Practical Multi-Objective Optimization Approaches for Decision Making in Health Care Considering Infectious Disease Dynamics and Uncertainties

Chelsea Greene

A dissertation
submitted in partial fulfillment of the requirements for the degree of

Doctor of Philosophy

University of Washington

2023

Reading Committee:

Zelda B. Zabinsky, Chair

Jennifer Ross

Shan Liu

Program Authorized to Offer Degree:
Industrial and Systems Engineering

University of Washington

Abstract

Practical Multi-Objective Optimization Approaches for Decision Making in Health Care Considering Infectious Disease Dynamics and Uncertainties

Chelsea Greene

Chair of the Supervisory Committee:
Zelda B. Zabinsky
Industrial and Systems Engineering

Operations research methods have been commonly used to inform decisions in health care related to inventory management, policy implementation, and resource allocation. However, the current research does not address many of the unique challenges and objectives faced by decision makers and stakeholders involved in managing infectious diseases. The aim of my dissertation research is to develop practical and effective methods that address these challenges and objectives, with the goal of improving health outcomes and promoting equity. To achieve this goal, my research combines state-of-the-art mathematical modeling methodologies with the perspectives of several organizations and researchers across multiple disciplines. It employs various methodologies, including mathematical optimization, dynamic transmission compartmental modeling, and statistics. The challenges and objectives addressed in this research, include but are not limited to dynamics and uncertainties in demand, supply, and health outcomes, multiple objectives, and vulnerabilities of populations,

This research contributes to three realistic applications, including:

(i) inventory and order management for multiple healthcare commodities and populations during an infectious disease outbreak;

(ii) policy analysis of tuberculosis (TB) and HIV health care program interventions in KwaZulu-Natal, South Africa;

(iii) budget allocation to regional TB and HIV health care programs across the nine provinces of South Africa.

These applications address the critical challenges and objectives of managing infectious diseases. In order to identify and address these critical challenges and objectives, I collaborated with several organizations and researchers across multiple disciplines, including epidemiologists, economists, and public health officials. One of the common challenges identified during these collaborations was the discrepancy between available and required input data to execute current modeling approaches. Therefore, one contribution of this dissertation is to develop approaches that use readily available data and incorporate uncertainty to offer practical decision support.

In addition to incorporating uncertainty, this research creates decision support approaches that account for the dynamic nature of infectious diseases. For instance, the inventory and order management application considers not only uncertainties in lead time, supply, and demand over time, but also accounts for the rippling effects of various supply chain components on optimal inventory and order management decisions. Furthermore, it is designed to generate recourse decisions that take into account these rippling effects when new information arises. I also introduce two versions of a dynamic transmission compartmental model of TB and HIV disease progression to project health outcomes under health care program interventions across the nine provinces of South Africa. Both versions of the dynamic transmission compartmental model are calibrated using available data, and identify a range of accepted parameter sets that represent uncertainties in TB- and HIV-related health outcomes. The budget allocation application uses the projections from the second version of the dynamic transmission compartmental model across accepted parameter sets to estimate the mean and variance of health outcomes to statistically capture uncertainty.

A second contribution is the consideration of multiple objectives and providing trade-off analyses to decision makers. For instance, the inventory and order management application

balances the impact of commodity substitutions with delays in meeting demand forecasts with the use of a new Healthcare Commodity Metric in the objective function. The policy analysis of TB and HIV health care program interventions evaluates the trade-offs between improved health outcomes and additional costs of implementing program interventions compared to the standard of care. The multiple objective optimization for the budget allocation application balances overall health outcomes with equity, and identifies a set of Pareto optimal solutions that probabilistically meet a budget constraint and are probabilistically non-dominated.

A third contribution is to take into account the unique vulnerabilities of different populations. For example, the inventory and order management application allows users to prioritize populations with specific commodities based on their criticality. This is particularly important for vulnerable populations, who may be disproportionately impacted by delays or substitutions in meeting their demand for healthcare commodities. To ensure that these populations are given priority, the Healthcare Commodity Metric integrates a user-specified criticality measure. The budget allocation application considers the unique vulnerabilities of regional populations by calibrating the second version of the dynamic transmission model of TB and HIV disease to regional calibration targets that correspond to each of the nine provinces of South Africa. Regional projections are used to estimate the overall health outcome and equity objectives used in the budget allocation approach.

Decision makers and stakeholders face unique challenges and objectives when managing infectious diseases. The three applications and methodologies provide practical approaches that address these challenges and objectives and pave the way for new, more practical, effective, and equitable approaches to decision making in health care to manage infectious diseases.

TABLE OF CONTENTS

LIST OF FIGURES

LIST OF TABLES

ACKNOWLEDGMENTS

I would like to express my sincere gratitude to my advisor, Professor Zelda B. Zabinsky, for her knowledge, guidance, and support during my Ph.D. I would also like to thank Dr. Jennifer Ross for introducing me to the fascinating world of epidemiology. Their encouragement to explore innovative ways of managing infectious diseases and emphasis on critical thinking from different perspectives has been invaluable. I would also like to extend my thanks to my other committee members, Professors Shan Liu and Shi Chen, for their comments and willingness to be a part of my committee. My dissertation was supported by the University of Washington's Department of Industrial and Systems Engineering and the Department of Global Health, as well as the National Science Foundation. My gratitude goes to my colleagues at the University of Washington Larissa Prates Guimarães Petroianu, Klass Fiete Krutien, Seyma Günes, Gabriela Giron-Valderrama, José Luis Machado León, Audur Anna Jonsdottir, Serin Lee, and Pariyakorn Maneekul for their support and friendship throughout my doctoral program.

My mother for her support, she always believed in me even when she did not understand what I was doing. Thanks to my former coworkers and friends, Lauren Finnegan, Hanna Moreland, Quynh-Chau Ha, Allison Pfaendler, and Anna Ferrante for supporting my vision of bridging the gap between research and practice and believing in my ability to do so.

My husband Casey, for his unconditional love and support. Without him by my side, completing this Ph.D. would not have been possible. His willingness to take on extra responsibilities without any hesitation is something I am truly grateful for. Last but not least, I would like to thank my loving, smart, and curious daughter Addison for the love, hugs, and laughs that got me through the final stretch of the Ph.D.

DEDICATION

To my grandfather, who encouraged me to pursue a Ph.D. in engineering. He inspires me to persevere through adversity and to always remain curious, loving, and optimistic.

Chapter 1

INTRODUCTION

Key stakeholders worldwide have continually emphasized that operations research methods are a critical component in alleviating challenges in health care decision making [41, 99]. As a result, there have been concerted efforts of these stakeholders to engage operations researchers [3, 149] to create models that can inform decisions related to inventory and order management [14, 154], policy decisions [65, 133], and resource allocation [9, 82].

However, managing infectious diseases is challenging due to uncertainties and dynamics of infectious diseases, complex issues involving multiple criteria and stakeholders, and the differing vulnerabilities of populations. To address the challenges in managing infectious diseases, my dissertation research combines mathematical optimization, dynamic transmission compartmental modeling, and statistical methods in the development of practical approaches for decision makers in health care. I collaborated with public health officials, epidemiologists, and economists to identify and determine how to best address these challenges in three realistic applications, including:

(i) inventory and order management for multiple healthcare commodities and populations during an infectious disease outbreak;

(ii) policy analysis of tuberculosis (TB) and HIV health care program interventions in KwaZulu-Natal, South Africa;

(iii) budget allocation to regional TB and HIV health care programs across the nine provinces of South Africa.

1.1 Motivation

The dynamic and uncertain nature of infectious diseases makes it difficult to reliably project health outcomes, demand and supply of healthcare commodities, and costs over time. These complex and uncertain projections make it challenging to reliably inform decisions related to inventory and order management, policy decisions, and resource allocation to manage the negative impacts of infectious disease. Dynamic transmission compartmental models have been widely used to project health outcomes, demand and supply of healthcare commodities, and costs over time [65, 133, 143]. However, in the absence of decision making tools that consider these dynamics and uncertainties, it is difficult for decision makers to understand and plan for uncertainties associated with their possible decisions. Additionally, the lack of models that enable decision makers to adapt to new information as it becomes available only compounds these difficulties in managing uncertainties. Without adaptable models, decision makers are forced to make quick adaptations with inadequate information when new data reveals changes to projections [97, 141].

When decisions are not properly planned for and adapted, it can have a negative impact on stakeholders affected by the decision making process. To avoid any negative impacts, it is important to involve various stakeholders and consider their challenges and objectives. However, due to the lack of collaborative approaches, siloed decision makers are forced to make guesses regarding the potential impact of their decision on others [84, 97, 106, 128]. Furthermore, coordinating multiple decision makers often require the consideration of multiple objectives. However, the majority of mathematical optimization approaches focus on improving a single health outcome and disregard other goals, such as equity between regions, that may be important to stakeholders [9, 65]. Disregarding objectives related to health equity can result in a disproportionate impact of infectious diseases among the most vulnerable communities. These complex challenges and objectives require new model formulations and solution techniques that account for the dynamics and uncertainties of demand, supply, and health outcomes, multiple objectives of relevant stakeholders and decision makers, and

varying population vulnerabilities [9, 82].

1.2 Research Applications and Contributions

The primary objective of this dissertation research is to develop practical approaches that balance overall health outcomes and equity objectives while simultaneously accounting for the uncertainties and dynamic nature of infectious diseases. In this dissertation, I present three research applications that address gaps in the existing literature and account for the unique challenges and objectives related to managing infectious diseases. My research contributes to applications that consider: (1) dynamics and uncertainties of demand, supply, and health outcomes, (2) multiple objectives, and (3) varying population vulnerabilities.

1.2.1 Inventory and Order Management for Healthcare Commodities During an Infectious Disease Outbreak

During the coronavirus (COVID-19) pandemic, limited supply, global supply chain disruptions, and demand volatility for healthcare commodities, such as personal protective equipment (PPE), resulted in shortages of commodities needed to limit transmission rates and treat infected individuals. To alleviate the impacts of these shortages, various governmental, non-governmental, private, and non-profit organizations expanded and established programs to acquire, store, and distribute healthcare commodities to organizations and individuals within their jurisdictions [61, 68, 114, 122, 150]. Unfortunately, there is a lack of modeling approaches to support the unique challenges and objectives of these organizations during an infectious disease outbreak [33, 107, 141].

The inventory and order management optimization model presented in Chapter 2 was built in collaboration with several organizations managing inventory for healthcare commodities during the COVID-19 pandemic to identify and address these challenges and objectives. It aims to minimize the consequences of delays and substitutions for multiple healthcare commodities and populations that vary in vulnerability. It uses linear optimization to pro-

vide optimal ordering schedules (amount and timing) for a set of healthcare commodities and populations, such as masks for healthcare providers, during an infectious disease outbreak.

The first contribution is to methods that incorporate dynamics and uncertainties of demand and supply into inventory and order management. During the COVID-19 pandemic, decision makers were forced to quickly adapt supply chain decisions to dynamic demand and supply patterns, geopolitics, and infection rates on a global scale with little information or guidance. These adaptions had a rippling effect on all supply chain management processes, from procurement to inventory management to resource allocation. Limitations in inventory and order management modeling forced supply chain managers to guess how decisions outside of their specific role might change and account for the potentially rippling effects of these decisions on theirs [84, 106, 128]. For example, it was difficult to determine how new information regarding the arrival time of ordered healthcare commodities would impact optimal ordering plans and the budgetary needs for ordering healthcare commodities. A compounding issue was the lack of effective communication between supply chain levels to coordinate decisions. The magnitude of external influences and factors that impact healthcare outcomes, and the lack of agile and collaborative decision-making tools forced supply chain managers to adapt quickly without adequate information.

To address these challenges, the inventory and order management model is designed to manage uncertainty across supply chain levels over time. The optimization model accounts for uncertainties at different levels of the supply chain (e.g., procurement, inventory management) that can impact an organization's ability to deliver healthcare commodities to their final destination. The model uses future demand projections (possibly from an infectious disease model) and supply projections (possibly from supplier information) to formulate a chance constraint and approximate lead times through a discretized probability distribution. Furthermore, it is agile so that it can be adapted quickly to new information regarding demand, supply capacities, supply costs, and lead times. The model is collaborative in that it considers the impacts of warehouse capacities, supplier portfolios, and budgets so that the

same model can support strategic and operational decision making.

The second contribution is to multiple objective models that balance the impacts of substitutions with delays of healthcare commodities. During the COVID-19 pandemic, organizations faced challenges in obtaining the supply needed to fulfill the demand for healthcare commodities in a timely manner. To mitigate delays in fulfilling demand, they substituted healthcare commodities with comparable items. However, these substitutions were often not ideal as they could reduce protection, lower treatment effectiveness, and increase ordering costs. To address this challenge, the optimization formulation considers both the negative impacts of commodity substitutions and delays in meeting demand. The created model balances the impacts of substitutions with delays and allows decision makers to evaluate the trade-offs.

The third contribution is to models that account for the disproportionate impact of inadequate healthcare commodities on vulnerable populations. Delays and substitutions can have a disproportionate effect on vulnerable populations. For instance, health care workers are generally more vulnerable to infection without medical-grade masks than other populations. To address this issue, a new Healthcare Commodity Metric is introduced that quantifies the relative consequences of delays and substitutions on various populations and commodities using suitability- and criticality-based inputs. This Healthcare Commodity Metric is used in the optimization model to balance the impacts of delays and substitutions on populations with varying vulnerabilities.

1.2.2 Policy Analysis of Healthcare Interventions for TB and HIV Care Delivery Programs in KwaZulu-Natal, South Africa

People living with HIV (PLWH) are at increased risk of progression to active TB disease and death due to their weakened immune systems from HIV disease [2, 12, 23, 96, 101, 103, 158]. Antiretroviral therapy (ART) is used to treat HIV and reduces the risk of progression

to active TB disease and dying while infected with TB [134]. TB preventative treatment (TPT) with isoniazid, when given with ART, further reduces the risk of progression to active TB disease [116].

ART and TPT are both part of the recommended care for PLWH. However, not all PLWH receive ART or TPT care [16, 50]. Public health officials in South Africa are interested in policy analysis to evaluate the impact of interventions that increase the uptake of ART and TPT. Recently, the Delivery Optimization for Antiretroviral Therapy (DO ART) household-randomized trial of community-based ART with TPT care delivery in South Africa and Uganda demonstrated that community-based care increases ART and TPT uptake, particularly among men [16]. However, the longer-term impact of increased ART and TPT uptake on incident TB and deaths from community-based care delivery was not quantified among trial participants, nor were TB incidence or deaths quantified among community members who were not in the trial.

The policy analysis presented in Chapter 4 was built in collaboration with epidemiologists and health economists to evaluate the impact of three care delivery programs in KwaZulu-Natal, South Africa, including: standard facility-based ART and TPT care delivery, community-based ART care delivery and facility-based TPT care delivery, and community-based ART with TPT care delivery. It uses the dynamic transmission compartmental model of TB and HIV transmission and disease progression presented in Chapter 3 (version one) to project health outcomes among 100,000 adults, ages 15-59, in KwaZulu-Natal, South Africa.

The first contribution is to methods that project dynamics and uncertainties of TB- and HIV-related health outcomes and costs. Reliable projection of TB and HIV health outcomes and costs requires the consideration of several complex factors. For example, PLWH have an increased likelihood of developing active TB disease and dying with active TB, which depends on their stage of HIV [2, 12, 23, 56, 80, 96, 101, 103, 134, 135, 158]. Increased uptake of ART and TPT from community-based care can reduce the risk of developing active TB disease among PLWH [109, 116, 137], and can indirectly impact TB health outcomes among people

without HIV through reduced community TB transmission.

To simulate these complex dynamics, I collaborated with epidemiologists to develop a dynamic transmission compartmental model that considers the implications of TB and HIV co-infection. It accounts for factors such as the increased likelihood of developing active TB disease and the risk of mortality among PLWH, and the reduced risk of developing active TB for PLWH treated with ART and TPT. The model includes people without HIV to allow the model to estimate the indirect health benefits of community-based ART with TPT for people without HIV.

Model parameters reflect findings from the DO ART trial [16] and other scientific literature. The model is calibrated over 34 parameters. A range of accepted parameter sets are identified through calibration by comparing model projections for a set of candidate parameter sets against ten regional calibration targets, including TB incidence and TB mortality estimates by HIV status (HIV-positive and HIV-negative) and gender, and HIV prevalence by gender across two years in KwaZulu-Natal, South Africa. Projections of TB- and HIV-related health outcomes and costs are provided across a range of accepted parameter sets that meet all calibration targets to represent uncertainties.

The second contribution is developing methods that aid decision makers in evaluating the trade-offs of improved health outcomes and additional costs with community-based care relative to standard, facility-based care. The model projects TB incidence, TB mortality, disability-adjusted life years (DALYs), and program costs under the three care delivery programs. We compare the number of TB cases, deaths, DALYs averted, and additional program costs with community-based care relative to standard, facility-based care. To evaluate the trade-offs of improved health outcomes with additional costs, we quantify incremental cost-effectiveness ratios from the provider perspective.

The third contribution is to insights into how community-based care delivery programs can reduce gender disparities in TB health outcomes. Across nearly all regions globally, and in South Africa specifically, under standard facility-based ART and TPT care delivery,

there is a smaller proportion of men living with HIV that achieve viral suppression, as compared to women living with HIV [142]. The community-based care arm of the DO ART trial observed an increased proportion of all PLWH with HIV achieving viral suppression, particularly among men as compared to women, [16], thus reducing gender disparity in HIV viral suppression.

To analyze the impacts of community-based care delivery on reducing gender disparities, we compare model projections on TB incidence and TB mortality by gender under the three care delivery programs. The model accounts for other gender differences identified in the literature, including mortality rates, HIV incidence, effective contact rates, and CD4 decline. The analysis shows a reduction in gender disparities related to TB incidence and TB mortality under community-based care, compared to standard facility-based care.

1.2.3 Allocation of Budget to TB and HIV Health Care Programs across South Africa's Nine Provinces

While community-based ART with TPT care has been shown to improve health outcomes, the higher costs associated with community-based care may make implementation throughout a country unaffordable [9]. Allowing the implementation of programs by region could enhance health outcomes while remaining within a fixed national budget [7, 35, 83]. However, there is a lack of approaches that consider regional dynamics and uncertainties of health outcomes and costs, the complex issues involving multiple criteria and stakeholders, and the unique regional population characteristics needed to inform budget allocation decisions to regional health care interventions [9].

The budget allocation optimization approach presented in Chapter 5 explores the best combinations of regions to prioritize for community-based HIV and TB care delivery programs, given a national budget. It aims to minimize inequities in TB- and HIV-related mortality rates between regions as well as minimize national TB- and HIV-related deaths. It integrates multiple objective optimization, a dynamic transmission model of TB and HIV

disease (the second version presented in Chapter 3), and statistical methods to generate a set of Pareto optimal solutions that are probabilistically non-dominated and probabilistically meet the budget constraint.

The first contribution is to methods that project dynamics and uncertainties of TB- and HIV-related health outcomes and costs. Model projections of infectious disease progression are inherently uncertain. An optimization model that does not consider uncertainties in TB- and HIV-related health outcomes and costs might disregard factors important to decision makers and stakeholders, such as variability in health outcomes and financial risks.

In the budget allocation application, dynamics and uncertainties in health outcomes and costs are projected with the use of the dynamic transmission model of TB and HIV disease (the second version presented in Chapter 3). Model uncertainties in TB- and HIV-related health outcomes by region are considered by identifying a range of accepted parameter sets that meet all calibration targets. The projected health outcomes for all accepted parameter sets are used to estimate the mean and variance of each health outcome to statistically capture uncertainty.

The second contribution is to consider multiple objectives that balance equity and effectiveness. The majority of budget allocation approaches aim to reduce the overall health burden. However, reducing the overall health burden is often not a health system's only objective. There are other factors, such as equity, financial risk and other political factors, that are important to stakeholders and decision makers.

The optimization approach in the budget allocation application considers two objectives that quantify inequity and effectiveness and a budget constraint. The first objective function represents inequity in TB- and HIV-related mortality rates across regions. The second objective function is the total TB- and HIV-related deaths summed over all regions. The budget constraint captures the risk of exceeding a national budget. The approach uses the sample mean and sample variance for each objective function. The approach returns a set of Pareto optimal solutions that probabilistically meet the budget constraint and are probabilistically

non-dominated.

The third contribution is to analyses that account for regional differences. It is crucial to account for regional differences in TB- and HIV-related health outcomes when evaluating interventions to ensure that vulnerable populations are considered in allocating limited budgetary resources. However, identifying regional differences in health outcomes and evaluating the impact of various combinations of regional interventions across a nation can be challenging.

To capture regional differences, the approach considers 31 calibrated model parameters, nine that vary by region (e.g., HIV incidence rates) and 22 that are constant over all regions (e.g., reduced risk of progression from TPT). The model projects health outcomes by region under two care delivery programs.

The analyses indicate that health benefits of the two programs differ by region, and regions with a high-burden of TB and HIV disease show greater improvement compared to regions with a low-burden of TB and HIV disease. However, the increased cost also varies by region characteristics. The analyses considers both health outcomes and costs when evaluating the allocation of limited budget to care delivery programs.

The following chapters describe the development of practical multi-objective optimization approaches for decision making in healthcare to manage infectious diseases. Chapter 2 provides the inventory and order optimization model. Chapter 3 describes the two versions of the dynamic transmission compartmental model of TB and HIV disease progression. Chapter 4 provides a policy analysis of TB and HIV health care program interventions in KwaZulu-Natal, South Africa. Chapter 5 provides the approach for the budget allocation application for regional TB and HIV care delivery programs across the nine provinces of South Africa. Finally, Chapter 6 gives concluding remarks and future research.

Chapter 2

AN INVENTORY AND ORDER MANAGEMENT OPTIMIZATION MODEL FOR HEALTHCARE COMMODITIES DURING AN INFECTIOUS DISEASE OUTBREAK

This chapter presents an inventory and order management model that accounts for a healthcare commodity supply chains' unique risks and objectives during an infectious disease outbreak to inform ordering plans and inventory strategies. Most of this chapter was submitted for publication in the Annals of Operations Research Journal in February 2022, and a revision was submitted in May 2023.

To guide the development of the inventory and order management model presented in this chapter, I collaborated with several organizations managing inventory for healthcare commodities during the coronavirus (COVID-19) pandemic. Through these collaborations, I identified the unique challenges, decisions, and objectives they faced during this time and determined how these factors could be reflected in the optimization model. One challenge was uncertainties along the supply chain. To address this challenge, the model accounts for risks such as demand surges, supply shortages, and lead-time uncertainties. Furthermore, to manage dynamics and uncertainties along the supply chain, the approach is adaptable and collaborative to inform recourse decisions as new information arises. The model is adaptable and can be modified quickly to respond to changes in demand, supply capacities, supply costs, and lead times. It facilitates collaborative decision-making by providing estimates of the impacts of both operational decisions (such as ordering) and strategic decisions (such as budgeting).

Another challenge was the lack of supply available to meet the demand. When supply was unavailable, decision makers were forced to substitute with comparable commodities.

However, these substitutions were not always ideal and could result in lower protective effectiveness and increased ordering costs. To address this challenge, the model enables item substitution to reduce delays in fulfilling demand and considers budgeting, supply, and warehouse constraints. When supply is limited, the model balances the impact of commodity substitutions with delays in meeting demand forecasts. To balance these impacts, I introduce a Healthcare Commodity Metric that quantifies the relative consequences of delay and substitutions and is used in the objective function. To account for the vulnerabilities of populations, the Healthcare Commodity Metric considers the varying impact of delays and substitutions on vulnerable populations with specific commodities with the use of a user-specified criticality input parameter.

The rest of the chapter is organized as follows. Section 2.1 describes the unique challenges and objectives of a healthcare inventory and order management role during a pandemic and provides an overview of how this model addresses these challenges and objectives. Section 2.2 describes the optimization model and the properties of our Healthcare Commodity Metric. Section 2.3 presents an example use case to illustrate how model outputs can be used to support an agile and collaborative decision making process. Section 2.4 discusses managerial implications, model assumptions, and limitations. Finally, Section 2.5 presents conclusions and future work.

2.1 Introduction and Background

During the coronavirus (COVID-19) pandemic, limited supply, global supply chain disruptions, and demand volatility for healthcare commodities, such as personal protective equipment (PPE), resulted in shortages of commodities needed to limit transmission rates and treat infected individuals. To alleviate the impacts of these shortages, various governmental, non-governmental, private, and non-profit organizations expanded and established programs to acquire, store, and distribute healthcare commodities to organizations and in-

dividuals within their jurisdictions [61, 68, 114, 122, 150].

However, there is a lack of modeling approaches to support these organizations during a pandemic [33, 107, 141]. I collaborated with several organizations during the COVID-19 pandemic, including the City of Seattle (M. Rathke, personal communication, 2020), John Snow, Inc. [62], Restart Partners [114], the International Association of Public Health Logisticians, and the Washington Global Health Alliance [157], to build a practical optimization model that supports an inventory and order management process for healthcare commodities.

This research addresses the following research questions: (1) what are the unique challenges and objectives of a healthcare inventory and order management role during a pandemic? (2) how can these unique challenges and objectives be reflected in an optimization model to support inventory and order management decisions for healthcare commodities during a pandemic? (3) how can the model be used to support agile and collaborative decision making across inventory and order management functions as new information arises?

In this research, I identify the unique challenges and objectives of organizations managing inventory for healthcare commodities during the COVID-19 pandemic. These findings are used to construct an optimization model that generates optimal ordering plans for multiple healthcare commodities (e.g., masks and ventilators) and populations (e.g., health care providers, essential businesses, the general public). The optimization model employs data readily available to these organizations to effectively inform the decisions made by these organizations during the COVID-19 pandemic. Specifically, the optimization model considers the increased consequences of delays and substitutions for highly critical healthcare commodities and populations. For example, delays in fulfilling the demand for masks for health care providers has more significant consequences than for the general public. Similarly, substituting a medical-grade N95 mask with a medical-grade surgical mask has more significant consequences when those masks are for healthcare providers versus the general public. The model balances the consequences of delays and substitutions for multiple healthcare commodities. also considers factors that impact inventory and order management decisions, such as lead times for receiving commodities, supplier capacity, demand forecasts, budgets, and

warehouse space. These considerations enable the optimization model to support an agile and collaborative decision-making process needed in a constantly changing environment, such as a pandemic. This work contributes to the literature by identifying unique challenges and objectives faced by inventory and order management decision makers during a pandemic. Another contribution is a practical optimization model that balances the impacts of fulfillment delays and substitutions to support agile and collaborative decision-making, as illustrated in the example use case.

2.1.1 Unique Challenges and Objectives during a Pandemic

This section presents the unique challenges and objectives of a healthcare inventory and order management role during a pandemic identified from collaborations, research articles, and reports. These unique challenges and objectives are discussed in Section 2.1.1 and summarized in Table 2.1. These challenges, objectives, and modeling gaps guide the development of the model.

Description of Challenges and Objectives

One of the challenges faced by organizations managing inventory for healthcare commodities is fluctuating and uncertain demand of healthcare commodities. During a pandemic, the demand for healthcare commodities fluctuates based on different factors such as disease outbreaks, hospitalization rates, and government mandates that are uncertain and can change over time [10, 30, 49, 58, 64, 110, 127]. For example, at the start of the COVID-19 pandemic, the City of Seattle established a process to distribute multiple PPE types (e.g., masks and gloves) from a centralized warehouse to their employees (e.g., firefighters, police, etc.). Demand for PPE was sporadic due to unexpected outbreaks that increased demand for testing centers supported by the City of Seattle workers and events (M. Rathke, personal communication, 2020).

Not only does a pandemic impact demand fluctuations and uncertainty, but it also brings

Unique Challenges and Objectives	References
Fluctuating and uncertain demand of healthcare commodities	[10, 30, 49, 58, 64, 110, 127]
Global supply chain disruptions and demand surges resulting in impacts to lead times and supplier capacities	[60, 61, 120, 123, 145, 146]
Limited buffer stocks due to supply shortages, warehouse capacities and strained budgets	[48, 58, 113, 122, 145]
Fulfill demand requests with minimal delays and substitutions, particularly for the most critical population and commodity types	[48, 100, 106, 107, 119, 122, 139, 144]
Lack of modeling approaches that support agile and coordinated decision-making required in a rapidly evolving supply chain environment	[18, 33, 48, 60, 61, 94, 113, 141]

Table 2.1: Summary of the unique challenges and objectives of a healthcare inventory and order management role during a pandemic and relevant references.

about global supply chain disruptions and demand surges resulting in impacts to lead times and supplier capacities [61, 120, 123, 145, 146]. For example, during the COVID-19 pandemic, to meet surges in demand, many suppliers expanded their capacities to provide healthcare commodities. However, reduced workforces, due in part to disease outbreaks, resulted in reduced supplier capacities, extended lead times, and constantly changing supplier capacities [60, 146]. For the City of Seattle, this meant that orders would commonly arrive delayed, partially fulfilled, or damaged (M. Rathke, personal communication, 2020).

A common strategy to alleviate shortages in the case of uncertain demand and supply is to store large buffer stocks. However, during the COVID-19 pandemic, there was limited inventory due to supply shortages, warehouse capacities, and strained budgets [48, 58, 113, 145]. Due to difficulty in maintaining buffer stocks, another strategy employed during the COVID-19 pandemic to alleviate these shortages and subsequent delays in fulfilling demand was to substitute stock-keeping units (SKUs) with comparable SKUs (e.g., N95 medical-grade masks substituted with medical-grade surgical masks). However, these substitutions can reduce protection, lower treatment effectiveness, and increase ordering costs [48, 106, 119].

For example, the State of Utah established a PPE push pack program aimed at helping small businesses get back to work. PPE push packs included masks, hand sanitizer, gloves, and other healthcare commodities depending on state inventory and workers' exposure at their place of work [122]. When medical-grade surgical masks were not available to fulfill the demand for masks for workers with medium risk exposure, the state substituted a reusable face shield with products needed to decontaminate the face shield following Occupational Safety and Health Administration guidelines [100].

Fulfillment delays and substitutions have increased implications for specific populations and healthcare commodities [139, 144]. For example, delays and substitutions of fulfilling the demand for highly critical commodities such as masks for health care providers increase infection and mortality rates and impact future demand more than the general public [100, 107, 144]. As a result, during the COVID-19 pandemic, highly critical healthcare commodities and populations were prioritized to reduce delays and substitutions in fulfilling demand when supply and inventory are limited [122, 144]. For example, for the State of Utah's PPE push pack program, when medical-grade surgical masks were available but in an inadequate quantity to satisfy the demand for medium and low-exposure risk workers, the state prioritized fulfilling the demand for masks for medium exposure risk workers with medical-grade surgical masks and distributed less suitable but comparable items, such as reusable face shields and products to decontaminate the face shields to those at low risk to exposure [100, 122].

The continually evolving assumptions and uncertainty in demand, supplier capacities, and lead times during a pandemic require increased coordination within organizations managing inventory and orders for healthcare commodities to quickly and effectively modify decisions. While the need for model agility and coordination is not a new challenge during a humanitarian crisis [6, 19, 33, 40] and routine global health supply chain management in a low resource setting [59, 106], decision makers face more severe consequences during a pandemic from suboptimal decisions [33, 60, 61, 94, 113, 141]. For example, John Snow Inc. is a non-governmental organization that helps countries, states, and public health systems world-

wide in supply chain management for medicines and related supplies. The organization faced many of the same challenges during the COVID-19 pandemic in routine healthcare commodity distribution in a low-resource setting. However, these challenges were exacerbated due to strict financial cycle restrictions, extended and uncertain lead times, and strained warehouse capacities [59, 61].

The rapidly evolving environment and more severe consequences require tools that support agile and coordinated decision-making. However, many models to determine strategic decisions for inventory and order management are relayed to operational decision-makers with no ability to easily adjust as the situation changes [18, 48]. Consequently, during the COVID-19 pandemic, healthcare commodity inventory managers were forced to make decisions quickly without adequate information [61, 141]. For example, in March 2020, the Federal Emergency Management Agency (FEMA) activated its national resource coordination center to support states, tribes, territories, and local governments across the United States in responding to COVID-19 [141]. FEMA supported these governmental agencies by coordinating the delivery of healthcare commodities such as N95 respirator masks, surgical gowns, face shields, and gloves to their jurisdictions. As per FEMA's national incident management system, decisions such as outstanding resource requests and delays were discussed daily by leaders of the various emergency support functions [140]. The current tools available to support FEMA's incident management frameworks for coordination required significant time to manually process outstanding requests and make recourse decisions as needed, stressing FEMA's workforce, resulting in challenges in coordination along the supply chain and transparency.

Relevant Inventory and Order Management Literature

The nature of a pandemic, such as the COVID-19 pandemic, reflects elements of an inventory management process for both a humanitarian crisis (e.g., earthquake, hazardous material spill) and routine global health supply chain management in a low resource setting. Interested readers can refer to literature reviews regarding humanitarian logistics [6, 15, 19,

33, 40, 71, 105] and routine global health supply chain management in a low resource setting [34, 106, 125]. While inventory management in these contexts has become an increasingly studied topic in the Operations Research field, I did not find any model that addresses the unique challenges and objectives faced by organizations managing inventory and order management processes for healthcare commodities during the COVID-19 pandemic [5, 26, 63, 70, 107, 108]. Specifically, the model provides an inventory and order management approach for multiple commodities that vary in criticality, allows for substitutions of products to fulfill demand when the most suitable product is unavailable, and supports agile and collaborative decision making.

Several studies in these applications support inventory management decisions for multiple commodities that vary in criticality. Little and Coughlan (2008) generate an inventory policy (delivery frequency and amount of stock to hold) for multiple healthcare commodities to maximize service levels (proportion of scenarios in which demand is satisfied for each commodity) in a space constrained environment [74]. Commodity criticality is considered by enforcing highly critical commodities to meet high service. Uthayakumar and Priyan (2013) developed a model that determine optimal lot sizes, lead times, and the number of deliveries for multiple pharmaceuticals that vary in unit costs, unit size, and considers lead times, however they do not consider commodity criticality [151]. There are various studies that support inventory management in a humanitarian crisis, primarily focused on pre-positioning multiple commodities of varying criticality through shortage penalties, however these models do not support ordering decisions [1, 11, 13, 36, 87, 112, 147].

There are inventory management models that consider substitutions in a private sector context [20, 27, 28, 51, 66, 77, 92, 126, 138] however, substitution penalties focus on increased costs, reduced profit and customer retention. Despite substitution being a common practice in global health and humanitarian logistics inventory management processes [10, 106, 119], I found very few studies that account for the quality impacts of substitutions in this context [15]. Yadavalli et al. (2015) present a model that generates an adjustable reorder point policy for two perishable products that are substitutable [160]. This model

balances penalties associated with substitution, unsatisfied demand, and waste of product due to expiry. Other models consider the additional costs associated with emergency orders through additional monetary costs, but do not consider quality impacts from substitutions [17, 115, 138, 162]. Zahiri et al. (2018) designed a model to support pharmaceutical supply chain design establishment of distribution center and manufacturer locations, inventory levels, and product flows for two perishable and substitutable pharmaceutical products with uncertainties in supplies and demands [162]. In Zahiri et al. (2018) it is assumed there is no penalty for substituting one product for another as long as the two products are substitutable [162]. Criticality of products and demand regions are considered by weighting the objective function (to minimize the maximum unsatisfied demand of all products and demand regions). I did not find any modeling approaches that balance delay and substitution impacts for multiple populations and healthcare commodities that vary in criticality when supply and inventory is limited.

Furthermore, many literature reviews of models applied in a humanitarian crisis and routine global health supply chain management in a low resource setting contexts state there is a lack of modeling approaches that support agile and collaborative decision making [6, 15, 33, 40, 106]. A common approach to integrate strategic and operational decision making for optimization models is two-stage stochastic programming with recourse, where the first stage supports strategic decisions (e.g., warehouse location, amount to preposition) given a set of probabilistic scenarios and the second stage can be used to support operational decisions (e.g., assignment of inventory to a demand region) when a given scenario is realized [19, 32, 87, 98, 156]. However, I did not find any models that support agile and collaborative decision-making that addresses the unique challenges and objectives faced by inventory and order management decision makers during a pandemic.

2.1.2 Overview

The discussed challenges, objectives, and modeling gaps guide the development of the model and example use case. The optimization model generates optimal ordering plans including quantities and timing of orders for a set of suppliers and SKUs over a user-specified forecasting period (e.g., twelve weeks) and time intervals (e.g., one week.) The supply received is added to the available inventory that can be used to fulfill demand for a set of healthcare commodities and populations in each time interval. The optimization model allows demand requests to be carried over when not fulfilled during the requested time interval but penalizes delays. The model allows substitution of healthcare commodities (e.g., medical-grade N95 masks with medical-grade surgical masks) when the most suitable items are not available. The user specifies the set of supplier-SKUs that can satisfy the demand for each healthcare and population type to indicate possible substitutions, and the suitability score that acts as a penalty when the substitution reduces protection or treatment effectiveness. The user also specifies a criticality score that represents the prioritization for each healthcare commodity and population type based on the relative consequences of delays and substitution. The new Healthcare Commodity Metric, employed in the objective function of the optimization model combines criticality and suitability scores to quantify the relative impact of delays and substitutions for each healthcare commodity and population type considered in the model set. The Healthcare Commodity Metric is designed to ensure that highly critical populations and healthcare commodities are prioritized in terms of minimizing delays and substitutions when supply, inventory, budgets, or warehouse space is limited.

This research contributes to the development of an inventory and order management optimization model for healthcare commodities during a pandemic by creating an optimization model that:

1. generates ordering plans that balance the negative impacts of delays and substitution for a set of populations and healthcare commodities, such as masks for health care providers, through a new Healthcare Commodity Metric,

2. is capable of agile decision making, to quickly and effectively update optimal ordering plans as information emerges by considering the up-to-date supply limitations, inventory availability and demand information, and
3. supports strategic decisions that can impact inventory and order management decisions (e.g., budgets).

I introduce a use case example that illustrates how the Healthcare Commodity Metric meets the objectives of an inventory and order management process for healthcare commodities during a pandemic. The use case example follows a similar process of many standard operating procedures for inventory and order management [59, 140]. It is based on conversations with organizations faced with both operational and strategic inventory and order management decisions during the COVID-19 pandemic. The example use case demonstrates the significance of combining up-to-date information from experts to modify ordering plans and in evaluating the impact of strategic decisions such as budgets periodically on inventory and order management objectives.

2.1.3 Managerial Implications

This work has several managerial implications. First, the optimization model is practical. Many optimization models require data not readily available to users. The proposed model employs data readily available to the organizations I collaborated with. For example, after organizations place orders, they are given an expected range of delivery dates or a single delivery date. The model incorporates a lead time constraint that allows the user to specify a range of projected lead times or a single lead time. Also, absolute consequences (e.g., number of additional infections) of delays and substitutions of multiple population and commodity types that vary in criticality are difficult to quantify and compare. A Healthcare Commodity Metric is introduced that quantifies the relative consequence of delays and substitutions for multiple commodities and populations using user-specified input parameters (criticality and suitability scores) that are easy to quantify and have transparent mathematical properties.

Specifically, the Healthcare Commodity Metric uses a criticality score between zero and one for each population and healthcare commodity type, where a value closer to one indicates higher criticality and a value closer to zero indicates lower criticality. The Healthcare Commodity Metric prioritizes the fulfillment of population and healthcare commodity types that are highly critical with minimal delay and substitution.

Second, the model supports an agile and collaborative decision-making process needed in a constantly changing environment, such as a pandemic. The optimization model is agile in that it can incorporate up-to-date information on lead times, supplier capacity, and demand forecasts to re-optimize ordering schedules as needed. The optimization model is collaborative in that it can support strategic decisions related to budgets and warehouse capacities and evaluate these decisions against the same metrics as operational ordering plan decisions.

2.2 Optimization Model

The optimization model is formulated as a linear program that provides optimal ordering decisions. Section 2.2.1 presents the notation used to describe the sets, input parameters, and decision variables used in the optimization model. Section 2.2.2 defines the Healthcare Commodity Metric used in the objective function of the optimization model to meet the objectives of a healthcare commodity inventory and order management process during a pandemic. Lastly, Section 2.2.3 provides the complete formulation.

2.2.1 Notation

See Table 2.2 for the notation used to describe sets and input parameters and Table 2.3 for the notation used to describe decision variables used in the optimization model. The forecasting period T (e.g., 12 weeks) is discretized into time intervals (e.g., days, weeks, months), where the set of time intervals is notated by $\mathcal{T} = \{1, \ldots, t, \ldots, T\}$. Orders are placed to fulfill demand requests in each time interval. All received commodities are placed

in a central warehouse and used for distribution. Each demand request is associated with a population and commodity type (e.g., masks for healthcare providers), where the set of population and commodity (population-commodity) types is notated by $\mathcal{K} = \{1, \ldots, k, \ldots, K\}$. In the use case example, the user can specify masks for healthcare providers ($k = 1$), masks for essential businesses ($k = 2$), and masks for non-essential businesses ($k = 3$). To fulfill demand requests there is a set of suppliers and SKUs (supplier-SKUs) they can provide, notated by $\mathcal{I} = \{1, \ldots, i, \ldots, I\}$. In the use case example, Supplier A provides medical-grade N95 masks ($i = 1$), Supplier B provides medical-grade N95 masks ($i = 2$), Supplier A also provides medical-grade surgical masks ($i = 3$), and Supplier C provides non-medical grade KN95 masks ($i = 4$). The set of supplier-SKUs that are suitable to fulfill demand for population-commodity type k is defined by $\mathcal{I}_k$, $\mathcal{I}_k \subseteq \mathcal{I}$, for all $k \in \mathcal{K}$. For example, a non-medical grade KN95 mask from Supplier C ($i = 4$) may not be suitable to fulfill demand requests for a mask for health care providers ($k = 1$). This is also how the user can specify, for example, that a gown is not suitable to fulfill demand requests for masks.

Healthcare Commodity Metric parameters (as in Table 2.2) include a user-specified *criticality score* denoted r_k for each population-commodity type k, $k \in \mathcal{K}$. The criticality score r_k takes on values between zero and one, where a value of one indicates that fulfilling demand for population-commodity type k is highly critical, and a value close to zero indicates low criticality. The Healthcare Commodity Metric uses the criticality score to prioritize fulfilling demand requests with minimal delay and substitutions for each population-commodity type k. Each supplier-SKU i that can be used to satisfy demand for population-commodity type k, $i \in \mathcal{I}_k$, is associated with a user-specified *suitability score* based on protective or treatment effectiveness, denoted $q_{k,i}$. The suitability score $q_{k,i}$ takes on values between zero and one, where a value of one indicates that supplier-SKU i is most suitable to fulfill demand requests of population-commodity type k and a value closer to zero indicates low suitability. For example, a medical-grade N95 mask from Supplier A ($i = 1$) may be more suitable than a medical-grade surgical mask from Supplier A ($i = 3$) to fulfill demand for masks for health care providers ($k = 1$). In this case, the user can set the suitability scores ($q_{k,i}$) such that

$q_{1,1} > q_{1,3}$, to represent that a medical-grade N95 mask from Supplier A ($i = 1$) is more suitable to satisfy the demand for masks for health care providers ($k = 1$) than medical-grade surgical mask from Supplier A ($i = 3$).

The *demand* input parameters to the model (see Table 2.2) include incoming demand requests and outstanding unfulfilled demand at the start of the forecasting period. Incoming demand requests for each population-commodity type k are estimated for each time interval t, represented by the parameter $d_{k,t}$, for all $k \in \mathcal{K}, t \in \mathcal{T}$. One way to estimate incoming demand is to employ statistical methods, but another is to ask experts about their forecasts. Various organizations and researchers have developed forecasting tools that provide estimates and ranges (minimum, maximum, most likely, or mean and standard deviation) to quantify demand for healthcare commodities [25, 143]. The proposed model can use multiple estimates and uncertainty ranges to incorporate uncertainty. To be conservative, the demand parameter $d_{k,t}$ could be set to the maximum range of the forecast, or to the mean plus one or two standard deviations. The goal is to fulfill demand as soon as possible, however the optimization model allows for unfulfilled demand to be carried over and fulfilled later in the forecasting period. Unfulfilled demand requests for each population-commodity type k at the start of the forecasting period are initialized with the parameters n_k^{init} for all $k \in \mathcal{K}$.

The model considers limitations on warehouse capacity, budget and inventory. The input parameter h represents the total warehouse capacity (e.g., 3,000 cubic feet), and the parameter s_i for all $i \in \mathcal{I}$ represents the size of a unit of supplier-SKU i in the same units as h (e.g., cubic feet). The input parameter b represents the total budget over the forecasting period, and the parameter c_i for all $i \in \mathcal{I}$ represents the cost for a unit from supplier-SKU i. The model allows input parameters for initial inventory levels at the start of the forecasting period for each supplier-SKU $i \in \mathcal{I}$ with the parameters z_i^{init}. When orders have been placed before the start of the forecasting period the parameter $o_{i,t}^{init}$ represents the number of units from supplier-SKU i expected to arrive during time interval t. For example, if there are 100 units of N95 medical-grade masks from Supplier A ($i = 1$) projected to arrive in the first week ($t = 1$) the user can set $o_{1,1}^{init} = 100$ to represent this projected additional inventory. For

Notation	Description
Sets	
$\mathcal{T}$	Set of time intervals in the forecasting period T, $\mathcal{T} = \{1, \ldots, t, \ldots, T\}$
$\mathcal{K}$	Set of population-commodity types $\mathcal{K} = \{1, \ldots, k, \ldots, K\}$
$\mathcal{I}$	Set of supplier-SKUs, $\mathcal{I} = \{1, \ldots, i, \ldots, I\}$
$\mathcal{I}_k$	Set of supplier-SKUs i that can satisfy demand for population-commodity type k, $\mathcal{I}_k \subseteq \mathcal{I},\ k \in \mathcal{K}$
Healthcare Commodity Metric Parameters	
r_k	Criticality score of population-commodity type k where one indicates a population-commodity type is highly critical and a value close to zero indicates a population-commodity type is not very critical, $0 < r_k \leq 1, k \in \mathcal{K}$
$q_{k,i}$	Suitability score for fulfilling demand of population-commodity type k with supplier-SKU i, where a score of one indicates a supplier-SKU i is best suited to fulfill demand for population-commodity type k and a value closer to zero indicates low suitability, $0 < q_{k,i} \leq 1, k \in \mathcal{K}, i \in \mathcal{I}_k$
Demand Parameters	
$d_{k,t}$	The projected incoming demand for population-commodity type k during time interval t, $k \in \mathcal{K}, t \in \mathcal{T}$
n_k^{init}	Unfulfilled demand for population-commodity type k at the beginning of the forecasting period, $k \in \mathcal{K}$
Warehouse Capacity Parameters	
h	Warehouse space capacity
s_i	Size per ordering unit of supplier-SKU i, $i \in \mathcal{I}$
Budget and Cost Parameters	
b	Available budget for orders placed during the forecasting period
c_i	Cost per unit of supplier-SKU i, $i \in \mathcal{I}$
Inventory Availability Parameters	
z_i^{init}	Initial inventory of supplier-SKU i at the beginning of the forecasting period, $i \in \mathcal{I}$
$o_{i,t}^{init}$	Units from outstanding orders of supplier-SKU i placed prior to the forecasting period that are expected to arrive during time interval t, $i \in \mathcal{I}, t \in \mathcal{T}$
Supply Parameters	
$cap_{i,t}$	The capacity for supplier-SKU i during time interval t, $i \in \mathcal{I}, t \in \mathcal{T}$
$f_{i,l}$	The fraction of an order from supplier-SKU i that is projected to arrive l time intervals after placing the order, $i \in \mathcal{I}, l \in \{0, \ldots, T\}$

Table 2.2: Sets and input parameters used in the inventory and order management model.

any time interval t where no units of supplier-SKU i are projected to arrive, set $o_{i,t}^{init} = 0$.

The model also considers supply parameters including capacities and lead times for each supplier-SKU. The model can handle supplier-SKU capacities that change over time according to changes in production and workforce through the parameter $cap_{i,t}$, which represents the unit capacity that supplier-SKU i can provide for orders placed during time interval t, for all $i \in \mathcal{I}, t \in \mathcal{T}$. Lead times are represented by the parameter $f_{i,l}$ which represents the fraction of an order from supplier-SKU i projected to arrive l time intervals after the initial order was placed, $i \in \mathcal{I}, l \in \{0, \ldots, T\}$, where $\sum_{l=0}^{T} f_{i,l} \leq 1$, for all $i \in \mathcal{I}$. In the use case example, the entire order placed for non-medical grade KN95 masks from Supplier C ($i = 4$) is projected to arrive in the same time interval after placing the order than, $f_{4,0} = 1$, and $f_{4,t} = 0$ for all $t \in \{1, \ldots, T\}$. However in the use case example, half of the order placed for medical-grade N95 masks from Supplier A ($i = 1$) is projected to arrive in one time interval and the other half is projected to arrive in two time intervals after placing the order so $f_{1,1} = f_{1,2} = 0.5$, and $f_{1,t} = 0$ for all $t \in \{0, 3, \ldots, T\}$. To incorporate uncertainties, lead-time parameters can be interpreted as the probability that an order will arrive within a certain number of time intervals t after placing the order.

The decision variables are defined in Table 2.3. The primary decision variable is $x_{i,t}$ which represents the number of units ordered for supplier-SKU i during time interval t, for $i \in \mathcal{I}$, $t \in \mathcal{T}$. There are also secondary decision variables that are impacted by the primary decision variables. The number of units of supplier-SKU i projected to arrive during time interval t are represented by $y_{i,t}$, for $i \in \mathcal{I}, t \in \mathcal{T}$. The number of units of supplier-SKU i available in the warehouse at the start of the time interval t is represented by $z_{i,t}$, for $i \in \mathcal{I}, t \in \mathcal{T}$. The number of units of unfulfilled demand of population-commodity type k at the start of the time interval t is represented by $n_{k,t}$, for $k \in \mathcal{K}, t \in \mathcal{T}$. The number of units of fulfilled demand for population-commodity type k from supplier-SKU i fulfilled during time interval t is represented by $m_{k,i,t}$, for $k \in \mathcal{K}$, $i \in \mathcal{I}$, $t \in \mathcal{T}$.

Notation	Description
$x_{i,t}$	Units of supplier-SKU i ordered during time interval t, $i \in \mathcal{I}, t \in \mathcal{T}$
$y_{i,t}$	Units of supplier-SKU i projected to arrive during time interval t, $i \in \mathcal{I}, t \in \mathcal{T}$
$z_{i,t}$	Units of inventory of supplier-SKU i available in the warehouse at the beginning of the time interval t, $i \in \mathcal{I}, t \in \mathcal{T}$
$n_{k,t}$	Unfulfilled demand for population-commodity type k at the beginning of time interval t, $k \in \mathcal{K}$, $t \in \mathcal{T}$
$m_{k,i,t}$	Fulfilled demand for population-commodity type k with supplier-SKU i during time interval t, $k \in \mathcal{K}, i \in \mathcal{I}_k, t \in \mathcal{T}$

Table 2.3: Decision variables used in the inventory and order management model.

2.2.2 Healthcare Commodity Metric

The optimization model maximizes the Healthcare Commodity Metric to ensure that the ordering plan generated by the optimization model best meets the goals of reducing the consequences of projected delays and substitutions for multiple population-commodity types that vary in criticality. The Healthcare Commodity Metric is a quantifiable measure with mathematical properties that:

1. Fulfill demand requests with minimal delay,
2. Prioritize fulfillment of demand requests for highly critical population-commodity types, and
3. Fulfill demand requests with the most suitable supplier-SKU available in the warehouse.

The Healthcare Commodity Metric denoted $\Phi_{k,i,t}$ integrates criticality scores r_k, suitability scores $q_{k,i}$, the projected time interval t a demand request is fulfilled, and the total number of time intervals in the forecasting period T for each $k \in \mathcal{K}, i \in \mathcal{I}, t \in \mathcal{T}$. Delay penalties are calculated using a modified version of a present value formula where the relative present value of fulfilling demand at the start of the forecasting period, $t = 1$, is set to $q_{k,i} r_k (1 + r_k)^T$ and the relative discounting rate per time interval t is set to $1/(1 + r_k)$ for population-commodity type k fulfilled with supplier-SKU i. The Healthcare Commodity

Metric is defined as,

$$\Phi_{k,i,t} = q_{k,i}\ r_k(1+r_k)^T \left(\frac{1}{1+r_k}\right)^t. \tag{2.1}$$

Property 1 The Healthcare Commodity Metric decreases as the time to fulfillment increases, thus prioritizing ordering decisions that minimize delay in fulfilling demand requests.

The Healthcare Commodity Metric is higher for population-commodity types associated with higher criticality scores compared to population-commodity types associated with lower criticality scores when fulfilled with a supplier-SKU with the same suitability score over each time interval. Given a criticality score r_k and a suitability score $q_{k,i}$ for a population-commodity type k and supplier-SKU i, the Healthcare Commodity Metric value decreases as delay increases, and is penalized by $1-(1/(1+r_k))$ each time interval that is delayed. To see this, consider the difference between $\Phi_{k,i,t}$ and $\Phi_{k,i,t+1}$ representing the impact of delay of one time interval,

$$\begin{aligned}\Phi_{k,i,t} - \Phi_{k,i,t+1} &= \left(q_{k,i}\ r_k(1+r_k)^T\right)\left(\frac{1}{1+r_k}\right)^t - \left(q_{k,i}\ r_k(1+r_k)^T\right)\left(\frac{1}{1+r_k}\right)^{t+1} \\ &= \left(q_{k,i}\ r_k(1+r_k)^T\right)\left(\frac{1}{1+r_k}\right)^t \left[1-\left(\frac{1}{1+r_k}\right)\right].\end{aligned}$$

Thus the Healthcare Commodity Metric has a greater value earlier in the forecasting period, so when the model maximizes the Healthcare Commodity Metric, it prioritizes fulfilling demand as soon as possible. A delay of n time periods results in further decrease in the Healthcare Commodity Metric, since

$$\begin{aligned}\Phi_{k,i,t} &= q_{k,i}\ r_k(1+r_k)^T \left(\frac{1}{1+r_k}\right)^t \\ &> q_{k,i}\ r_k(1+r_k)^T \left(\frac{1}{1+r_k}\right)^{t+n} = \Phi_{k,i,t+n}\end{aligned}$$

for $1 \le t < t+n \le T$. Thus $1/(1+r_k)$ can be interpreted as a discounting factor.

Property 2 The Healthcare Commodity Metric is higher for population-commodity types associ-

ated with higher criticality scores compared to population-commodity types associated with lower criticality scores when fulfilled with a supplier-SKU with the same suitability score over each time interval.

Consider the Healthcare Commodity Metric for a population-commodity type k with a higher criticality score compared to a population-commodity type $\bar{k}$ associated with a lower criticality score, where $r_k > r_{\bar{k}}$, in any given time interval t. Fixing the suitability score to be the same, $q_{k,i} = q_{\bar{k},i}$, we see that

$$\begin{aligned}\Phi_{k,i,t} &= q_{k,i}\ r_k(1+r_k)^T\left(\frac{1}{1+r_k}\right)^t = q_{k,i}\ r_k(1+r_k)^{T-t} \\ &> q_{\bar{k},i}\ r_{\bar{k}}(1+r_{\bar{k}})^{T-t} = \Phi_{\bar{k},i,t}.\end{aligned}$$

The percent decrease in Healthcare Commodity Metric for one time interval for population-commodity type k of $1-(1/(1+r_k))$ is larger than the delay of one time interval for population-commodity type $\bar{k}$ of $1-(1/(1+r_{\bar{k}}))$, since $r_k > r_{\bar{k}}$ delay penalties are higher for population-commodity types of relatively high criticality, and the Healthcare Commodity Metric prioritizes fulfilling demand for these highly critical population-commodity types relatively quickly.

Property 3 The Healthcare Commodity Metric prioritizes substitutions based on the suitability score $q_{k,i}$ for using the supplier-SKU i to fulfill a demand request for population-commodity k.

The Healthcare Commodity Metric prioritizes ordering decisions that minimize substitutions because $\Phi_{k,i,t}$ decreases as the suitability score $q_{k,i}$ decreases, thus choosing the most suitable supplier-SKU possible. Consider the suitability score $q_{k,i}$ for using the supplier-SKU i to fulfill a demand request for population-commodity k, and a lower suitability score $q_{k,\bar{i}}$ for using the supplier-SKU $\bar{i}$, $q_{k,i} > q_{k,\bar{i}}$. Then $\Phi_{k,i,t} > \Phi_{k,\bar{i},t}$, from the Healthcare Commodity Metric definition in Equation (2.1).

The three mathematical properties summarize the changes in the Healthcare Commodity Metric $\Phi_{k,i,t}$ by varying one element at a time. It is also possible to combine the properties and inves-

tigate the Healthcare Commodity Metric for different critical population and commodities with different suitability scores. Consider a highly critical population-commodity k versus a less critical population-commodity $\bar{k}$, with $r_k > r_{\bar{k}}$. Also suppose that the suitability score $q_{k,i}$ for using the supplier-SKU i to fulfill a demand request for population-commodity k is higher than the suitability score $q_{\bar{k},\bar{i}}$ for using the supplier-SKU $\bar{i}$ to fulfill a demand request for population-commodity $\bar{k}$. Then,

$$\begin{aligned}\Phi_{k,i,t} &= q_{k,i}\ r_k(1+r_k)^T\left(\frac{1}{1+r_k}\right)^t = q_{k,i}\ r_k(1+r_k)^{T-t} \\ &> q_{\bar{k},\bar{i}}\ r_{\bar{k}}(1+r_{\bar{k}})^{T-t} = \Phi_{\bar{k},\bar{i},t}\end{aligned}$$

indicating that the Healthcare Commodity Metric will prioritize using the most suitable supplier-SKU with as little delay as possible for the highly critical population-commodity k. The use case example illustrates some of these tradeoffs.

2.2.3 Formulation

The linear optimization model generates optimal ordering decisions through maximization of the Healthcare Commodity Metric as defined in Equation (2.1) over all time intervals $t \in \mathcal{T}$, population-commodity types $k \in \mathcal{K}$ and supplier-SKUs $i \in \mathcal{I}$ against demand, supply, inventory availability, warehouse capacity and budget constraints. As such, the mathematical formulation is as follows:

$$\max \quad \sum_{k\in\mathcal{K}}\sum_{i\in\mathcal{I}_k}\sum_{t\in\mathcal{T}} \Phi_{k,i,t} m_{k,i,t} \tag{2.2}$$

$$n_{k,1} = n_k^{init} \qquad \forall k \in \mathcal{K} \tag{2.3}$$

$$\sum_{i\in\mathcal{I}_k} m_{k,i,t} - n_{k,t} + n_{k,t+1} = d_{k,t} \qquad \forall k \in \mathcal{K}, t \in \{1,\ldots,T-1\} \tag{2.4}$$

$$\sum_{i\in\mathcal{I}_k} m_{k,i,T} - n_{k,T} \leq d_{k,T} \qquad \forall k \in \mathcal{K} \tag{2.5}$$

$$\sum_{i\in\mathcal{I}} s_i z_{i,t} \leq h \qquad \forall t \in \mathcal{T} \tag{2.6}$$

$$\sum_{i\in\mathcal{I}}\sum_{t\in\mathcal{T}} c_i x_{i,t} \leq b \tag{2.7}$$

$$z_{i,1} = z_i^{init} \qquad \forall i \in \mathcal{I} \tag{2.8}$$

$$z_{i,t-1} + y_{i,t-1} - \sum_{k\in\mathcal{K}} m_{k,i,t-1} - z_{i,t} = 0 \qquad \forall i \in \mathcal{I}, t \in \{2,\ldots,T\} \tag{2.9}$$

$$\sum_{k\in\mathcal{K}} m_{k,i,t} - z_{i,t} - y_{i,t} \leq 0 \qquad \forall i \in \mathcal{I}, t \in \mathcal{T} \tag{2.10}$$

$$x_{i,t} \leq cap_{i,t} \qquad \forall i \in \mathcal{I}, t \in \mathcal{T} \tag{2.11}$$

$$y_{i,t} = \sum_{\substack{\tilde{t}\leq t \\ \tilde{t}\in\mathcal{T}}} f_{i,t-\tilde{t}} x_{i,\tilde{t}} + o_{i,t}^{init} \qquad \forall i \in \mathcal{I}, t \in \mathcal{T} \tag{2.12}$$

$$x_{i,t}, y_{i,t}, z_{i,t}, n_{k,t}, m_{k,i,t} \geq 0 \qquad \forall k \in \mathcal{K}, i \in \mathcal{I}, t \in \mathcal{T} \tag{2.13}$$

The objective function (2.2) maximizes the Healthcare Commodity Metric. Constraints (2.3) – (2.5) are demand constraints. Constraint (2.3) initializes unfulfilled demand for each population-commodity type k. Constraints (2.4) and (2.5) ensure the amount of demand fulfilled is not more than cumulative unfulfilled demand which is equal to incoming demand and unfulfilled demand at the beginning of each time interval. Constraint (2.5) is also used to calculate unfulfilled demand at the beginning of each time interval in the forecasting period. Constraints (2.6) and (2.7) are the warehouse capacity and budget constraints. Constraints (2.8) – (2.10) are inventory availability constraints. Constraint (2.8) initializes available inventory at the beginning of the first time interval. Constraint (2.9) calculates the available inventory at the start of each time interval by setting it equal to beginning inventory minus demand fulfilled plus number of units received in the previous time interval. Constraint (2.10) ensures the amount of stock fulfilled is not more than the available inventory which is equal to beginning inventory plus any orders that arrived in each time interval. Constraints (2.11) – (2.12) are supply constraints. Constraint (2.11) ensures that the unit capacity for each supplier-SKU is respected. Constraint (2.12) calculates the units of each supplier-SKU projected to arrive during each time interval given outstanding placed prior to the forecasting period and new orders placed within the forecasting period. Note that the lead time l, used as a subscript in the parameter $f_{i,l}$, is represented by the number of time intervals between the time interval $\tilde{t}$ when the order is placed, and the time interval t when the order is projected to arrive,

i.e., $l = t - \tilde{t}$. Finally, constraint set (2.13) specifies the non-negative properties of the decision variables.

2.3 Example Use Case: State Masks for All Program

The example use case is built to reflect the scenario and decisions faced by organizations managing inventory for healthcare commodities during the COVID-19 pandemic, such as Utah's Push Pack Program [122]. The use case considers a state-wide program that provides masks to health care providers and businesses in response to a pandemic. The state will generate ordering plans over the next twelve weeks, in line with their budgeting period, for the program. Once a week, the state meets with representatives of the different stakeholders and decision-makers along the supply chain to discuss up-to-date weekly demand estimates, inventory levels, the status of previously placed orders, and resulting updates to the ordering plan, if any. Once all of the updates are discussed, model inputs are updated, model outputs are generated and new orders are placed.

This section illustrates how the model can be used to generate ordering schedules, update ordering schedules in the case of an unexpected situation, and support strategic decision making, such as budgets. Section 2.3.1 describes example input data that relates back to the sets and input parameters described in Table 2.2. Section 2.3.2 presents optimal ordering plans and evaluates subsequent projected fulfillment delay and substitution consequences to illustrate how the model balances these impacts. Section 2.3.3 considers a situation with an unexpected demand surge, increased unit costs, and updated lead time information to illustrate how the model can be used to update ordering plans to support agile decision making. Finally, in Section 2.3.4, budgeting decisions and the subsequent impact on projected fulfillment delay and substitutions are evaluated to illustrate how the model can be used to support collaborative decision making among strategic and operational decision makers.

2.3.1 Description of Input Data

The forecasting period is 12-weeks, $T = 12$, and the time interval t is one week. The state provides masks to health care providers, essential businesses, and non-essential businesses. As such, the state defines three population-commodity types, including masks for health care providers

($k = 1$), masks for essential businesses ($k = 2$), and masks for non-essential businesses ($k = 3$). The state considers supplying masks for health care providers the most critical, masks for essential businesses to be the second most critical, and masks for non-essential businesses to be the least critical. The state represents these priorities through criticality scores, r_k, for each population-commodity type k. The state assigns criticality scores of 1 for masks for health care providers ($r_1 = 1$), 0.4 for masks for essential businesses ($r_2 = 0.4$), and 0.2 for masks for essential businesses ($r_3 = 0.2$). Incoming demand requests, $d_{k,t}$ for each population-commodity type k are estimated over each week t in the forecasting period, where fluctuations in demand may be due to changes to hospitalization, infection rates, and reopening plans. Figure 2.1 describes the current projections for the number of units of incoming demand requests for each population-commodity type per week. At the start of the forecasting period, there is no unfulfilled demand, $n_k^{init} = 0$, for any of the three population-commodity types.

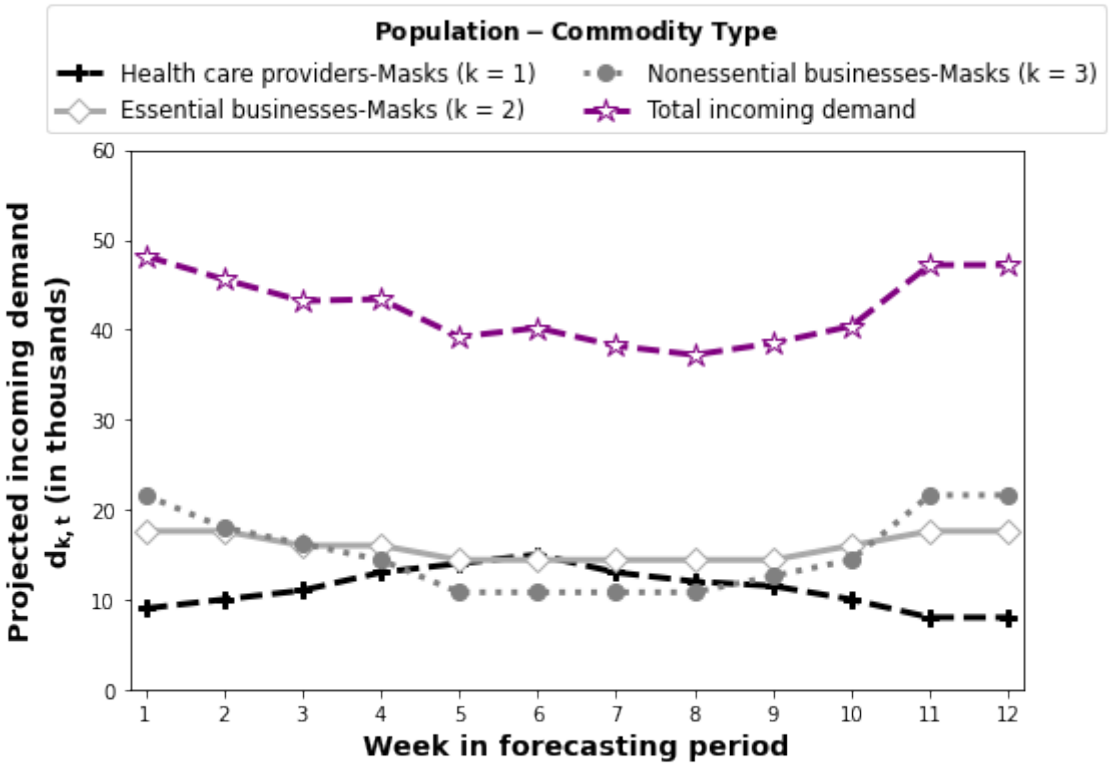

Figure 2.1: Projected weekly incoming demand by population and commodity type.

The state established relationships with three suppliers that provide three different types of masks for a total of four supplier-SKU combinations. Supplier A provides medical-grade N95 masks, Supplier A-N95:MG ($i = 1$), and medical-grade surgical masks, Supplier A-SUR:MG ($i = 3$), Supplier B provides medical-grade N95 masks, Supplier B-N95:MG ($i = 2$), and Supplier C provides non-medical-grade KN95 masks, Supplier C-KN95:NonMG ($i = 4$). All four supplier-SKUs can satisfy demand for masks for essential and non-essential businesses, however only the three medical-grade supplier-SKUs can satisfy demand for masks for health care providers. The state assigns suitability scores, $q_{k,i}$, based on their protective effect. Supplier A-N95:MG ($i = 1$) and Supplier B-N95:MG ($i = 2$) are most suitable to fulfill demand for masks so the state assigns these supplier-SKUs a suitability score of one, $q_{k,1} = q_{k,2} = 1$ for all population-commodity types, $k \in \{1, 2, 3\}$. Supplier A-SUR:MG ($i = 3$) is the second most suitable so the state assigns a suitability score of 0.9, $q_{k,3} = 0.9$ for all population-commodity types, $k \in \{1, 2, 3\}$. Supplier C-KN95:NonMG ($i = 4$) is the least suitable so the state assigns a suitability score of 0.4, $q_{k,4} = 0.4$, for the fitting population-commodity types, $k \in \{2, 3\}$. Notice that Supplier C-KN95:NonMG ($i = 4$) cannot be used to fulfill demand for masks for health care providers.

Table 2.4 describes the unit size, unit cost, capacities, and lead times for each supplier-SKU. While Supplier A-N95:MG ($i = 1$) and Supplier B-N95:MG ($i = 2$) have the same suitability score for all population-commodity types, they vary in costs, capacities, and lead times as described in Table 2.4. For example, Supplier A-N95:MG ($i = 1$) is \$15 cheaper than Supplier B-N95:MG ($i = 2$), however, Supplier A-N95:MG ($i = 1$) has lower weekly capacities of 8,000 units over the entire 12-week forecasting period, $cap_{1,t} = 8,000$ for $t \in \{1, \ldots, 12\}$, whereas Supplier B-N95:MG ($i = 2$) has higher projected weekly capacities of 14,000 units in the first two weeks of the forecasting period, $cap_{2,t} = 14,000$ for $t \in \{1, 2\}$ and is planning to increase their weekly capacities to 18,000 units after week two, $cap_{2,t} = 18,000$ for $t \in \{3, \ldots, 12\}$.

Supplier A-N95:MG ($i = 1$) has projected lead times of one to two weeks, so the state estimates that 50% of the order will arrive one week after the order is placed and the other 50% will arrive two weeks after the order is placed, $f_{1,1} = f_{1,2} = 0.5$. Supplier B-N95:MG ($i = 2$) has projected lead times of three to five weeks, so the state estimates that a third of the order will arrive 3, 4, and 5 weeks after the order was placed, $f_{2,3} = f_{2,4} = f_{2,5} = 0.33$. Supplier C-KN95:NonMG ($i = 4$)

Supplier-SKU set ID	Supplier-SKU name	Unit size	Unit cost	Capacity (thousands)	Lead time (fractional orders)
i		s_i	c_i	$cap_{i,t}$	$f_{i,l}$
1	Supplier A-N95:MG	1	\$20	8 for $t \in \{1, \ldots, 12\}$	0 for $l = 0$ 0.5 for $l = 1$ 0.5 for $l = 2$ 0 for $l \in \{3, \ldots, 12\}$
2	Supplier B-N95:MG	1	\$35	14 for $t \in \{1, 2\}$ 18 for $t \in \{3, \ldots, 12\}$	0 for $l \in \{0, 1, 2\}$ 0.33 for $l = 3$ 0.33 for $l = 4$ 0.33 for $l = 5$ 0 for $l \in \{6, \ldots, 12\}$
3	Supplier A-SUR:MG	1	\$15	25 for $t \in \{1, \ldots, 12\}$	0 for $l = 0$ 0.5 for $l = 1$ 0.5 for $l = 2$ 0 for $l \in \{3, \ldots, 12\}$
4	Supplier C-KN95:NonMG	1	\$4	20 for $t \in \{1, 2\}$ 40 for $t \in \{3, \ldots, 12\}$	1 for $l = 0$ 0 for $\{1, \ldots, 12\}$

Table 2.4: Description of supplier and SKU attributes.

has weekly capacities of $20,000$ units for weeks 1 and 2, $cap_{4,t} = 20,000$ for $t \in \{1, 2\}$ and $40,000$ units thereafter, $cap_{4,t} = 40,000$ for $t \in \{3, \ldots, 12\}$. Supplier C-KN95:NonMG ($i = 4$) are readily available in store and so the associated lead time is zero, $f_{4,0} = 1$.

At the start of the forecasting period, there is no available inventory in the warehouse, i.e., $z_i^{init} = 0$ for all supplier-SKUs, and no incoming orders, i.e., $o_{i,t}^{init} = 0$ for all supplier-SKUs and time intervals. The state has 150,000 cubic feet of warehouse space available and has established a budget of $7 million over the forecasting period.

2.3.2 Generate Ordering Plans

The state ran the optimization model to generate optimal ordering schedules for each week in the 12-week forecasting period under a budget of $7 million and a warehouse capacity of 150,000 cubic feet. As illustrated in Figure 2.2 in the first week the state orders 8,000 units of medical-grade N95 masks from Supplier A, $x_{1,1} = 8,000$, 14,000 units of medical-grade N95 masks from Supplier B, $x_{2,1} = 14,000$, 25,000 units of medical-grade surgical masks from Supplier A, $x_{3,1} = 25,000$ and 20,000 units of non-medical-grade KN95 masks from Supplier C, $x_{4,1} = 20,000$. The model assumes orders will arrive according to the lead time input parameters described in Table 2.4. For example, the lead time input parameters indicate that 50% of an order for medical-grade N95 masks from Supplier A is projected to arrive in one week, and the remaining 50% of the order will arrive in two weeks. So, the optimal ordering schedule for medical-grade N95 masks from Supplier A illustrated in Figure 2.2(a) indicates that of the 8,000 units ordered in week one, 4,000 units will arrive in week two (one week after the initial order was placed) and the remaining 4,000 units ordered will arrive in week three (two weeks after the initial order was placed).

Before placing the orders, the state reviews the projected impacts of the optimal ordering schedule in Figure 2.2 on delays and substitutions. Figure 2.3 illustrates the projected cumulative, total incoming, fulfilled, and unfulfilled demand summed over all population-commodity types for each week in the forecasting period projected as a result of the optimal ordering schedule. As illustrated in Figure 2.3 at the start of the forecasting period, between weeks one to six, there is not enough supply to meet demand. To limit delays, the optimal ordering schedule for Supplier C-KN95:NonMG ($i = 4$), illustrated in Figure 2.2(d), suggests ordering non-medical-grade KN95

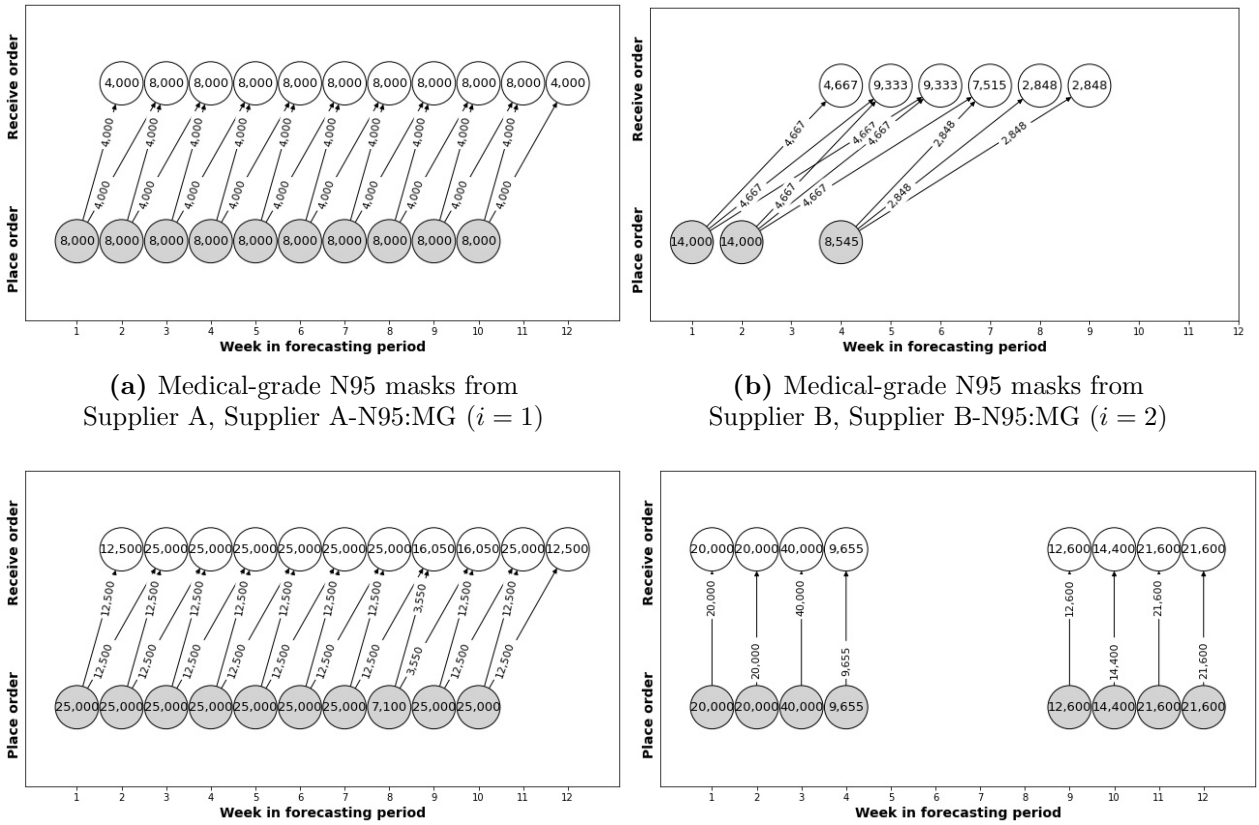

(a) Medical-grade N95 masks from Supplier A, Supplier A-N95:MG ($i = 1$)

(b) Medical-grade N95 masks from Supplier B, Supplier B-N95:MG ($i = 2$)

(c) Medical-grade surgical masks from Supplier A, Supplier A-SUR:MG ($i = 3$)

(d) Non-medical-grade KN95 masks from Supplier C, Supplier C-KN95:NonMG ($i = 4$)

Figure 2.2: Optimal ordering schedules for each supplier and SKU under a budget of $7 million.

masks from Supplier C in the first few weeks until the orders of more suitable supplier-SKUs arrive in the warehouse for distribution. This is in line with the first property of the Healthcare Commodity Metric to fulfill demand requests with minimal delay.

Towards the end of the forecasting period, between weeks nine and twelve, the optimal ordering plan reduces the order for Supplier B-SUR:MG ($i = 2$) and increases the order of Supplier C-KN95:NonMG ($i = 4$) as illustrated in Figure 2.2(b) and Figure 2.2(d) due to budget limitations. Even though the two N95 masks available from the state's suppliers, Supplier A-N95:MG ($i = 1$) and Supplier B-N95:MG ($i = 2$), have the same suitability score for all masks, more units are ordered from Supplier A-N95:MG ($i = 1$) than Supplier B-N95:MG ($i = 2$) because of cost differences. In weeks four to ten, when N95 masks are available, they are distributed; however, when KN95

masks from Supplier C are available, and N95 masks are limited, KN95 masks are used to fulfill demand. This is in line with the third property of the Healthcare Commodity Metric to fulfill demand requests with the most suitable supplier-SKU available in the warehouse.

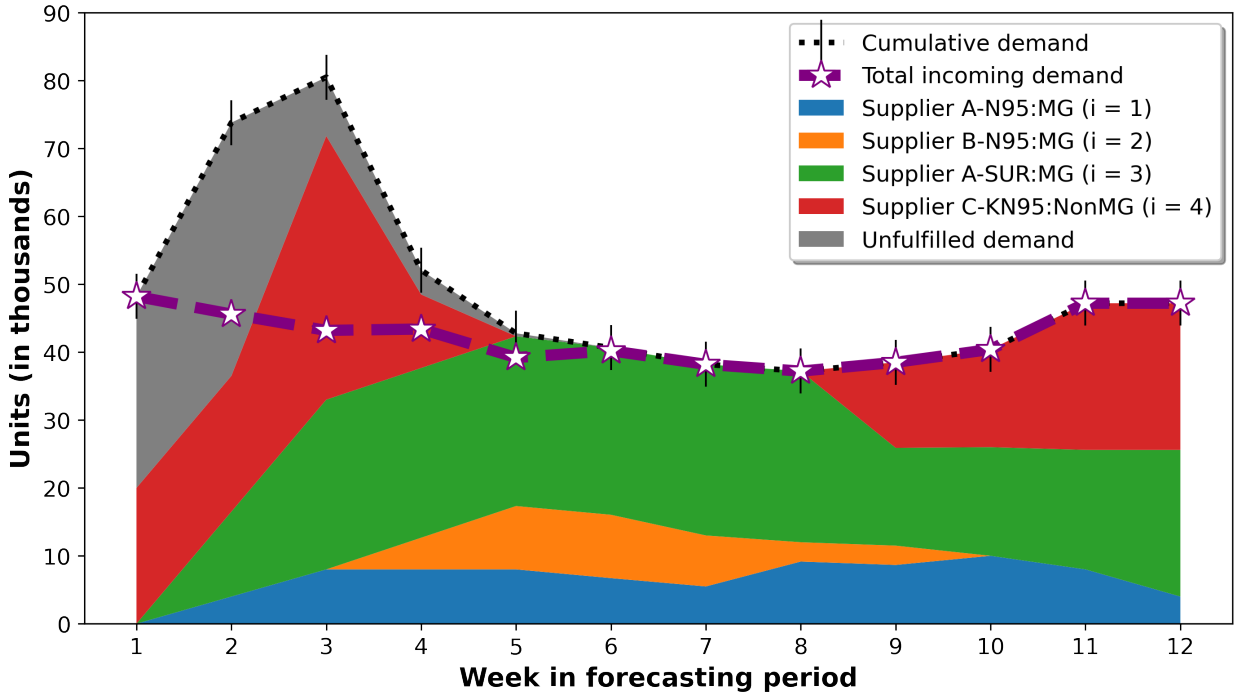

Figure 2.3: The cumulative, total incoming, unfulfilled demand, and fulfilled by each supplier and SKU for each week in the forecasting period summed over all population and commodity types, projected as a result of the optimal ordering schedule, under a budget of $7 million.

Figure 2.4 and Figure 2.5 illustrate the projected impacts of delays and substitutions by population-commodity type summarised over the forecasting period under the optimal ordering schedule. The figures show how the Healthcare Commodity Metric prioritizes fulfillment of demand requests according to their criticality in line with the second property of the Healthcare Commodity Metric. Figure 2.4 illustrates the projected impacts of the optimal ordering schedule on delays by summarising the percent of incoming demand requests delayed by one week and two weeks or more by population-commodity type. As shown in Figure 2.4, masks for healthcare providers ($k = 1$) are prioritized in terms of minimizing delay, as they have the lowest projected percentage of incoming demand delayed by one week at 8% and two weeks or more at 0% compared

to the less critical population-commodity types, masks for essential businesses ($k = 2$), and masks for non-essential businesses ($k = 3$).

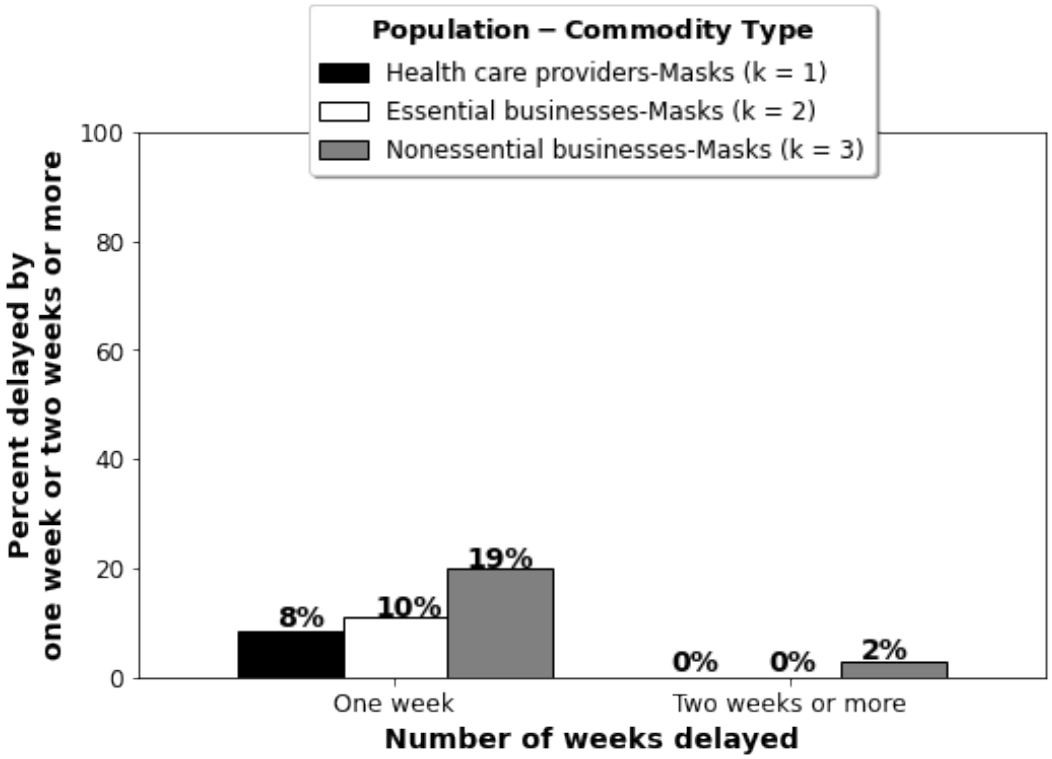

Figure 2.4: Projected percent of demand requests delayed by one week and two weeks or more by population and commodity type, as a result of the optimal ordering schedule, to illustrate prioritization in terms of *delays*.

Figure 2.5 illustrates the projected impacts of the optimal ordering schedule on substitutions by summarising the percent of incoming demand requests fulfilled by each supplier-SKU by population-commodity type. As shown in Figure 2.5, masks for healthcare providers ($k = 1$) are also prioritized in terms of minimizing substitutions, as 83% of demand for masks for health care providers ($k = 1$) are projected to be fulfilled by the supplier-SKUs with the highest suitable scores, Supplier A - N95:MG masks ($i = 1$) and Supplier B - N95:MG masks ($i = 2$), while less than 2% of demand for masks for essential businesses ($k = 2$) and 0% of demand for masks for non-essential businesses ($k = 3$) are projected to be fulfilled the most suitable supplier-SKUs.

Using similar logic it is clear from Figure 2.4 and Figure 2.5 that the second-most critical

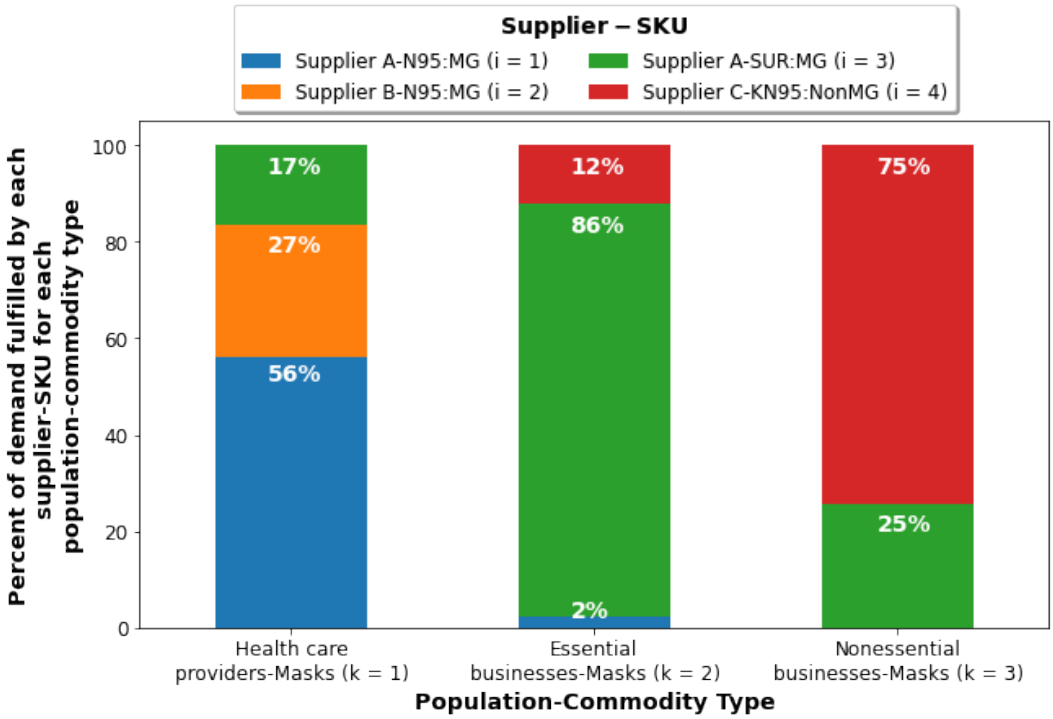

Figure 2.5: The projected percent of demand requests fulfilled by each supplier and SKU by population and commodity type, as a result of the optimal ordering schedule, to illustrate prioritization in terms of *substitutions*.

population-commodity type, masks for essential businesses ($k = 2$), is prioritized over the least critical population-commodity type, masks for non-essential businesses ($k = 3$). As shown in Figure 2.5, no non-medical grade KN95 masks from Supplier C, Supplier C-KN95:NonMG ($i = 4$), are used to fulfill the demand for health care providers because the state specified it is not fitting to do so.

2.3.3 Update Ordering Schedule given a Demand Surge and Increased Unit Costs

Suppose in the second week of the forecasting period, up-to-date information revealed changes in demand projections, unit supply costs, and projected arrival of an incoming order. Orders have already been placed and received in the first week of the forecasting period, however, the state has

the opportunity to update ordering plans and to employ the model to re-optimize ordering plans between weeks two and twelve to account for the impact of these changes.

Specifically, up-to-date information revealed an increase in demand projections for masks for health care providers ($k = 1$), while demand projections for masks for essential businesses ($k = 2$) and non-essential businesses ($k = 3$) stayed the same. Updated demand projections for masks for health care providers ($i = 1$) and resulting total incoming demand are shown in Figure 2.6. Supplier B increased the cost per unit for their medical-grade N95 masks, Supplier B-N95:MG ($i = 2$), from \$35 to \$45, and the entire order placed for 8,000 units medical-grade N95 masks from Supplier A, Supplier A-N95:MG ($i = 1$) is now projected to arrive in week two.

To re-optimize the ordering plans for weeks two through 12, the state updated input parameters in the model according to the most up-to-date information. The demand parameters for health care providers are updated, $d_{1,t}$ for $t \in \{2, \ldots, 12\}$. In the first ordering period, \$1.365 million dollars of the \$7 million dollar budget was used so the remaining budget is \$5.635 million dollars, $b = 5,635,000$. The cost for a unit of supplier-SKU, Supplier B-N95:MG ($i = 2$) is updated to reflect the increased cost, $c_2 = 45$. All initialization parameters for unfulfilled demand (n_k^{init}), inventory levels (z_i^{init}), and projected arrivals of outstanding orders ($o_{i,t}^{init}$) are updated to reflect the their status at the start of week two in the forecasting period. There are no other changes, so all other model parameters stay the same.

The updated optimal ordering schedule for each Supplier-SKU is illustrated in Figure 2.7. Orders previously placed and received in the first week of the forecasting period are highlighted in black. The update to the expected arrival of the 8,000 units placed for Supplier A-N95:MG ($i = 1$) in week two are reflected in Figure 2.7(a). The ordering schedule for Supplier A-N95:MG ($i = 1$) stays the same, however there are modifications to the ordering schedules for the other three supplier-SKUs. For example, there is an increase in the number of units ordered of Supplier-SKU Supplier B-N95:MG ($i = 2$) in weeks two and three, to meet increased demand for masks for health care providers ($k = 1$). The increased order for Supplier B-N95:MG ($i = 2$) results in a decreased order for Supplier A-SUR:MG ($i = 3$) after week five, due to budget limitations. To alleviate delays in fulfilling demand from reduced orders of Supplier A-SUR:MG ($i = 3$) the optimal ordering schedule increases orders for Supplier C-KN95:NonMG ($i = 4$) after week five.

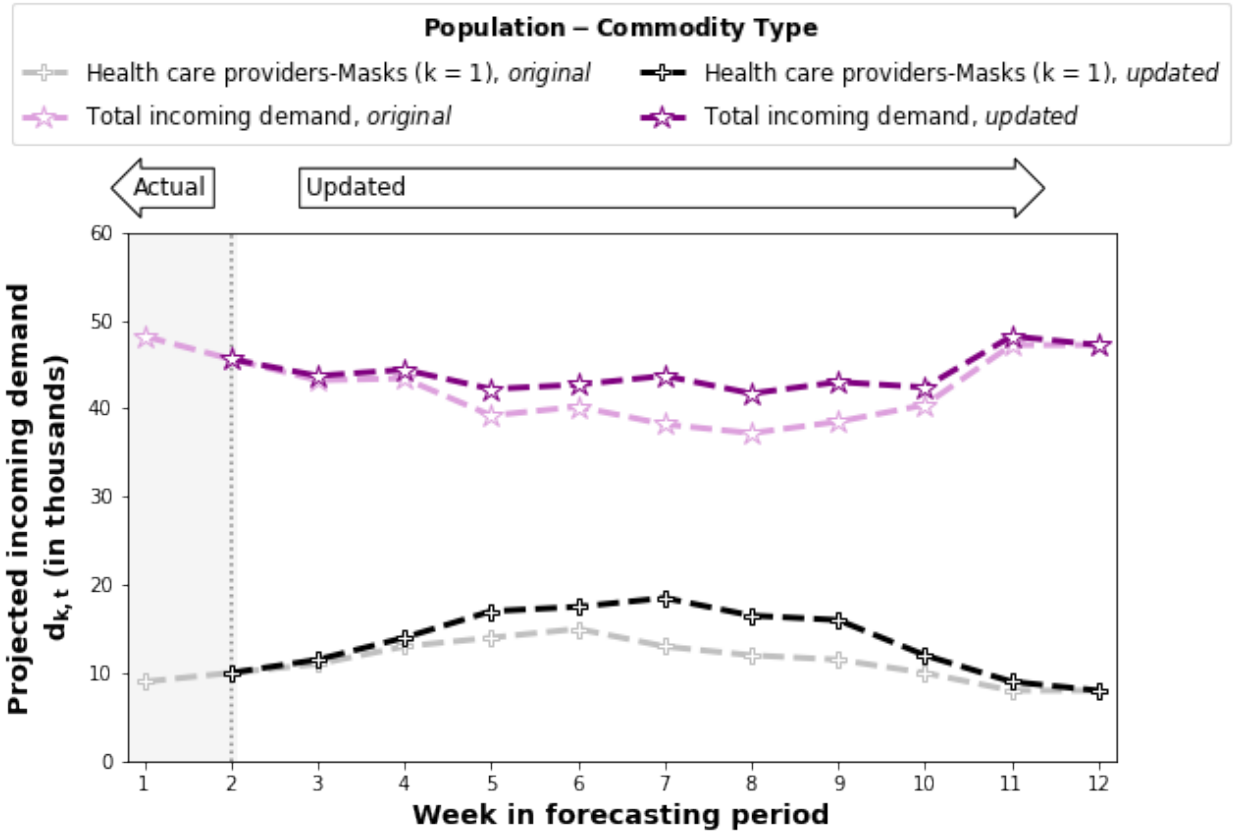

Figure 2.6: Updated projected weekly demand for masks for health care providers and total incoming demand for masks for all populations, compared to original projections. The surge in demand is evident in weeks 5-9.

Figure 2.8(a) represents the projected impact of re-optimized ordering schedules on overall delays and substitutions under revised demand and costs. While as illustrated in Figure 2.3 a budget of $7 million is adequate to satisfy all incoming demand for masks under the original demand projections and unit costs, as illustrated in Figure 2.8(a) under the updates it is projected that there will be not enough supply to satisfy demand by week 10.

2.3.4 Evaluate the Impacts of Budgeting Decisions

The state wants to evaluate the budget's impact on delays, substitutions, and unsatisfied demand under updated demand projections and unit costs at the end of the forecasting period. Fig-

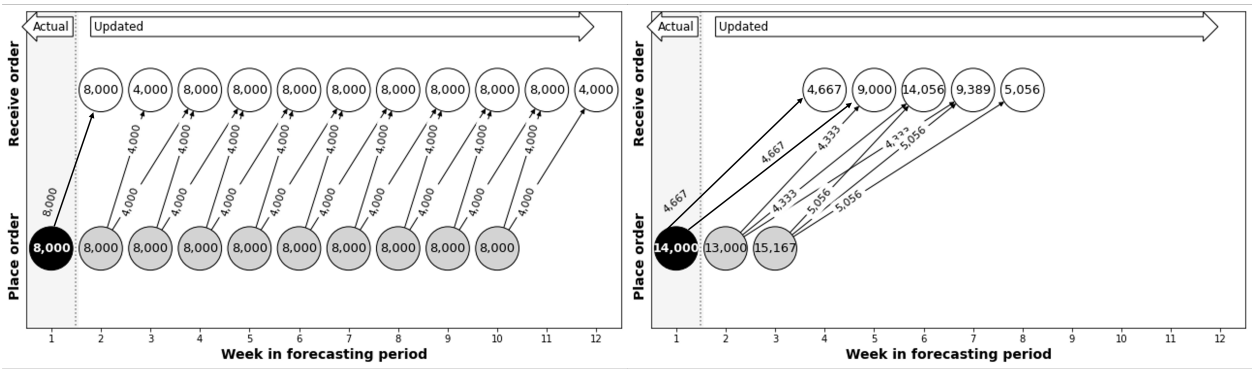

(a) Medical-grade N95 masks from Supplier A, Supplier A-N95:MG ($i = 1$)

(b) Medical-grade N95 masks from Supplier B, Supplier B-N95:MG ($i = 2$)

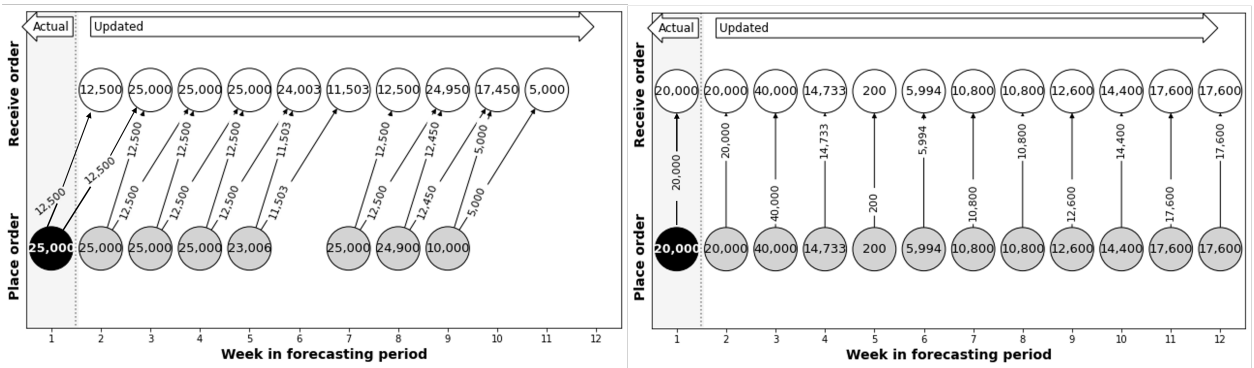

(c) Medical-grade surgical masks from Supplier A, Supplier A-SUR:MG ($i = 3$)

(d) Non-medical-grade KN95 masks from Supplier C, Supplier C-KN95:NonMG ($i = 4$)

Figure 2.7: Updated ordering schedules for each supplier and SKU under a budget of $7 million. Orders previously placed and received in the first week of the forecasting period are highlighted in black.

ure 2.8 evaluates the cumulative, total incoming, unfulfilled demand, and fulfilled by supplier-SKU for each week in the forecasting period summed over all population-commodity types, under revised demand and costs, under a budget of $7, $8 and $9 million. The model projects that increasing the budget from $7 to $8 million will eliminate unfulfilled demand at the end of the forecasting period and increase the proportion of demand requests for masks fulfilled by the most suitable supplier-SKUs. An increase in the budget from $8 million to $9 million provides enough funds for the state to increase the number of N95 masks they can order from Supplier B to reduce the proportion of fulfilled demand for masks substituted with KN95 masks from Supplier C. However,

if they choose to order more N95 masks from Supplier B and fewer KN95 masks from Supplier C, it is projected that there will be a slight increase in delay of fulfilling demand. The Healthcare Commodity Metric in the optimization model selects ordering the N95 medical grade masks with a slight delay in fulfilling demand.

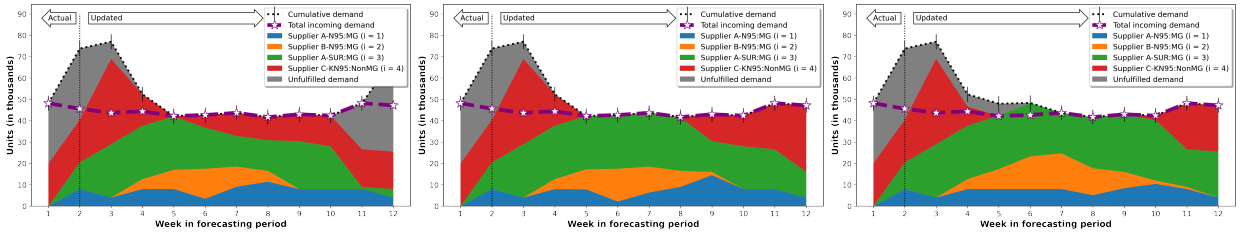

(a) Budget of $7 million **(b)** Budget of $8 million **(c)** Budget of $9 million

Figure 2.8: The cumulative, total incoming, fulfilled, and unfulfilled demand for each week in the forecasting period summed over all population and commodity types, for re-optimized ordering schedules under revised demand and costs, and various budget options.

Figure 2.9 illustrates the projected percent of incoming demand requests by population-commodity type delayed by one week and two weeks or more with budgets of $7, $8, and $9 million. Figure 2.10 shows the projected percent of incoming demand requests by population-commodity type fulfilled by each supplier-SKU under revised demand and costs and budgets of $7, $8, and $9 million. The model projects that under an optimized ordering schedule increasing the budget from $7 to $8 million will reduce delays for masks for non-essential businesses ($k = 3$) but will have no impact on delays on fulfilling the demand for masks for health care providers ($k = 1$) or masks for essential businesses ($k = 2$). However, as shown in Figure 2.10 the model projects that increasing the budget from $7 to $8 million will improve the suitability of supplier-SKUs used to fulfill the demand for all population-commodity types. As illustrated in Figure 2.9(c) it is projected that under a re-optimized ordering schedule the increased delays seen in Figure 2.8 will only impact the proportion of masks for nonessential businesses ($k = 3$) delayed by one week and will not impact delays in fulfilling demand for masks for healthcare providers ($k = 1$) or masks for essential businesses ($k = 2$). However, it will further improve the suitability of supplier-SKUs used to fulfill the demand for all population-commodity types.

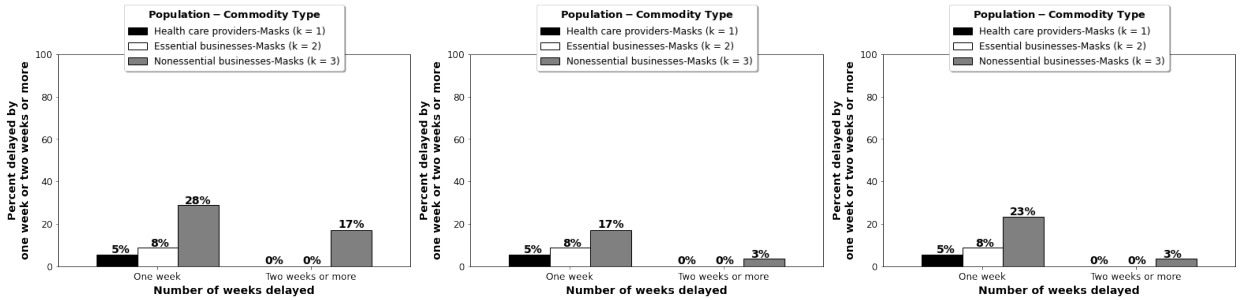

(a) Budget of $7 million **(b)** Budget of $8 million **(c)** Budget of $9 million

Figure 2.9: Projected percent of incoming demand requests by population and commodity type delayed by one week and two weeks or more, as a result of re-optimized ordering schedules, under revised demand and costs, and various budget options.

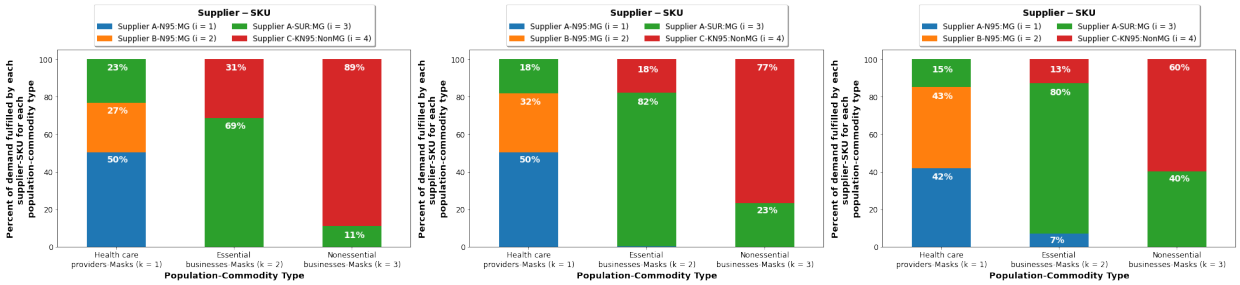

(a) Budget of $7 million **(b)** Budget of $8 million **(c)** Budget of $9 million

Figure 2.10: Projected percent of fulfilled demand satisfied by each supplier and SKU by population and commodity type, as a result of re-optimized ordering schedules, under revised demand and costs, and various budget options.

2.4 Discussion

This research was motivated by the gap in modeling approaches for inventory and order management in a pandemic context. It addresses three research questions. *To address the first question*, I discussed challenges and objectives faced by the collaborators during the COVID-19 pandemic, and related these experiences to published research articles and reports.

To address the second research question, we developed an optimization model that addresses these unique challenges and objectives. For example, a unique challenge addressed is how to fulfill demand requests with minimal delays and allow substitutions when the delay is too long. The

introduction of a Healthcare Commodity Metric provides a quantifiable measure to tradeoff delays with substitutable commodities when inventory is limited, as illustrated in Figure 2.3. This same metric also addresses the critical populations to target for priority fulfillment. Given limited and uncertain availability of commodities, the prioritization in terms of delays and substitutions is met with the approach. Figures 2.4 and 2.5 illustrate the impacts of prioritization.

To address the third research question, scenarios faced by organizations managing inventory for healthcare commodities during a pandemic that require model agility and collaboration are presented. To support agile decision-making, a situation with an unexpected demand surge, increased unit costs, and updated lead time information is presented to illustrate how the model can be used to update ordering plans. To illustrate collaborative decision-making, this chapter presents an evaluation of budgeting decisions at a strategic level and discusses the operational impact on projected fulfillment delay and substitutions.

There are several assumptions and limitations of the proposed model. It assumes there is a distinct number of time intervals (e.g., weeks, days) when orders are placed, orders arrive, and demand is fulfilled. It also assumes if demand is not fulfilled when requested, it can be fulfilled at a later time interval or substituted with a comparable supplier-SKU. The model implements uncertain lead times by creating partial orders. It does not consider incoming demand outside of the forecasting period, however, the model could be solved over a rolling forecasting horizon if the user wants to extend the forecasting period. It assumes the user knows initial unfulfilled demand, inventory levels, and projected arrivals of outstanding orders and can reasonably project demand and supply parameters.

2.5 Conclusion and Future Work

This work submitted for publication in Feburary, 2022 to Annals of Operations Research introduces an optimization model that generates ordering plans that balance the negative impacts of delays and substitution for a set of healthcare commodities and populations that vary in criticality. It allows the fulfillment of the demand for a healthcare commodity and population type from multiple supplier-SKUs as appropriate to reduce delays in fulfilling healthcare commodities requests but considers the impacts of substitutions through a user-specified suitability score. It considers the

relative consequences of delays and substitutions for each healthcare commodity and population type by allowing the user to specify a criticality score. This chapter introduces a new Healthcare Commodity Metric used in the objective function of the optimization model to balance the relative impacts of delays and substitutions according to each healthcare commodity and population's criticality.

The optimization model considers the challenges exacerbated by a pandemic, including demand and supplier-SKU unit capacities that change over time and lead-time uncertainties. The model can be updated and re-optimized to reflect up-to-date information on projected demand, unfulfilled demand, inventory levels, lead times, unit costs, and supplier capacities as the situation changes. The optimization model can inform ordering, budgeting, and warehouse capacity decisions iteratively under the same set of metrics to allow coordinated changes in strategic and operational decisions as needed. As such, the model supports an agile and collaborative approach to inventory and order management decisions required in a constantly changing situation, such as a pandemic. This chapter illustrates how the optimization model can support operational and strategic decisions through a use case example built to reflect the various situations during the COVID-19 pandemic faced by organizations managing inventory and orders for healthcare commodities.

There are several future research directions worth investigating. The model does not account for dynamic pricing due to constant changes in demand and supply. It also does not account for possible re-use of items (supplier-SKUs). It does not consider shipping costs or reduced prices from bulk orders to keep the model linear for simplicity. Regarding model extension, it would be interesting to develop an approach that integrates other supply chain management functions (e.g., final-mile distribution) to reduce decision-making silos even further.

Chapter 3

DYNAMIC TRANSMISSION COMPARTMENTAL MODELS OF TB AND HIV DISEASE PROGRESSION

This chapter presents two versions of a dynamic transmission compartmental model that describes tuberculosis (TB) and HIV disease progression. The models presented in this chapter consider the health implications of TB and HIV co-infection and are designed to measure the effects of increased uptake of antiretroviral therapy (ART) and TB preventive therapy (TPT) with isoniazid on TB- and HIV-related health outcomes. Version one of the model is used to project health outcomes and costs under three care delivery programs in KwaZulu-Natal, South Africa. The first version of the model is provided in the appendix of a paper that was submitted for publication to the Journal of the International AIDS Society in May 2023, and is currently under second revision. A preprint appears in [117]. Version two is modified from version one for better generalizability across the nine provinces of South Africa. Version two of the model is in the appendix of the manuscript submitted to the Health Care Management Science Journal in October 2023.

To guide the development of two versions of the dynamic transmission model of TB and HIV disease, I collaborated with a team of epidemiologists and health economists to identify key dynamics and uncertainties involved in modeling TB and HIV disease progression and regional differences. The factors that describe TB and HIV disease progression considered in the model include, but are not limited to, the implications of TB- and HIV-co-infection, TB drug resistance, recent and remote latent TB infections, and gender differences. Regional differences include HIV incidence, TB effective contact rates, delays in TB treatment, mortality rates, ART coverage, and TPT initiation. Furthermore, through these collaborations, we identified the key health outcomes and program costs that could be estimated from the model outputs needed to aid decision makers and stakeholders in their final program decisions. These key health outcomes include, but are not limited to TB incidence, HIV prevalence, TB- and HIV-related mortality, and disability-adjusted life years.

The rest of the chapter is organized as follows. Section 3.1 provides background and an overview of the TB and HIV dynamic transmission model. Section 3.2 to Section 3.7 provides a description and equations for the two versions of the model. Section 3.2 provides the model compartments. Section 3.3 provides the model transitions. Section 3.4 provides calculations for time-varying parameters impacted by population states. Section 3.5 provides the differential equations that describe TB and HIV progression. Section 3.6 describes how the model is executed. Section 3.7 describes the program health outcomes and costs generated from model outputs. Finally, Section 3.8 provides input parameters, and Section 3.9 provides the conclusion and future work.

3.1 Introduction and Background

People living with HIV (PLWH) are at increased risk of progression to active TB disease and dying while infected with TB due to their weakened immune systems from HIV disease [2, 12, 23, 96, 101, 103, 158]. Antiretroviral therapy (ART) is used to treat HIV and reduces the risk of progression to active TB disease and dying while infected with TB [134]. TB preventative treatment (TPT), when given with ART, further reduces the risk of progression to active TB disease [116]. ART and TPT are both part of the recommended care for people living with HIV. As a result, ART and TPT care are often integrated in regions where the burden of TB and HIV co-infection is high [50]. However, not all people living with HIV receive ART or TPT care [50]. Community-based ART with TPT care delivery programs that extend beyond standard facility-based care have been shown to increase uptake of ART and TPT but are often more costly than standard facility-based care [16, 47, 75, 117]. Assessing the impact of community-based ART with TPT care delivery programs involves critical considerations such as TB and HIV co-infection, gender differences, TB drug resistance, and regional differences.

This chapter presents two versions of a dynamic transmission compartmental model of TB and HIV disease. The model is designed to evaluate the impact of implementing community-based ART with TPT care delivery, compared to standard facility-based ART and TPT care. The model considers critical factors and aims to provide a better understanding of regional disease dynamics to support stakeholders and decision makers in policy decisions.

Model parameters are drawn from a community-based ART initiation and resupply trial in

sub-Saharan Africa (Delivery Optimization for Antiretroviral Therapy, DO ART) [16] and other scientific literature. Model parameters are calibrated and reflect regional targets in TB incidence, HIV prevalence, and TB- and HIV-related mortality from the 2019 Global Burden of Disease Study (GBD 2019) [44]. The model projects health outcome metrics related to TB and HIV mortality, TB and HIV prevalence, TB incidence, and disability-adjusted life years (DALYs) based on population states and transition rates. DALYs represent the years of life lost (YLL) and years lived with disability (YLD) from TB and HIV disease.

The first version of the dynamic transmission compartmental model is applied to KwaZulu-Natal, South Africa, under three care delivery programs presented in Chapter 4. The second version of the dynamic transmission compartmental model is modified for generalizability to simulate TB and HIV disease progression among 100,000 adults ages 15-59 in all nine provinces in South Africa under two care delivery programs. Model outputs are proportionally weighted by population estimates from GBD 2019 [44] and integrated into a budget allocation approach as described in Chapter 5. In this chapter, I highlight the differences between these two versions of the model, including model compartments, transition, equations, and execution.

3.2 Model Compartments

Section 3.2.1 and Section 3.2.2 present the model compartments considered in the first and second versions of the model, respectively.

3.2.1 Version One: Model Compartments

Version one of the dynamic transmission compartmental model considers eight TB compartments, two TB drug resistance (DR) compartments, four HIV compartments, and two gender compartments. Version one of the dynamic transmission model is applied to a policy analysis that evaluates three care delivery programs in KwaZulu-Natal, South Africa presented in Chapter 4.

Set of Tuberculosis (TB) Compartments

Version one of the model consists of eight TB compartments. TB compartments consist of uninfected, latent TB infection (LTBI), active TB, and recovered/treated TB compartments. LTBI

compartments not associated with individuals treated with TPT are separated into recent (less than two years since exposure) and remote (at least two years after exposure to TB) to account for the difference in risk of progression [31, 38, 45, 79].

Uninfected and LTBI compartments are tracked by those who are on TPT and those not on TPT. Those who are on TPT benefit from a reduced risk of infection (or reinfection). Those with LTBI who are on TPT or have completed their course of TPT benefit from a reduced risk of progression to active TB after completion of TPT [4, 116, 137]. Those with LTBI, on TPT, and LTBI after TPT are not differentiated by recent or remote infection and progress to active TB at a rate that considers a regional-specific estimation of the proportion of the LTBI population infected recently or remotely. Let TB' denote the set of eight TB compartments containing the following elements:

1. Uninfected, not on TPT
2. Uninfected, on TPT
3. LTBI, infected recently (exposed within the past two years)
4. LTBI, infected remotely (exposed more than two years ago)
5. LTBI, on TPT
6. Active TB
7. Recovered/Treated
8. LTBI, after TPT

Set of Tuberculosis Drug Resistance (DR) Compartments

The model differentiates drug-susceptible TB (DS TB) and multidrug-resistant TB (MDR TB) infections. MDR TB is defined as resistant to treatment with isoniazid and rifampicin. Uninfected individuals on TPT have a reduced risk of acquiring DS LTBI, but the model assumes no reduced risk of acquiring MDR LTBI [37]. Individuals with DS LTBI on TPT have a reduced risk of progression to active TB, but the model assumes those with MDR LTBI on TPT do not benefit from a reduced risk of progression to active TB [2, 12, 23, 134, 135, 158]. The set of two DR compartments, denoted DR, contains the following elements:

1. Drug-susceptible (DS)
2. Multidrug-resistant (MDR)

For individuals who are uninfected, it is not possible to distinguish by DR status, so all uninfected individuals are assigned to DR compartment 1. Only individuals with DS LTBI gain the benefits of TPT. As such, in the first version of the model, the possible combinations of TB and DR compartments are:

- TB compartment 1, DR compartment 1 only
- TB compartment 2, DR compartment 1 only
- TB compartment 3, both DR compartments 1 and 2
- TB compartment 4, both DR compartments 1 and 2
- TB compartment 5, DR compartment 1 only
- TB compartment 6, both DR compartments 1 and 2
- TB compartment 7, DR compartments 1 and 2
- TB compartment 8, both DR compartment 1 only

Set of HIV Compartments

The model consists of four HIV compartments, which include people living without HIV, people living with HIV (PLWH) with CD4>200, PLWH with CD4$\leq$ 200, and PLWH taking ART (any CD4 count). These HIV compartments are differentiated by their relative transmissibility of TB, risk of progression from LTBI to active TB, duration of active TB and mortality rates [2, 12, 23, 56, 80, 96, 101, 103, 134, 135, 158]. Only PLWH are eligible to initiate ART, and only those on ART initiate TPT treatment [16]. PLWH are eligible for TPT regardless of LTBI infection status, reflecting guidance that TPT should not be delayed among PLWH for lack of available LTBI testing. PLWH not on ART are distinguished by CD4 count to account for increased risk of progression from LTBI to active TB, duration of active TB, and mortality rates for those with lower CD4 counts. The set of four HIV compartments, denoted HIV, contains the following elements:

1. HIV–
2. HIV+, not on ART, CD4 $>$ 200
3. HIV+, not on ART, CD4 $\leq$ 200
4. HIV+, and on ART

Set of Gender Compartments

The model consists of two gender compartments, denoted G, that are differentiated by the rate of ART and TPT initiation, HIV incidence, CD4 decline, effective contact rates, and mortality rates [52, 53, 73, 78, 118, 124]. The set of two gender compartments, denoted G, contains the following elements:

1. Male
2. Female

Set of Regions and Programs

The model considers a set of regions, denoted $\mathcal{I}$, and a set of programs, denoted $\mathcal{P}$. The specific set of regions and programs considered in the program analysis application are provided in Chapter 4.

3.2.2 Version Two: Model Compartments

Version two of the dynamic transmission compartmental model considers the same DR, HIV, and gender compartments as version one of the model; however, version two includes seven TB compartments that differ from the first version of the model to allow for better generalizability of the impact of TPT across regions. The second version of the dynamic transmission compartmental model is used in the budget allocation application to project health outcomes across the nine regions of South Africa under two care delivery programs presented in Chapter 5.

Set of TB Compartments

Version two of the model consists of seven TB compartments. In version two of the model, those

with LTBI treated with TPT are categorized by recent and remote infection. The reduced risk of progression from those who are LTBI and treated with TPT is modeled with a parameter that diminishes the rate of progression for those with recent and remote LTBI. However, for simplicity, version two of the model, does not account for reduced risk of infection (or re-infection) while on TPT. This is a reasonable assumption because under version one of the model, the health benefits from reduced risk of infection (or re-infection) while on TPT were minimal for the modeled six-month course of TPT; however, for a longer course of TPT, this might not be a reasonable assumption. Therefore, if individuals uninfected with TB (in TB compartment 1) start taking TPT, they remain in TB compartment 1 and gain no benefits from TPT. Individuals with LTBI treated with TPT immediately gain the full benefits of reduced risk of progression to active TB and enter a post-TPT compartment; however, they do not gain benefits from reduced risk of reinfection from TPT. Let TB'' denote the set of seven TB compartments containing the following elements:

1. Uninfected
2. LTBI, infected recently, no TPT
3. LTBI, infected remotely, no TPT
4. LTBI, infected recently, post-TPT
5. LTBI, infected remotely, post-TPT
6. Active TB
7. Recovered/Treated

Similar to version one, for individuals who are uninfected, it is not possible to distinguish by DR status, so all uninfected individuals are assigned to DR compartment 1. Only individuals with DS LTBI gain the benefits of TPT. As such, in the second version of the model, the possible combinations of TB and DR compartments are:

- TB compartment 1, DR compartment 1 only
- TB compartment 2, both DR compartments 1 and 2
- TB compartment 3, both DR compartments 1 and 2

- TB compartment 4, DR compartment 1 only
- TB compartment 5, DR compartment 1 only
- TB compartment 6, both DR compartments 1 and 2
- TB compartment 7, both DR compartments 1 and 2

Set of Regions and Programs

The model considers a set of regions, denoted $\mathcal{I}$, and a set of programs, denoted $\mathcal{P}$. The specific set of regions and programs considered in the budget allocation application are provided in Chapter 5.

3.3 Model Transitions

The total population in TB compartment t, DR compartment r, HIV compartment h, and gender compartment g at time τ in region i under program p is defined as $N^{i,p}_{t,r,h,g}(\tau)$. The descriptions of transitions in version one and version two of the model are provided in Section 3.3.1 and Section 3.3.2, respectively.

The description and notation for the parameters used in versions one and two of the dynamic transmission model are summarized in Table 3.1. The parameters that are directly impacted by care delivery programs (ART and TPT initiation rates) are highlighted in green in Table 3.1. The parameters that are indirectly impacted by care delivery programs (TB and HIV incidence) are highlighted in blue in Table 3.1.

Time-varying parameters are indicated by τ. The time-varying parameters that are calculated using the population states $N^{i,p}_{t,r,h,g}(\tau)$, specifically TB force of infection rates for populations in DR compartment r at time τ, $\lambda^{i,p}_r(\tau)$, ART initiation rates for gender g, $\eta^{i,p}_{2,4,g}(\tau)$ and $\eta^{i,p}_{3,4,g}(\tau)$, and the total population entering the model, $B^{i,p}(\tau)$, are calculated using the equations defined in Section 3.4. The remaining time-varying parameters are input parameters as described in Section 3.8.

Most parameters are the same for both versions of the model; however, the five parameters that differ are highlighted in red in Table 3.1. The rate of moving off of TPT per year (ω) is only applicable to version one of the model since version two of the model does not track individuals

on TPT. The partially protective effect of TPT against acquiring a DS TB infection (ι_r) is only applicable to version one of the model since version two of the model does not account for the reduced risk of infection while on TPT. In both versions of the model, those with LTBI not treated with TPT are distinguished by recent and remote infection. However, in version one, those with LTBI treated with TPT (on or after TPT), are not distinguished by recent or remote infection and progress at a rate of $\pi^i_{on\_TPT\_prog}$ and $\pi^i_{after\_TPT\_prog}$, for region i, respectively. Whereas in version two of the model those with LTBI treated with TPT, are distinguished by recent or remote infection, and the base rate of TB progression from LTBI to active TB is reduced with the parameter χ, $0 < \chi < 1$.

Notation	Description
	Parameters that Impact TB Force of Infection
$\lambda_r^{i,p}(\tau)$	TB force of infection for populations in DR compartment r at time τ for region i under program p.
ι_r	Diminished risk of acquiring a latent TB infection for those exposed to DS TB while on TPT, such that $0 < \iota_1 < 1$ and $\iota_2 = 1$ (only applicable in version one of the model.
ξ	Increased risk of reinfection after recovery/treatment of active TB.
ζ	Partially-protective effect of LTBI against acquiring a new TB infection
ω	Rate of moving off of TPT, per year (only applicable in version one of the model).
	Parameters that Describe TB Progression
γ_r	Indicator to reflect that those infected with DS LTBI ($r = 1$) yield benefits of TPT ($\gamma_1 = 1$), whereas those with MDR LTBI ($r = 2$) do not yield benefits of TPT ($\gamma_2 = 0$).
π_{recent_remote}	Rate of TB progression from recent LTBI to remote LTBI, per year.
π_{recent_prog}	Rate of TB progression from recent LTBI to active TB, per year.
π_{remote_prog}	Rate of TB progression from remote LTBI to active TB, per year.

Continued on next page

Table 3.1 – continued from previous page

Notation	Description
θ_h	Relative risk for TB progression from LTBI to active TB by HIV compartment h, where those who are HIV negative ($h = 1$) progress at the base rate, $\theta_1 = 1$, and θ_h for $h \in \{2, 3, 4\}$ accounts for an increased risk of TB progression, $\theta_h > 1$.
χ	Relative risk of TB progression for those with LTBI treated with TPT, $0 < \chi < 1$ (only applicable in version two of the model).
$\pi_{recover}$	Rate of recovery/treatment from active TB, per year.
$\pi_{relapse}$	Rate of relapse from recovered/treated to active TB, per year.
$\pi^i_{on\_TPT\_prog}$	Rate of TB progression from LTBI on TPT to active TB per year in region i (only applicable in version one of the model).
$\pi^i_{after\_TPT\_prog}$	Rate of TB progression from LTBI after TPT to active TB, per year in region i (only applicable in version one of the model).
υ^i_h	Relative reduction of recovery/treatment rate by HIV compartment h in region i, $0 < \upsilon^i_h \leq 1$.
$\kappa^{i,p}_{h,g}(\tau)$	Rate of TPT initiation from HIV compartment h for gender g at time τ for region i under program p, per year, where only individuals in HIV compartment 4 (HIV+, on ART) initiate TPT, such that $\kappa^{i,p}_{h,g} = 0$ for $h \in \{1, 2, 3\}$, $0 \leq \kappa_{h,g} \leq 1$ for $h \in \{4\}$ for all g.
Parameters that Describe HIV Progression	
$\eta^{i,p}_{1,2,g}(\tau)$	Rate of HIV incidence from HIV compartment 1 (HIV–) to HIV compartment 2 (HIV+, not on ART, CD4 > 200) for gender g at time τ for region i under program p.
$\eta_{2,3,g}$	Rate of HIV progression from HIV compartment 2 (HIV+, not on ART, CD4 > 200) to HIV compartment 3 (HIV+, not on ART, CD4 $\leq$ 200) for gender g.

Continued on next page

Table 3.1 – continued from previous page

Notation	Description
$\eta^{i,p}_{2,4,g}(\tau)$	Rate of ART initiation from HIV compartment 2 (HIV+, not on ART, CD4 $>$ 200) to HIV compartment 4 (HIV+, on ART) for gender g at time τ, for region i under program p, per year.
$\eta^{i,p}_{3,4,g}(\tau)$	Rate of ART initiation from HIV compartment 3 (HIV+, not on ART, CD4 $\leq$ 200) to HIV compartment 4 (HIV+, on ART) for gender g at time τ, for region i under program p per year.
Parameters that Describe Entries and Exits from the Population	
$B^{i,p}(\tau)$	Total population aging into the model at time τ for region i under program p.
$\alpha\_out^{i}_{t,h,g}(\tau)$	Rate of the population exiting the model due to mortality or aging out in TB compartment t, HIV compartment h, and gender compartment g at time τ in region i, per year.
$\alpha\_in^{i}_{t,r,h,g}(\tau)$	Proportion of the total population aging into the model that enters into TB compartment t, DR compartment r, HIV compartment h, and gender compartment g at time τ in region i due to aging in.

Table 3.1: Description and notation for parameters used in the equations that describe TB and HIV disease progression, treatment rates, and entries and exits from the model. Parameters that depend on the care delivery program are highlighted in green. TB force of infection and HIV incidence rates are highlighted in blue to indicate the care delivery program indirectly impacts them. Time-varying parameters are notated as functions of τ. Parameters that are only applicable to version one or version two of the model are highlighted in red.

3.3.1 Version One: Model Transitions

Figure 3.1 illustrates transitions to and from each TB compartment in the set TB' with the mathematical notation in Table 3.1. Figure 3.2 illustrates transitions to and from each HIV compartment in HIV. Although not depicted in Figure 3.1 and Figure 3.2, there are transitions that reflect those aging into and exiting the model as described at the end of this section. The rates of flow between each compartment are governed by differential equations as described in Section 3.5.1.

TPT initiation rates ($\kappa_{t,h}^{i,p}(\tau)$) and ART initiation rates ($\eta_{1,2,g}^{i,p}(\tau)$) are highlighted in green in Figure 3.1 and Figure 3.2 to emphasize that care programs directly impact them. TB force of infection ($\lambda_r^{i,p}(\tau)$) and HIV infection rates ($\eta_{1,2,g}^{i,p}(\tau)$) are highlighted in blue in Figure 3.1 and Figure 3.2 to emphasize that care programs indirectly impact them. The parameters that describe the diminished risk of acquiring LTBI for those exposed to DS TB while on TPT (ι_r), rate of completion of TPT (ω), rate of progression from LTBI on TPT to active TB ($\pi_{on\_TPT\_prog}^{i}$) and rate of progression from LTBI after TPT to active TB ($\pi_{after\_TPT\_prog}^{i}$) are highlighted in red in Figure 3.1 to emphasize that they are only applicable in version one of the model.

TB Disease Progression

Figure 3.1 illustrates transitions to and from each TB compartment using mathematical notation as defined in Table 3.1. Individuals exit TB compartment 1 (uninfected, not on TPT) through TB infection or TPT initiation. While all individuals in TB compartment 1 are arbitrarily assigned to DR compartment 1 when transitioning to TB compartment 3 (LTBI, infected recently), the force of infection is differentiated by drug resistance status ($\lambda_r^{i,p}(\tau)$), which is based on a proportion of those infected with DS TB and MDR TB. Uninfected individuals who initiate TPT enter TB compartment 2 (uninfected, on TPT) and DR compartment 1. Individuals in TB compartment 2 (uninfected, on TPT) that contract TB while on TPT and transition to TB compartment 3 (LTBI, infected recently) are differentiated by drug resistance status according to the force of infection ($\lambda_r^{i,p}(\tau)$) and a parameter that accounts for the reduced risk of infection of DS-TB while on TPT (ι_r).

The transition rate for all those that move into TB compartment 3 (LTBI, infected recently) by reinfection (from TB compartments 4, 7, and 8) accounts for the individual's most recent TB strain type. The transition rate of reinfection from TB compartments 4 and 8 is determined by the force of infection $\lambda_r^{i,p}(\tau)$ and the partially-protective effect of LTBI against acquiring a new TB infection (ζ). However, individuals in TB compartment 7 (Recovered/Treated) have an increased risk of reinfection, where the force of infection is modified by an increased risk of reinfection (ξ).

Individuals in TB compartment 3 (LTBI, infected recently) will on average, progress to TB compartment 4 (LTBI, infected remotely) after two years. Some proportion of individuals in TB

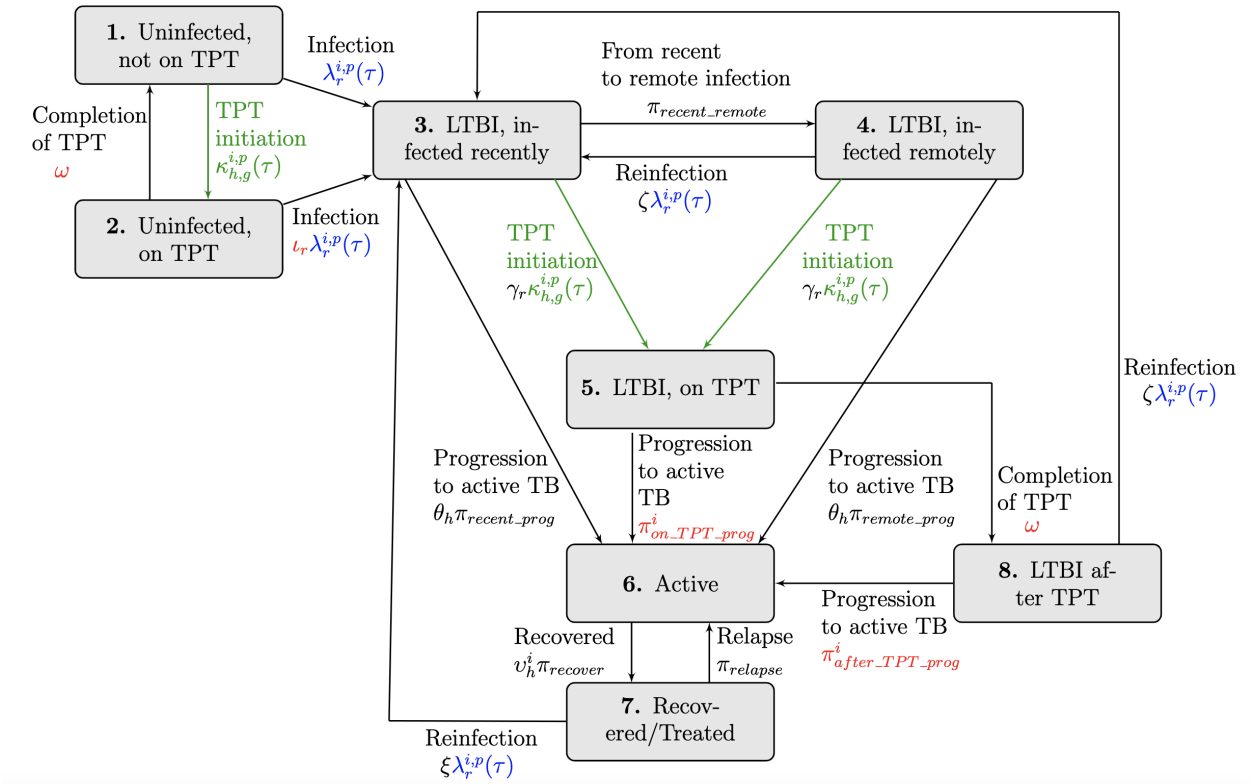

Figure 3.1: Illustration of TB transitions for version one of the TB and HIV disease dynamic transmission model. Although not visualized here, each of the eight tuberculosis compartments is stratified across two TB drug-resistance compartments, four HIV compartments, and two genders. Individuals can age out or die from any compartment. The parameters that are only applicable to version one of the model are highlighted in red. TB preventative therapy (TPT) initiations are highlighted in green to emphasize that care programs directly impact them. TB force of infection is highlighted in blue to indicate the care program indirectly impacts them.

compartment 3 will progress to TB compartment 6 (active TB) or TB compartment 5 (LTBI, on TPT). We assume only PLWH on ART will initiate TPT, which is captured by the TPT initiation rates. We assume individuals with MDR LTBI do not benefit from a reduced risk of progression to active TB (TB compartment 6) by disallowing those with MDR LTBI to move into TB compartment 5 (LTBI, on TPT) and subsequently TB compartment 8 (LTBI, after TPT). Those with LTBI who complete their course of TPT move into TB compartment 8 (LTBI after TPT) to account for the reduced risk of progression even after completing their TPT course.

Individuals who progress to TB compartment 4 (LTBI, infected remotely) have a reduced risk

of progression to active TB compared to those in TB compartment 3 (LTBI, infected recently). PLWH have an increased risk of progression to TB compartment 6 (active TB). Rates of recovery are estimated by HIV status ($\upsilon_h^i \pi_{recovered}$) to represent varying expected delays to treatment. A proportion of those who recover from active TB will relapse or become reinfected.

HIV Disease Progression

Figure 3.2 illustrates transitions to and from each HIV compartment using mathematical notation as defined in Table 3.1. Some proportion of those in HIV compartment 2 (HIV+, not on ART, CD4 > 200) will initiate ART and transition into HIV compartment 4 (HIV+, on ART), and others experience CD4 decline and transition into HIV compartment 3 (HIV+, not on ART, CD4 ≤ 200). Net ART initiations from HIV compartment 2 (HIV+, not on ART, CD4 > 200) and HIV compartment 3 (HIV+, not on ART, CD4 ≤ 200) are based on ART coverage estimates over time, and the guidance on eligibility for PLWH to initiate ART is based on their CD4 count in South Africa as outlined in Section 3.4.

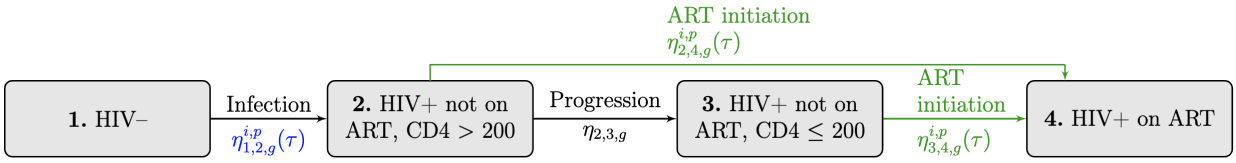

Figure 3.2: Illustration of transitions between HIV compartments for each gender compartment g at time τ. Antiretroviral therapy (ART) initiation rates (highlighted in green) are directly impacted by ART coverage for each care delivery program. ART coverage is used to calculate ART initiation rates so that the proportion of PLWH on ART by gender corresponds to ART coverage assumptions. HIV incidence rates are highlighted in blue to indicate the care delivery program indirectly impacts them. Although not visualized here, each HIV compartment is stratified across eight TB compartments, two TB drug resistance and two gender compartments.

Entries and Exits

The model includes an adult population representative of each region i between the ages of 15 and 59 under each program p, with no immigration or emigration between regions. The size of the

population is kept constant at all time steps such that

$$\sum_{t\in TB'}\sum_{r\in DR}\sum_{h\in HIV}\sum_{g\in G} N^{i,p}_{t,r,h,g}(\tau) = 100,000 \qquad \forall i \in \mathcal{I}, p \in \mathcal{P}. \tag{3.1}$$

The population is held constant by setting the total amount of population entering the model to the total amount exiting the model (due to aging out or dying). Some proportion of the population aging into the model ages into TB compartments corresponding to those uninfected with TB, LTBI, infected recently not treated with TPT, LTBI infected remotely not treated with TPT, and active TB according to yearly population, LTBI prevalence, and TB prevalence estimates by gender and region. LTBI prevalence and TB prevalence estimates are provided by drug resistance when indicated by estimates. Some proportion of the population ages into the HIV negative compartment and the HIV positive compartment for those not on ART with a CD4 count greater than 200 according to yearly HIV prevalence estimates. Changes in population characteristics of those aging into the model over time are accounted for by adjusting the proportion of the population aging into each TB, HIV, and gender compartment according to yearly estimates from the 2019 Global Burden of Disease Study (GBD 2019) for the corresponding region i [44].

3.3.2 Version Two: Model Transitions

Figure 3.3 illustrates transitions to and from each TB compartment in the set TB'' with the mathematical notation in Table 3.1. Transitions that describe HIV disease progression and entries and exits are the same for both versions of the model and are illustrated in Figure 3.2 and described in Section 3.3.1. The rates of flow between each compartment are governed by differential equations as described in Section 3.5.2.

TPT initiation rates ($\kappa^{i,p}_{h,g}(\tau)$) are highlighted in green in Figure 3.3 to emphasize that care programs directly impact them. TB force of infection ($\lambda^{i,p}_{r}(\tau)$) is highlighted in blue in Figure 3.3 to emphasize that care programs indirectly impact them. The parameter that describes the relative risk of TB progression for those with LTBI treated with TPT (χ) is highlighted in red in Figure 3.3 to emphasize that the parameter is only applicable in version two of the model.

TB Disease Progression

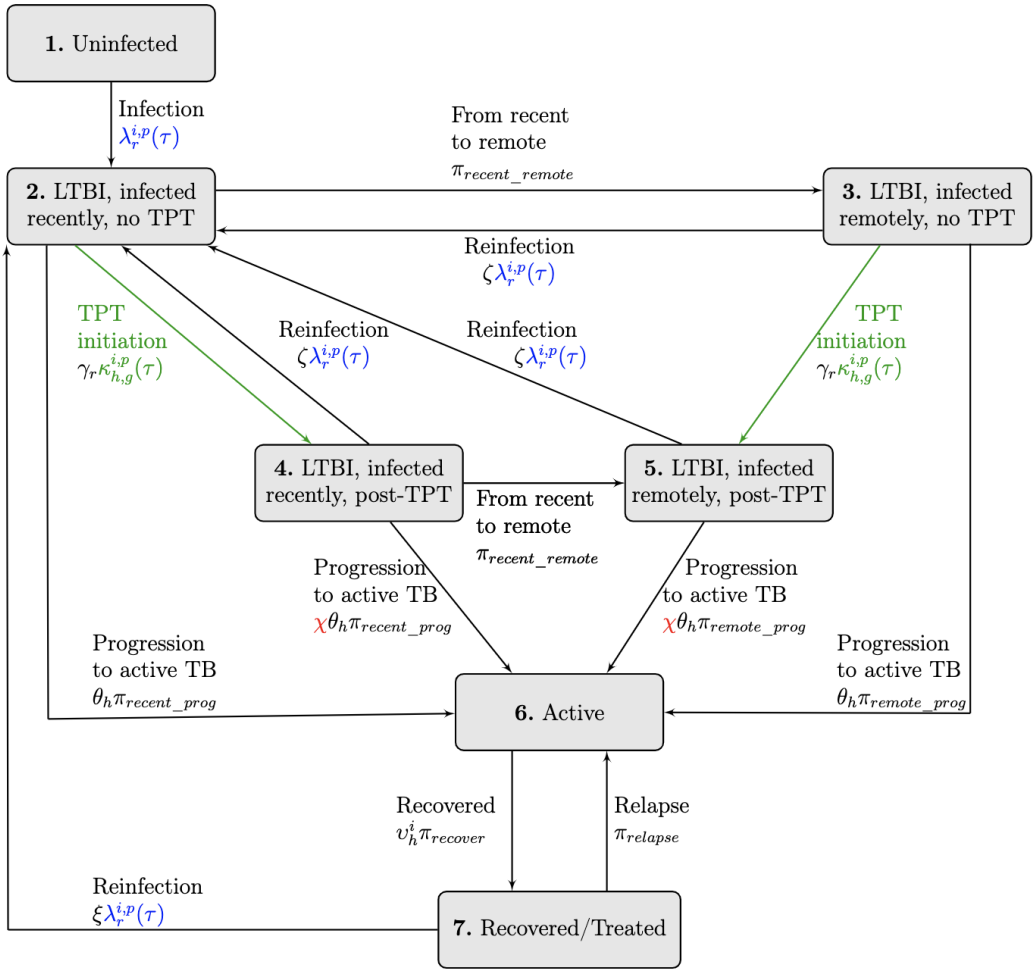

Figure 3.3: Illustration of TB transitions for version two of the TB and HIV disease dynamic transmission model. Although not visualized here, each of the seven tuberculosis compartments is stratified across two TB drug-resistance compartments, four HIV compartments, and two genders. Individuals can age out or die from any compartment. The parameter that is only applicable to version two of the model is highlighted in red. TB preventative therapy (TPT) initiations are highlighted in green to emphasize that care programs directly impact them. TB force of infection is highlighted in blue to indicate the care program indirectly impacts them.

In this section, the TB compartments correspond to those in the set TB'' for version two of the model. While all individuals in TB compartment 1 (uninfected) are arbitrarily assigned to DR compartment 1, when transitioning to TB compartment 2 (LTBI, infected recently, no TPT), they

may transition to DR compartment 1 (infected with DS TB) or 2 (infected with MDR TB) because the force of infection ($\lambda_r^{i,p}(\tau)$) are estimated by drug resistance status based on a proportion of those infected with DS TB ($r = 1$) and MDR TB ($r = 2$).

The transition rate for all those that move into TB compartment 2 (LTBI, infected recently, no TPT) by infection or reinfection (from TB compartments 3, 4, 5, and 7) accounts for the individual's most recent TB strain type. The transition rate of reinfection from TB compartments 3, 4, and 5 is determined by the force of infection ($\lambda_r^{i,p}(\tau)$) and the partially protective effect of LTBI against acquiring a new TB infection (ζ). However, individuals in TB compartment 7 (Recovered/Treated) have an increased risk of reinfection, where the force of infection ($\lambda_r^{i,p}(\tau)$) is modified by an increased risk of reinfection (ξ). Those in TB compartments 2, 3, 4, 5, and 7 can progress to TB compartment 6 (active TB). PLWH have an increased risk of progression to TB compartment 6 (active TB), which is represented by the parameter (θ_h).

Individuals in TB compartment 2 (LTBI, infected recently, no TPT) will, on average, progress to TB compartment 3 (LTBI, infected remotely, no TPT) after two years. Individuals who progress to TB compartment 3 (LTBI, infected remotely, no TPT) have a reduced risk of progression to active TB compared to those in TB compartment 2 (LTBI, infected recently, no TPT).

Those in TB compartment 2 (LTBI, infected recently, no TPT) and TB compartment 3 (LTBI, infected remotely, no TPT) with DS LTBI who initiate TPT enter TB compartment 4 (LTBI, infected recently, post-TPT) and TB compartment 5 (LTBI, infected remotely, post-TPT), respectively. The reduced risk of TB progression from TPT (χ) is used to reduce the risk of TB progression for those with recent and remote LTBI.

We assume those who initiate TPT with DS LTBI immediately gain the full benefits of TPT and enter the post-TPT state. We assume only PLWH on ART will initiate TPT, which is captured by the TPT initiation rates ($\kappa_{t,h}^{i,p}(\tau)$). We assume individuals with MDR LTBI do not benefit from a reduced risk of progression to active TB (TB compartment 6) by disallowing those with MDR LTBI to move into post-TPT compartments, TB compartment 4 or 5 with the indicator γ_r. Those in TB compartment 4 will, on average, progress to TB compartment 5 (LTBI, infected remotely, post-TPT) after two years. Rates of recovery are estimated by HIV status ($\upsilon_h^i \pi_{recovered}$) to represent varying expected delays to treatment. A proportion of those who recover from active

TB will relapse or become reinfected.

3.4 Time-Varying Parameters Impacted by Population States

A description of the parameters used in the calculations for TB force of infection, ART initiation rates, and entries to and exits from the population is given in Table 3.2. These parameters are calculated based on the total population in TB compartment t, DR compartment r, HIV compartment h, and gender compartment g in the region i under program p at time τ, denoted $N^{i,p}_{t,r,h,g}(\tau)$. The population states will differ between version one and version two of the model, however the equations for time-varying parameters are the same as provided in Section 3.4.1.

Notation	Description
Parameters that Impact TB Force of Infection ($\lambda^{i,p}_r(\tau)$)	
β^i_g	Number of effective contacts for TB transmission per year for gender g in region i.
ϕ_h	Relative transmissibility of TB in populations in HIV compartment h, such that $\phi_1 = 1$ and $0 < \phi_h < 1$ for $h = 2, 3$, or 4.
ε	Fraction of new TB infections that are MDR TB.
Parameters that Impact ART Initiation ($\eta^{i,p}_{2,4,g}(\tau)$ and $\eta^{i,p}_{3,4,g}(\tau)$)	
$\sigma^{i,p}_g(\tau)$	ART coverage for gender g at time τ in region i under program p.
$\varrho_g(\tau)$	Proportion of the population in HIV compartment 2 (HIV+, not on ART, CD4 $>$ 200) eligible to initiate ART by gender g at time τ.
Parameters that Impact Entries ($B^{i,p}(\tau)$) and Exits ($\alpha\_out^i_{t,h,g}(\tau)$) from the Population	
$\mu^i_{t,h,g}(\tau)$	Mortality rates from populations in TB compartment t, HIV compartment h, and gender compartment g at time τ, per year in region i.
$1/(60-15)$	Rate of exit from the population due to aging.

Table 3.2: Description and notation for parameters used in calculations of time-varying parameters impacted by population states. The parameter that is directly impacted by program is highlighted in green.

3.4.1 Version One: Time-Varying Parameters Impacted by Population States

TB Force of Infection

The TB force of infection for DR compartment r at time τ in region i under program p is denoted $\lambda_r^{i,p}(\tau)$, and is calculated at each time step using Equations (3.2a) and (3.2b), for DS TB ($r = 1$) and MDR TB strains ($r = 2$), respectively. The population with active TB contributes to the force of infection for new LTBI among the susceptible population. The number of individuals infected with active DS TB (in TB compartment 6 and DR compartment 1), HIV compartment h, and gender g in region i under program p at time τ is indicated by $N_{6,1,h,g}^{i,p}(\tau)$. The number of effective contacts varies by gender g and region i and is represented by the parameter β_g^i. Relative transmissibility varies by HIV compartment h, and is represented by the parameter ϕ_h [56, 80]. The model allows different effective contact rates by gender, which are calibrated but assume homogeneous mixing in the population.

The estimated fraction of new TB infections that are projected to be MDR are represented by the parameter ε. These parameters are used to calculate the TB force of infection for each DR compartment r, region i, and program p at each time step τ as follows

$$\lambda_1^{i,p}(\tau) = \sum_{h \in HIV} \sum_{g \in G} \left(\frac{\beta_g^i}{100,000} \right) \phi_h N_{6,1,h,g}^{i,p}(\tau) \qquad \forall i \in \mathcal{I},\ p \in \mathcal{P} \tag{3.2a}$$

$$\lambda_2^{i,p}(\tau) = \frac{\varepsilon \lambda_1^{i,p}(\tau)}{(1-\varepsilon)} \qquad \forall i \in \mathcal{I},\ p \in \mathcal{P}. \tag{3.2b}$$

ART Initiation Rates

ART initiation rates ($\eta_{2,4,g}^{i,p}(\tau)$ and $\eta_{3,4,g}^{i,p}(\tau)$) are calculated at each time step using Equation (3.6) and Equation (3.5). In addition to the population states $N_{t,r,h,g}^{i,p}(\tau)$, the calculations are based on: ART coverage by gender g at time τ for region i under program p, denoted $\sigma_g^{i,p}(\tau)$; and the proportion of those who are in HIV compartment 2 (HIV+, not on ART, CD4 > 200) and are eligible to initiate ART by gender g at time τ, denoted $\varrho_g(\tau)$. ART coverage, $\sigma_g^{i,p}(\tau)$, is used to calculate ART initiation rates so that the proportion of PLWH on ART by gender g corresponds to ART coverage assumptions for each region i and program p. There are four distinct time periods

that impact the input parameter values for ART coverage, $\sigma_g^{i,p}(\tau)$, and the proportion of those in HIV compartment 2 (HIV+, not on ART, CD4 > 200) that are eligible to initiate ART, $\varrho_g(\tau)$ [111],

1. Before 2004: ART was not available in this setting (South Africa).
2. Between 2004-2010: Individuals living with HIV with CD4 $\leq$ 200 were eligible for ART.
3. Between 2011-2015: CD4 eligibility levels were increased to 350 for all individuals who were HIV positive.
4. After 2016: All individuals who are HIV positive are eligible for ART.

The input values for ART coverage at time τ, by gender g in region i under program p, $\sigma_g^{i,p}(\tau)$ and the proportion of those in HIV compartment 2 (HIV+, not on ART, CD4 > 200) that are eligible to initiate ART by gender g, $\varrho_g(\tau)$, reflect these time periods. The values for ART coverage over time, by gender, $\sigma_g^{i,p}(\tau)$, are described in Section 3.8.2. The proportion of those in HIV compartment 2 (HIV+, not on ART, CD4 > 200) that are eligible to initiate ART by gender, $\varrho_g(\tau)$, is described in Section 3.8.2. The model assumes all those eligible to initiate ART, initiate at the same rate.

Before 2004, all ART initiation rates are set to zero, i.e. $\eta_{2,4,g}^{i,p}(\tau) = \eta_{3,4,g}^{i,p}(\tau) = 0$, to represent that ART is not available before 2004. After 2004, ART initiation rates are calculated in Equation (3.5) and Equation (3.6) using intermediate calculations in Equation (3.3), Equation (3.4). Equation (3.3) calculates the current proportion of those who are HIV positive in each HIV compartment h, $h \in \{2,3,4\}$ by gender g at time τ in region i under program p, $V_{h,g}^{i,p}(\tau)$, given as

$$V_{h,g}^{i,p}(\tau) = \frac{\sum\limits_{t\in TB}\sum\limits_{r\in DR} N_{t,r,h,g}^{i,p}(\tau)}{\sum\limits_{t\in TB'}\sum\limits_{r\in DR}\sum\limits_{\hat{h}\in\{2,3,4\}} N_{t,r,\hat{h},g}^{i,p}(\tau)} \qquad \forall h \in \{2,3,4\},\ g \in G,\ i \in \mathcal{I},\ p \in \mathcal{P}. \tag{3.3}$$

Equation (3.4) calculates a general ART initiation rate for all PLWH, not on ART (in HIV compartment 2 and HIV compartment 3) eligible to initiate ART by gender, denoted $\eta\_all_g^{i,p}(\tau)$ (assuming that all those eligible to initiate ART, initiate at the same rate). The numerator represents the difference in ART coverage for gender g at time τ in region i under program p, $\sigma_g^{i,p}(\tau)$, and model projected ART coverage for gender g at time τ in region i under program p, $V_{4,g}^{i,p}(\tau)$.

The denominator represents the proportion of PLWH, not on ART (in HIV compartment 2 and HIV compartment 3) eligible to initiate ART at time τ by gender g in region i under program p. The general ART initiation rate is calculated as

$$\eta\_all_g^{i,p}(\tau) = \frac{\sigma_g^{i,p}(\tau) - V_{4,g}^{i,p}(\tau)}{\varrho_g(\tau)V_{2,g}^{i,p}(\tau) + V_{3,g}^{i,p}(\tau)} \qquad \forall g \in G,\ i \in \mathcal{I},\ p \in \mathcal{P}. \tag{3.4}$$

Since all those in HIV compartment 2 (HIV+, not on ART, CD4 $>$ 200) are eligible to initiate ART for all times associated with the years after 2004, Equation (3.5) sets ART initiation rates for those in HIV compartment 2, $\eta_{2,4,g}^{i,p}(\tau)$, to the general ART initiation rate for all PLWH, not on ART, $\eta\_all_g^{i,p}(\tau)$, as

$$\eta_{2,4,g}^{i,p}(\tau) = \eta\_all_g^{i,p}(\tau) \qquad \forall g \in G,\ i \in \mathcal{I},\ p \in \mathcal{P}. \tag{3.5}$$

Finally, Equation (3.6) provides ART initiation rates from HIV compartment 3 (HIV+, not on ART, CD4 $\leq$ 200) to HIV compartment 4 (HIV+, on ART), by gender at time τ as

$$\eta_{3,4,g}^{i,p}(\tau) = \varrho_g(\tau)\eta\_all_g^{i,p}(\tau) \qquad \forall g \in G,\ i \in \mathcal{I},\ p \in \mathcal{P}. \tag{3.6}$$

Population Entering and Exiting the Model

This section describes how the rate of population exiting the model is calculated based on aging out rates and mortality rates at time τ; $\alpha\_out_{t,h,g}^{i}(\tau)$ for TB compartment t, DR compartment r, HIV compartment h and gender compartment g, in region i in Equation (3.7), and the total population aging into the model at time τ, $B^{i,p}(\tau)$ in region i under program p, in Equation (3.8).

Exits from the model can occur due to mortality at a rate of $\mu_{t,h,g}^{i}(\tau)$ for TB compartment t, HIV compartment h and gender compartment g at time τ in region i or aging out. The model only considers populations with ages between 15 and 59, that is, they enter on their 15th birthday and exit on their 60th birthday so the model assumes aging out of the population occurs at a rate of $1/(60-15)$ per year which is the inverse of the duration of time between population entry at age

15 and exit at age 60. Note that, $\mu^{i}_{t,h,g}(\tau)/(60-15)$, is subtracted to ensure an individual can only age out or die, but cannot both age out and die. The rate of population exiting the model based on aging out rates and mortality rates is calculated as

$$\alpha\_out^{i}_{t,h,g}(\tau) = \mu^{i}_{t,h,g}(\tau) + \frac{1}{(60-15)}(1-\mu^{i}_{t,h,g}(\tau)) \quad \forall t \in TB',\ h \in HIV,\ g \in G,\ i \in \mathcal{I}. \tag{3.7}$$

This model assumes a constant population size of 100,000. In order to keep the population size constant, the entries to the population are set to the total population leaving the model from aging out or dying. The total population aging into the model is calculated as

$$B^{i,p}(\tau) = \sum_{t\in TB}\sum_{r\in DR}\sum_{h\in HIV}\sum_{g\in G}\alpha\_out^{i}_{t,h,g}(\tau)N^{i,p}_{t,r,h,g}(\tau) \qquad \forall i \in \mathcal{I},\ p \in \mathcal{P}. \tag{3.8}$$

New entries are assigned to TB uninfected, latent TB (no TPT), and active TB compartments. As well as, HIV- and HIV+, not on ART, CD4 $>$ 200, all DR compartments, and all gender g compartments, at time τ in region i with the input parameter $\alpha\_in^{i}_{t,r,h,g}(\tau)$.

3.4.2 Version Two: Time-Varying Parameters Impacted by Population States

The calculations of time-varying parameters impacted by population states remain unchanged between version one and version two. In version two of the model, these parameters are computed by substituting TB' with TB'' in the relevant equations, from Equation (3.2a) to Equation (3.8).

3.5 Differential Equations that Govern TB and HIV Transitions

Section 3.5.1 describes the differential equations in version one of the model used to represent transitions between the eight TB compartments, two DR compartments, four HIV compartments, and two gender compartments. Section 3.5.2 describes the differential equations in version two of the model used to represent transitions between the seven TB compartments, two DR compartments, four HIV compartments, and two gender compartments.

3.5.1 Version One: Differential Equations

In this section, $N^{i,p}_{t,r,h,g}(\tau)$ represents the total population in TB compartment for $t \in TB'$, DR compartment $r \in DR$, HIV compartment $h \in HIV$, gender compartment $g \in G$, in region $i \in \mathcal{I}$, and program $p \in \mathcal{P}$.

*TB compartment 1: Uninfected, not on TPT**

$$\begin{aligned}
\frac{dN^{i,p}_{1,1,h,g}(\tau)}{dt} = \quad & \alpha_in^{i}_{1,1,h,g}(\tau)B^{i,p}(\tau) \\
& - \alpha_out^{i}_{1,h,g}(\tau)N^{i,p}_{1,1,h,g}(\tau) \\
& - \kappa^{i,p}_{h,g}(\tau)N^{i,p}_{1,1,h,g}(\tau) \\
& + \omega N^{i,p}_{2,1,h,g}(\tau) \\
& - \sum_{\hat{r}\in DR} \lambda^{i,p}_{\hat{r}}(\tau)N^{i,p}_{1,1,h,g}(\tau) \\
& + \sum_{\substack{\hat{h}\in HIV,\\ \hat{h}\neq h}} \eta^{i,p}_{\hat{h},h,g}(\tau)N^{i,p}_{1,1,\hat{h},g}(\tau) \\
& - \sum_{\substack{\hat{h}\in HIV,\\ \hat{h}\neq h}} \eta^{i,p}_{h,\hat{h},g}(\tau)N^{i,p}_{1,1,h,g}(\tau) \qquad (3.9)
\end{aligned}$$

$$\forall h \in HIV, g \in G, i \in \mathcal{I}, p \in \mathcal{P}$$

**Note: The model does not distinguish TB uninfected, not on TPT, compartments by drug resistance, and as such, all initial uninfected populations are assigned to DR compartment 1, and all exits and entries into TB uninfected compartments are from DR compartment 1.*

Equation (3.9) *Description*

The first line in Equation (3.9) calculates the entries into TB compartment 1 as a proportion of the population enters at age 15. The second line calculates the population leaving the compartment from aging out or dying. The third and fourth lines calculate the total population leaving and entering compartment 1 from initiation (only those who are HIV+ and on ART) and completion

of TPT, respectively. The fifth line calculates the population leaving after being infected with TB. The last two lines calculate entries and exits between HIV compartments.

*TB compartment 2: Uninfected, on TPT**

$$\begin{aligned}\frac{dN^{i,p}_{2,1,h,g}(\tau)}{dt} = \quad & -\alpha\_out^{i}_{2,h,g}(\tau)N^{i,p}_{2,1,h,g}(\tau) \\ & +\kappa^{i,p}_{h,g}(\tau)N^{i,p}_{1,1,h,g}(\tau) \\ & -\omega N^{i,p}_{2,1,h,g}(\tau) \\ & -\sum_{\hat{r}\in DR}\iota_{\hat{r}}\lambda^{i,p}_{\hat{r}}(\tau)N^{i,p}_{2,1,h,g}(\tau) \\ & +\sum_{\substack{\hat{h}\in HIV,\\ \hat{h}\neq h}}\eta^{i,p}_{\hat{h},h,g}(\tau)N^{i,p}_{2,1,\hat{h},g}(\tau) \\ & -\sum_{\substack{\hat{h}\in HIV,\\ \hat{h}\neq h}}\eta^{i,p}_{h,i,g}(\tau)N^{i,p}_{2,1,h,g}(\tau) \qquad (3.10)\end{aligned}$$

$$\forall h \in HIV, g \in G, i \in \mathcal{I}, p \in \mathcal{P}$$

**Note: The model does not distinguish TB uninfected, not on TPT, compartments by drug resistance, and as such, all initial uninfected populations are assigned to DR compartment 1, and all exits and entries into TB uninfected compartments are from DR compartment 1.*

Equation (3.10) *Description*

The first line in Equation (3.10) calculates the population leaving the compartment from aging out or dying (note: we do not let individuals age into TPT compartments). The second and third lines calculate the total population entering and leaving compartment 2 from initiation and completion of TPT. The fourth line calculates the population leaving after being infected with TB, diminished for those infected with DS TB to represent the partially protective effects of becoming infected with TB while on TPT. The last two lines calculate entries and exits between HIV compartments.

TB compartment 3: LTBI, infected recently

$$
\begin{aligned}
\frac{dN^{i,p}_{3,r,h,g}(\tau)}{dt} = \quad & \alpha\_in^{i}_{3,r,h,g}(\tau)B^{i,p}(\tau) \\
& - \alpha\_out^{i}_{3,h,g}(\tau)N^{i,p}_{3,r,h,g}(\tau) \\
& + \lambda^{i,p}_{r}(\tau)N^{i,p}_{1,1,h,g}(\tau) \\
& + \iota_r\lambda^{i,p}_{r}(\tau)N^{i,p}_{2,1,h,g}(\tau) \\
& + \zeta\lambda^{i,p}_{r}(\tau)\sum_{\hat{r}\in DR} N^{i,p}_{4,\hat{r},h,g}(\tau) \\
& + \xi\lambda^{i,p}_{r}(\tau)\sum_{\hat{r}\in DR} N^{i,p}_{7,\hat{r},h,g}(\tau) \\
& + \zeta\lambda^{i,p}_{r}(\tau)\sum_{\hat{r}\in DR} N^{i,p}_{8,\hat{r},h,g}(\tau) \\
& - \pi_{recent\_remote}N^{i,p}_{3,r,h,g}(\tau) \\
& - \gamma_r\kappa^{i,p}_{h,g}(\tau)N^{i,p}_{3,r,h,g}(\tau) \\
& - \theta_h\pi_{recent\_prog}N^{i,p}_{3,r,h,g}(\tau) \\
& + \sum_{\substack{\hat{h}\in HIV,\\ \hat{h}\neq h}} \eta^{i,p}_{\hat{h},h,g}(\tau)N^{i,p}_{3,r,\hat{h},g}(\tau) \\
& - \sum_{\substack{\hat{h}\in HIV,\\ \hat{h}\neq h}} \eta^{i,p}_{h,\hat{h},g}(\tau)N^{i,p}_{3,r,h,g}(\tau) \qquad (3.11)
\end{aligned}
$$

$$\forall r \in DR, h \in HIV, g \in G, i \in \mathcal{I}, p \in \mathcal{P}$$

Equation (3.11) *Description*

Line one in Equation (3.11) calculates entries into TB compartment 3 as a proportion of the population enters at age 15. Line two calculates the population leaving the compartment from aging out or dying. Lines three through seven calculate entries from infections (and re-infections) from TB compartments 1 (uninfected, not on TPT), 2 (uninfected, on TPT), 4 (LTBI, remote), 8 (LTBI, on TPT), and 7 (recovered/treated). For the purpose of this model, we assume in regards to reinfection, that the most recent TB strain type determines the DR compartment. As such,

we sum the total populations from compartments 4, 7, and 8 over drug-resistant compartments to allow populations to transition between DR compartments (DS and MDR). For individuals in TB compartments 4 and 8, re-infection is diminished by the partially protective effect of previous infections on reinfection. For individuals in TB compartment 8, infection rates are increased to account for the increased risk of reinfection after active TB. Lines eight through ten calculate exits due to movements from recent to remote, going onto TPT, and progression to active TB. We only allow individuals with DS LTBI and HIV+ and on ART to move into TB compartment 5, we assume those with MDR LTBI on TPT continue to progress according to the annual risk of progression for recent LTBI. The last two lines calculate transitions between HIV compartments for entries and exits.

TB compartment 4: LTBI, infected remotely

$$\begin{aligned}
\frac{dN^{i,p}_{4,r,h,g}(\tau)}{dt} = \quad & \alpha_in^{i}_{4,r,h,g}(\tau)B^{i,p}(\tau) \\
& - \alpha_out^{i}_{4,h,g}(\tau)N^{i,p}_{4,r,h,g}(\tau) \\
& + \pi_{recent_remote}N^{i,p}_{3,r,h,g}(\tau) \\
& - \zeta \sum_{r\in\hat{r}} \lambda^{i,p}_{\hat{r}}(\tau)N^{i,p}_{4,r,h,g}(\tau) \\
& - \gamma_r \kappa^{i,p}_{h,g}(\tau)N^{i,p}_{4,r,h,g}(\tau) \\
& - \theta_h \pi_{remote_prog}N^{i,p}_{4,r,h,g}(\tau) \\
& + \sum_{\substack{\hat{h}\in HIV,\\ \hat{h}\neq h}} \eta^{i,p}_{\hat{h},h,g}(\tau)N_{4,r,\hat{h},g}(\tau) \\
& - \sum_{\substack{\hat{h}\in HIV,\\ \hat{h}\neq h}} \eta^{i,p}_{h,\hat{h},g}(\tau)N^{i,p}_{4,r,h,g}(\tau) \qquad (3.12)
\end{aligned}$$

$$\forall r \in DR, h \in HIV, g \in G, i \in \mathcal{I}, p \in \mathcal{P}$$

Equation (3.12) *Description*

Line one in Equation (3.12) calculates entries into TB compartment 4 as a proportion of the

population enters at age 15. Line two calculates the population leaving the compartment from aging out or dying. Line three calculates entries from LTBI, recent to remote, two years after the initial LTBI. Lines three to six calculate exits due to re-infection, which is diminished for the partially-protective effect of previous LTBI infections against acquiring a new TB infection, going onto TPT, and progression to active TB. We only allow individuals with DS LTBI and HIV+ and on ART to move into TB compartment 5. We assume those with MDR LTBI on TPT continue to progress according to the annual risk of progression for remote LTBI. The last two lines calculate transitions between HIV compartments.

TB compartment 5: LTBI, on TPT

$$\begin{aligned}\frac{dN^{i,p}_{5,r,h,g}(\tau)}{dt} = \quad & -\alpha\_out^{i}_{5,h,g}(\tau)N^{i,p}_{5,r,h,g}(\tau) \\ & +\gamma_r\kappa^{i,p}_{h,g}(\tau)(N^{i,p}_{3,r,h,g}(\tau)+N^{i,p}_{4,r,h,g}(\tau)) \\ & -\pi^{i}_{on\_TPT\_prog}N^{i,p}_{5,r,h,g}(\tau) \\ & -\omega N^{i,p}_{5,r,h,g}(\tau) \\ & +\sum_{\substack{\hat{h}\in HIV,\\ \hat{h}\neq h}}\eta^{i,p}_{\hat{h},h,g}(\tau)N^{i,p}_{5,r,\hat{h},g}(\tau) \\ & -\sum_{\substack{\hat{h}\in HIV,\\ \hat{h}\neq h}}\eta^{i,p}_{h,\hat{h},g}(\tau)N^{i,p}_{5,r,h,g}(\tau) \end{aligned} \tag{3.13}$$

$$\forall r \in DR, h \in HIV, g \in G, i \in \mathcal{I}, p \in \mathcal{P}$$

Equation (3.13) *Description*

Line one in Equation (3.13) calculates the population leaving the compartment from aging out or dying (note: we do not let individuals age into TPT compartments). Line two calculates the rate at which populations move onto TPT from the LTBI, infected recently, and LTBI, infected remotely compartments, respectively. Lines three and four calculate exits due to active TB progression and completion of TPT. The last two lines calculate transitions between HIV compartments for entries and exits.

TB compartment 6: Active TB

$$\begin{aligned}\frac{dN^{i,p}_{6,r,h,g}(\tau)}{dt} = \quad & \alpha\_in^{i}_{6,r,h,g}(\tau)B^{i,p}(\tau) \\ & - \alpha\_out^{i}_{6,h,g}N^{i,p}_{6,r,h,g}(\tau) \\ & + \theta_h \pi_{recent\_prog} N^{i,p}_{3,r,h,g}(\tau) \\ & + \theta_h \pi_{remote\_prog} N^{i,p}_{4,r,h,g}(\tau) \\ & + \pi^{i}_{on\_TPT\_prog} N^{i,p}_{5,r,h,g}(\tau) \\ & + \pi^{i}_{after\_TPT\_prog} N^{i,p}_{8,r,h,g}(\tau) \\ & + \pi_{relapse} N^{i,p}_{7,r,h,g}(\tau) \\ & - \upsilon^{i}_{h} \pi_{recover} N^{i,p}_{6,r,h,g}(\tau) \\ & + \sum_{\substack{\hat{h}\in HIV, \\ \hat{h}\neq h}} \eta^{i,p}_{\hat{h},h,g}(\tau) N^{i,p}_{6,r,\hat{h},g}(\tau) \\ & - \sum_{\substack{\hat{h}\in HIV, \\ \hat{h}\neq h}} \eta^{i,p}_{h,\hat{h},g}(\tau) N^{i,p}_{6,r,h,g}(\tau) \end{aligned} \tag{3.14}$$

$$\forall r \in DR, h \in HIV, g \in G, i \in \mathcal{I}, p \in \mathcal{P}$$

Equation (3.14) *Description*

Line one in Equation (3.14) calculates entries into TB compartment 6 as a proportion of the population enters at age 15. Line two calculates the population leaving the compartment from aging out or dying. Lines three through six calculate the rate at which populations with LTBI who are recently and remotely infected (relative to HIV state), on TPT, and after TPT (for those who are HIV+ and on ART) progress to active TB. Line seven calculates entries from relapse. Line eight calculates exits from recovery and accounts for the increased duration of active TB due to delays in treatment. The last two lines calculate transitions between HIV compartments for entries and exits.

TB compartment 7: Recovered/Treated

$$\begin{aligned}\frac{dN^{i,p}_{7,r,h,g}(\tau)}{dt} = \quad & -\alpha\_out^{i}_{7,h,g} N^{i,p}_{7,r,h,g}(\tau) \\ & + \upsilon^{i}_{h} \pi_{recover} N^{i,p}_{6,r,h,g}(\tau) \\ & - \xi \sum_{r \in \hat{r}} \lambda^{i,p}_{\hat{r}}(\tau) N^{i,p}_{7,r,h,g}(\tau) \\ & - \pi_{relapse} N^{i,p}_{7,r,h,g}(\tau) \\ & + \sum_{\substack{\hat{h} \in HIV, \\ \hat{h} \neq h}} \eta^{i,p}_{\hat{h},h,g}(\tau) N^{i,p}_{7,r,\hat{h},g}(\tau) \\ & - \sum_{\substack{\hat{h} \in HIV, \\ \hat{h} \neq h}} \eta^{i,p}_{h,\hat{h},g}(\tau) N^{i,p}_{7,r,h,g}(\tau) \end{aligned} \tag{3.15}$$

$$\forall r \in DR, h \in HIV, g \in G, i \in \mathcal{I}, p \in \mathcal{P}$$

Equation (3.15) *Description*

Line one in Equation (3.15) calculates the population leaving the compartment from aging out or dying (note: we do not let individuals age into the TB recovered/treated compartment). Line two calculates entries from recovery/treatment and accounts for the increased duration of active TB due to delays in treatment. Line three calculates exits from reinfection, which accounts for the increased risk of acquiring a new TB infection after active TB. Line four calculates exits from relapse. The last two lines calculate transitions between HIV compartments.

TB compartment 8: LTBI after TPT

$$\begin{aligned}\frac{dN^{i,p}_{8,r,h,g}(\tau)}{dt} = \quad & -\alpha\_out^{i}_{8,h,g} N^{i,p}_{8,r,h,g}(\tau) \\ & + \omega N^{i,p}_{5,r,h,g}(\tau) \\ & - \pi^{i}_{after\_TPT\_prog} N^{i,p}_{8,r,h,g}(\tau) \\ & - \zeta \sum_{r \in \hat{r}} \lambda^{i,p}_{\hat{r}}(\tau) N^{i,p}_{8,r,h,g}(\tau) \\ & + \sum_{\substack{\hat{h} \in HIV, \\ \hat{h} \neq h}} \eta^{i,p}_{\hat{h},h,g}(\tau) N^{i,p}_{8,r,\hat{h},g}(\tau) \\ & - \sum_{\substack{\hat{h} \in HIV, \\ \hat{h} \neq h}} \eta^{i,p}_{h,\hat{h},g}(\tau) N^{i,p}_{8,r,h,g}(\tau) \end{aligned} \tag{3.16}$$

$$\forall r \in DR, h \in HIV, g \in G, i \in \mathcal{I}, p \in \mathcal{P}$$

Equation (3.16) *Description*

Line one in Equation (3.16) calculates the population leaving the compartment from aging out or dying (note: we do not let individuals age into TPT compartments). Line two calculates the total population entering TB compartment 8 after completing TPT with LTBI. Lines three and four calculate exits due to progression to active TB and reinfection, which is diminished for the partially-protective effect of LTBI from TB against acquiring a new TB infection. The last two lines calculate transitions between HIV compartments for entries and exits.

3.5.2 Version Two: Differential Equations

In this section, $N^{i,p}_{t,r,h,g}(\tau)$ represents the total population in TB compartment for $t \in TB''$, DR compartment $r \in DR$, HIV compartment $h \in HIV$, gender compartment $g \in G$, in region $i \in \mathcal{I}$, and program $p \in \mathcal{P}$.

*TB compartment 1: Uninfected**

$$\begin{aligned}\frac{dN^{i,p}_{1,1,h,g}(\tau)}{dt} &= \alpha\_in^{i}_{1,1,h,g}(\tau)B^{i,p}(\tau) \\ &- \alpha\_out^{i}_{1,h,g}(\tau)N^{i,p}_{1,1,h,g}(\tau) \\ &- \sum_{\hat{r}\in DR}\lambda^{i,p}_{\hat{r}}(\tau)N^{i,p}_{1,1,h,g}(\tau) \\ &+ \sum_{\substack{\hat{h}\in HIV,\\ \hat{h}\neq h}}\eta^{i,p}_{\hat{h},h,g}(\tau)N^{i,p}_{1,1,\hat{h},g}(\tau) \\ &- \sum_{\substack{\hat{h}\in HIV,\\ \hat{h}\neq h}}\eta^{i,p}_{h,\hat{h},g}(\tau)N^{i,p}_{1,1,h,g}(\tau) \qquad (3.17)\end{aligned}$$

$$\forall h \in HIV, g \in G, i \in \mathcal{I}, p \in \mathcal{P}$$

**Note: The model does not distinguish TB uninfected compartments by drug resistance, and as such, all initial uninfected populations are assigned to DR compartment 1, and all exits and entries into TB uninfected compartments are from DR compartment 1.*

Equation (3.17) *Description*

The first line in Equation (3.17) calculates the entries into TB compartment 1 as a proportion of the population enters at age 15. The second line calculates the population leaving the compartment from aging out or dying. The third line calculates the population leaving after being infected with TB. The last two lines calculate transitions between HIV compartments.

TB compartment 2: LTBI, infected recently, no TPT

$$
\begin{aligned}
\frac{dN^{i,p}_{2,r,h,g}(\tau)}{dt} = \; & \alpha\_in^{i}_{2,r,h,g}(\tau)B^{i,p}(\tau) \\
& - \alpha\_out^{i}_{2,h,g}(\tau)N^{i,p}_{2,r,h,g}(\tau) \\
& + \lambda^{i,p}_{r}(\tau)N^{i,p}_{1,1,h,g}(\tau) \\
& + \zeta\lambda^{i,p}_{r}(\tau)\sum_{\hat{r}\in DR} N^{i,p}_{3,\hat{r},h,g}(\tau) \\
& + \zeta\lambda^{i,p}_{r}(\tau)\sum_{\hat{r}\in DR} N^{i,p}_{4,\hat{r},h,g}(\tau) \\
& + \zeta\lambda^{i,p}_{r}(\tau)\sum_{\hat{r}\in DR} N^{i,p}_{5,\hat{r},h,g}(\tau) \\
& + \xi\lambda^{i,p}_{r}(\tau)\sum_{\hat{r}\in DR} N^{i,p}_{7,\hat{r},h,g}(\tau) \\
& - \pi_{2,3}N^{i,p}_{2,r,h,g}(\tau) \\
& - \gamma_{r}\kappa^{i,p}_{h,g}(\tau)N^{i,p}_{2,r,h,g}(\tau) \\
& - \theta_{h}\pi_{2,6}N^{i,p}_{2,r,h,g}(\tau) \\
& + \sum_{\substack{\hat{h}\in HIV,\\ \hat{h}\neq h}} \eta^{i,p}_{\hat{h},h,g}(\tau)N^{i,p}_{2,r,\hat{h},g}(\tau) \\
& - \sum_{\substack{\hat{h}\in HIV,\\ \hat{h}\neq h}} \eta^{i,p}_{h,\hat{h},g}(\tau)N^{i,p}_{2,r,h,g}(\tau)
\end{aligned}
\tag{3.18}
$$

$$\forall r \in DR, h \in HIV, g \in G, i \in \mathcal{I}, p \in \mathcal{P}$$

Equation (3.18) *Description*

Line one in Equation (3.18) calculates entries into TB compartment 2 as a proportion of the population enters at age 15. Line two calculates the population leaving the compartment from aging out or dying. Lines three through seven calculate entries from infections (and re-infections) from TB compartments 1 (uninfected), 3 (LTBI, infected remotely, no TPT), 4 (LTBI, infected recently, post-TPT), 5 (LTBI, infected remotely, post-TPT), and 7 (recovered/treated). For the purpose of

this model, we assume, in regard to reinfection, that the most recent TB strain type determines the DR compartment. As such, we sum the total populations from TB compartments 3, 4, 5, and 7 over drug-resistant compartments to allow populations to transition between DR compartments (DS and MDR). For individuals in TB compartments 3, 4 and 5, re-infection is diminished by the partially protective effect of previous infections on reinfection. For individuals in TB compartment 7, infection rates are increased to account for the increased risk of reinfection after active TB. Lines eight through ten calculate exits due to movements from recent to remote, going onto TPT, and progression to active TB. We only allow individuals with DS LTBI and HIV+ and on ART to move into TB compartment 4. We assume those with MDR LTBI on TPT continue to progress according to the annual risk of progression for recent LTBI. The last two lines calculate transitions between HIV compartments.

TB compartment 3: LTBI, infected remotely, no TPT

$$\begin{aligned}
\frac{dN^{i,p}_{3,r,h,g}(\tau)}{dt} = \; & \alpha_in^{i}_{3,r,h,g}(\tau)B^{i,p}(\tau) \\
& - \alpha_out^{i}_{3,h,g}(\tau)N^{i,p}_{3,r,h,g}(\tau) \\
& + \pi_{2,3}N^{i,p}_{2,r,h,g}(\tau) \\
& - \zeta \sum_{\hat{r}\in DR} \lambda^{i,p}_{\hat{r}}(\tau)N^{i,p}_{3,r,h,g}(\tau) \\
& - \gamma_r \kappa^{i,p}_{h,g}(\tau)N^{i,p}_{3,r,h,g}(\tau) \\
& - \theta_h \pi_{recent_prog}N^{i,p}_{3,r,h,g}(\tau) \\
& + \sum_{\substack{\hat{h}\in HIV,\\ \hat{h}\neq h}} \eta^{i,p}_{\hat{h},h,g}(\tau)N^{i,p}_{3,r,\hat{h},g}(\tau) \\
& - \sum_{\substack{\hat{h}\in HIV,\\ \hat{h}\neq h}} \eta^{i,p}_{h,\hat{h},g}(\tau)N^{i,p}_{3,r,h,g}(\tau). \qquad (3.19)
\end{aligned}$$

$$\forall r \in DR, h \in HIV, g \in G, i \in \mathcal{I}, p \in \mathcal{P}$$

Equation (3.19) *Description*

Line one in Equation (3.19) calculates entries into TB compartment 3 as a proportion of the population enters at age 15. Line two calculates the population leaving the compartment from aging out or dying. Line three calculates entries from LTBI, recent to remote, two years after the initial LTBI. Line four calculates exits due to re-infection, which is diminished for the partially protective effect of previous LTBI infections against acquiring a new TB infection. Those who are reinfected can be reinfected with DS LTBI or MDR LTBI. We assume that the most recent infection determines if the TB strain is DS or MDR. Lines five and six calculate exits due to going onto TPT and progression to active TB. We only allow individuals with DS LTBI and HIV+ and on ART to move into the post-TPT state. We assume those with MDR LTBI on TPT continue to progress according to the annual risk of progression for remote LTBI. The last two lines calculate transitions between HIV compartments.

TB compartment 4: LTBI, infected recently, post-TPT

$$
\begin{aligned}
\frac{dN^{i,p}_{4,r,h,g}(\tau)}{dt} &= -\alpha\_out^{i}_{4,h,g}(\tau)N^{i,p}_{4,r,h,g}(\tau) \\
&+ \gamma_r \kappa^{i,p}_{h,g}(\tau)N^{i,p}_{2,r,h,g}(\tau) \\
&- \zeta \sum_{\hat{r}\in DR} \lambda^{i,p}_{\hat{r}}(\tau)N^{i,p}_{4,r,h,g}(\tau) \\
&- \chi\theta_h\pi_{2,6}N^{i,p}_{4,r,h,g}(\tau) \\
&- \pi_{2,3}N^{i,p}_{4,r,h,g}(\tau) \\
&+ \sum_{\substack{\hat{h}\in HIV,\\ \hat{h}\neq h}} \eta^{i,p}_{\hat{h},h,g}(\tau)N^{i,p}_{4,r,\hat{h},g}(\tau) \\
&- \sum_{\substack{\hat{h}\in HIV,\\ \hat{h}\neq h}} \eta^{i,p}_{h,\hat{h},g}(\tau)N^{i,p}_{4,r,h,g}(\tau) \qquad (3.20)
\end{aligned}
$$

$$\forall r \in DR, h \in HIV, g \in G, i \in \mathcal{I}, p \in \mathcal{P}$$

Equation (3.20) *Description*

Line one in Equation (3.20) calculates the population leaving the compartment from aging out or dying (note: we do not let individuals age into post-TPT compartments). Line two calculates the rate at which populations initiate TPT from TB compartment 2. Lines three to five calculate exits due to reinfection, progression to active TB diminished based on the relative risk of TB progression for those on TPT, and movements from recent to remote, respectively. The last two lines calculate transitions between HIV compartments.

TB compartment 5: LTBI, infected remotely, post-TPT

$$\begin{aligned}\frac{dN^{i,p}_{5,r,h,g}(\tau)}{dt} &= -\alpha\_out^{i,p}_{5,h,g} N^{i,p}_{5,r,h,g}(\tau) \\ &+ \pi_{2,3} N^{i,p}_{4,r,h,g}(\tau) \\ &+ \gamma_r \kappa^{i,p}_{h,g}(\tau) N^{i,p}_{3,r,h,g}(\tau) \\ &- \chi \theta_h \pi_{recent\_prog} N^{i,p}_{5,r,h,g}(\tau) \\ &- \zeta \sum_{\hat{r} \in DR} \lambda^{i,p}_{\hat{r}} N^{i,p}_{5,r,h,g}(\tau) \\ &+ \sum_{\substack{\hat{h} \in HIV, \\ \hat{h} \neq h}} \eta^{i,p}_{\hat{h},h,g}(\tau) N^{i,p}_{5,r,\hat{h},g}(\tau) \\ &- \sum_{\substack{\hat{h} \in HIV, \\ \hat{h} \neq h}} \eta^{i,p}_{h,\hat{h},g}(\tau) N^{i,p}_{5,r,h,g}(\tau) \end{aligned} \tag{3.21}$$

$$\forall r \in DR, h \in HIV, g \in G, i \in \mathcal{I}, p \in \mathcal{P}$$

Equation (3.21) *Description*

Line one in Equation (3.21) calculates the population leaving the compartment from aging out or dying (note: we do not let individuals age into post-TPT compartments). Line two calculates the total population entering TB compartment 5 due to movements from recent to remote LTBI. Line three calculates the rate at which populations initiate TPT from TB compartment 3. Lines

four and five calculate exits due to progression to active TB (diminished for the reduced risk of progression for those on TPT) and reinfection (diminished for the partially protective effect of LTBI from TB against acquiring a new TB infection.) The last two lines calculate transitions between HIV compartments.

TB compartment 6: Active TB

$$\begin{aligned}
\frac{dN^{i,p}_{6,r,h,g}(\tau)}{dt} &= \alpha_in^{i}_{6,r,h,g}(\tau)B^{i,p}(\tau) \\
&- \alpha_out^{i}_{6,h,g}N^{i,p}_{6,r,h,g}(\tau) \\
&+ \theta_h \pi_{2,6} N^{i,p}_{2,r,h,g}(\tau) \\
&+ \theta_h \pi_{recent_prog} N^{i,p}_{3,r,h,g}(\tau) \\
&+ \chi\theta_h \pi_{2,6} N^{i,p}_{4,r,h,g}(\tau) \\
&+ \chi\theta_h \pi_{recent_prog} N^{i,p}_{5,r,h,g}(\tau) \\
&+ \pi_{relapse} N^{i,p}_{7,r,h,g}(\tau) \\
&- \upsilon^{i}_{h} \pi_{recover} N^{i,p}_{6,r,h,g}(\tau) \\
&+ \sum_{\substack{\hat{h}\in HIV, \\ \hat{h}\neq h}} \eta^{i,p}_{\hat{h},h,g}(\tau) N^{i,p}_{6,r,\hat{h},g}(\tau) \\
&- \sum_{\substack{\hat{h}\in HIV, \\ \hat{h}\neq h}} \eta^{i,p}_{h,\hat{h},g}(\tau) N^{i,p}_{6,r,h,g}(\tau) \qquad (3.22)
\end{aligned}$$

$$\forall r \in DR, h \in HIV, g \in G, i \in \mathcal{I}, p \in \mathcal{P}$$

Equation (3.22) *Description*

Line one in Equation (3.22) calculates entries into TB compartment 6 as a proportion of the population enters at age 15. Line two calculates the population leaving the compartment from aging out or dying. Lines three to six calculate the population progressing to active TB from TB compartments 2, 3, 4, and 5. Line seven calculates entries from relapse. Line eight calculates exits

from recovery and accounts for the increased duration of active TB due to delays in treatment. The last two lines calculate transitions between HIV compartments.

TB compartment 7: Recovered/Treated

$$\begin{aligned}\frac{dN^{i,p}_{7,r,h,g}(\tau)}{dt} &= -\alpha\_out^{i}_{7,h,g} N^{i,p}_{7,r,h,g}(\tau) \\ &+ \upsilon^{i}_{h} \pi_{recover} N^{i,p}_{6,r,h,g}(\tau) \\ &- \xi \sum_{\hat{r} \in DR} \lambda^{i,p}_{\hat{r}}(\tau) N^{i,p}_{7,r,h,g}(\tau) \\ &- \pi_{relapse} N^{i,p}_{7,r,h,g}(\tau) \\ &+ \sum_{\substack{\hat{h} \in HIV, \\ \hat{h} \neq h}} \eta^{i,p}_{\hat{h},h,g}(\tau) N_{7,r,\hat{h},g}(\tau) \\ &- \sum_{\substack{\hat{h} \in HIV, \\ \hat{h} \neq h}} \eta^{i,p}_{h,\hat{h},g}(\tau) N_{7,r,h,g}(\tau) \end{aligned} \tag{3.23}$$

$$\forall r \in DR, h \in HIV, g \in G, i \in \mathcal{I}, p \in \mathcal{P}$$

Equation (3.23) *Description*

Line one in Equation (3.23) calculates the population leaving the compartment from aging out or dying (note: we do not let individuals age into the TB recovered/treated compartment). Line two calculates entries from recovery/treatment. Line three calculates exits from reinfection, which accounts for the increased risk of acquiring a new TB infection after active TB. Line four calculates exits from relapse. The last two lines calculate transitions between HIV compartments.

3.6 Model Execution

In both versions, I ran the model independently for each region $i \in \mathcal{I}$ and program $p \in \mathcal{P}$ with parameters specific to each region i under program p. Both versions assume no immigration or emigration between regions and a constant model population of 100,000 individuals in each region.

The system of differential equations is solved using a time step τ of one month or 1/12 (0.083) of a year. Each time step τ is associated with a year, y. For example time steps $\tau \in \{1990.0, 1990.083, \ldots, 1990.833, 1990.917\}$ are associated with the year 1990 or $y = 1990$.

In both versions, I ran the model for each region over a warmup and calibration period from the beginning of 1940 to the end of 2017. HIV incidence is introduced in 1980. In order to calibrate the parameters used in the dynamic transmission model, I generate candidate parameter sets with Latin hypercube sampling [132] using the range of values described in Section 3.8. Model outputs for each candidate parameter set are evaluated against calibration target ranges. Parameter sets that meet all calibration target ranges are accepted. A detailed description of calibration for version one and version two of the model is provided in Chapter 4 and Chapter 5, respectively.

For each accepted parameter set, I continue to execute the model in each region under each care delivery program over a ten-year intervention period from the start of 2018 to the end of 2027. The parameters that depend on the care delivery program are held constant over the intervention period. Program health outcomes and costs are calculated for each region and care delivery program based on the equations in Section 3.7.

The dynamic transmission model was programmed in R version 3.5.2 and the system of differential equations was solved with the deSolve package [130]. I ran the code on Hyak, the University of Washington's supercomputing system, to allow for computations at scale [57].

3.7 Program Health Outcomes and Costs

The calculations of program health outcomes and costs for version one and version two of the model are provided in Section 3.7.1 and Section 3.7.2, respectively. The notation for program health outcomes and costs projected from version one and version two of the model and are summarised in Table 3.3 and Table 3.5, respectively. These metrics are generated based on population states and transition rates in versions one and two of the model. These metrics are used in the application results presented in Chapter 4 and Chapter 5.

3.7.1 Version One: Program Health Outcomes and Costs Equations

This section describes how TB incidence, TB mortality, TB and HIV prevalence, and disability-adjusted life years (DALYs) are projected using population states and transition rates in version one of the model. DALYs represent the years of life lost (YLL) and years lived with disability (YLD) for TB and HIV disease. These metrics are used to calculate discounted and undiscounted program health outcomes and costs over the 10-year intervention period from the start of 2018 to the end of 2027, and discounted and undiscounted incremental cost-effectiveness ratios per TB incidence, TB deaths, and DALYs averted between the care delivery programs as provided in the results of Chapter 4. Model outputs are generated for each care delivery program during the intervention period.

Notation	**Description**
	TB Incidence
$\widehat{TBinc\_per}^{i,p}(y)$	TB incidence rate in year y, per 100,000 individuals in region i under program p
$TBinc\_per\_HIVpos_g^{i,p}(y)$	TB incidence rate for the HIV positive population in year y by gender g, per 100,000 males or females in region i under program p
$TBinc\_per\_HIVneg_g(y)$	TB incidence rate for the HIV negative population in year y by gender g, per 100,000 males or females in region i under program p
	TB Mortality
$TBmort\_per^{i,p}(y)$	TB mortality rate in year y, per 100,000 individuals in region i under program p
$TBmort\_per\_HIVpos_g^{i,p}(y)$	TB mortality rate for the HIV positive population in year y by gender g, per 100,000 males or females in region i under program p

Continued on next page

Table 3.3 – continued from previous page

Notation	Description
$TBmort\_per\_HIVneg_g^{i,p}(y)$	TB mortality rate for the HIV negative population in year y by gender g, per 100,000 males or females in region i under program p
TB and HIV prevalence	
$TBprev\_per^{i,p}(y)$	TB prevalence rate in year y, per 100,000 individuals in region i under program p
$\widehat{HIVprev\_per}_g^{i,p}(y)$	HIV prevalence rate in year y by gender g, per 100,000 males or females in region i under program p,
Disability-Adjusted Life Years (DALYs)	
$YLL\_per^{i,p}(y)$	YLL in year y, per 100,000 individuals in region i under program p
$YLD\_per^{i,p}(y)$	YLD in year y, per 100,000 individuals in region i under program p
$DALY\_per^{i,p}(y)$	DALYs in year y, per 100,000 individuals in region i under program p
Costs	
$\widehat{Cost\_per}^{i,p}(y)$	Costs in year y, per 100,000 individuals in region i under program p
Program Health Outcomes and Costs (Undiscounted)	
$UTBinc\_total^{i,p}$	Total undiscounted incident TB cases over the 10-year intervention period from 2018 to 2027 in region i under program p
$UTBmort\_total^{i,p}$	Total undiscounted TB deaths over the 10-year intervention period from 2018 to 2027 in region i under program p
$UDALY\_total^{i,p}$	Total undiscounted DALYs over the 10-year intervention period from 2018 to 2027 in region i under program p

Continued on next page

Table 3.3 – continued from previous page

Notation	Description
$UCost\_total^{i,p}$	Total undiscounted costs over the 10-year intervention period from 2018 to 2027 in region i under program p
Program Health Outcomes and Costs (Discounted)	
$DTBinc\_total^{i,p}$	Total discounted incident TB cases over the 10-year intervention period from 2018 to 2027 in region i under program p
$DTBmort\_total^{i,p}$	Total discounted TB deaths over the 10-year intervention period from 2018 to 2027 in region i under program p
$DDALY\_total^{i,p}$	Total discounted DALYs over the 10-year intervention period from 2018 to 2027 in region i under program p
$DCost\_total^{i,p}$	Total discounted costs over the 10-year intervention period from 2018 to 2027 in region i under program p
Incremental Cost-Effectiveness Ratios (Undiscounted)	
$UICER\_TBinc^{i}_{\tilde{p},p}$	Undiscounted incremental cost per TB incidence case averted from 2018 to 2027 between the intervention program $\tilde{p}$ and program p in region i
$UICER\_TBmort^{i}_{\tilde{p},p}$	Undiscounted incremental cost per TB death averted from 2018 to 2027 between the intervention program $\tilde{p}$ and program p in region i
$UICER\_DALY^{i}_{\tilde{p},p}$	Undiscounted incremental cost per DALY from 2018 to 2027 between the intervention program $\tilde{p}$ and program p in region i
Incremental Cost-Effectiveness Ratios (Discounted)	
$DICER\_TBinc^{i}_{\tilde{p},p}$	Discounted incremental cost per TB incidence case averted over the intervention period between the intervention program $\tilde{p}$ and program p in region i

Continued on next page

Table 3.3 – continued from previous page

Notation	Description
$DICER\_TBmort^{i}_{\tilde{p},p}$	Discounted incremental cost per TB death averted over the intervention period between the intervention program $\tilde{p}$ and program p in region i
$DICER\_DALY^{i}_{\tilde{p},p}$	Discounted incremental cost per DALY averted over the intervention period between the intervention program $\tilde{p}$ and program p in region i

Table 3.3: Description and notation for program health outcomes and costs generated from version one of the model.

TB Incidence

TB incidence rates per 100,000 individuals are calculated by summing those progressing to active TB (TB compartment 6) from TB compartments 3 (LTBI, recent), 4 (LTBI, remote), 5 (LTBI, on TPT), and 8 (LTBI, after TPT). In this section, $N^{i,p}_{t,r,h,g}(\tau)$ represents the total population in TB compartment $t \in TB'$, DR compartment $r \in DR$, HIV compartment $h \in HIV$, gender compartment $g \in G$, in region $i \in \mathcal{I}$ under program $p \in \mathcal{P}$. Note: only those in HIV compartment 4 (HIV+, and on ART) can initiate TPT and enter TB compartments 5 and 8. TB progression rates from TB compartments 5 and 8 are defined for PLWH on ART. TB incidence rates are calculated by summing over all time steps τ in year y in region i under program p as,

$$\begin{aligned}
\widehat{TBinc_per}^{i,p}(y) = &\sum_{\tau \in y} \sum_{r \in DR} \sum_{h \in HIV} \sum_{g \in G} \theta_h \pi_{recent_prog} N^{i,p}_{3,r,h,g}(\tau) \\
&+ \sum_{\tau \in y} \sum_{r \in DR} \sum_{h \in HIV} \sum_{g \in G} \theta_h \pi_{remote_prog} N^{i,p}_{4,r,h,g}(\tau) \\
&+ \sum_{\tau \in y} \sum_{r \in DR} \sum_{g \in G} \pi^{i}_{on_TPT_prog} N^{i,p}_{5,r,4,g}(\tau) \\
&+ \sum_{\tau \in y} \sum_{r \in DR} \sum_{g \in G} \pi^{i}_{after_TPT_prog} N^{i,p}_{8,r,4,g}(\tau) \qquad \forall i \in \mathcal{I},\ p \in \mathcal{P}. \qquad (3.24)
\end{aligned}$$

Equations for TB incidence rates by year and by gender (per 100,000 males or females) for those who are HIV positive are given in Equation (3.26) and for those who are HIV negative in Equation (3.27). In order to scale rates by gender, model population estimates for each gender compartment g at time τ for region i under program p are calculated and denoted $M\_POP_g^{i,p}(\tau)$. Population estimates for gender compartment g at time τ in region i under program p are calculated as,

$$M\_POP_g^{i,p}(\tau) = \sum_{t \in TB'} \sum_{r \in DR} \sum_{h \in HIV} N_{t,r,h,g}(\tau) \qquad \forall g \in G,\ i \in \mathcal{I},\ p \in \mathcal{P}. \tag{3.25}$$

Equation (3.26) provides the number of TB incident cases for the HIV positive population by gender g at time τ, then scales TB incidence rates for those who are HIV positive per 100,000 males $g = 1$ and 100,000 females $g = 2$ by dividing by population estimates for each gender g, summing over all time steps τ in year y and multiplying by 100,000,

$$\begin{aligned} TBinc\_per\_HIVpos_g^{i,p}(y) = 100,000 \sum_{\tau \in y} & \left(\frac{\sum_{r \in DR} \sum_{h \in \{2,3,4\}} \theta_h \pi_{recent\_prog} N_{3,r,h,g}^{i,p}(\tau)}{M\_POP_g^{i,p}(\tau)} \right) \\ + 100,000 \sum_{\tau \in y} & \left(\frac{\sum_{r \in DR} \sum_{h \in \{2,3,4\}} \theta_h \pi_{remote\_prog} N_{4,r,h,g}^{i,p}(\tau)}{M\_POP_g^{i,p}(\tau)} \right) \\ + 100,000 \sum_{\tau \in y} & \left(\frac{\sum_{r \in DR} \pi_{on\_TPT\_prog}^{i} N_{5,r,4,g}^{i,p}(\tau)}{M\_POP_g^{i,p}(\tau)} \right) \\ + 100,000 \sum_{\tau \in y} & \left(\frac{\sum_{r \in DR} \pi_{after\_TPT\_prog}^{i} N_{8,r,4,g}^{i,p}(\tau)}{M\_POP_g^{i,p}(\tau)} \right) \\ & \forall g \in G,\ i \in \mathcal{I},\ p \in \mathcal{P}. \end{aligned} \tag{3.26}$$

Similarly, Equation (3.27) provides the number of TB incident cases for the HIV negative population by gender g at time τ in program p, and divides by population estimates for each gender g, then summing over all time steps τ in year y and multiplying by 100,000,

$$TBinc\_per\_HIVneg_g^{i,p}(y) = 100,000 \sum_{\tau \in y} \left(\frac{\sum_{r \in DR} \pi_{recent\_prog} N_{3,r,1,g}^{i,p}(\tau)}{M\_POP_g^{i,p}(\tau)} \right) + 100,000 \sum_{\tau \in y} \left(\frac{\sum_{r \in DR} \pi_{remote\_prog} N_{4,r,1,g}^{i,p}(\tau)}{M\_POP_g^{i,p}(\tau)} \right) \quad \forall g \in G,\ i \in \mathcal{I},\ p \in \mathcal{P}. \tag{3.27}$$

The aggregated TB incidence rate in year y, per 100,000 males ($g = 1$) and females ($g = 2$) in region i under program p, is equal to the sum of $TBinc\_per\_HIVpos_g^{i,p}(y)$ plus $TBinc\_per\_HIVneg_g^{i,p}(y)$ by gender g.

TB Mortality

TB mortality per 100,000 individuals projected by the model in region i under program p is calculated by summing those departing the active TB compartment (TB compartment 6) due to death for all time steps τ in year y and is given as,

$$TBmort\_per^{i,p}(y) = \sum_{\tau \in y} \sum_{r \in DR} \sum_{h \in HIV} \sum_{g \in G} \mu_{6,h,g}^{i}(\tau)\ N_{6,r,h,g}^{i,p}(\tau) \qquad \forall i \in \mathcal{I},\ p \in \mathcal{P}. \tag{3.28}$$

TB mortality in region i under program p by gender (per 100,000 males or females) for those who are HIV positive is given in Equation (3.29) and for those who are HIV negative in Equation (3.30). Model population estimates, $M\_POP_g^{i,p}(\tau, p)$, are used to scale TB mortality by gender as described in Equation (3.25). Equation (3.29) provides the number of HIV positive individuals who died at time τ, divided by the number of individuals who are HIV positive by population estimates for each gender g, and summed over all time steps τ in year y and multiplied by 100,000,

$$TBmort\_per\_HIVpos_g^{i,p}(y) = 100,000 \sum_{\tau \in y} \left(\frac{\sum_{r \in DR} \sum_{h \in \{2,3,4\}} \mu_{6,h,g}^{i}(\tau)\ N_{6,r,h,g}^{i,p}(\tau)}{M\_POP_g^{i,p}(\tau)} \right)$$

$$\forall g \in G,\ i \in \mathcal{I},\ p \in \mathcal{P}. \tag{3.29}$$

Similarly, Equation (3.30) provides the number of individuals who died that are HIV negative by gender g at time τ, scaled by population estimates for each gender g, summed over all time steps τ in year y and multiplied by 100,000,

$$TBmort\_per\_HIVneg_g^{i,p}(y) = 100,000 \sum_{\tau \in y} \left(\frac{\sum_{r \in DR} \mu_{6,1,g}^{i}(\tau)\ N_{6,r,1,g}^{i,p}(\tau)}{M\_POP_g^{i,p}(\tau)} \right)$$

$$\forall g \in G,\ i \in \mathcal{I},\ p \in \mathcal{P}. \tag{3.30}$$

The aggregated TB mortality rate in year y, per 100,000 males ($g = 1$) and females ($g = 2$) in region i under program p, is equal to the sum of $TBmort\_per\_HIVpos_g^{i,p}(y)$ and $TBmort\_per\_HIVneg_g^{i,p}(y)$ by each gender g.

TB and HIV Prevalence

TB prevalence represents the proportion of the population in the model with active TB. HIV prevalence represents the proportion of the population that is living with HIV. TB prevalence is provided by year per 100,000 individuals in Equation (3.31). Equation (3.31) calculates the number of individuals with active TB (in TB compartment 6), then sets TB prevalence for year y in region i under program p based on the average TB prevalence over time steps τ in year y,

$$TBprev\_per^{i,p}(y) = \frac{1}{12} \sum_{\tau \in y} \sum_{r \in DR} \sum_{h \in HIV} \sum_{g \in G} N_{6,r,h,g}^{i,p}(\tau) \qquad \forall i \in \mathcal{I},\ p \in \mathcal{P}. \tag{3.31}$$

HIV prevalence represents the proportion of the population who are living with HIV (in HIV

compartments 2, 3, and 4). HIV prevalence is calculated by gender (per 100,000 males and per 100,000 females) and year in Equation (3.32). Equation (3.32) provides the number of HIV positive individuals at time τ, divided by population estimates for each gender g and multiplied by 100,000, and taking the average over all time steps τ in year y,

$$\widehat{HIV prev\_per}_g^{i,p}(y) = 100,000 \left(\frac{1}{12}\right) \sum_{\tau \in y} \left(\frac{\sum_{t \in TB'} \sum_{r \in DR} \sum_{h \in \{2,3,4\}} N_{t,r,h,g}^{i,p}(\tau)}{M\_POP_g^{i,p}(\tau)} \right)$$
$$\forall g \in G,\ i \in \mathcal{I},\ p \in \mathcal{P}. \tag{3.32}$$

Disability-Adjusted Life Years

Disability-adjusted life years (DALYs) are calculated based on years of life lost (YLL) and years lived with disability (YLD) per 100,000 individuals. The years of life lost in year y per 100,000 individuals in region i under program p, $YLL\_per(y)$, is calculated in Equation (3.33) as a measure that represents the number of years lost from premature death for those with active TB and/or HIV positive. It is assumed that any individual with active TB or HIV positive during the intervention period would have survived to the end of the intervention period if they had not died, so YLL is $2028 - \tau$. Equation (3.33) multiplies YLL by the projected number of individuals dying with active TB (in TB compartment 6) and/or HIV positive compartments (HIV 2, 3 and 4), per 100,000 individuals in year y as,

$$\begin{aligned} YLL\_per^{i,p}(y) = & \sum_{\tau \in y} \sum_{r \in DR} \sum_{h \in HIV} \sum_{g \in G} (2028 - \tau)(\mu_{6,h,g}^{i}(\tau)\ N_{6,r,h,g}^{i,p}(\tau)) \\ & + \sum_{\tau \in y} \sum_{\substack{t \in TB' \\ t \neq 6}} \sum_{r \in DR} \sum_{h \in \{2,3,4\}} \sum_{g \in G} (2028 - \tau)(\mu_{t,h,g}^{i}(\tau)\ N_{t,r,h,g}^{i,p}(\tau)) \end{aligned}$$
$$\forall i \in \mathcal{I},\ p \in \mathcal{P}. \tag{3.33}$$

The years lived with disability in year y per 100,000 individuals in region i under program p, $YLD\_per^{i,p}(y)$, is calculated in Equation (3.34) to quantify the impact on quality of life for those

with active TB or living with HIV using disability weights. The parameter $D_{t,h}$ is the disability weight for those in TB compartment t and HIV compartment h. Input parameter values for disability weights $D_{t,h}$ are defined for a year living with TB and/or HIV and are given in Section 3.8.4, Table 3.8. To convert disability weights to monthly estimates, disability weights are multiplied by 1/12,

$$YLD\_per^{i,p}(y) = \sum_{\tau \in y} \left(\sum_{t \in TB'} \sum_{h \in HIV} \frac{1}{12} D_{t,h} \sum_{r \in DR} \sum_{g \in G} N^{i,p}_{t,r,h,g}(\tau) \right) \qquad \forall i \in \mathcal{I},\ p \in \mathcal{P}. \tag{3.34}$$

Disability-adjusted life years (DALYs) are calculated for each program p in each region i by year y, per 100,000 individuals, as the sum of years of life lost (YLL) and years lived with disability (YLD) for each program p by year y such that,

$$DALY\_per^{i,p}(y) = YLL\_per^{i,p}(y) + YLD\_per^{i,p}(y) \qquad \forall i \in \mathcal{I},\ p \in \mathcal{P}. \tag{3.35}$$

Program Costs

Program costs include costs for inpatient and outpatient care for PLWH for causes other than TB, costs to administer TPT, TB treatment costs, and HIV testing costs. The cost in year y per 100,000 individuals in region i under program p, $\widehat{Cost\_per}^{i,p}(y)$, is provided in Equation (3.36). These costs are generated by combining HIV prevalence, the number of individuals on TPT, TB prevalence, and ART initiation estimates from model projections with the cost parameters summarised in Table 3.4.

The input cost parameters $OUTcost^p_h$ and $INcost_h$ represent the yearly cost to administer ART and inpatient cost of care for PLWH for causes other than TB in HIV compartment h, for $h \in \{2, 3, 4\}$. The cost to provide a course of TPT under program p is represented by the parameter $TPTcost^p$. Costs to provide TB treatment are differentiated by drug-resistance status to account for costs associated with the treatment regimens for DS-TB versus MDR-TB. These costs are represented by the parameters $TBCAREcost_r$, for $r \in DR$. The costs of HIV diagnosis to identify a person to initiate ART under care delivery program p is represented by the parameter

$HIVTESTcost^p$.

Notation	Description
	Costs
$OUTcost_h^p$	Annual outpatient HIV care for PLWH in HIV compartment h under program p, for $h \in \{2,3,4\}, p \in \mathcal{P}$
$INcost_h$	Annual inpatient HIV care for PLWH in HIV compartment h, for $h \in \{2,3,4\}$
$TPTcost^p$	Cost to provide a course of TPT for care delivery program p
$TBCAREcost_r$	Cost to provide a course of TB treatment for those with active TB (in TB compartment 6) in DR compartment r, for $r \in DR$
$HIVTESTcost^p$	Cost of HIV testing to find one person to initiate ART for care delivery program p

Table 3.4: Description and notation for parameters used to generate program costs.

The first line in Equation (3.36) calculates outpatient and inpatient costs for PLWH (in HIV compartments 2, 3 and 4) for causes other than TB by multiplying the number of individuals in each HIV positive compartment at time τ by monthly costs of HIV care, where the annual costs of ART and inpatient care, $OUTcost_h^p$ and $INcost_h$, are converted to monthly costs by multiplying by 1/12. ART costs are differentiated by program to account for the additional costs of community-based care. The second line of Equation (3.36) calculates the cost to administer TPT by multiplying the number of individuals on TPT at time τ by monthly costs of administering TPT. Since the TPT cost, $TPTcost^p$, is defined for an entire course of TPT, $TPTcost^p$ is multiplied by $\omega/12$ to get a monthly cost, where $12/\omega$ represents the duration of a TPT course in months. Line three calculates the inpatient and outpatient cost of TB care for those with active TB (in TB compartment 6) and DR compartment r by multiplying the number of individuals with active DS-TB and MDR-TB by monthly TB care costs. The TB care cost, $TBCAREcost_r$, is defined for a course of TB treatment. TB treatment costs are multiplied by $\upsilon_h^i \pi^{recover}/12$ to get monthly costs, where $12/\upsilon_h^i \pi^{recover}$ represents the duration of recovery/treatment in months. Line four calculates HIV testing costs by multiplying the number of individuals initiating ART by the average cost per ART diagnosis and ART initiation. To get yearly costs, monthly costs are summed over each time τ in year y,

$$\begin{aligned}\widehat{Cost\_per}^{i,p}(y) = &\sum_{\tau\in y}\sum_{h\in\{2,3,4\}}\frac{1}{12}(OUTcost_h^p + INcost_h)\sum_{t\in TB'}\sum_{r\in DR}\sum_{g\in G}N_{t,r,h,g}^{i,p}(\tau)\\ &+\sum_{\tau\in y}\frac{1}{12}\omega TPTcost^p\sum_{t\in\{2,5\}}\sum_{r\in DR}\sum_{g\in G}N_{t,r,4,g}^{i,p}(\tau)\\ &+\sum_{\tau\in y}\sum_{r\in DR}\sum_{h\in HIV}\frac{1}{12}\upsilon_h^i\pi^{recover}TBCAREcost_r\sum_{g\in G}N_{6,r,h,g}^{i,p}(\tau)\\ &+\sum_{\tau\in y}\sum_{t\in TB'}\sum_{r\in DR}\sum_{h\in\{2,3\}}\sum_{g\in G}HIVTESTcost^p\eta_{h,4,g}^{i,p}(\tau)N_{t,r,h,g}^{i,p}(\tau)\\ &\forall i\in\mathcal{I},\ p\in\mathcal{P}.\end{aligned}\tag{3.36}$$

Incremental Health Outcomes, Costs, and Cost-Effectiveness Ratios

Discounted and undiscounted health outcomes and costs are calculated for TB incident cases, TB deaths, DALYs, and program costs. Undiscounted incident TB cases, TB deaths, DALYs, and costs are accumulated over the 10-year intervention period from 2018 to 2027 for each program p, and are specified in Equation (3.37), Equation (3.38), Equation (3.39), and Equation (3.40), respectively,

$$UTBinc\_total^{i,p} = \sum_{y\in[2018,2027]}\widehat{TBinc\_per}^{i,p}(y) \qquad \forall i\in\mathcal{I},\ p\in\mathcal{P} \tag{3.37}$$

$$UTBmort\_total^{i,p} = \sum_{y\in[2018,2027]}TBmort\_per^{i,p}(y) \qquad \forall i\in\mathcal{I},\ p\in\mathcal{P} \tag{3.38}$$

$$UDALY\_total^{i,p} = \sum_{y\in[2018,2027]}DALY\_per^{i,p}(y) \qquad \forall i\in\mathcal{I},\ p\in\mathcal{P} \tag{3.39}$$

$$UCost\_total^{i,p} = \sum_{y\in[2018,2027]}\widehat{Cost\_per}^{i,p}(y) \qquad \forall i\in\mathcal{I},\ p\in\mathcal{P}. \tag{3.40}$$

Discounted health outcomes and costs are calculated similarly but are multiplied by a discounting factor, $F(y)$. Metrics are discounted at a rate of 3% (i.e., 0.03) to the present value at the start

of the intervention period in 2018 for each year in the intervention period, *year* $y \in [2018, 2027]$ as,

$$F(y) = \frac{1}{(1+0.03)^{(y-2018)}}. \tag{3.41}$$

Discounted incident TB cases, TB deaths, DALYs, and costs over the 10-year intervention period from 2018 to 2027 are calculated for each program p and converted to 2018 present values with the discounting factor $F(y)$ in Equation (3.42), Equation (3.43), Equation (3.44), and Equation (3.45), respectively,

$$DTBinc\_total^{i,p} = \sum_{y\in[2018,2027]} F(y)\widehat{TBinc\_per}^{i,p}(y) \qquad \forall i \in \mathcal{I},\ p \in \mathcal{P} \tag{3.42}$$

$$DTBmort\_total^{i,p} = \sum_{y\in[2018,2027]} F(y)TBmort\_per^{i,p}(y) \qquad \forall i \in \mathcal{I},\ p \in \mathcal{P} \tag{3.43}$$

$$DDALY\_total^{i,p} = \sum_{y\in[2018,2027]} F(y)DALY\_per^{i,p}(y) \qquad \forall i \in \mathcal{I},\ p \in \mathcal{P} \tag{3.44}$$

$$DCost\_total^{i,p} = \sum_{y\in[2018,2027]} F(y)\widehat{Cost\_per}^{i,p}(y) \qquad \forall i \in \mathcal{I},\ p \in \mathcal{P}. \tag{3.45}$$

These metrics are used to generate undiscounted and discounted incremental cost-effectiveness ratios (ICERs) to assess the per-dollar cost per incident TB case averted, TB death averted, and DALYs averted to compare care delivery intervention programs $\tilde{p}$ to programs p.

For the three combinations of $\tilde{p}$ and p described above and each region $i \in \mathcal{I}$, undiscounted ICERs are calculated for incident TB cases averted, TB deaths averted, and DALYs averted are calculated as in Equation (3.46), Equation (3.47), and Equation (3.48), respectively,

$$UICER\_TBinc^{i}_{\tilde{p},p} = \frac{UCost\_total^{i,\tilde{p}} - UCost\_total^{i,p}}{UTBinc\_total^{i,\tilde{p}} - UTBinc\_total^{i,p}} \tag{3.46}$$

$$UICER\_TBmort^{i}_{\tilde{p},p} = \frac{UCost\_total^{i,\tilde{p}} - UCost\_total^{i,p}}{UTBmort\_total^{i,\tilde{p}} UTBmort\_total^{i,p}} \tag{3.47}$$

$$UICER\_DALY^{i}_{\tilde{p},p} = \frac{UCost\_total^{i,\tilde{p}} - UCost\_total^{i,p}}{UDALY\_total^{i,\tilde{p}} UDALY\_total^{i,p}}. \tag{3.48}$$

For the three combinations of $\tilde{p}$ and p described above and each region $i \in \mathcal{I}$, discounted ICERs are calculated for incident TB cases averted, TB deaths averted, and DALYs averted as in Equation (3.49), Equation (3.50) and Equation (3.51), respectively,

$$DICER\_TBinc^{i}_{\tilde{p},p} = \frac{DCost\_total^{i,\tilde{p}} - DCost\_total^{i,p}}{DTBinc\_total^{i,\tilde{p}} - DTBinc\_total^{i,p}} \tag{3.49}$$

$$DICER\_TBmort^{i}_{\tilde{p},p} = \frac{DCost\_total^{i,\tilde{p}} - DCost\_total^{i,p}}{DTBmort\_total^{i,\tilde{p}} DTBmort\_total^{i,p}} \tag{3.50}$$

$$DICER\_DALY^{i}_{\tilde{p},p} = \frac{DCost\_total^{i,\tilde{p}} - DCost\_total^{i,p}}{DDALY\_total^{i,\tilde{p}} DDALY\_total^{i,p}}. \tag{3.51}$$

3.7.2 Version Two: Program Health Outcomes and Costs Equations

In version two of the model, $N^{i,p}_{t,r,h,g}(\tau)$ represents the total population in TB compartment $t \in TB''$, DR compartment $r \in DR$, HIV compartment $h \in HIV$, gender compartment $g \in G$, in region $i \in \mathcal{I}$ under program $p \in \mathcal{P}$. This section describes how TB incidence, TB- and HIV-related mortality, and HIV prevalence are projected based on population states and transition rates in version two of the model. While yearly TB incidence, HIV prevalence, and program cost rates are also calculated in version one of the model, the variations in model states and transition rates in version one and version two of the model require modified equations to generate health outcome and cost metrics. These metrics are integrated into the multi-objective optimization approach in Chapter 5. Before the intervention period, model outputs represent the standard of care (facility-based ART and TPT care). Model outputs are generated for each care delivery program during the intervention period.

Population estimates for region i in year y are denoted as $GBD\_POP_i(y)$. From 1990 to 2017, $GBD\_POP_i(y)$ is set to yearly regional estimates from GBD 2019 [44]. After 2018, $GBD\_POP_i(y)$ is set to 2017 regional estimates from GBD 2019 [44].

Notation	Description
	TB Incidence
$\widetilde{TBinc\_per}^{i,p}(y)$	TB incidence rate per 100,000 individuals in region i under program p in year y, $i \in \mathcal{I}, p \in \mathcal{P}$ (using the states and transitions in version two)
	HIV Prevalence
$\widetilde{HIVprev\_per}^{i,p}(y)$	HIV prevalence rate per 100,000 individuals in region i under program p in year y, $i \in \mathcal{I}, p \in \mathcal{P}$ (using the states and transitions in version two)
	TB- and HIV-related Mortality
$TBHIVmort\_per^{i,p}(y)$	TB- and HIV-related mortality rate per 100,000 individuals in region i under program p in year y, $i \in \mathcal{I}, p \in \mathcal{P}$,
$TBHIVmort\_pop^{i,p}(y)$	Population-level TB and HIV related deaths in region i under program p in year y, $i \in \mathcal{I}, p \in \mathcal{P}$
	Program Costs
$\widetilde{Cost\_per}^{i,p}(y)$	Cost of administering ART and TPT per 100,000 individuals in region i under program p in year y, $i \in \mathcal{I}, p \in \mathcal{P}$ (using the states and transitions in version two)
$Cost\_pop^{i,p}(y)$	Population-level cost of administering ART and TPT in region i under program p in year y, $i \in \mathcal{I}, p \in \mathcal{P}$

Table 3.5: Description and notation for program health outcomes and costs generated from version two of the model.

TB Incidence

The TB incidence rate per 100,000 individuals for region i under program p in year y, denoted $\widetilde{TBinc\_per}^{i,p}(y)$, is defined in Equation (3.52). The TB incidence rate is calculated by summing those progressing to active TB (TB compartment 6) from TB compartments associated with latent

TB infections (TB compartments 2, 3, 4 and 5) over all time steps τ associated with year y as,

$$\begin{aligned}\widetilde{TBinc\_per}^{i,p}(y) = &\sum_{\tau\in y}\sum_{h\in HIV}\theta_h\pi_{2,6}N^{i,p}_{2,r,h,g}(\tau)\\ &+\sum_{\tau\in y}\sum_{h\in HIV}\theta_h\pi_{recent\_prog}N^{i,p}_{3,r,h,g}(\tau)\\ &+\sum_{\tau\in y}\sum_{h\in HIV}\chi\theta_h\pi_{2,6}N^{i,p}_{4,r,h,g}(\tau)\\ &+\sum_{\tau\in y}\sum_{h\in HIV}\chi\theta_h\pi_{recent\_prog}N^{i,p}_{5,r,h,g}(\tau)\\ &+\sum_{\tau\in y}\sum_{h\in HIV}\pi_{relapse}N^{i,p}_{7,r,h,g}(\tau) \qquad \forall i\in\mathcal{I}, p\in\mathcal{P}. \end{aligned} \tag{3.52}$$

HIV Prevalence

The HIV prevalence rate per 100,000 individuals in region i under program p in year y, denoted $\widetilde{HIVprev\_per}^{i,p}(y)$, is defined in Equation (3.53). The HIV prevalence rate represents the number of individuals living with HIV (in HIV compartments 2, 3, and 4) and is calculated in year y by taking the average number of people living with HIV over all time steps τ in year y as,

$$HIVprev\_per^{i,p}(y) = \left(\frac{1}{12}\right)\sum_{\tau\in y}\sum_{t\in TB''}\sum_{r\in DR}\sum_{h\in\{2,3,4\}}\sum_{g\in G}N^{i,p}_{t,r,h,g}(\tau) \qquad \forall i\in\mathcal{I}, p\in\mathcal{P}. \tag{3.53}$$

TB- and HIV-related Mortality

TB- and HIV-related mortality rate per 100,000 individuals, for region i under program p in year y, denoted $TBHIVmort\_per^{i,p}(y)$, is defined in Equation (3.54) by summing those dying with active TB (in TB compartment 6) and HIV negative (in HIV compartment 1), those with both active TB (in TB compartment 6) and HIV positive (in HIV compartments 2, 3 and 4), those without active TB (not in TB compartment 6) and HIV positive (in HIV compartments 2, 3 and

4) over all time steps τ associated with year y as,

$$\begin{aligned} TBHIVmort\_per^{i,p}(y) = &\sum_{\tau \in y} \sum_{r \in DR} \sum_{g \in G} \mu^{i}_{6,1,g}(\tau)\ N^{i,p}_{6,r,1,g}(\tau) \\ &+ \sum_{\tau \in y} \sum_{r \in DR} \sum_{h \in \{2,3,4\}} \sum_{g \in G} \mu^{i}_{6,h,g}(\tau)\ N^{i,p}_{6,r,h,g}(\tau) \\ &+ \sum_{\tau \in y} \sum_{\substack{t \in TB'', \\ t \neq 6}} \sum_{r \in DR} \sum_{h \in \{2,3,4\}} \sum_{g \in G} \mu^{i}_{t,h,g}(\tau)\ N^{i,p}_{t,r,h,g}(\tau) \\ &\forall i \in \mathcal{I}, p \in \mathcal{P}. \end{aligned} \tag{3.54}$$

The population-level TB- and HIV-related deaths are estimated for region i under program p in year y in Equation (3.55) by scaling TB- and HIV-related mortality rates per 100,000 individuals to population estimates for region i in year y denoted $GBD\_POP_i(y)$ as,

$$TBHIVmort\_pop^{i,p}(y) = \frac{GBD\_POP_i(y)}{100,000} TBHIVmort\_per^{i,p}(y) \forall i \in \mathcal{I}, p \in \mathcal{P}. \tag{3.55}$$

Program Cost

In version two of the model, program costs include the costs to administer ART and TPT, and HIV testing costs in region i under program p in year y per 100,000 individuals denoted $\widetilde{Cost\_per}^{i,p}(y)$ as defined in Equation (3.56). The cost parameter notation is provided in Table 3.4.

The first line in Equation (3.56) calculates the cost to administer TPT per 100,000 individuals by multiplying the number of individuals initiating TPT (from TB compartments 2 and 3) at time τ by the per person cost of administering a 6-month course of TPT under program p denoted, $TPTcost^p$. The second line calculates the cost to administer ART per 100,000 individuals by multiplying the number of individuals on ART (in HIV compartment 4) at time τ by the annual cost per person cost of administering ART under program p denoted $OUTcost^p_4$ scaled to monthly costs. Lines three and four calculate HIV testing costs by multiplying the number of individuals initiating ART by the average cost per ART diagnosis and ART initiation denoted $HIVTESTcost^p$. We sum the costs to administer ART and TPT, and HIV testing costs per 100,000 individuals for all time steps τ associated with year y to calculate program costs per 100,000 individuals in year y

as,

$$\widetilde{Cost\_per}^{i,p}(y) = TPTcost^p \sum_{\tau \in y} \sum_{t \in \{2,3\}} \sum_{r \in DR} \sum_{g \in G} \kappa_{4,g}^{i,p} N_{t,r,4,g}^{i,p}(\tau)$$
$$+ OUTcost_4^p \left(\frac{1}{12}\right) \sum_{\tau \in y} \sum_{t \in TB''} \sum_{r \in DR} \sum_{g \in G} N_{t,r,4,g}^{i,p}(\tau)$$
$$+ HIVTESTcost^p \sum_{\tau \in y} \sum_{t \in TB''} \sum_{r \in DR} \sum_{h \in \{2,3\}} \sum_{g \in G} \eta_{h,4,g}^{i,p}(\tau)\ N_{t,r,h,g}^{i,p}(\tau)$$
$$\forall i \in \mathcal{I}, p \in \mathcal{P}. \tag{3.56}$$

The population-level program costs are estimated for region i under program p in year y in Equation (3.57) by scaling program costs per 100,000 individuals to population estimates for region i in year y denoted $GBD\_POP_i(y)$ as,

$$Cost\_pop^{i,p}(y) = \frac{GBD\_POP_i(y)}{100,000} \widetilde{Cost\_per}^{i,p}(y) \qquad \forall i \in \mathcal{I}, p \in \mathcal{P}. \tag{3.57}$$

3.8 Description of Input Parameters

This section describes the input parameters needed to execute the two versions of the dynamic transmission model and generate program health outcomes and costs. Section 3.8.1 describes how the population in the dynamic transmission model is initialized at the start of 1940 in each region. Section 3.8.2 provides the input parameter values and calibration ranges. Section 3.8.3 describes how parameter values, specifically ART coverage and TPT initiation are calculated for three care delivery programs over the intervention period from the start of 2018 to the end of 2027 based on findings from the DO ART trial [16]. Finally, Section 3.8.4 provides disability weights used to calculate DALYs, and Section 3.8.5 provides the parameter values used to generate costs.

3.8.1 Population

Initial population state values at the start of 1940 are assigned according to estimates for 1990 on the total population, TB prevalence, and LTBI prevalence by gender from GBD 2019 for 15 to 59-year-olds for each region (province) in South Africa [44]. The initial population state values are

scaled proportionally to 100,000 to match the model population.

In version one of the model, the non-zero population compartments in 1940 include TB compartments 1 (Uninfected, not on TPT), 3 (LTBI, recent), 4 (LTBI, remote), and 6 (active TB), HIV compartment 1 (HIV-), and both gender compartments. To estimate the number of individuals uninfected, not on TPT (in TB compartment 1), TB prevalence and LTBI prevalence estimates from GBD 2019 are subtracted from total population estimates. It is assumed that 3.7% of those in LTBI and active TB compartments (TB compartments 3, 4, and 6) are infected with MDR TB [159].

In version two of the model, the non-zero population compartments in 1940 include TB compartments 1 (Uninfected), 2 (LTBI, recent, no TPT), 3 (LTBI, remote, no TPT), and 6 (active TB), HIV compartment 1 (HIV–), and both gender compartments. GBD 2019 estimates the total population, active TB, and LTBI for 1990 by gender. To estimate the number of individuals uninfected with TB (in TB compartment 1), TB prevalence and LTBI prevalence estimates from GBD 2019 are subtracted from total population estimates. It is assumed that 3.7% of those in LTBI and active TB compartments (TB compartments 2, 3, and 6) are infected with MDR TB [159].

3.8.2 Input Parameter Values

Table 3.6 includes the input parameter values and calibration ranges for the parameters needed to execute version one and version two of the dynamic transmission model as summarised in Table 3.1 and Table 3.2. A range of 25% above and below the mean value is used from cited sources for calibrated parameters. A description of the parameters included in the calibration and a description of how the calibration is used to represent model uncertainty in health outcomes and costs for each application of the model is described in Chapter 4 and Chapter 5.

The input parameter values and ranges that are regional-specific are specified by region. The set of regions, $\mathcal{I} = \{1, \ldots, i, \ldots, 9\}$ is defined to correspond to the nine provinces in South Africa, including Eastern Cape ($i = 1$), Free State ($i = 2$), Gaunteng ($i = 3$), KwaZulu-Natal ($i = 4$), Limpopo ($i = 5$), Mpumalanga ($i = 6$), Northern Cape ($i = 7$), North-West ($i = 8$) and Western Cape ($i = 9$). Most input parameters are the same for both version of the model; the input parameters that are only applicable to version one or version two of the model are highlighted

in red in Table 3.6. They include $\iota_r, \chi, \omega, \pi^i_{on\_TPT\_prog}$ and $\pi^i_{after\_TPT\_prog}$. The regional-specific parameters ($\pi^i_{on\_TPT\_prog}$ and $\pi^i_{after\_TPT\_prog}$) are only applicable to version one and are specified for KwaZulu-Natal ($i = 4$), South Africa.

Most input parameters are not time-dependent. Time-varying input parameters are notated as functions of τ in Table 3.6. The values for these parameters are described after Table 3.6 and include rate of TPT initiation for HIV compartment h and gender g in region i under program p, denoted $\kappa^{i,p}_{h,g}(\tau)$, HIV incidence rates for gender g in region i under program p, denoted $\eta^{i,p}_{1,2,g}(\tau)$, ART coverage for gender g for region i under program p, denoted $\sigma^{i,p}_g(\tau)$, the proportion of PLWH (not on ART, with CD4 $>$ 200) of gender g eligible to initiate ART, denoted $\varrho_g(\tau)$, mortality rates for TB compartment t, HIV compartment h and gender g in region i, denoted $\mu^i_{t,h,g}(\tau)$, and allocation of births to TB compartment t, DR compartment r, HIV compartment h and gender compartment g in region i, denoted $\alpha\_in^i_{t,r,h,g}(\tau)$.

Table 3.6: Input parameters used in the dynamic transmission model to describe TB and HIV disease progression. The mean value of calibrated parameters is given with the 25% calibration range. The parameters that are regional-specific are provided by region. The input parameters that are only applicable to version one or version two of the model are highlighted in red. Time-varying parameters, notated as a function of τ, are described after the table. Program-specific parameters are highlighted in green. HIV infection rates are highlighted in blue to indicate that they are indirectly impacted by program.

Parameter description	Value [Calibration Range]	Reference
Parameters that Impact TB Force of Infection		
β^i_g Number of effective contacts for TB transmission per year for gender g in region i:		[152]
Males in Eastern Cape, β^1_1	14 [10.5, 17.5]	
Females in Eastern Cape, β^1_2	14 [10.5, 17.5]	
Males in Free State, β^2_1	14 [10.5, 17.5]	
Females in Free State, β^2_2	14 [10.5, 17.5]	
Males in Gauteng, β^3_1	14 [10.5, 17.5]	
Females in Gauteng, β^3_2	14 [10.5, 17.5]	
Males in KwaZulu-Natal, β^4_1	14 [10.5, 17.5]	
Females in KwaZulu-Natal, β^4_2	14 [10.5, 17.5]	

Continued on next page

Table 3.6 – continued from previous page

Parameter description	Value [Calibration Range]	Reference
Males in Limpopo, β_1^5	14 [10.5, 17.5]	
Females in Limpopo, β_2^5	14 [10.5, 17.5]	
Males in Mpumalanga, β_1^6	14 [10.5, 17.5]	
Females in Mpumalanga, β_2^6	14 [10.5, 17.5]	
Males in Northern Cape, β_1^7	14 [10.5, 17.5]	
Females in Northern Cape, β_2^7	14 [10.5, 17.5]	
Males in North-West, β_1^8	14 [10.5, 17.5]	
Females in North-West, β_2^8	14 [10.5, 17.5]	
Males in Western Cape, β_1^9	14 [10.5, 17.5]	
Females in Western Cape, β_2^9	14 [10.5, 17.5]	
ϕ_h Relative transmissibility of TB for those in HIV compartment h:		[56, 80]
HIV−, ϕ_1	1 (fixed value)	
HIV+, Not on ART, CV4 $>$ 200, ϕ_2	0.9 [0.675, 1.125]	
HIV+, Not on ART, CV4 $\leq$ 200, ϕ_3	0.6 [0.45, 0.75]	
HIV+, On ART, ϕ_4	0.9 [0.675, 1.125]	
ε Fraction of new TB infections that are MDR TB	0.037 [0.02775, 0.04625]	[159]
ι_r Diminished risk of acquiring a latent TB infection of strain r while uninfected and on TPT (only applicable in version one), such that:		
DS TB, ι_1	0.43 [0.3225, 0.5375]	[37]
MDR TB, ι_2	1 (fixed value)	
ξ Increased risk of reinfection after recovery/treatment of active TB	4 [3, 5]	[153]
ζ Partially protective effect of LTBI against acquiring a new TB infection	0.4 [0.3, 0.5]	[37, 56, 76, 153]
Parameters that Describe TB Progression		
$1/\omega$ Duration of TPT course (years) (only applicable to version one)	0.5 (fixed value)	[16]
γ_r Indicator to reflect that those infected with DS LTBI ($r = 1$) yield benefits of TPT, whereas those with MDR LTBI do not yield benefits of TPT:		

Continued on next page

Table 3.6 – continued from previous page

Parameter description	Value [Calibration Range]	Reference
DS strain, γ_1	1 (fixed value)	
MDR strain, γ_2	0 (fixed value)	
$1/\pi_{recent\_remote}$ Duration of LTBI recently infected period (years)	2 (fixed value)	[155]
π_{recent_prog} Rate of TB progression from recent LTBI to active TB	0.025 [0.01875, 0.03125]	[38, 79]
π_{remote_prog} Rate of TB progression from remote LTBI to active TB	0.001 [0.00075, 0.00125]	[31, 45]
$\pi_{relapse}$ Rate of TB progression from recovered/treated to active TB,	0.01 [0.0075, 0.0125]	[29]
$\pi^4_{on\_TPT\_prog}$ Rate of TB progression from LTBI on TPT to active TB in KwaZulu-Natal (only applicable to version one of the model)	0.0113 [0.0085, 0.0142]	[116]
$\pi^4_{after\_TPT\_prog}$ Rate of TB progression from LTBI after TPT to active TB in KwaZulu-Natal (only applicable to version one of the model)	0.0113 [0.0085, 0.0142]	[116]
θ_h Relative risk of TB progression from LTBI to active TB for individuals in HIV compartment h:		
HIV−, θ_1	1 (fixed value)	
HIV+, not on ART, CD4 $>$ 200, θ_2	10 [7.5, 12.5]	[12, 158]
HIV+, not on ART, CD4 $\leq$ 200, θ_3	17 [12.75, 21.25]	[2, 23]
HIV+, on ART, θ_4	3 [2.25, 5.25]	[134, 135]
χ Relative risk of TB progression for those with LTBI treated with TPT (only applicable in version two of the model)	0.68 [0.51, 0.85]	[116]
$\pi_{recover}$ Rate of recovery/treatment from active TB	2 (fixed value)	[69]
$1/(\upsilon^i_h \pi_{recover})$ Duration of active TB (years) that reflect differences in treatment for individuals by HIV compartment h in:		[69]
Eastern Cape and HIV−, $1/(\upsilon^1_1 \pi_{recover})$	2.0 [1.6, 2.7]	
Eastern Cape and HIV+, not on ART, CD4 $>$ 200, $1/(\upsilon^1_2 \pi_{recover})$	1.5 [1.2, 2.0]	

Continued on next page

Table 3.6 – continued from previous page

Parameter description	Value [Calibration Range]	Reference
Eastern Cape and HIV+, not on ART, CD4 $\leq$ 200, $1/(\upsilon_3^1\pi_{recover})$	1.5 [1.2, 2.0]	
Eastern Cape and HIV+, on ART, $1/(\upsilon_4^1\pi_{recover})$	1.5 [1.2, 2.0]	
Free State and HIV−, $1/(\upsilon_1^2\pi_{recover})$	2.0 [1.6, 2.7]	
Free State and HIV+, not on ART, CD4 $>$ 200, $1/(\upsilon_2^2\pi_{recover})$	1.5 [1.2, 2.0]	
Free State and HIV+, not on ART, CD4 $\leq$ 200, $1/(\upsilon_3^2\pi_{recover})$	1.5 [1.2, 2.0]	
Free State and HIV+, on ART, $1/(\upsilon_4^2\pi_{recover})$	1.5 [1.2, 2]	
Gauteng and HIV−, $1/(\upsilon_1^3\pi_{recover})$	2.0 [1.6, 2.7]	
Gauteng and HIV+, not on ART, CD4 $>$ 200, $1/(\upsilon_2^3\pi_{recover})$	1.5 [1.2, 2.0]	
Gauteng and HIV+, not on ART, CD4 $\leq$ 200, $1/(\upsilon_3^3\pi_{recover})$	1.5 [1.2, 2.0]	
Gauteng and HIV+, on ART, $1/(\upsilon_4^3\pi_{recover})$	1.5 [1.2, 2]	
KwaZulu-Natal and HIV−, $1/(\upsilon_1^4\pi_{recover})$	2.0 [1.6, 2.7]	
KwaZulu-Natal and HIV+, not on ART, CD4 $>$ 200, $1/(\upsilon_2^4\pi_{recover})$	1.5 [1.2, 2.0]	
KwaZulu-Natal and HIV+, not on ART, CD4 $\leq$ 200, $1/(\upsilon_3^4\pi_{recover})$	1.5 [1.2, 2.0]	
KwaZulu-Natal and HIV+, on ART, $1/(\upsilon_4^4\pi_{recover})$	1.5 [1.2, 2.0]	
Limpopo and HIV−, $1/(\upsilon_1^5\pi_{recover})$	2.0 [1.6, 2.7]	
Limpopo and HIV+, not on ART, CD4 $>$ 200, $1/(\upsilon_2^5\pi_{recover})$	1.5 [1.2, 2.0]	
Limpopo and HIV+, not on ART, CD4 $\leq$ 200, $1/(\upsilon_3^5\pi_{recover})$	1.5 [1.2, 2.0]	
Limpopo and HIV+, on ART, $1/(\upsilon_4^5\pi_{recover})$	1.5 [1.2, 2.0]	
Mpumalanga and HIV−, $1/(\upsilon_1^6\pi_{recover})$	2.0 [1.6, 2.7]	
Mpumalanga and HIV+, not on ART, CD4 $>$ 200, $1/(\upsilon_2^6\pi_{recover})$	1.5 [1.2, 2.0]	
Mpumalanga and HIV+, not on ART,	1.5 [1.2, 2.0]	

Continued on next page

Table 3.6 – continued from previous page

Parameter description	Value [Calibration Range]	Reference
CD4 $\leq$ 200, $1/(\upsilon_3^6 \pi_{recover})$		
Mpumalanga and HIV+, on ART, $1/(\upsilon_4^6 \pi_{recover})$	1.5 [1.2, 2.0]	
Northern Cape and HIV−, $1/(\upsilon_1^7 \pi_{recover})$	2.0 [1.6, 2.7]	
Northern Cape and HIV+, not on ART, CD4 $>$ 200, $1/(\upsilon_2^7 \pi_{recover})$	1.5 [1.2, 2.0]	
Northern Cape and HIV+, not on ART, CD4 $\leq$ 200, $1/(\upsilon_3^7 \pi_{recover})$	1.5 [1.2, 2.0]	
Northern Cape and HIV+, on ART, $1/(\upsilon_4^7 \pi_{recover})$	1.5 [1.2, 2.0]	
North-West and HIV−, $1/(\upsilon_1^8 \pi_{recover})$	2 [1.6, 2.7]	
North-West and HIV+, not on ART, CD4 $>$ 200, $1/(\upsilon_2^8 \pi_{recover})$	1.5 [1.2, 2.0]	
North-West and HIV+, not on ART, CD4 $\leq$ 200, $1/(\upsilon_3^8 \pi_{recover})$	1.5 [1.2, 2.0]	
North-West and HIV+, on ART, $1/(\upsilon_4^8 \pi_{recover})$	1.5 [1.2, 2.0]	
Western Cape and HIV−, $1/(\upsilon_1^9 \pi_{recover})$	2 [1.6, 2.7]	
Western Cape and HIV+, not on ART, CD4 $>$ 200, $1/(\upsilon_2^9 \pi_{recover})$	1.5 [1.2, 2.0]	
Western Cape and HIV+, not on ART, CD4 $\leq$ 200, $1/(\upsilon_3^9 \pi_{recover})$	1.5 [1.2, 2.0]	
Western Cape and HIV+, on ART, $1/(\upsilon_4^9 \pi_{recover})$	1.5 [1.2, 2.0]	
$\kappa_{h,g}^{i,p}(\tau)$ Rate of TPT initiation for those in HIV compartment h and gender g at time τ in region i under program p. The rate of TPT initiation is based on mean TPT initiation rates in year y for those in HIV compartment h and gender compartment g under program p, denoted $\kappa\_VAL_{h,g}^{p}(y)$, and the TPT calibration factor for region i, denoted κ_FACTOR^{i}, defined below.		

Continued on next page

Table 3.6 – continued from previous page

Parameter description	Value [Calibration Range]	Reference
$\kappa\_VAL^{p}_{h,g}(y)$ Mean TPT initiation rates in year y for those in HIV compartment h and gender compartment g under program p	Time-varying	[16, 117]
κ_FACTOR^{i} TPT calibration factor for individuals in:		
Eastern Cape κ_FACTOR^{1}	1 [0.75, 1.25]	
Free State κ_FACTOR^{2}	1 [0.75, 1.25]	
Gauteng κ_FACTOR^{3}	1 [0.75, 1.25]	
KwaZulu-Natal κ_FACTOR^{4}	1 [0.75, 1.25]	
Limpopo κ_FACTOR^{5}	1 [0.75, 1.25]	
Mpumalanga κ_FACTOR^{6}	1 [0.75, 1.25]	
Northern Cape κ_FACTOR^{7}	1 [0.75, 1.25]	
North-West κ_FACTOR^{8}	1 [0.75, 1.25]	
Western Cape κ_FACTOR^{9}	1 [0.75, 1.25]	
Parameters that Describe HIV Progression		
$\eta^{i,p}_{1,2,g}(\tau)$ Rate of HIV incidence from HIV compartment (HIV–) to HIV compartment 2 (HIV+, not on ART, CD4 $>$ 200) for gender g at time τ in region i under program p. The rate of HIV incidence is based on regional mean HIV incidence rates for gender g in year y in region i under program p, $\eta\_VAL^{i,p}_{1,2,g}(y)$, and the HIV incidence rate calibration factor for region i by gender g, denoted $\eta\_FACTOR^{i}_{1,2,g}$, defined below.		
$\eta\_VAL^{i,p}_{1,2,g}(y)$ Mean HIV incidence rates for gender g in year y in region i under program p	Time-varying	[44, 111]
$\eta\_FACTOR^{i}_{1,2,g}$ HIV incidence rate calibration factor for individuals in:		
Males in Eastern Cape $\eta\_FACTOR^{1}_{1,2,1}$	1 [0.75, 1.25]	
Females in Eastern Cape $\eta\_FACTOR^{1}_{1,2,2}$	1 [0.75, 1.25]	

Continued on next page

Table 3.6 – continued from previous page

Parameter description	Value [Calibration Range]	Reference
Males in Free State $\eta\_FACTOR^{2}_{1,2,1}$	1 [0.75, 1.25]	
Females in Free State $\eta\_FACTOR^{2}_{1,2,1}$	1 [0.75, 1.25]	
Males in Gauteng $\eta\_FACTOR^{3}_{1,2,1}$	1 [0.75, 1.25]	
Females in Gauteng $\eta\_FACTOR^{3}_{1,2,2}$	1 [0.75, 1.25]	
Males in KwaZulu-Natal $\eta\_FACTOR^{4}_{1,2,1}$	1 [0.75, 1.25]	
Females in KwaZulu-Natal $\eta\_FACTOR^{4}_{1,2,2}$	1 [0.75, 1.25]	
Males in Limpopo $\eta\_FACTOR^{5}_{1,2,1}$	1 [0.75, 1.25]	
Females in Limpopo $\eta\_FACTOR^{5}_{1,2,2}$	1 [0.75, 1.25]	
Males in Mpumalanga $\eta\_FACTOR^{6}_{1,2,1}$	1 [0.75, 1.25]	
Females in Mpumalanga $\eta\_FACTOR^{6}_{1,2,2}$	1 [0.75, 1.25]	
Males in Northern Cape $\eta\_FACTOR^{7}_{1,2,1}$	1 [0.75, 1.25]	
Females in Northern Cape $\eta\_FACTOR^{7}_{1,2,2}$	1 [0.75, 1.25]	
Males in North-West $\eta\_FACTOR^{8}_{1,2,1}$	1 [0.75, 1.25]	
Females in North-West $\eta\_FACTOR^{8}_{1,2,2}$	1 [0.75, 1.25]	
Males in Western Cape $\eta\_FACTOR^{9}_{1,2,1}$	1 [0.75, 1.25]	
Females in Western Cape $\eta\_FACTOR^{9}_{1,2,2}$	1 [0.75, 1.25]	
$1/\eta_{2,3,g}$ Duration of time spent in HIV compartment 2 (HIV+, not on ART, CD4 < 200) for gender g:		[118]
Males $1/\eta_{2,3,1}$	7.72 [5.79, 9.65]	
Females $1/\eta_{2,3,2}$	10.25 [7.6875, 12.8125]	
$\sigma_g^{i,p}(\tau)$ ART coverage for gender g at time τ in region i under program p. ART coverage is based on mean ART coverage for gender g in year y under program p, $\sigma\_VAL_g^p(y)$, and the ART calibration factor for PLWH in region i, denoted σ_FACTOR^i, defined below.		
$\sigma\_VAL_g^p(y)$ Mean ART coverage for gender g in year y under program p	Time-varying	[16, 117]
σ_FACTOR^i ART coverage calibration factor for PLWH in:		

Continued on next page

Table 3.6 – continued from previous page

Parameter description	Value [Calibration Range]	Reference
Eastern Cape σ_FACTOR^1	1 [0.75, 1.25]	
Free State σ_FACTOR^2	1 [0.75, 1.25]	
Gauteng σ_FACTOR^3	1 [0.75, 1.25]	
KwaZulu-Natal σ_FACTOR^4	1 [0.75, 1.25]	
Limpopo σ_FACTOR^5	1 [0.75, 1.25]	
Mpumalanga σ_FACTOR^6	1 [0.75, 1.25]	
Northern Cape σ_FACTOR^7	1 [0.75, 1.25]	
North-West σ_FACTOR^8	1 [0.75, 1.25]	
Western Cape σ_FACTOR^9	1 [0.75, 1.25]	
$\varrho_g(\tau)$ Proportion of the population in HIV compartment 2 (HIV+, not on ART, CD4 $>$ 200) eligible to initiate ART by gender at time τ.	Time-varying	[111]
Parameters that Describe Entries and Exits from the Population		
$\mu^i_{t,h,g}(\tau)$ Mortality rates for those in TB compartment t, HIV compartment h, and gender compartment g in region i at time τ. Mortality rates are calculated based on the regional mean baseline mortality rates by gender g in year y in region i, denoted $\mu\_VAL^i_g(y)$, and three calibrated parameters including the mortality rate calibration factor, denoted $\mu\_FACTOR^i_g$ for region i and gender g, the increased risk of HIV-related mortality for those without active TB, denoted $\hat{R}_h$ and HIV-related mortality for those with active TB, denoted $\tilde{R}_h$ for those in HIV compartment h, defined below.		
$\mu\_VAL^i_g(y)$ Mean baseline mortality rates by gender g in year y in region i	Time-varying	[44]
$\mu\_FACTOR^i_g$ Mortality rate calibration factor for:		

Continued on next page

Table 3.6 – continued from previous page

Parameter description	Value [Calibration Range]	Reference
Males in Eastern Cape $\mu\_FACTOR_1^1$	1 [0.75, 1.25]	
Females in Eastern Cape $\mu\_FACTOR_2^1$	1 [0.75, 1.25]	
Males in Free State $\mu\_FACTOR_1^2$	1 [0.75, 1.25]	
Females in Free State $\mu\_FACTOR_2^2$	1 [0.75, 1.25]	
Males in Gauteng $\mu\_FACTOR_1^3$	1 [0.75, 1.25]	
Females in Gauteng $\mu\_FACTOR_2^3$	1 [0.75, 1.25]	
Males in KwaZulu-Natal $\mu\_FACTOR_1^4$	1 [0.75, 1.25]	
Females in KwaZulu-Natal $\mu\_FACTOR_2^4$	1 [0.75, 1.25]	
Males in Limpopo $\mu\_FACTOR_1^5$	1 [0.75, 1.25]	
Females in Limpopo $\mu\_FACTOR_2^5$	1 [0.75, 1.25]	
Males in Mpumalanga $\mu\_FACTOR_1^6$	1 [0.75, 1.25]	
Females in Mpumalanga $\mu\_FACTOR_2^6$	1 [0.75, 1.25]	
Males in Northern Cape $\mu\_FACTOR_1^7$	1 [0.75, 1.25]	
Females in Northern Cape $\mu\_FACTOR_2^7$	1 [0.75, 1.25]	
Males in North-West $\mu\_FACTOR_1^8$	1 [0.75, 1.25]	
Females in North-West $\mu\_FACTOR_2^8$	1 [0.75, 1.25]	
Males in Western Cape $\mu\_FACTOR_1^9$	1 [0.75, 1.25]	
Females in Western Cape $\mu\_FACTOR_2^9$	1 [0.75, 1.25]	
$\hat{R}_h$ Increased risk of mortality for those with no active TB that are:		[2, 12, 96, 101, 103]
HIV–, $\hat{R}_1$	1 (fixed value)	
HIV+, not on ART, CD4 $>$ 200, $\hat{R}_2$	8 [6, 10]	
HIV+, not on ART, CD4 $\leq$ 200, $\hat{R}_3$	26 [19.5, 32.5]	
HIV+, on ART, $\hat{R}_4$	1.35 [1.2, 1.5]	
$\tilde{R}_h$ Increased risk of mortality for those with active TB that are:		[2, 8, 12, 96, 101, 103]
HIV–, $\tilde{R}_1$	15.5 [11.625, 19.375]	
HIV+, not on ART, CD4 $>$ 200, $\tilde{R}_2$	26 [19.5, 32.5]	
HIV+, not on ART, CD4 $\leq$ 200, $\tilde{R}_3$	50 [37.5, 62.5]	
Active TB and HIV+, on ART, $\tilde{R}_4$	18.5 [13.875, 23.125]	

Continued on next page

Table 3.6 – continued from previous page

Parameter description	Value [Calibration Range]	Reference
$\alpha\_in^{i}_{t,r,h,g}(\tau)$ Proportion of the population in region i that enters into TB compartment t, DR compartment r, HIV compartment h, and gender compartment g and time τ in region i	Time-varying	[44, 159]
Rate of exit from the population due to aging	$1/(60-15)$ (fixed value)	

TPT Initiation Rates

TPT initiation rates, $\kappa^{i,p}_{h,g}(\tau)$ for those in HIV compartment h and gender g in region i under program p, vary over time according to the calculated mean yearly TPT initiation rate estimates, $\kappa\_VAL^{p}_{h,g}(y)$. A calibrated regional multiplication factor, κ_FACTOR^{i}, is used to capture regional diversities in TPT initiation rates and is used to adjust all yearly TPT initiation rate estimates in region i for both genders using the range indicated in Table 3.6. The mean yearly TPT rate estimate is multiplied by the regional calibration factor, and it is assumed the monthly TPT initiation rate is the same for all months within the year y, that is,

$$\kappa^{i,p}_{h,g}(\tau) = \kappa\_FACTOR^{i}\ \kappa\_VAL^{p}_{h,g}(y) \qquad \forall h \in HIV,\ g \in G,\ \tau \in y,\ i \in \mathcal{I},\ p \in \mathcal{P}. \tag{3.58}$$

Only those in HIV compartment 4 (HIV+, on ART) are assumed to initiate TPT, so mean yearly TPT initiation rates are set to zero for those not in HIV compartment 4, i.e., $\kappa\_VAL^{p}_{1,g}(y) = \kappa\_VAL^{p}_{2,g}(y) = \kappa\_VAL^{p}_{3,g}(y) = 0$ for all y, $g \in G$, $p \in \mathcal{P}$. For those in HIV compartment 4, mean yearly TPT initiation rates $\kappa\_VAL^{p}_{4,g}(y)$ change over time according to TPT availability and program (during the intervention period). From 1940 to 2004, the mean yearly TPT initiation rates are set to zero for those in HIV compartment 4, i.e., $\kappa\_VAL^{p}_{4,g}(y) = 0$, to indicate that TPT was not widely available in South Africa.

Mean yearly TPT initiation rates for those in HIV compartment 4 by gender g are linearly interpolated from zero in 2004 (the year before TPT became widely available) to the value in 2018 for the standard facility-based ART and TPT program. During the intervention period from

2018 to 2027, the yearly mean TPT initiation rate for gender g, $\kappa\_VAL^{p}_{4,g}(y)$, is held constant and is provided by program p based on findings from the DO ART study [16, 117] as described in Section 3.8.3.

HIV Incidence Rates

HIV incidence rates, $\eta^{i,p}_{1,2,g}(\tau)$ for gender g in region i under program p, vary over time according to calculated mean yearly HIV incidence rates by gender g in region i under program p, $\eta\_VAL^{i,p}_{1,2,g}(y)$. A calibrated regional multiplication factor by gender, $\eta\_FACTOR^{i}_{1,2,h}$, is used to adjust yearly regional HIV incidence rate estimates by gender g in region i under all programs using the range indicated in Table 3.6. Each mean yearly incidence rate estimate is multiplied by the regional multiplication factor by gender and assume the monthly incidence rate is the same for all months within the year, that is,

$$\eta^{i,p}_{1,2,g}(\tau) = \eta\_FACTOR^{i}_{1,2,g}\ \eta\_VAL^{i,p}_{1,2,g}(y) \qquad \forall g \in G,\ \tau \in y,\ i \in \mathcal{I},\ p \in \mathcal{P}. \tag{3.59}$$

From 1940 to 1979, the mean yearly HIV incidence estimates are set to zero, i.e., $\eta\_VAL^{i,p}_{1,2,g}(y) = 0$, to represent the assumption that there is no HIV incidence in the model during the time. HIV incidence is introduced at the beginning of 1980. Between 1980 and 1990, the mean yearly HIV incidence rate is linearly interpolated from zero in 1979 to the regional estimate in 1990. Between 1990 and 2017, the mean yearly HIV incidence estimates are set to yearly estimates from GBD 2019 for males and females between the ages of 15 to 59-year-olds in each region in South Africa [44]. For the years in the intervention period, starting at the beginning of 2018 and continuing through the end of 2027, the mean yearly regional HIV incidence estimates are projected for each program by applying rate of change, denoted $\eta\_ROC^{p}_{1,2,g}(y)$ for year y under program p, that decrease regional HIV incidence estimates from the prior year, as

$$\eta\_VAL^{i,p}_{1,2,g}(y) = \eta\_ROC^{p}_{1,2,g}(y)\eta\_VAL^{i,p}_{1,2,g}(y-1) \qquad \forall g \in G,\ i \in \mathcal{I},\ p \in \mathcal{P}. \tag{3.60}$$

The rate of change $\eta\_ROC^{p}_{1,2,g}(y)$, are projected by the Data-driven Recommendations for Interventions against Viral Infection (DRIVE) model [111] using the mean ART coverage values for

each program provided in Table 3.7. While the DRIVE model [111] projects that HIV incidence will decrease each year for all programs, it projects that HIV incidence for community-based ART programs (community-based ART with standard facility-based TPT and community-based ART with TPT) will decrease at a higher rate than the standard facility-based ART program (standard facility-based ART and TPT) due to the indirect impacts of increased ART coverage on HIV incidence rates.

Regional HIV incidence yearly estimates by gender under each program are represented in Figure 3.4, where the values for community-based ART programs (community-based ART with standard facility-based TPT and community-based ART with TPT) are distinct from the standard facility-based ART program (standard facility-based ART and TPT) during the intervention period for the years between 2018 and 2027.

ART Coverage

ART coverage, $\sigma_g^{i,p}(\tau)$ for gender g in region i under program p, varies over time according to the calculated mean yearly ART coverage estimate $\sigma\_VAL_g^p(y)$. A regional calibrated multiplication factor, σ_FACTOR^i, is used to capture regional diversities in ART coverage and is used to adjust all yearly ART coverage estimates in region i for both genders using the range indicated in Table 3.6. Each mean yearly ART coverage estimate is multiplied by the regional multiplication factor, and it is assumed the monthly ART coverage is the same for all months within the year y, that is,

$$\sigma_g^{i,p}(\tau) = \sigma\_FACTOR^i \ \sigma\_VAL_g^p(y) \qquad \forall g \in G,\ \tau \in y,\ i \in \mathcal{I},\ p \in \mathcal{P}. \tag{3.61}$$

The mean yearly ART coverage estimates are the same under both versions for the corresponding programs described in Section 3.8.3. Mean yearly ART coverage estimates $\sigma\_VAL_g^p(y)$ change over time according to ART availability in South Africa and program as described in Section 3.4. Before 2004, ART is not available, so mean yearly ART coverage for both genders are set to zero, i.e., $\sigma\_VAL_1^p(y) = \sigma\_VAL_2^p(y) = 0$, to represent that ART is not available until the start of 2004. Between 2004 (when ART became widely available) and 2018, ART coverage estimates are linearly interpolated from zero in 2003 to the value in 2018 for the standard facility-based ART and TPT program. During the intervention period, ART coverage varies by program and is held constant

from the beginning of 2018 to the end of 2027, with the values for $\sigma\_VAL_g^p(y)$ based on findings from the DO ART study [16, 117] and provided in Table 3.7.

Proportion of PLWH (not on ART, with CD4 >200) Eligible to Initiate ART

The proportion of PLWH not on ART with CD4 >200 that are eligible to initiate ART, denoted $\varrho_g(\tau)$ by gender g at time τ, correspond to changes in clinical guidance on ART eligibility described in Section 3.4. Between the start of 1940 and the end of 2010, no one in HIV compartment 2 (HIV+, not on ART, CD4 > 200) is eligible to initiate ART, i.e., $\varrho_g(\tau) = 0$. Between the start of 2011 to the end of 2015, the proportions of those in HIV compartment 2 (HIV+, not on ART, CD4 > 200) by gender that are eligible to initiate ART are set to estimates projected by the DRIVE model [111], such that $0 < \varrho_g(\tau) < 1$. From the start of 2016, all those in HIV compartment 2 (HIV+, not on ART, CD4 > 200) are eligible to initiate ART, i.e., $\varrho_g(\tau) = 1$.

Regional Mortality Rates by TB and HIV Compartments

Mortality rates for populations in TB compartment t, HIV compartment h for gender g at time τ in region i, denoted $\mu^i_{t,h,g}(\tau)$, represent mortality due to causes that are not TB-related or HIV-related. Mortality rates vary over time according to calculated yearly regional mean baseline mortality rate estimates, denoted $\mu\_VAL^i_g(y)$ in region i and gender g. A calibrated regional multiplication factor, $\mu\_FACTOR^i_g$, is used to adjust all yearly regional mean baseline mortality rate estimates in region i by gender g using the range indicated in Table 3.6. The increased risk of mortality is represented by $\hat{R}_h$ (for those in TB compartments 1, 2, 3, 4, 5, 7, or 8 in TB' and TB compartments 1, 2, 3, 4, 5, or 7 in TB'') and $\tilde{R}_h$ (for those in TB compartment 6 in TB' or TB''). It is calibrated with the ranges provided in Table 3.6. To obtain $\mu^i_{t,h,g}(\tau)$, the regional mean baseline mortality rates for each gender are multiplied by the increased risk of mortality and the regional multiplication factor, and we assume the monthly mortality rate is the same for all months within the year, that is,

$$\mu^i_{t,h,g}(\tau) = \begin{cases} \mu\_VAL^i_g(y)\ \mu\_FACTOR^i_g \hat{R}_h, & \text{for } t \in TB', t \neq 6 \text{ or for } t \in TB'', t \neq 6 \\ \mu\_VAL^i_g(y)\ \mu\_FACTOR^i_g \tilde{R}_h, & \text{for } t \in \{6\}, \end{cases}$$

$$\forall h \in HIV, g \in G,\ \tau \in y,\ i \in \mathcal{I}. \tag{3.62}$$

The yearly baseline mortality rates, $\mu\_VAL^i_g(y)$, are calculated in Equation (3.63) using yearly regional GBD 2019 estimates (provided for the years 1990 to 2017) on the number of deaths from all causes, denoted $ALLMORT^i_g(y)$ the number of TB- and HIV-related deaths, denoted $TBHIVMORT^i_g(y)$ and population estimates, denoted $GBD\_POP^i_g(y)$ by gender g in year y in region i for males and females between the ages of 15 to 59-year-olds in each region South Africa. In Equation (3.63), the number of TB-related and HIV-related deaths are subtracted from deaths from all causes to calculate the number of deaths from causes not related to TB or HIV. This value is divided by population estimates to convert the number of deaths into a rate. This data is used to calculate the yearly baseline mortality rates, $\mu\_VAL^i_g(y)$, for the years 1990 to 2017 as,

$$\mu\_VAL^i_g(y) = \frac{ALLMORT^i_g(y) - TBHIVMORT^i_g(y)}{GBD\_POP^i_g(y)} \qquad \forall g \in G,\ i \in \mathcal{I}. \tag{3.63}$$

From the start of 1940 to the end of 1989, the yearly baseline mortality rates, $\mu\_VAL^i_g(y)$, are set to the 1990 estimates. During the intervention period, for the years 2018 to 2027, yearly baseline mortality rates are held constant at 2017 estimates. Mean yearly baseline mortality rates $\mu\_VAL^i_g(y)$ for each gender g in year y in region i are illustrated in Figure 3.5.

Regional Allocation of Births to TB and HIV Compartments

A proportion of births entering the model at time τ, $\alpha\_in^i_{t,r,h,g}(\tau)$, are based on GBD 2019 projections for 10 to 15-year-olds for each region i in South Africa [44]. GBD 2019 provides regional projections on the number of males and females with active TB living with HIV, LTBI, and population estimates for the years 1990 to 2017. We use these estimates to allocate a proportion of births to uninfected (TB compartment 1 in both versions), LTBI compartments (TB compartments

3 and 4 in version one; TB compartments 2 and 3 in version two), and active TB (TB compartment 6 in both versions), distinguished by drug resistance, HIV status, and gender that are representative of changes in population characteristics over time. We scale population estimates in each of these compartments for each year to percentages so that the total number of individuals aging into the model equals the total number of individuals aging out of the model as described in Section 3.4.

Since GBD 2019 does not estimate the number of individuals uninfected with TB (in TB compartment 1 in both versions) and HIV negative, the number of males and females uninfected with TB (TB compartment 1 in both versions) and HIV negative (HIV compartment 1 in both versions) is calculated by subtracting out the number of males and females with active TB, LTBI or HIV positive from population estimates. We do not allocate births to TB compartments associated with TPT (TB compartments 2, 5, and 8 in version one; TB compartments 4 and 5 in version two) or recovery from TB (TB compartment 7 in both versions), such that $\alpha\_in^{i}_{t,r,h,g}(\tau) = 0$ for $t \in \{2, 5, 8, 7\} \subset TB'$, $t \in \{4, 5, 7\} \subset TB''$ for all τ.

GBD 2019 does not distinguish LTBIs by LTBI infected recently, no TPT (TB compartment 3 in version one; TB compartment 2 in version two), and LTBI infected remotely, no TPT (TB compartment 3 in version one; TB compartment 3 in version two). We assume that those aging into the model (on their 15th birthday) were equally likely to be exposed in each year prior to aging into the model, such that 2/15 of LTBIs are recent (exposed within the past two years), and 13/15 of LTBI are remote (exposed more than two years ago). The GBD 2019 study also does not differentiate LTBI projections by drug resistance or HIV status. We assume that the proportion of LTBIs that are MDR corresponds to estimates from the 2020 Global Tuberculosis Report [2] and that the proportion of LTBIs that are associated with PLWH correspond to yearly HIV prevalence estimates from GBD 2019. GBD 2019 does not provide HIV prevalence among levels of HIV disease severity, so we assign all PLWH who age into the model into HIV compartment 2 (HIV+, not on ART, CD4 $>$ 200).

For τ associated with the years between 1940 and 1979 (before HIV incidence is introduced in the model) new entries are only assigned to HIV compartment 1 (HIV–) according to 1990 estimates (aggregated over HIV status), such that $\alpha\_in^{i}_{t,r,h,g}(\tau) = 0$ for $h \in \{2, 3, 4\}$ for all time steps τ associated with the years 1940 to 1979. After 1980, all those with HIV are assigned to HIV

compartment 2 (HIV+, not on ART, CD4 > 200).

For τ associated with the years between 1980 and 1989, $\alpha\_in^{i}_{t,r,h,g}(\tau)$ is set to 1990 estimates. Between the start of 1990 to the end of 2017, the proportion of births allocated to each compartment changes according to yearly estimates. From 2018 and 2027, we assign new entries based on 2017 estimates.

3.8.3 Parameter Values for Care Delivery Programs

This section describes three modeled care delivery programs: standard facility-based ART and TPT care, community-based ART with standard facility-based TPT care, and community-based ART with TPT care. The programs considered in each application of the model are defined in Chapter 4 and Chapter 5.

The input parameters that depend on the care program include ART coverage for gender g under program p, denoted $\sigma\_VAL^{p}_{g}(\tau)$, and TPT initiation rates for those in HIV compartment h and gender g under program p, $\kappa\_VAL^{p}_{h,g}(\tau)$. ART coverage for gender g under program p, $\sigma\_VAL^{p}_{g}(\tau)$, represents the proportion of PLWH on ART, that is, the ratio of those in HIV compartment 4 to those in HIV positive compartments (in HIV compartments 2, 3, and 4). TPT initiation rates under program p, $\kappa\_VAL^{p}_{h,g}(\tau)$, represent the proportion of those in HIV compartment h and gender g that initiate TPT. The model assumes only PLWH on ART (in HIV compartment 4) initiate TPT, such that $\kappa\_VAL^{p}_{h,g}(\tau) = 0,\ h \in \{1, 2, 3\}$.

ART coverage and TPT initiation rates vary for each program based on observations from the DO ART trial [16]. The impact of the programs on ART coverage and TPT initiation rates among PLWH on ART over the program intervention period from the beginning of 2018 to the end of 2027 are provided in Table 3.7. These input parameters are held constant over the intervention period for the times associated with the years between 2018 and 2027.

Standard facility-based ART and TPT care delivery reflects the levels of ART coverage and TPT initiation rates among PLWH on ART observed in the facility-based care arm of the DO ART trial [16]. Community-based ART with TPT care delivery reflects the levels of ART coverage and TPT initiation rates observed in the community-based care arm of the DO ART trial. Community-based ART was only tested in the DO ART trial with a nested community-based TPT care program;

however, in Chapter 4, community-based ART without community-based TPT is evaluated to test the independent effects of community-based ART on TB incidence and TB mortality. We do this by setting ART coverage for community-based ART with standard facility-based TPT to the same values as in the community-based ART with TPT care delivery program. We back out the TPT initiation percentage among PLWH on ART for community-based ART with standard facility-based TPT by equating the TPT initiation percentage among all PLWH (including those on ART and not on ART) to the values from standard facility-based ART and TPT care delivery.

Program Name	**ART Coverage %** $\sigma\_VAL_g^p(\tau)$		**TPT initiation % among PLWH on ART** $\kappa\_VAL_{4,g}^p(\tau)$	
	Male $g=1$	*Female* $g=2$	*Male* $g=1$	*Female* $g=2$
Standard facility-based ART and TPT care	49	69	29	27
Community-based ART with standard facility-based TPT care	82	83	17	22
Community-based ART with TPT care	82	83	70	75

Table 3.7: Care delivery programs and parameter values for time periods associated with the years in the intervention period from 2018 to 2027.

ART Coverage

Mean ART coverage estimates for gender g, $\sigma\_VAL_g^p(\tau)$ are provided in Equation (3.64). Mean ART coverage estimates vary for each program p, based on the proportion of participants in the DO ART trial that achieved viral suppression under program p, denoted VS_g^p. The estimates account for the proportion of PLWH on ART of gender g under program p who achieve viral suppression with the parameter AT_g^p, and the proportion of PLWH diagnosed with HIV by gender g under program p with the parameter DH_g^p. The proportion of PLWH on ART of gender g under program p who achieve viral suppression, AT_g^p, and the proportion of PLWH diagnosed with HIV of gender g under program p, DH_g^p, is based on findings from the 2017 South African National HIV Prevalence, Incidence, Behaviour, and Communication Survey [129]. It is assumed all those who are virally

suppressed are on ART; however, some proportion of those on ART are not virally suppressed. The proportions of male and female participants that achieved viral suppression in the DO ART trial, VS_g^p, are divided by the proportion of PLWH on ART of gender g who achieve viral suppression under program p, AT_g^p, in Equation (3.64) to calculate the proportion of participants in the trial who are on ART, including participants that are both virally suppressed on ART and not virally suppressed on ART. All participants in the trial on ART know their status; however, our model considers PLWH who do not know their status. The proportion of the HIV positive population on ART is calculated by gender g under program p, $\sigma\_VAL_g^p(\tau)$, in Equation (3.64) by multiplying the proportion of participants in the trial who are on ART (VS_g^p/AT_g^p) by the proportion of PLWH diagnosed with HIV, DH_g^p, as

$$\sigma\_VAL_g^p(\tau) = DH_g^p \left(\frac{VS_g^p}{AT_g^p} \right) \qquad \forall g \in G,\ \mathcal{P}. \tag{3.64}$$

ART coverage estimates are based on the proportion of PLWH who achieve viral suppression under facility-based care and community-based care in the DO ART trial [16]. Under the standard facility-based care arm in the DO ART trial, 51% of male participants and 70% of female participants achieved viral suppression, i.e., $VS_1^p = 51\%, VS_2^p = 70\%$. Under the community-based care arm in the DO ART trial, 72% of male participants and 73% of female participants achieved viral suppression, i.e., $VS_1^p = 72\%, VS_2^p = 73\%$ [44].

The proportion of PLWH on ART who achieve viral suppression and the proportion of PLWH diagnosed with HIV are based on population-based survey data [129]. The 2017 South African National HIV Prevalence, Incidence, Behaviour, and Communication Survey [129] estimates 82% of males, 90% of females, and 88% of both males and females are virally suppressed given they are on ART. It is assumed that the proportion of PLWH on ART of gender g who achieve viral suppression, AT_g varies by gender under facility-based care, but is the same for both genders under community-based care to account for one of the findings from the DO ART trial that the community-based ART care intervention closed the gender gap in terms of the proportion of individuals virally suppressed given they are on ART treatment compared to the standard facility-based care [16]. Under standard facility-based ART and TPT care, $AT_1^p = 82\%$ and $AT_2^p = 90\%$. Under community-based ART

with TPT care, it is assumed that the proportion of PLWH who achieve viral suppression is the same for both genders, $AT_1^p = AT_2^p = 88\%$.

The 2017 South African National HIV Prevalence, Incidence, Behaviour, and Communication Survey [129] estimates 78% and 90% of males and females living with HIV know their status. Under the standard facility-based ART and TPT care program, $DH_1^p = 78\%, DH_2^p = 90\%$. The community-based care arm of the DO ART trial includes community-wide HIV testing, so it is assumed that all PLWH in community-based ART with TPT care program know their status such that $DH_1^p = DH_2^p = 100\%$.

These values are used to generate the ART coverage estimates as presented in Table 3.7 for standard facility-based ART and TPT care delivery for males ($78\% \times 51\%/82\% = 49\%$) and females ($90\% \times 70\%/90\% = 69\%$); and community-based ART with TPT care delivery for males ($100\% \times 72\%/88\% = 82\%$) and females ($100\% \times 73\%/88\% = 83\%$). The same ART coverage is assumed under community-based ART with standard facility-based TPT care delivery as in community-based ART with TPT care delivery.

TPT Initiation Rates

TPT initiation rates $\kappa\_VAL_{h,g}^p(\tau)$, $h = 4$ for standard facility-based ART and TPT care delivery are based on observations from the DO ART trial of the proportion of PLWH on ART who initiated TPT in the standard facility-based ART and TPT care trial group (29% among men on ART, 27% among women on ART). TPT initiation rates for community-based ART with TPT care delivery are also based on observations from the DO ART trial of the proportion of PLWH on ART who initiated TPT in the community-based ART and TPT care group (70% among men on ART, 75% among women on ART).

Community-based ART with standard facility-based TPT care delivery was not observed in the DO ART trial but is modeled to test the independent effect of community-based ART without changing the proportion of PLWH who initiate TPT. We infer the proportion of PLWH on ART who initiate TPT by gender g, $\kappa\_VAL_{h,g}^p(\tau), h = 4$ for community-based ART with standard TPT care delivery, so that TPT initiation rates among all PLWH are the same in standard facility-based ART and TPT care delivery as in community-based ART with standard TPT care delivery

while accounting for the differences in ART coverage under community-based ART care. The TPT initiation rates among all PLWH for standard facility-based ART and TPT care delivery is approximately equal to $\sigma\_VAL_g^p \kappa\_VAL_{4,g}^p(\tau)$, i.e., for males $40\% \times 29\% = 0.1421$, and for females $69\% \times 27\% = 0.1863$. Given values for $\sigma\_VAL_g^p(\tau)$ for community-based ART with standard TPT care delivery, as in Table 3.7, we solve for $\kappa\_VAL_{4,g}^p(\tau)$ for community-based ART with standard TPT care delivery. Hence, for community-based ART with standard TPT care delivery, for males, $\kappa\_VAL_{4,1}^p(\tau) = 0.1421/82\% = 17\%$, and for females, $\kappa\_VAL_{4,2}^p(\tau) = 0.1863/83\% = 22\%$.

3.8.4 Parameter Values for Disability-Adjusted Life Years

In version one of the model, disability weights are used in conjunction with projected model states to calculate Disability-Adjusted Life Years (DALYs) as described in Section 3.7.1, Equation (3.35). Since these parameter values only apply to version one of the model, all TB compartments in this section refer to those in TB'. Disability weights for those in TB compartment t and HIV compartment h, denoted $D_{t,h}$ are provided in Table 3.8. Those without active TB (not in TB compartment 6) or without HIV (in HIV compartment 1) have an associated disability weight of zero. Disability weights associated with active TB (in TB compartment 6) or HIV (in HIV compartments 2, 3, and 4) are from GBD 2019 [43].

The disability weights associated with PLWH without active TB from GBD 2019 include stratification over CD4 levels, ART status and anemia levels. Since anemia levels of PLWH are not tracked in the dynamic transmission model, we apply the disability weight corresponding to mild anemia to all PLWH (in HIV compartments 2, 3 and 4) without active TB (not in TB compartment 6) since mild anemia is common among PLWH [24]. While TPT can affect levels of anemia, the impact is not substantial [137].

The disability weights associated with TB among PLWH from GBD 2019 are not distinguished among levels of HIV disease severity. We apply the disability weight associated with TB among PLWH to those in HIV compartment 2 (HIV+, not on ART, CD4 $>$ 200) and TB compartment 6 (active TB). For those in HIV compartment 3 (HIV+, not on ART, CD4 $\leq$ 200) and active TB (in TB compartment 6), We apply the disability weight associated with PLWH without active TB, with a CD4 count of less than 200, with mild anemia to reflect the severity of a CD4 count below

200. For PLWH on ART with active TB (in TB compartment 6 and HIV compartment 4), we assume the same disability as those with active TB who are not living with HIV.

Parameter Description	Value	Reference
$D_{t,h}$ Disability weights for those in TB compartment t and HIV compartment h, per year		[43]
No active TB and HIV-, $D_{t,1},\ \text{for } t \in TB',\ t \neq 6$	0 (no disability)	
No active TB and HIV+, not on ART, CD4 > 200, $D_{t,2},\ \text{for } t \in TB',\ t \neq 6$	0.016	
No active TB and HIV+, not on ART, CD4 $\leq$ 200 $D_{t,3},\ \text{for } t \in TB',\ t \neq 6$	0.583	
No active TB and HIV+, on ART $D_{t,4},\ \text{for } t \in TB',\ t \neq 6$	0.081	
Active TB and HIV-, $D_{6,1}$	0.333	
Active TB and HIV+, not on ART, CD4 > 200, $D_{6,2}$	0.411	
Active TB and HIV+, not on ART, CD4 $\leq$ 200, $D_{6,3}$	0.583	
Active TB and HIV+, on ART $D_{6,4}$	0.333	

Table 3.8: Input parameters values for disability weights used to calculate disability-adjusted life-years (DALYs).

3.8.5 Parameter Values for Program Costs

The costs in 2018 US dollars are estimated from cited sources for TB and HIV preventative treatments and care as provided in Table 3.9. These estimates are used to calculate the projected cost of each program using Equation (3.36) and Equation (3.56) in Section 3.7.1.

For PLWH on ART, outpatient HIV care costs include the costs associated with administering ART, which is differentiated by delivery method to account for additional costs associated with community-based care versus facility-based care [16]. The inpatient HIV care costs in Table 3.9 exclude costs of care for TB-related hospitalization. The total reported HIV inpatient care costs from cited sources include costs of TB-related hospitalization; however, the costs of TB-related inpatient care are subtracted from the total reported HIV inpatient care costs. The estimated HIV

Parameter Description	Value	Reference
$OUTcost_h$ Annual outpatient HIV care costs for PLWH who are:		
Not on ART $OUTcost_h, h \in \{2, 3\}$	135	[46]
On ART $OUTcost_h, h = 4$ under		
Standard facility-based ART care	249	[16]
Community-based ART care	310	[16]
$INcost_h$ Annual inpatient HIV care costs for PLWH who are:		
Not on ART, CD4 > 200 $OUTcost_2$	62	[88]
Not on ART, CD4 ≤ 200 $OUTcost_3$	162	[88]
On ART $OUTcost_4$	151	[88]
$HIVTESTcost^p$ Cost of HIV testing to find one person to initiate ART under all standard and facility-based care programs	24	[16, 90]
$TPTcost^p$ Cost of a 6-month course of TPT with isoniazid under all standard and facility-based care programs	20	[22, 67, 116, 131]
$TBCAREcost_r$ Cost of a course of TB treatment for people with		
DS-TB, $TBCARECost_1$	259	[22]
MDR-TB, $TBCARECost_2$	1,889	[81]

Table 3.9: Input parameter notation and values used in the cost model. Costs are provided in 2018 US dollars. Costs provided in the table are rounded to the nearest dollar.

testing cost is based on the assumption that programs typically test multiple individuals for HIV before finding an eligible person to initiate ART screening. Based on the screening and enrollment results from the DO ART trial [16], we use a ratio of 5.4 individuals tested for one individual found to be eligible, and the cost per HIV test of $4.44 [90]. To obtain the cost of HIV testing to find one person to initiate ART, we multiply 5.4 by $4.44. TPT community-based care is nested in the community-based ART care intervention and only provided to those already on ART, so there are no additional costs associated with community-based TPT care versus facility-based care [16]. TPT costs are defined over a six-month course of TPT and include the cost of the medication ($8) [131], provider time for counseling ($12) [22], outpatient care for TPT-associated drug-induced liver injury (DILI) ($6 \times 0.00293 \times \$4$) [67, 116], and provider laboratory costs for TPT-associated DILI ($6 \times 0.00293 \times \$14$) [67, 116], where 0.00293 reflects the probability of developing DILI per month of TPT use. Costs for TB treatment are defined for a course of TB treatment and differentiated

by DS-TB and MDR-TB infections to account for the different medication and provider time costs of these treatment regimens [81].

3.9 Conclusion and Future Work

In this chapter, I introduced two versions of a dynamic transmission compartmental model that describe TB and HIV disease progression with considerations for TB drug resistance and gender. Version one of the dynamic transmission compartmental model is applied to KwaZulu-Natal, South Africa, under three care delivery programs presented in Chapter 4. Version two of the dynamic transmission compartmental model is modified to simulate TB and HIV disease progression in all nine provinces in South Africa under two care delivery programs and integrated into a budget allocation approach as described in Chapter 5. Version one of the dynamic transmission model accounts for the reduced risk of infection while on TPT; however, it does not distinguish those with LTBI treated with TPT by recent and remote infection. The rate at which those with LTBI treated with TPT progress to active TB is specific to assumptions regarding the proportion of those LTBI treated with TPT with recent and remote infection in a region. In version two of the dynamic transmission model, those with LTBI are tracked according to recent and remote infection in order to better account for the reduced risk of TB progression across regions. However, to reduce complexity, version two does not account for the reduced risk of infection while on TPT. For a six-month course of TPT, which is modeled in version one, I found the impact of the reduced risk of infection while on TPT was minimal. However, for a longer course of TPT, this might not be a reasonable assumption.

The two versions of the dynamic transmission model do not take into account both the reduced risk of infection while on TPT and the differing rates of TB progression for those with recent and remote LTBI and treated with TPT. In future research, it would be interesting to develop a model that considers both of these factors. Figure 3.6 illustrates TB transitions for a possible future version of the model, where the dynamic transmission model considers both the reduced risk of infection while on TPT and the differing rates of TB progression for those with recent and remote LTBI and treated with TPT.

The two versions of the dynamic transmission model were created to answer specific questions

related to their applications, as presented in Chapter 4 and Chapter 5. It is crucial to incorporate reasonable assumptions into future model design to generate accurate outputs that can answer the critical questions posed by decision makers and stakeholders.

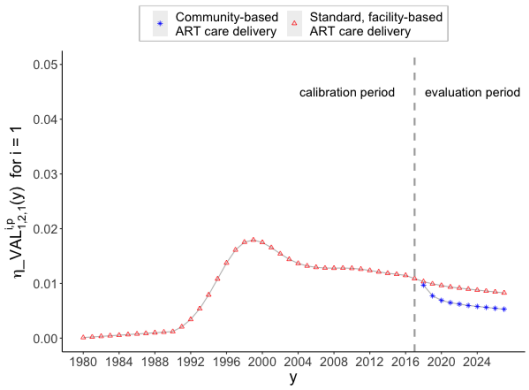

(a) Mean HIV incidence rate in year y for males in Eastern Cape, $\eta\_VAL^{1,p}_{1,2,1}(y)$

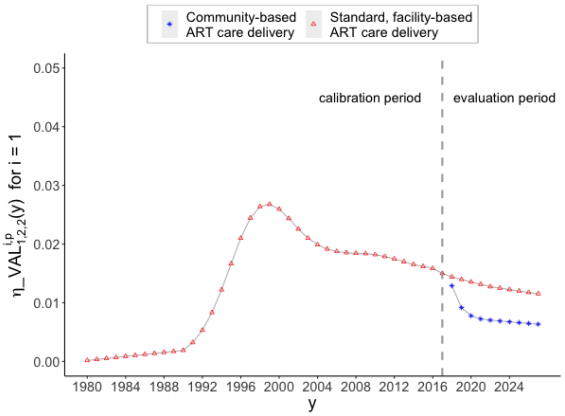

(b) Mean HIV incidence rate in year y for females in Eastern Cape, $\eta\_VAL^{1,p}_{1,2,2}(y)$

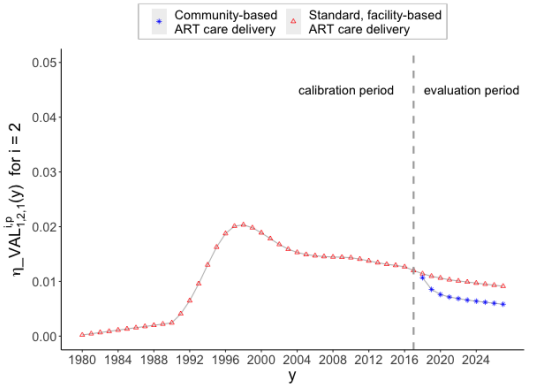

(c) Mean HIV incidence rate in year y for males in Free State, $\eta\_VAL^{2,p}_{1,2,1}(y)$

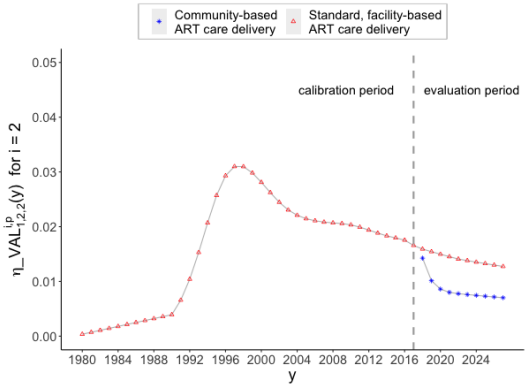

(d) Mean HIV incidence rate in year y for females in Free State, $\eta\_VAL^{2,p}_{1,2,2}(y)$

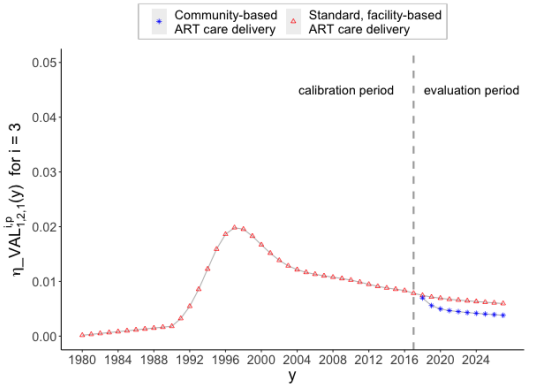

(e) Mean HIV incidence rate in year y for males in Gauteng, $\eta\_VAL^{3,p}_{1,2,1}(y)$

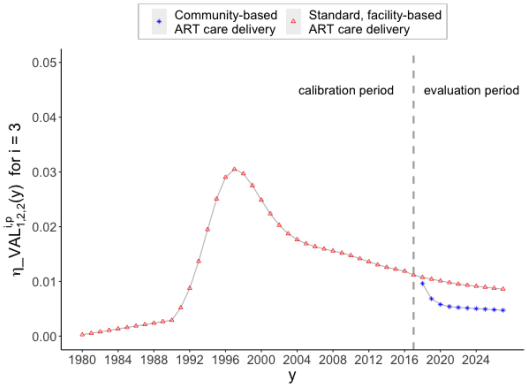

(f) Mean HIV incidence rate in year y for females in Gauteng, $\eta\_VAL^{3,p}_{1,2,2}(y)$

Figure continued on the next page

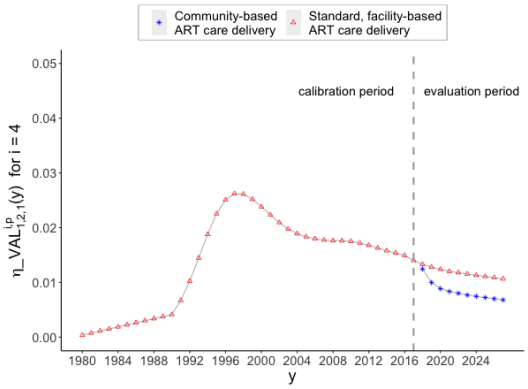

(a) Mean HIV incidence rate in year y for males in KwaZulu-Natal, $\eta\_VAL^{4,p}_{1,2,1}(y)$

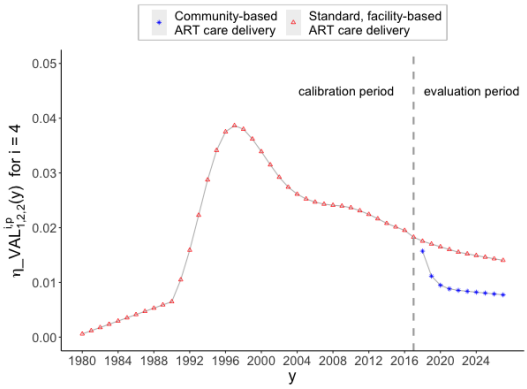

(b) Mean HIV incidence rate in year y for females in KwaZulu-Natal, $\eta\_VAL^{4,p}_{1,2,2}(y)$

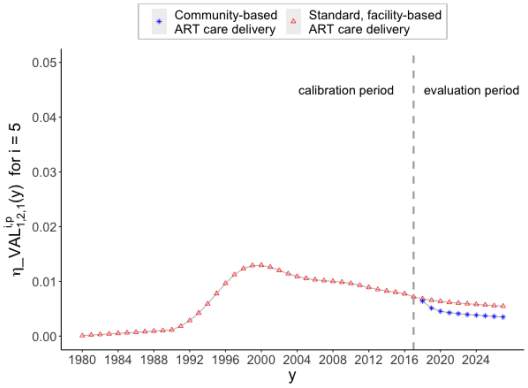

(c) Mean HIV incidence rate in year y for males in Limpopo, $\eta\_VAL^{5,p}_{1,2,1}(y)$

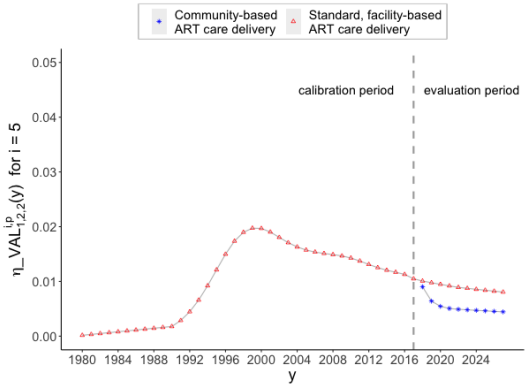

(d) Mean HIV incidence rate in year y for females in Limpopo, $\eta\_VAL^{5,p}_{1,2,2}(y)$

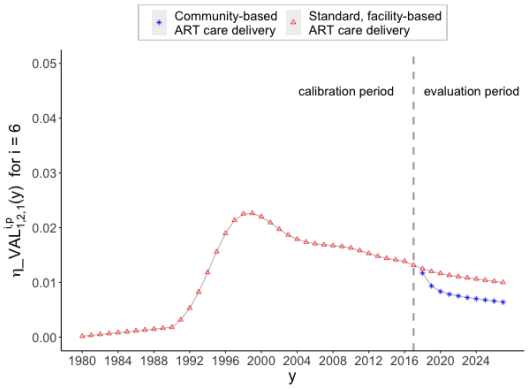

(e) Mean HIV incidence rate in year y for males in Mpumalanga, $\eta\_VAL^{6,p}_{1,2,1}(y)$

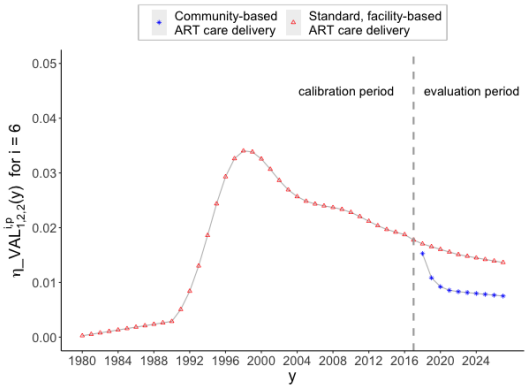

(f) Mean HIV incidence rate in year y for females in Mpumalanga, $\eta\_VAL^{6,p}_{1,2,2}(y)$

Figure continued on the next page

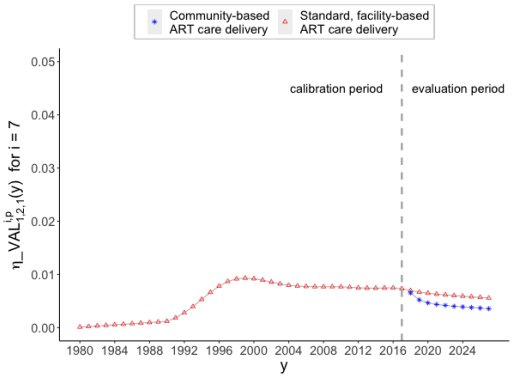

(a) Mean HIV incidence rate in year y for males in Northern Cape, $\eta\_VAL^{7,p}_{1,2,1}(y)$

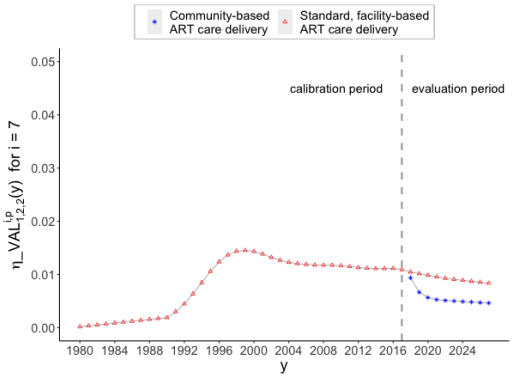

(b) Mean HIV incidence rate in year y for females in Northern Cape, $\eta\_VAL^{7,p}_{1,2,2}(y)$

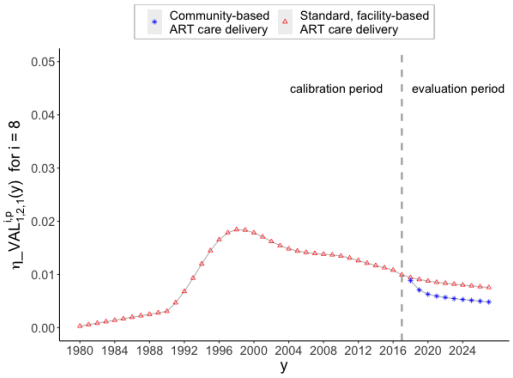

(c) Mean HIV incidence rate in year y for males in North-West, $\eta\_VAL^{8,p}_{1,2,1}(y)$

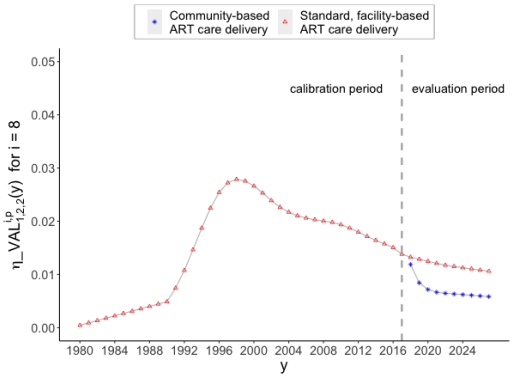

(d) Mean HIV incidence rate in year y for females in North-West, $\eta\_VAL^{8,p}_{1,2,2}(y)$

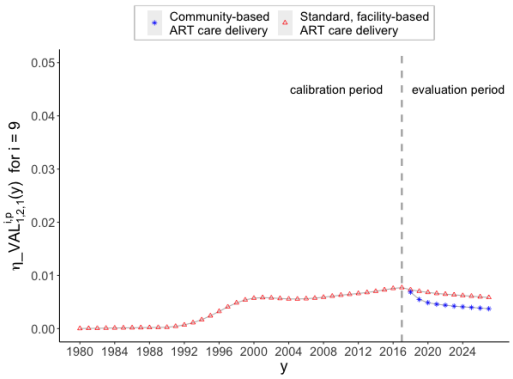

(e) Mean HIV incidence rate in year y for males in Western Cape, $\eta\_VAL^{9,p}_{1,2,1}(y)$

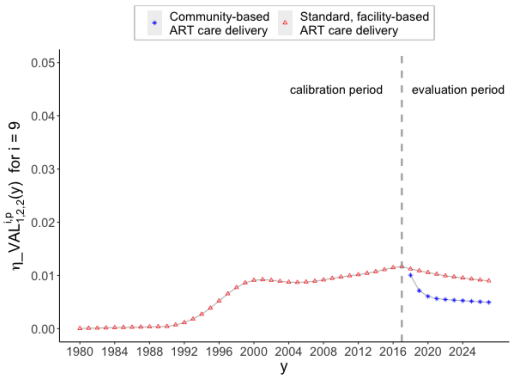

(f) Mean HIV incidence rate in year y for females in Western Cape, $\eta\_VAL^{9,p}_{1,2,2}(y)$

Figure 3.4: Yearly mean HIV incidence estimates for males, $\eta\_VAL^{i}_{1,2,1}(y)$, and females, $\eta\_VAL^{i}_{1,2,2}(y)$ for region i from 1980 to 2027. Over the intervention period between 2018 and 2027, HIV estimates are distinguished by facility-based and community-based ART programs. HIV incidence rate estimates for standard facility-based ART programs are in blue (stars), and incidence rate estimates for community-based ART programs are in red (triangles).

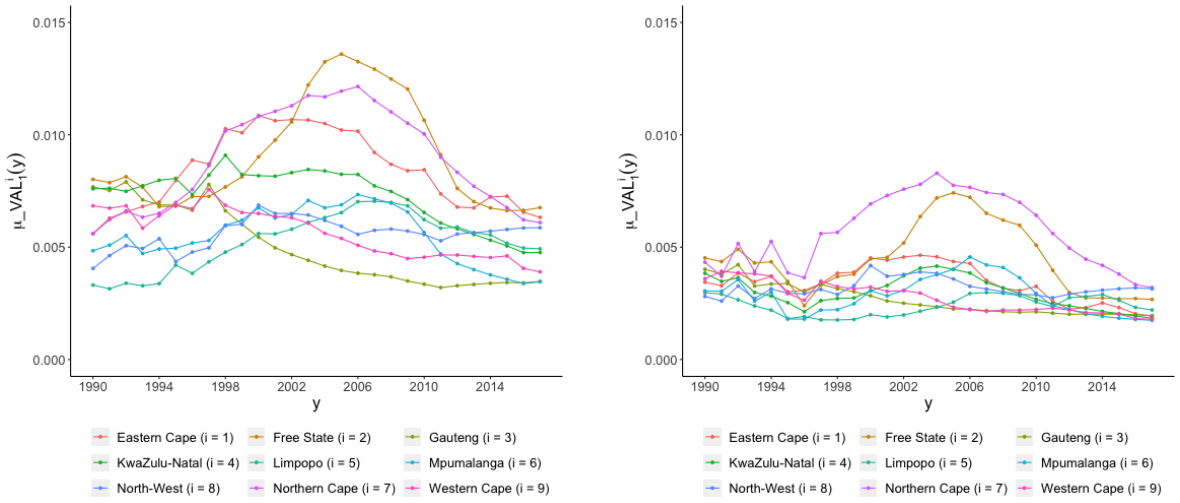

(a) Mean baseline mortality rates, for year y and males, $\mu\_VAL_1^i(y)$ by region i

(b) Mean baseline mortality rates, for year y and females, $\mu\_VAL_2^i(y)$ by region i

Figure 3.5: Mean yearly baseline mortality rate estimates for males, $\mu\_VAL_1^i(y)$, and females, $\mu\_VAL_2^i(y)$, by region i from 1990 to 2017 [44].

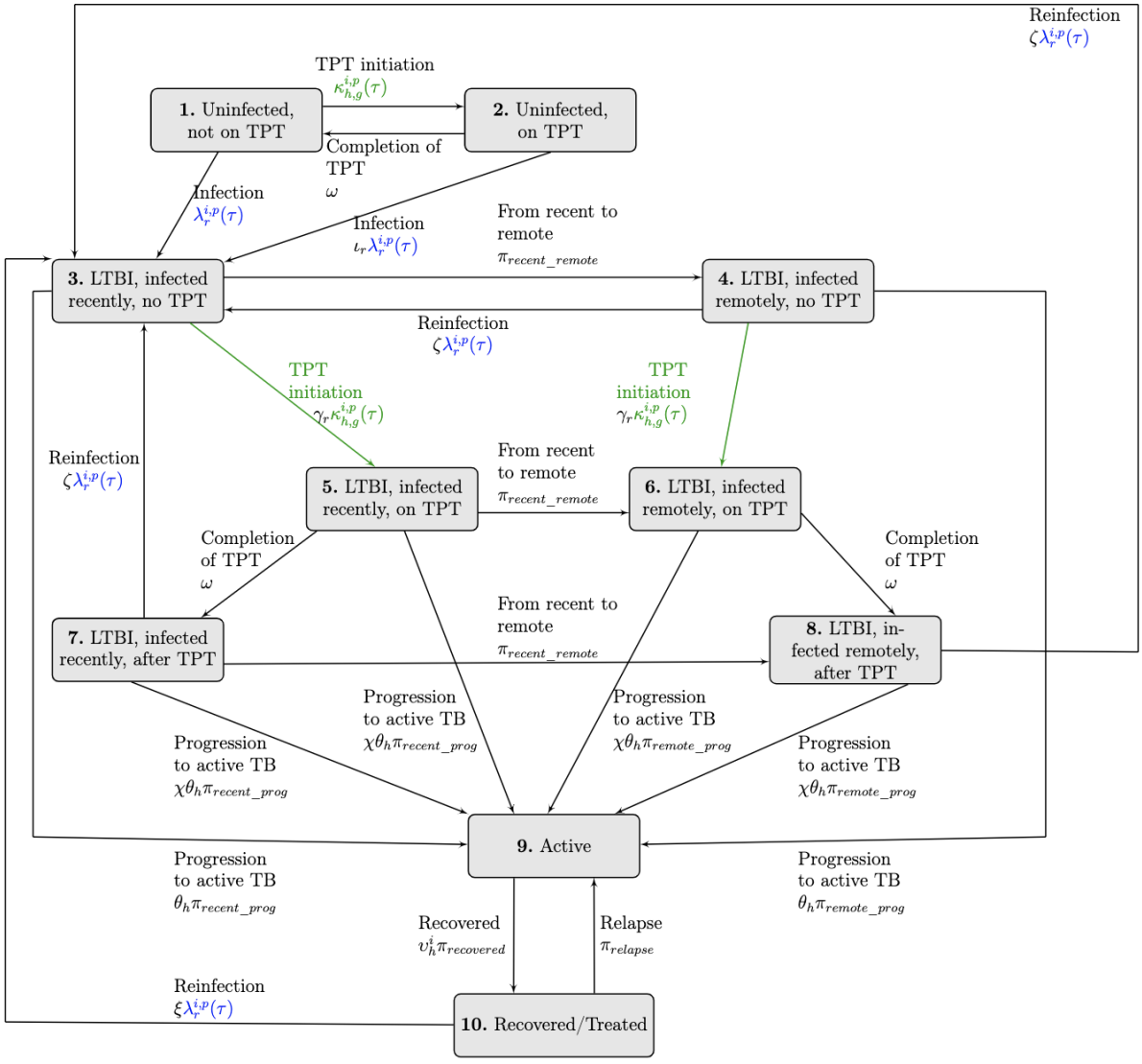

Figure 3.6: Illustration of TB transitions if the dynamic transmission model considers both reduced risk of TB progression from TPT by recent and remote infection and the reduced risk of infection while on TPT. Although not visualized here, each of the ten tuberculosis compartments would be stratified across two TB drug-resistance compartments, four HIV compartments, and two genders. Individuals can age out or die from any compartment. TB preventative therapy (TPT) initiations are highlighted in green to emphasize that care programs directly impact them. TB force of infection is highlighted in blue to indicate the care program indirectly impacts them.

Chapter 4

POLICY ANALYSIS OF IMPLEMENTING COMMUNITY-BASED CARE DELIVERY TO IMPROVE TB HEALTH OUTCOMES IN KWAZULU-NATAL, SOUTH AFRICA

This chapter provides a policy analysis that evaluates the health impact of extending community-based antiretroviral therapy (ART) and tuberculosis (TB) preventative therapy (TPT) care delivery to population scale in a TB-HIV high-burden setting of KwaZulu-Natal, South Africa, including an analysis of gender disparities in health outcomes. Disease progression is modeled with version one of the dynamic transmission model presented in Chapter 3 in KwaZulu-Natal under three facility-based and community-based ART and TPT care delivery programs. Most of this chapter was submitted to the Journal of the International AIDS Society in May 2023, and is currently under second revision. A preprint appears in [117].

In the development of the analysis presented in this chapter, I collaborated with epidemiologists and health economists to develop a policy analysis that evaluates the impacts of community-based ART with TPT care delivery in KwaZulu-Natal South Africa. Version one of the gender-stratified dynamic model of TB and HIV transmission and disease progression among 100,000 adults ages 15-59 in KwaZulu-Natal, South Africa, presented in Chapter 3, is used to project health outcomes and costs under three programs including, facility-based ART and TPT care delivery (Program 1), community-based ART and facility-based TPT care delivery (Program 2), and community-based ART with TPT care delivery (Program 3). To ensure that TB health outcomes are realistic, 34 parameters were calibrated against ten regional calibration targets, including TB incidence and TB mortality estimates by HIV status (HIV-positive and HIV-negative) and gender, and HIV prevalence by gender in KwaZulu-Natal, South Africa. The projections of TB- and HIV-related health outcomes and costs are presented across a range of accepted parameter sets identified through calibration that meet all calibration targets to represent uncertainty in health outcomes and costs.

The modeling study quantifies the health impact and cost-effectiveness of extending community-based ART and TPT to the population scale in a TB-HIV high-burden setting of KwaZulu-Natal, South Africa across all accepted parameter sets. Projections on the number of TB cases, deaths, and disability-adjusted life years (DALYs) averted relative to standard, clinic-based care are provided. Furthermore, program costs and incremental cost-effectiveness ratios are presented to evaluate the trade-offs between health gains and additional costs with community-based care, compared to standard facility-based care.

This chapter also presents an analysis of the impact of community-based ART with TPT programs on reducing gender disparities in TB incidence and TB mortality rates. To ensure the model accurately represents gender differences, the input parameters consider gender-specific differences, such as mortality rates, ART coverage, and TPT initiation rates, and are calibrated to TB incidence, HIV prevalence, and TB mortality targets by gender. Furthermore, it quantifies the indirect health benefits of these programs for the HIV negative population. To project these impacts, the model includes the HIV negative population, who are not served directly by these programs. To quantify these benefits, projections on TB incidence and TB mortality rates under the three care delivery programs by HIV status and gender are compared.

The rest of the chapter is organized as follows. Section 4.1 provides a background and introduces the analysis. Section 4.2 describes the calibration method and provides the results. Section 4.3 provides the analysis of care delivery programs. Section 4.4 provides a discussion of the results. Section 4.5 presents conclusions and future work.

4.1 Introduction and Background

Tuberculosis (TB) is the leading cause of death globally among people living with HIV (PLWH) [144]. The burden of HIV-associated TB is particularly high in South Africa, where more than 50% of people with incident TB in 2021 also had HIV, compared to a global mean of 6.7% [144]. In KwaZulu-Natal, approximately 70% of people who develop TB also have HIV [72]. Despite frequent co-occurrence, TB and HIV exhibit different gender disparity patterns in South Africa, where TB prevalence nationally is higher among men compared to higher HIV prevalence among

women [93, 129]. Multiple factors likely contribute to greater TB burden among men, including gender differences in accessing health care, gender-specific contact patterns, and higher prevalence of exposures that increase risk for TB infection and/or progression (e.g., mining, incarceration, use of alcohol, illicit substances, and tobacco) [52, 53, 73]. Additionally, gender disparities in HIV outcomes include lower levels of HIV viral suppression among men than women living with HIV across nearly all regions globally and in South Africa [142]. The higher detectable viral loads in men contribute in part to higher incidence among women [144].

TB preventive treatment (TPT) with isoniazid, when given with antiretroviral therapy (ART), reduces the risk of TB by approximately one-third [109, 116, 137]. Between 2018 and 2020, over six million PLWH accessed TPT globally, exceeding the target set at the 2018 UN High-Level Meeting on Tuberculosis. However, disruptions in care during the COVID-19 pandemic were associated with a 21% decline in the number of people taking TPT between 2019 and 2020 [144]. While global TPT figures are not disaggregated by gender, some studies conducted between 2020 and 2021 in sub-Saharan Africa found lower rates of TPT initiation and completion among men than among women [78, 124], while others did not find differences [136, 148].

Differentiated models of care tailor health care delivery to client health needs and often extend care beyond traditional facility settings and involve an additional cadre of health workers [47]. Differentiated community-based care models have been effective and cost-effective interventions for HIV and TB care in sub-Saharan Africa [75]. They can improve healthcare by caring for PLWH outside of health facilities. Recently, the Delivery Optimization for Antiretroviral Therapy (DO ART) household-randomized trial of community-based ART initiation and treatment in South Africa and Uganda demonstrated that community-based care delivery increases the proportion of PLWH who achieve viral suppression, particularly among men [16]. This overcame a gender disparity in viral suppression that was observed in clinic-based care models. At South African DO ART sites, asymptomatic participants without contraindications to TPT in the community-based care group were offered TPT starting one month after ART initiation, while the standard clinic group received TPT per routine clinic procedures. TPT uptake was higher among DO ART participants who received community-based care than participants who received facility-based care. A recent modeling analysis concluded that community-based HIV treatment was cost-effective in

preventing death and disability due to HIV [121]. However, the longer-term impact of increased ART and TPT uptake on incident TB and TB deaths were not quantified among trial participants, nor were TB incidence or deaths quantified among community members who were not in the trial. This modeling study aims to quantify the health impact and cost-effectiveness of extending community-based ART and TPT to the population scale in a TB-HIV high-burden setting of KwaZulu-Natal, South Africa, including analysis of gender disparities in health outcomes.

To meet this aim, version one of the dynamic compartmental transmission model of TB and HIV disease presented in Chapter 3 was used to simulate TB and HIV outcomes in KwaZulu-Natal, South Africa, for three care delivery programs, including

1. standard facility-based ART and TPT care delivery (Program 1),
2. community-based ART and standard facility-based TPT care delivery (Program 2) and,
3. community-based ART with TPT care (Program 3)

The model simulates a population of 100,000 persons representing the adult population (ages 15-59) of KwaZulu-Natal, South Africa, under the three programs that reflect findings from the DO ART trial [16] using the values described in Section 3.8.3.

The population moves through the compartments at transition rates reflecting TB and HIV infection, disease progression, treatment and recovery from TB, death, and aging into and out of the system as described in Section 3.3.1. The system of ordinary differential equations is described in Section 3.5.1, and the input parameters values and calibration ranges to run the model in KwaZulu-Natal under the three care delivery programs are provided in Section 3.8. The impacts of community-based ART and TPT delivery care programs are simulated over ten years, assuming that community-based ART and TPT were scaled up to similar levels as in the DO ART trial (i.e., ART coverage increasing from 49% to 82% among men and from 69% to 83% among women) and sustained for ten years. Community-based ART care delivery with standard facility-based TPT care was not implemented in DO ART but is considered in this analysis to evaluate the independent effects of community-based ART and TPT.

The model is executed from the beginning of 1940 to the end of 2027, with a warmup and calibration period from 1940 through the end of 2017 and the ten-year intervention period from the start of 2018 through the end of 2027. During the intervention period, the programs differ in

their gender-specific ART coverage and TPT initiation rates (see Table 3.7 in Chapter 3). It is assumed that programs take full effect at the start of the intervention period and are maintained over ten years. Over the ten-year intervention period, model outputs are used to project health and economic outcomes under each program. The calculations for program health and costs are provided in Section 3.7.1 and include, TB incidence, TB mortality, disability-adjusted life years (DALYs), and costs – for each care delivery program.

Discounted and undiscounted health outcomes are quantified, including TB incident cases, TB deaths, and DALYs, and costs for each program over the ten-year intervention period. These metrics are used to generate incremental cost-effectiveness ratios (ICERs) to assess the undiscounted and discounted per-dollar cost per incident TB case averted, TB death averted, and DALYs averted from care delivery intervention programs. The program comparisons include:

- Program 2 (community-based ART care with standard facility-based TPT care) to Program 1 (standard facility-based ART and TPT care) to quantify incremental health gains and additional costs of a community-based ART intervention,

- Program 3 (community-based ART with TPT care) compared to Program 1 (standard facility-based ART and TPT care) to quantify incremental health gains and additional costs of a community-based ART and TPT intervention, and

- Program 3 (community-based ART with TPT care) compared to Program 2 (community-based ART care with standard facility-based TPT care) to quantify incremental health gains and additional costs of a nested community-based TPT intervention.

Discounted ICERs are used to evaluate the cost-effectiveness of programs. The projection of TB incidence and TB mortality is evaluated by HIV status (HIV positive and HIV negative) and gender (male and female) to analyze the impacts of these programs on health outcomes by gender as well as their indirect health benefits on the HIV negative population, who are not directly served by the program.

4.2 Calibration of the Dynamic Transmission Compartmental Model

Version one of the dynamic transmission model (described in Chapter 3) is calibrated over 34 parameters for KwaZulu-Natal, South Africa. In this research, we assume TPT initiation rates ($\kappa_{h,g}^{i,p}(\tau)$) and ART coverage ($\sigma_g^{i,p}(\tau)$) estimates are held constant at the values in Table 3.6, and we do not calibrate these parameters, such that $\kappa\_FACTOR^4 = 1$ and $\sigma\_FACTOR^4 = 1$ in Equation (3.58) and Equation (3.61), respectively.

Latin hypercube sampling [132] was used to generate 100,000 candidate parameter sets from the calibrated parameters using the ranges specified in Table 3.6 applicable to version one of the model in KwaZulu-Natal, South Africa. For each candidate parameter set, the model is executed over a warm-up and calibration period from the start of 1940 to the end of 2017 under the standard facility-based ART and TPT care program.

Ten metrics are considered for calibration, including TB incidence rates by HIV status (HIV- and HIV+) and gender, TB mortality rates by HIV status (HIV- and HIV+) and gender, and HIV prevalence by gender. These ten metrics are evaluated in 2005, the peak of the HIV epidemic, and in 2017, the year prior to the start of the intervention period of the DO ART trial. Model values are calculated for each metric in 2005 and 2017 for the 100,000 candidate parameter sets using the equations provided in Section 3.7.1. Model values are compared to corresponding target calibration ranges in 2005 and 2017 based on 95% uncertainty intervals from the GBD Study 2019 for adults between 15 and 59 years old in KwaZulu-Natal, South Africa [44]. A candidate parameter set is considered if all 20 model values fall into all 20 target calibration ranges. A candidate parameter set is accepted if it shows a reduction in the total number of TB cases and deaths over the intervention period in community-based ART with TPT care delivery versus community-based ART with standard facility-based TPT care delivery. The calibration resulted in 859 accepted parameter sets. Figure 4.1 illustrates the mean, minimum, and maximum model values of the 859 accepted parameter sets for each of the ten calibration metrics between the years 1990 and 2017. In 2005 and 2017, model values were compared to target calibration ranges; target calibration ranges are emphasized lines.

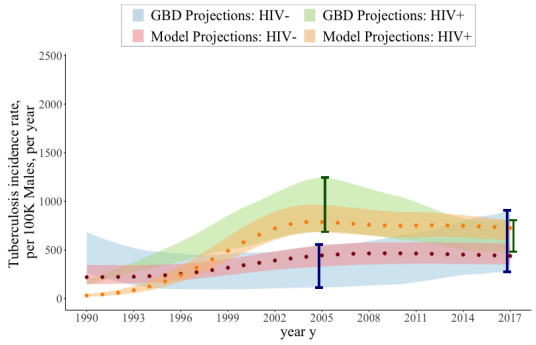

(a) TB incidence rate per 100,000 males in year y HIV positive and HIV negative

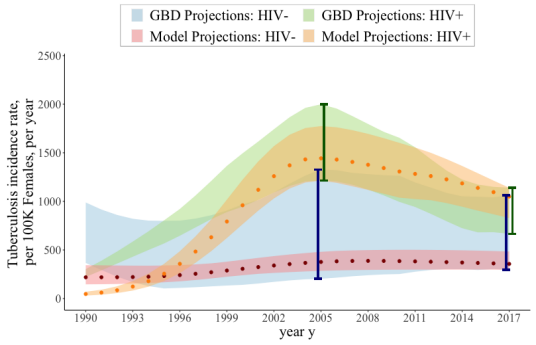

(b) TB incidence rate per 100,000 females in year y HIV positive and HIV negative

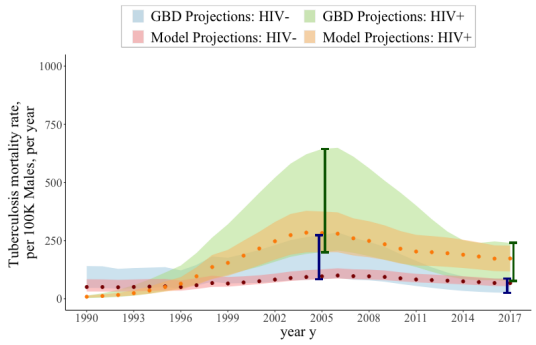

(c) TB mortality rate per 100,000 males in year y HIV positive and HIV negative

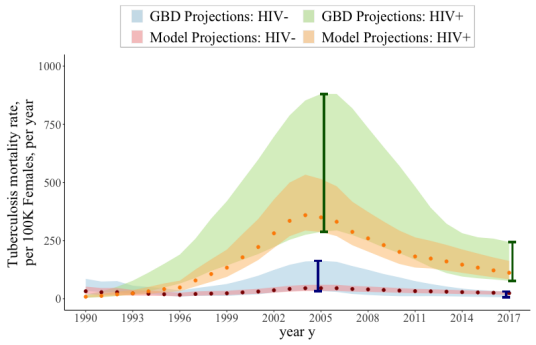

(d) TB mortality rate per 100,000 females in year y HIV positive and HIV negative

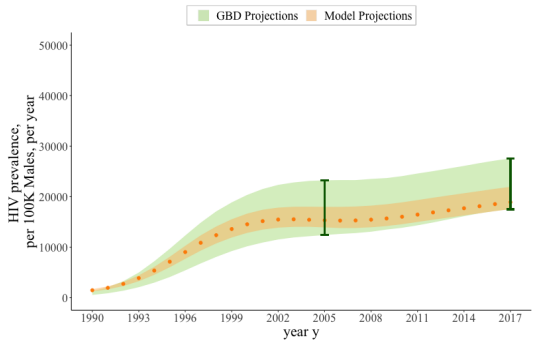

(e) HIV prevalence per 100,000 males in year y

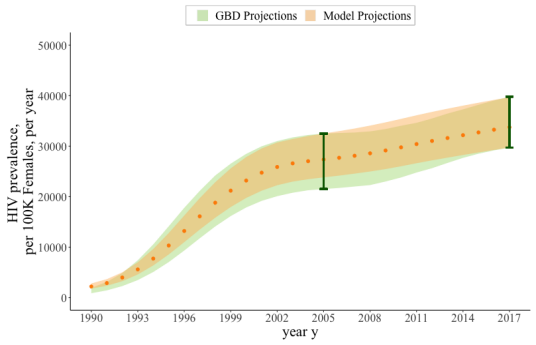

(f) HIV prevalence per 100,000 females in year y

Figure 4.1: Maximum, minimum, and mean ranges of TB incidence, TB mortality, and HIV prevalence metrics from the 859 accepted parameter sets for each year y under standard facility-based ART and TPT care from 1990 to 2017. Model values are shown in red and orange for HIV negative and HIV positive populations, respectively. Estimates from GBD 2019 for males and females between the ages of 15 and 59 in KwaZulu-Natal, South Africa, are shown in blue and green for HIV negative and HIV positive populations, respectively [44]. In 2005 and 2017, target calibration ranges are emphasized lines.

4.3 Analysis of Care Delivery Programs

The model was executed with the 859 accepted calibrated parameter sets for the three care delivery programs over a 10-year intervention period from the start of 2018 to the end of 2027. Figure 4.2 illustrates the projected annual TB incidence and mortality rates by gender from 1990 to 2027 over the 859 accepted calibrated parameter sets. In 2017, the year before the start of the intervention, the estimated annual incidence of active TB disease was slightly higher for women (1,406 per 100,000; range 1,141 – 1,577) than for men (1,165 per 100,000; range 989 – 1,362). In 2017, nearly 74.7% (1,050 out of 1,406) of women with incident TB were also living with HIV, compared to 62.4% (727 out of 1,165) of men with incident TB also living with HIV. However, the estimated TB mortality rate in 2017 was higher for men, with an estimate of 240 (range 174 – 309) per 100,000 men compared with 135 (range 103 – 188) per 100,000 women.

Over the 10-year intervention period, an estimated 31,009 (range 25,674 – 39,021) PLWH received a course of TPT in Program 3 compared to 17,264 (range 14,156 – 21,255) in Program 1 and 18,221 (range 15,305 – 22,370) in Program 2. The outputs from the model estimated the number needed to treat with TPT to prevent one case of active TB was 38. Section 4.3.1 describes the population level impact of the programs, and Section 4.3.2 describes the impact of the programs by gender and HIV status.

4.3.1 Analysis of the Population-Level Impact of Care Delivery Programs

Figure 4.3 illustrates the population-level impact of each program by comparing TB incidence and mortality rates per 100,000 individuals over the intervention period. The impact of offering community-based ART (without changing TPT uptake) is estimated by comparing Program 2 to Program 1 outcomes. In 2027, Program 2 could reduce the TB incidence rate by 27.0% (range 21.3% – 34.1%) and the TB mortality rate by 34.6% (range 24.8% – 42.2%) compared to Program 1. The impact of offering community-based TPT with ART is estimated by comparing Program 3 to Program 2 outcomes. In 2027, Program 3 could reduce TB incidence by an additional 3.6% (range 0.2% – 9.9%) and TB mortality rates by 2.2% (range 0.1% – 7.6%) compared to Program 2.

Health outcomes (DALYs, TB incident cases, TB deaths) and costs are summed over the 10-year intervention period for each care program, shown in Table 4.1. These program health outcomes and

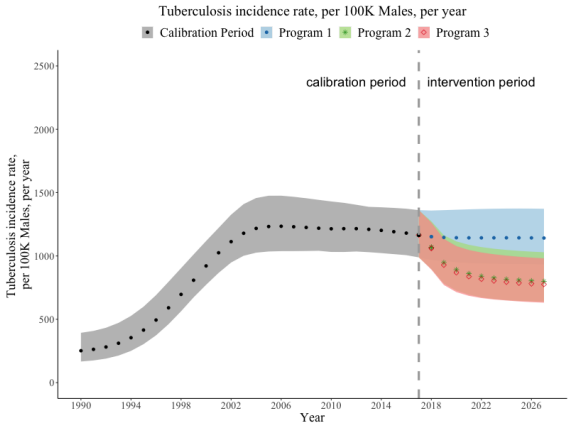

(a) TB incidence per 100,000 males

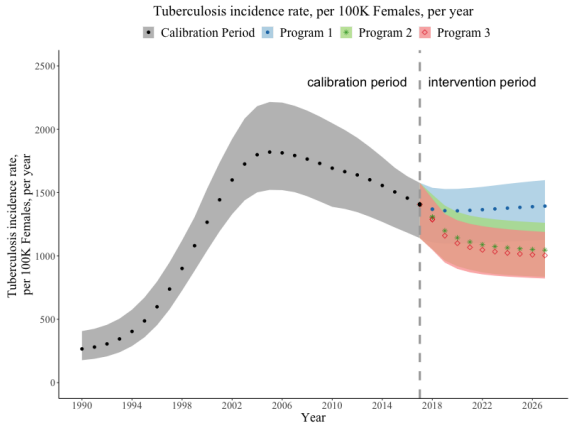

(b) TB incidence per 100,000 females

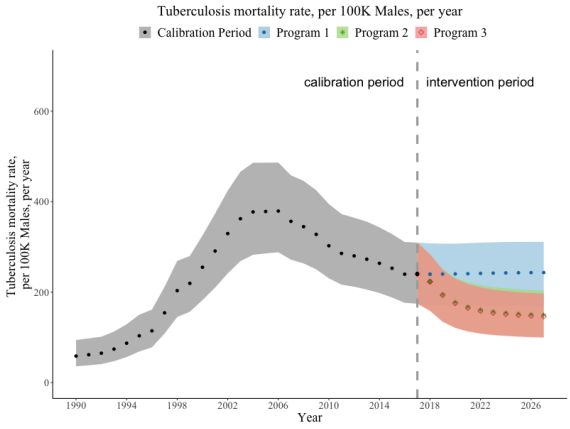

(c) TB mortality per 100,000 males

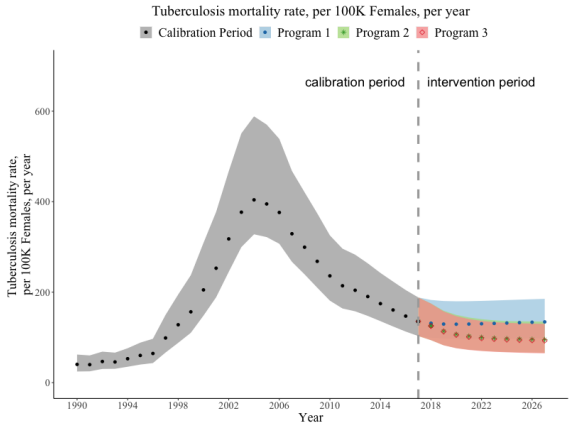

(d) TB mortality per 100,000 females

Figure 4.2: Estimated TB incidence and mortality by gender. The mean, maximum, and minimum yearly TB incidence and mortality rates from 1990-2017 over the 859 accepted parameter sets are shown in grey (dots). The mean, maximum, and minimum yearly TB incidence and mortality rates during the intervention period (2018-2027) over the 859 accepted parameter sets are illustrated by care delivery program. During the intervention period, Program 1 (standard facility-based ART and TPT care) is shown in blue (dots), Program 2 (community-based ART care with standard facility-based TPT care) is shown in green (stars), and Program 3 (community-based ART with TPT care) is shown in red (diamonds).

costs are used to calculate incremental health gains, costs, and ICERs for the outcomes of DALYs, incident TB cases, and TB deaths between facility-based and community-based care delivery programs, as in Table 4.2.

Cost-effectiveness is assessed relative to the threshold of $590 USD per DALY averted based

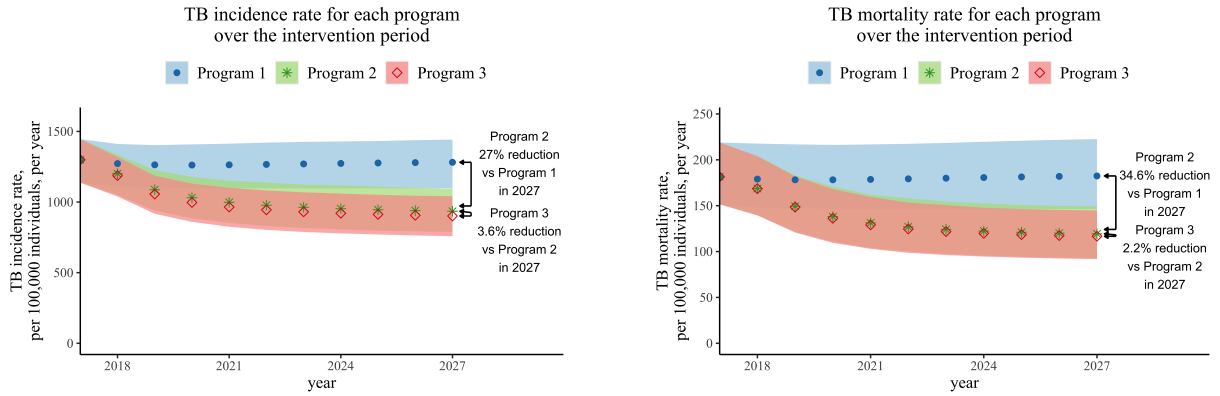

(a) TB incidence per 100,000 individuals

(b) TB mortality per 100,000 individuals

Figure 4.3: Estimated TB incidence and mortality by care-delivery program. The mean, maximum, and minimum yearly TB incidence and mortality rates are estimated over the 859 accepted parameter sets. Program 1 (standard facility-based ART and TPT care) is shown in blue (dots), Program 2 (community-based ART care with standard facility-based TPT care) is shown in green (stars), and Program 3 (community-based ART with TPT care) is shown in red (diamonds).

on the opportunity cost at the margin of the South African program [91, 104], as in [21]. The community-based ART with TPT care program (Program 3) did not meet the cost-effectiveness threshold of $590 USD per DALY averted with the input parameter costs given in Table 4.2.

A one-way sensitivity analysis of costs was conducted by varying the cost parameters in the model using the mean metrics from the 859 accepted parameter sets. Figure 4.4 shows the impact of varying costs on the discounted incremental cost per DALY averted under Program 3 versus Program 1. The discounted incremental cost per DALY was most sensitive to the cost of outpatient HIV care. If the cost of annual outpatient care for PLWH on ART under community-based ART programs (Programs 2 and 3) were to decrease from $310 to $283, or if the cost of annual outpatient care for PLWH on ART under standard facility-based ART and TPT care (Program 1) were to increase from $249 to $260, then the discounted incremental cost per DALY would achieve the cost-effectiveness threshold.

	Program 1 *Standard facility-based ART and TPT care*	**Program 2** *Community-based ART care with standard facility-based TPT care*	**Program 3** *Community-based ART with TPT care*
	Mean [Min, Max]	**Mean [Min, Max]**	**Mean [Min, Max]**
Health Outcomes and Costs (Undiscounted)			
DALYs (thousands)	82.0 [70.5, 92.2]	59.7 [52.4, 67.2]	59.5 [52.2, 66.9]
TB incident cases (thousands)	12.7 [10.5, 14.7]	10.0 [8.1, 12.1]	9.7 [8.1, 11.6]
TB deaths (thousands)	1.8 [1.4, 2.3]	1.3 [1.0, 1.7]	1.3 [1.0, 1.7]
Program costs (millions in USD)	99.3 [90.6, 114.1]	118.2 [107.4, 135.5]	118.4 [107.6, 135.8]
Health Outcomes and Costs (Discounted)			
DALYs (thousands)	73.4 [63.1, 82.5]	53.8 [47.1, 60.5]	53.6 [47.0, 60.2]
TB incident cases (thousands)	11.2 [9.2, 12.9]	8.8 [7.2, 10.7]	8.6 [7.1, 10.3]
TB deaths (thousands)	1.6 [1.2, 2.0]	1.2 [0.9, 1.5]	1.1 [0.9, 1.5]
Program costs (millions in USD)	87.1 [79.5, 100.1]	103.7 [94.3, 118.9]	103.9 [94.4, 119.2]

Table 4.1: Cumulative health outcomes and costs over the intervention period by program. Values are the mean, minimum, and maximum values of the 859 accepted parameter sets. Health outcomes and costs are summed over the 10-year intervention period for a population of 100,000 individuals. Discounted values are presented in 2018 values and use an annual discount rate of 3%.

4.3.2 Analysis of the Impact of Care Delivery Programs by Gender and HIV Status

TB incidence and mortality rates by gender under each program in the last year of the intervention period are provided in Table 4.3. Community-based ART with TPT care (Program 3) reduced gender disparities in TB mortality compared to standard facility-based ART and TPT care (Program 1). TB mortality declined by 39.9% (range 32.2%–46.3%) among men and 30.6% (range 25.3%-36.5%) among women under Program 3 versus Program 1.

The model projected that community-based care programs also had indirect health benefits for people with and without HIV through reduced community TB transmission even though ART and

	Program 2 vs. Program 1 *Community-based ART with standard facility-based TPT care vs. facility-based ART and TPT care*	**Program 3 vs. Program 1** *Community-based ART with TPT care vs. facility-based ART and TPT care*	**Program 3 vs. Program 2** *Community-based ART with TPT care vs. community-based ART with facility-based TPT care*
	Mean [Min, Max]	**Mean [Min, Max]**	**Mean [Min, Max]**
Incremental Health Outcomes and Costs (Undiscounted)			
DALYs averted (thousands)	22.3 [18.1, 27.0]	22.5 [18.2, 27.3]	0.2 [0.0, 0.5]
TB incident cases averted (thousands)	2.7 [2.1, 3.5]	3.0 [2.3, 3.7]	0.3 [0.0, 0.9]
TB deaths averted (thousands)	0.5 [0.3, 0.7]	0.5 [0.4, 0.7]	0.0 [0.0, 0.1]
Incremental costs (millions in USD)	18.8 [16.8, 21.5]	19.0 [17.0, 21.7]	0.2 [0.1, 0.3]
Incremental Health Outcomes and Costs (Discounted)			
DALYs averted (thousands)	19.7 [15.9, 23.8]	19.8 [16.0, 24.0]	0.1 [0.0, 0.4]
TB incident cases averted (thousands)	2.3 [1.8, 3.0]	2.6 [2.0, 3.2]	0.3 [0.0, 0.8]
TB deaths averted (thousands)	0.4 [0.3, 0.6]	0.4 [0.3, 0.6]	0.0 [0.0, 0.1]
Incremental costs (millions in USD)	16.6 [14.8, 18.9]	16.7 [14.9, 19.1]	0.2 [0.1, 0.3]
Incremental Cost-effectiveness Ratios *(Health gains and costs are discounted by 3%)*			
Cost per DALY averted (in USD)	843 [706, 1,017]	846 [709, 1,012]	1,967 [244, 20,282]
Cost per incident case averted (in USD)	7,192 [5,161, 10,010]	6,498 [4,823, 9,304]	1,109 [107, 13,012]
Cost per TB death averted (in USD)	40,692 [26,116, 62,157]	39,373 [25,606, 57,020]	19,737 [1,783, 470,597]

Table 4.2: Incremental health gains, costs, and incremental cost-effectiveness ratios (ICERs) between community-based and facility-based care delivery programs. Health outcomes and costs are summed over the 10-year intervention period for a population of 100,000 individuals. Values are the mean, minimum, and maximum values over 859 parameter sets. Discounted values are presented in 2018 values and use an annual discount rate of 3%.

TPT were only taken by PLWH. In 2027, TB incidence was 12.9% (range 8.3% – 18.1%) lower among men without HIV and 9.6% (range 4.7% – 15.1%) lower among women without in HIV under Program 3 versus Program 1. Figure 4.5 and Figure 4.6 present estimated reductions in TB incidence and mortality for people without HIV by gender. Table 4.4 provides the mean, maximum,

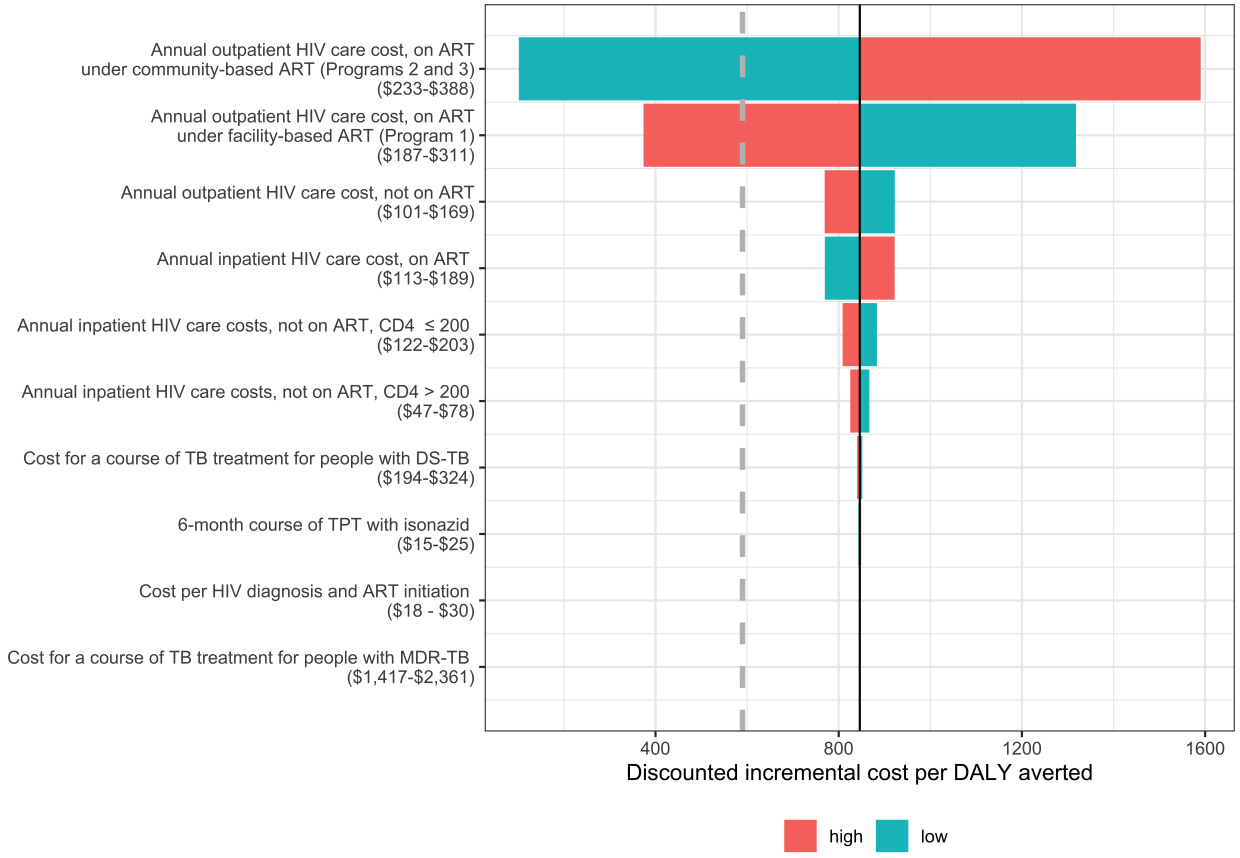

Figure 4.4: Sensitivity analysis of the discounted incremental cost per DALY averted by community-based ART with TPT care (Program 3) versus standard facility-based ART and TPT care (Program 1) over the intervention period. The solid line represents the mean discounted incremental cost per DALY averted over the 859 accepted parameter sets of $846 USD per DALY averted. The dashed vertical line represents the cost-effectiveness threshold of $590 USD per DALY averted. The horizontal bars represent the discounted incremental cost per DALY averted at bounds of 25% above of the modeled cost parameter (high) and 25% below the modeled cost parameter (low). All costs are in 2018 USD.

and minimum TB incidence and mortality rates in 2027 (the last year of the intervention period) per 100,000 males and females by HIV status and care program over the 859 accepted parameter sets.

	Program 1 *Standard facility-based ART and TPT care*	**Program 2** *Community-based ART care with standard facility-based TPT care*	**Program 3** *Community-based ART with TPT care*
	Mean [Min, Max]	**Mean [Min, Max]**	**Mean [Min, Max]**
TB incidence rate			
TB incidence rate per 100,000 males	1,141 [977, 1,301]	799 [665, 950]	775 [654, 902]
TB incidence rate per 100,000 females	1,394 [1,185, 1,561]	1,046 [883, 1,220]	1,004 [848, 1,155]
TB mortality rate			
TB mortality rate per 100,000 males	243 [184, 300]	149 [111, 191]	146 [110, 184]
TB mortality rate per 100,000 females	134 [103, 174]	95 [70, 125]	93 [69, 120]

Table 4.3: Estimated TB incidence and mortality by care-delivery programs and gender in the last year of the intervention period. The mean, maximum, and minimum yearly TB incidence and mortality rates are estimated over the 859 accepted parameter sets.

4.4 Discussion

Scaling up community-based ART with TPT to the population level in a high HIV-TB burden setting such as KwaZulu-Natal, South Africa, could avert substantial HIV and TB morbidity and mortality, if equivalent effectiveness is maintained as demonstrated in the DO ART trial. The increase in ART coverage achieved through community-based care reduced cumulative TB disease by 21% over ten years, and community-based TPT reduced it further by 3%. Additionally, though the interventions were only directly delivered to people living with HIV, the model captured indirect benefits of reduced TB incidence disease and mortality among people without HIV under the community ART and TPT scenarios. Prior modeling analyses in South Africa have also found that ART and TPT scale-up would be projected to reduce TB incidence among people living with and without HIV [54]. Gender disparities in HIV and TB outcomes in this setting are complex and are reflected in the model results. Specifically, the higher HIV prevalence among women (39%) compared to men (20%) in our model resulted in higher incidence and mortality of HIV-associated

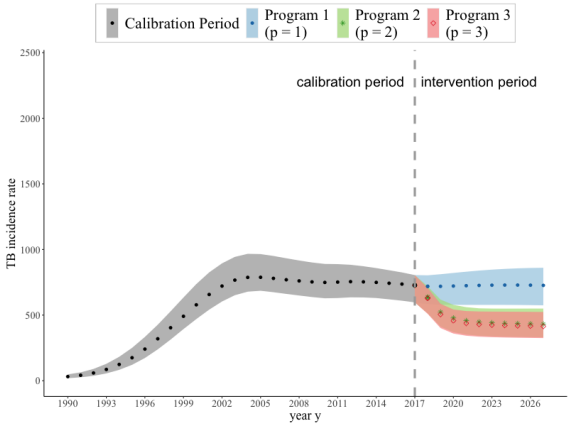

(a) TB incidence per 100,000 males HIV positive

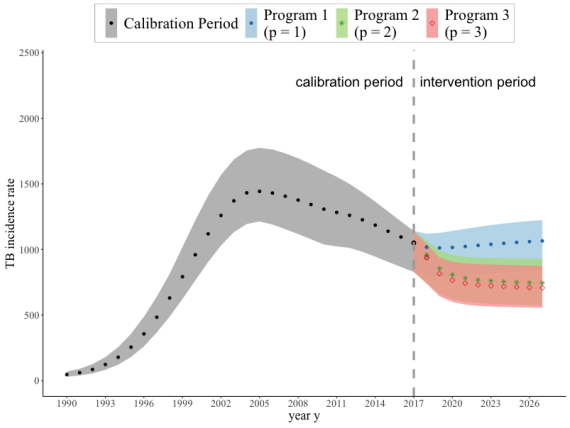

(b) TB incidence per 100,000 females HIV positive

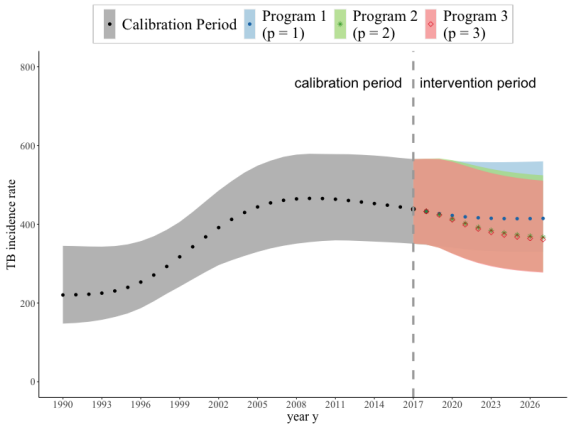

(c) TB incidence per 100,000 males HIV negative

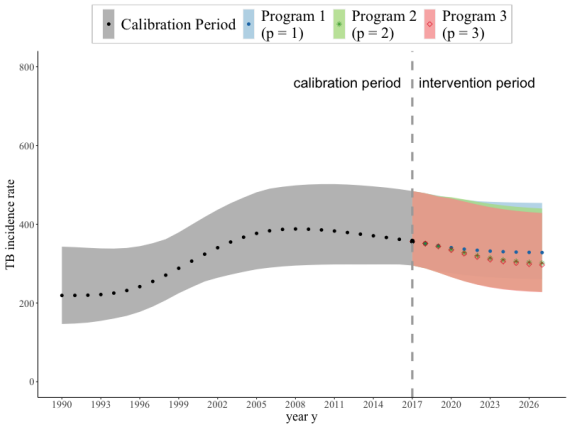

(d) TB incidence per 100,000 females HIV negative

Figure 4.5: Estimated TB incidence by gender in KwaZulu-Natal, South Africa during the calibration period and during the intervention period under the three care programs. Mean, maximum, and minimum yearly TB incidence rates from 1990 to 2017 over the 859 accepted parameter sets are shown in grey (dots). Mean, maximum, and minimum yearly TB incidence rates during the intervention period (2018-2027) over the 859 accepted parameter sets are illustrated by care program. During the intervention period, Program 1 (standard facility-based ART and TPT care) is shown in blue (dots), Program 2 (community-based ART care with standard facility-based TPT) is shown in green (stars), and Program 3 (community-based ART and TPT care) is shown in red (diamonds).

TB among women than among men, while HIV-negative women had lower TB incidence, prevalence, and mortality than HIV-negative men. The larger increase in ART coverage under the community-based care programs among men resulted in larger percent reductions in 10-year TB-associated

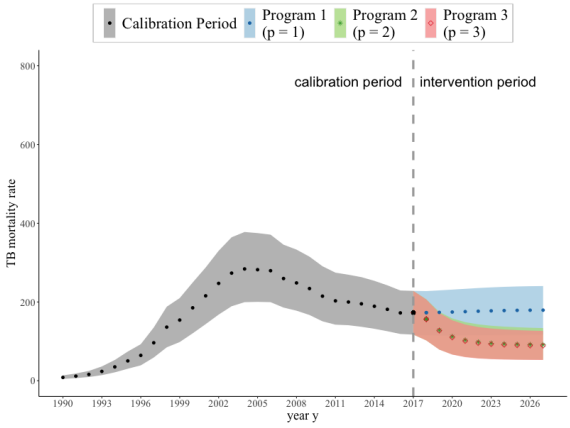

(a) TB mortality per 100,000 males and HIV positive

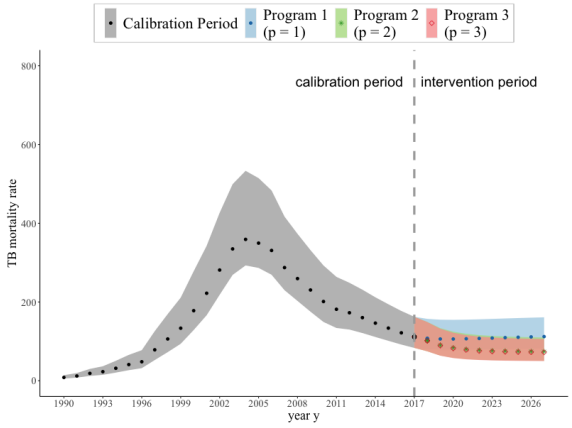

(b) TB mortality per 100,000 females and HIV positive

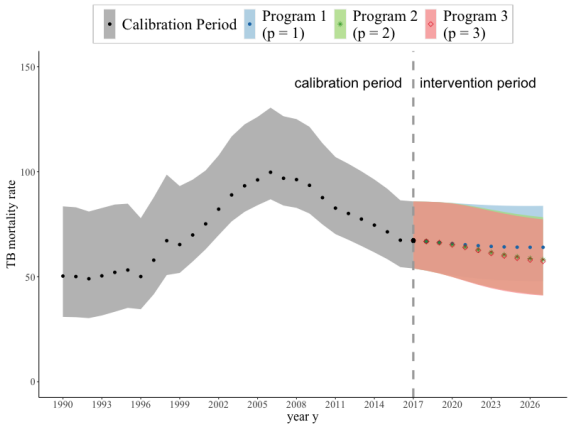

(c) TB mortality per 100,000 males and HIV negative

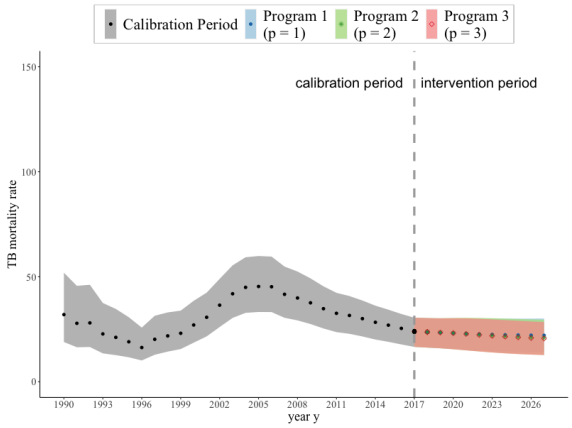

(d) TB mortality per 100,000 females and HIV negative

Figure 4.6: Estimated TB mortality rates by gender in KwaZulu-Natal, South Africa during the calibration period and during the intervention period under the three ART and TPT care programs. Mean, maximum, and minimum yearly TB mortality rates from 1990 to 2017 over the 859 accepted parameter sets are shown in grey (dots). Mean, maximum, and minimum yearly TB mortality rates during the intervention period (2018-2027) over the 859 accepted parameter sets are illustrated by care program. During the intervention period, Program 1 (standard facility-based ART and TPT care) is shown in blue (dots), Program 2 (community-based ART care with standard facility-based TPT) is shown in green (stars), and Program 3 (community-based ART and TPT care) is shown in red (diamonds).

mortality among men than among women compared to standard clinic-based care. Gender-specific model parameters included effective contact rates, HIV prevalence, HIV disease progression, ART coverage, and baseline (non-HIV and non-TB associated) mortality, though other features of TB

	Program 1 *Standard facility-based ART and TPT care*	**Program 2** *Community-based ART care with standard facility-based TPT care*	**Program 3** *Community-based ART with TPT care*
	Mean [Min, Max]	**Mean [Min, Max]**	**Mean [Min, Max]**
TB incidence rate			
TB incidence rate per 100,000 males and HIV positive	727 [609, 818]	432 [358, 515]	414 [345, 492]
TB incidence rate per 100,000 females and HIV positive	1,066 [899, 1,184]	745 [613, 863]	707 [586, 819]
TB incidence rate per 100,000 males and HIV negative	414 [340, 504]	367 [296, 456]	361 [293, 451]
TB incidence rate per 100,000 females and HIV negative	328 [269, 413]	301 [238, 388]	296 [235, 374]
TB mortality rate			
TB mortality rate per 100,000 males and HIV positive	179 [131, 230]	91 [62, 122]	89 [62, 117]
TB mortality rate per 100,000 females and HIV positive	112 [86, 150]	74 [55, 99]	72 [53, 97]
TB mortality rate per 100,000 males and HIV negative	64 [51, 81]	58 [44, 75]	57 [44, 74]
TB mortality rate per 100,000 females and HIV negative	22 [15, 29]	21 [14, 28]	21 [14, 27]

Table 4.4: Mean, minimum, and maximum TB incidence and mortality rates in 2027 (the last year of the intervention period) per 100,000 males and 100,000 females by HIV status and care program over the 859 accepted parameter sets.

epidemiology may also differ by gender, including care seeking behavior that may impact active TB duration and case fatality ratios. A recent gender-specific TB model in a setting with a low HIV prevalence found that interventions targeted to risk factors with a higher prevalence among men (e.g. tobacco smoking and harmful alcohol use) achieved the greatest projected TB incidence reductions among men, but also substantially reduced TB incidence among women and children [54]. Our cost analysis found that community-based ART with TPT was cost ineffective relative to the willingness-to-pay threshold based on the opportunity cost at the margin of the South African programme [21]. The sensitivity analysis of cost parameters indicated that variation in the costs of outpatient HIV care for PLWH on ART substantially affected the ICER. If the annual per person costs of outpatient HIV care for PLWH on ART under community-based care were to decrease from $310 to $283 or the

annual per-person costs of outpatient HIV care for PLWH on ART under facility-based care were to increase to from $249 to $260, then community-based ART with TPT (Program 3) could be cost effective. Other community-based interventions, including interval TB/HIV screening and linkage to care, were found to be cost-effective in a modeling analysis set in South Africa, though these did not include community-based HIV treatment and were evaluated against a higher GDP-based cost-effectiveness threshold [42]. Strengths of this analysis include that it is based in findings from the recent DO ART randomized controlled trial conducted in this setting. Additionally, the model is calibrated to gender- and province-specific estimates of TB and TB-HIV incidence and mortality at two time points that capture the declines in HIV-associated TB incidence and mortality in the setting of increased ART coverage [44]. To reflect these dynamics, time varying parameters for HIV incidence, prevalence, and ART coverage that incorporate historical changes in ART availability were included. Additionally, the model incorporates uncertainty in model parameters. Uncertainty remains in key aspects of TB epidemiology, including the rate of progression from latent to active TB, which is represented differently across models [86]. Finally, by using a model that differentiates compartments by gender, outcomes were able to be stratefied by gender, which is important for evaluating health program impacts on gender equity in health outcomes. This analysis also has limitations. First, the model assumed that the modeled care programs could take effect immediately and be sustained over ten years, which may not be feasible for already-strained health care workforce and budgets. However, dramatic increases in TPT initiation and completion have been observed in some HIV high-incidence settings through focused outreach campaigns [95]. Second, the model does not differentiate groups by age despite differences in HIV and TB incidence, prevalence, and mortality by age group due to the complexity of calibration across this additional dimension. Third, for simplicity, it was assumed that people taking TPT would not be protected from infection with an MDR-TB strain, though some evidence suggests that they may have partial protection from a resistant strain [55]. Finally, the economic analysis is from a health system perspective that does not include patient costs, despite numerous studies documenting patient costs and avoiding catastrophic costs as a key focus of TB goals [39].

4.5 Conclusion and Future Work

If community-based ART could be implemented with similar effectiveness to the DO ART trial, increased ART coverage could reduce TB incidence by 27.0% (range 21.3% - 34.1%) and TB mortality by 36.0% (range 26.9% - 43.8%) after ten years. Increasing both ART and TPT uptake through community-based ART with TPT care could reduce TB incidence by 29.7% (range 23.9% - 36.0%) and TB mortality by 36.0% (range 26.9% - 43.8%). Community-based ART care reduced gender disparities in TB mortality rates by reducing TB mortality among men by a projected 39.8% (range 32.2% - 46.3%) and by 30.9% (range 25.3% - 36.5%) among women. Differentiated models of HIV care can substantially reduce TB morbidity and mortality and reduce gender disparities in TB.

In order to address the limitations that were discussed in Section 4.4, it would be beneficial to test various scenarios that account for a ramp-up period where the programs do not take full effect immediately. Additionally, instead of assuming the programs are sustained over ten years, it would be beneficial to test realistic scenarios where ART coverage and TPT initiation fluctuate over time. This type of scenario testing would be particularly important if a decision maker wanted to evaluate the program's impacts over an intervention period that is longer than ten years. Furthermore, if the model were to be applied over a longer intervention period, it might need to take into account the evolving proportion of individuals who age into the model with active TB and HIV.

Chapter 5

A BUDGET ALLOCATION OPTIMIZATION APPROACH TO REGIONAL TB AND HIV CARE DELIVERY PROGRAMS

This chapter presents an optimization approach to budget allocation to regional tuberculosis (TB) and HIV care delivery programs in South Africa, considering regional differences, multiple objectives, and dynamics and uncertainties in disease progression. Disease progression is modeled with version two of the dynamic transmission model presented in Chapter 3 in the nine South African provinces under two facility-based and community-based antiretroviral therapy (ART) and TB preventative therapy (TPT) care delivery programs. Most of this chapter was submitted for publication in the Health Care Management Science Journal in October 2023.

To estimate uncertainties and dynamics of TB and HIV health outcomes and costs, the approach integrates health outcome and cost projections from version two of the dynamic transmission model (as described in Chapter 3) for each of the nine South African provinces under two programs including, facility-based ART and TPT care delivery (Program 1) and community-based ART with TPT care delivery (Program 2). The model is calibrated to regional calibration targets in TB incidence, HIV prevalence, and TB- and HIV-related mortality rates and a national calibration target for the total TB- and HIV-related deaths. Model calibration is used to identify a range of parameter sets that meet all calibration targets and represent health outcome uncertainties.

Calibrated model predictions are used to quantify health outcomes and program costs used in the multi-objective optimization approach. The two objective functions capture equity and effectiveness. The approach employs statistical methods that use model projections from the accepted parameter sets to identify a set of Pareto optimal solutions with sufficient statistical evidence that they satisfy a budget constraint and are non-dominated.

Instead of assuming all regions implement a single care delivery program, the approach allows for the implementation of programs by region. This allows consideration of the most vulnerable populations to be prioritized for community-based ART with TPT care delivery, under limited

resources. The optimization approach evaluates candidate solutions that represent combinations of regional implementations of the two care delivery programs. The two objective functions and cost function combine regional estimates for statistical quantification for each candidate solution. The approach generates a set of Pareto optimal solutions that provide optimal regional program implementation options.

The rest of this chapter is organized as follows. Section 5.1 provides an introduction and background to the budget allocation approach. Section 5.2 describes the regional calibration method and results. Section 5.3 presents the multi-objective optimization approach. Section 5.4 provides the results that describe the best regions to prioritize for community-based ART with TPT care across the nine provinces of South Africa. Section 5.5 discusses the trade-offs between TB- and HIV-related mortality rate inequities between regions and the total TB- and HIV-related deaths. Section 5.6 provides the conclusion and possible future research directions.

5.1 Introduction and Background

Due to the high costs of implementing community-based ART with TPT care delivery, it may not be practical to implement throughout a country [9]. This research introduces an approach for identifying regions within a country to prioritize for community-based ART with TPT care delivery. The problem of allocating a budget to regions for TB and HIV care is challenging due to unique regional population dynamics, complex issues involving multiple criteria and stakeholders, and uncertainties [9]. The multi-objective optimization approach presented in this chapter aims to address these challenges by integrating a regionally calibrated infectious disease dynamic transmission model, mathematical optimization, and statistical methods.

When it comes to optimizing budget allocation for a set of candidate healthcare programs, mathematical optimization is a widely used approach. However, most mathematical optimization approaches in this context only consider nationally administered programs that are implemented uniformly across all regions [9, 65, 133]. Despite research indicating that implementing programs by region could enhance health outcomes while remaining within a fixed national budget [7, 35, 83], most mathematical optimization methods overlook regional program implementation options. Our

approach considers regional differences and allows the implementation of community-based ART with TPT care delivery at the regional level.

To capture regional differences, version two of the TB and HIV dynamic transmission compartmental model presented in Chapter 3 is calibrated to reflect regional differences in yearly TB incidence, HIV prevalence, and TB- and HIV-related mortality rates. Model calibration is used to identify parameter sets that meet three regional calibration targets across the nine South African provinces and one national target. The targets are based on estimates from the 2019 Global Burden of Disease Study (GBD 2019) in South Africa [44]. For each of the identified parameter sets, the model is used to simulate disease progression and estimate health outcomes and costs in each region under each care delivery program.

Furthermore, the majority of mathematical optimization approaches focus on improving overall health outcomes (e.g., disability-adjusted life years) [9, 65]. However, reducing the overall burden of TB and HIV may not be a health system's only objective. Other goals, such as health equity between regions, financial risk, and other sociopolitical factors, are essential to stakeholders. The proposed approach considers two objectives to balance equity and effectiveness of TB- and HIV-related health outcomes against a budget constraint. The first objective function represents inequity in TB- and HIV-related mortality rates between regions. It calculates the maximum difference between the TB- and HIV-related mortality rates in each region and the average TB- and HIV-related mortality rate aggregated over all regions. The second objective function is the total TB- and HIV-related deaths summed over all regions.

Instead of aggregating the two objectives into a single objective with weights and returning a single solution, the approach generates a set of Pareto optimal solutions that provide a comprehensive view of the balance between inequity in TB- and HIV-related mortality rates between regions and the total TB- and HIV-related deaths summed over all regions. When making decisions related to budget allocation to TB and HIV programs by region, several crucial factors (e.g., practicalities and political pressures) must be considered. The Pareto optimal solutions can be considered in conjunction with these other factors to aid decision makers in their final decision.

Another important factor inherent to budget allocation for regional care delivery programs is uncertainty. Many optimization approaches only consider the expected value of the objective func-

tions and do not account for the uncertainty in the estimation [102, 161]. The proposed approach considers uncertainties in the total program costs and two objective functions by estimating their means and standard deviations across a range of parameter sets. The budget constraint considers the risk that program costs might exceed the budget through a chance constraint. Uncertainties are considered in the two objective functions with statistical tests that evaluate if a solution is probabilistically dominated. The multi-objective optimization approach returns Pareto optimal solutions with sufficient statistical evidence that they satisfy the budget constraint and are non-dominated.

This research contributes to the development of a multi-objective optimization approach to budget allocation for regional TB and HIV care delivery programs that:

1. accounts for regional differences and allows for the implementation of programs by region,
2. balances equity and effectiveness objectives and,
3. considers uncertainties in health outcomes and costs.

The multi-objective optimization approach considers two candidate programs across the nine provinces of South Africa. Version two of the dynamic transmission compartmental model of TB and HIV disease, presented in Chapter 3, is used to simulate TB and HIV outcomes in the nine provinces of South Africa, for two care delivery programs, including:

1. Standard facility-based ART and TPT care delivery (Program 1) and,
2. Community-based ART with TPT care delivery (Program 2).

The set of regions, $\mathcal{I} = \{1, \ldots, i, \ldots, 9\}$ are defined so they correspond to the nine provinces in South Africa, including Eastern Cape ($i = 1$), Free State ($i = 2$), Gaunteng ($i = 3$), KwaZulu-Natal ($i = 4$), Limpopo ($i = 5$), Mpumalanga ($i = 6$), Northern Cape ($i = 7$), North-West ($i = 8$) and Western Cape ($i = 9$). The set of programs $\mathcal{P} = \{1, 2\}$ includes standard facility-based ART and TPT care delivery ($p = 1$) and community-based ART with TPT care delivery ($p = 2$). The approach generates a set of Pareto optimal solutions that provide realistic and statistically valid insights into the best combination of regions to prioritize for community-based ART with TPT care delivery, given a national budget.

5.2 Calibration of the Dynamic Transmission Compartmental Model

Regional dynamics and uncertainties in TB and HIV disease progression across the nine provinces of South Africa are represented by parameter sets that are identified through model calibration. We calibrate 31 parameters in the dynamic transmission model, where 22 calibrated parameters are general parameters that are held constant over all regions, and nine calibrated parameters are regional-specific parameters that can vary by region. Details of the input parameter values are provided in Chapter 3 in Table 3.6. Since gender differences are not a critical part of the optimization approach presented in this chapter, calibrated parameters for the number of effective contacts for TB transmission per year, HIV incidence rates, and mortality rates are not calibrated by gender (e.g., $\beta_1^i = \beta_2^i$).

Latin hypercube sampling is used to generate 500 samples of the 22 general parameters and 40 samples of the nine regional-specific parameters from the 25% calibration ranges specified in Table 3.6. In each region, 20,000 candidate regional parameter sets are considered, which represent all combinations of the 500 samples of the general parameters and 40 samples of the regional-specific parameters ($500 \times 40 = 20,000$). In each region, the model is executed over the warm-up and calibration period from the beginning of 1940 to the end of 2017, with the 20,000 candidate regional parameter sets that are representative of standard facility-based ART and TPT care delivery (Program 1).

For each region and each of the 20,000 candidate regional parameter sets, model projections are compared to three regional calibration targets, TB incidence, HIV prevalence, and TB- and HIV-related mortality rates per 100,000 individuals using Equation (3.52), Equation (3.53) and Equation (3.54), respectively. Model projections are evaluated against the three calibration targets in 2005, at the peak of the HIV epidemic, and 2017, the year before the intervention period. Regional calibration target ranges are represented by 95% confidence intervals from GBD 2019 [44] for the corresponding South African province. Furthermore, since general parameters are held constant over all regions, we reject regional parameter sets associated with a set of general parameters that do not meet the regional calibration targets in one or more regions. The accepted regional parameter sets are notated as $\bar{\mathcal{K}}_i = \{1, \ldots, \bar{k}, \ldots, \bar{K}_i\}$ for each region $i \in \mathcal{I}$.

To generate candidate national parameter sets, we combine the accepted regional parameter

sets by taking their cross-product for a common general parameter set. Each candidate national parameter set contains 103 randomly generated values, including the 22 general parameters and nine regional-specific values for each of the nine regions ($22+9\times9 = 103$). After filtering for regional parameter sets that meet the regional targets across all regions, 24 common general parameter sets were left. If we considered all remaining candidate national parameter sets resulting from the filtered regional parameter sets, we would have 240,924,612 candidate national parameter sets. To reduce the number of candidate national parameter sets for tractable computation, we identified regional parameter sets that represent the minimum and maximum projections of the TB incidence, HIV prevalence, and TB- and HIV-related mortality rates in 2017, for each of the 24 common general parameter sets. With this reduction, the number of regional parameter sets associated with each of the 24 accepted sets of general parameters is between one and six. This reduced the number of candidate national parameter sets from 240,924,612 to 2,513,680.

Table 5.1 describes the components of the 2,513,680 candidate national parameter sets. The table provides the number of regional parameter sets accepted in region i across the 24 accepted general parameter sets. The total number of accepted regional parameter sets ($\bar{K}_i$ in region i) provided in the second to last row of the table is calculated by summing accepted regional parameter sets accepted in region i over all 24 accepted parameter sets. The number of combinations of regional parameter sets associated with each of the 24 accepted general parameter sets is calculated by taking the cross-product of the number of accepted regional parameter sets associated with each general parameter set (as shown in the last column of Table 5.1.) The total number of candidate national parameter sets (2,513,680) is provided in the last row and column of Table 5.1 and is calculated by summing the number of combinations of regional parameter sets over all 24 accepted general parameter sets.

For each of the candidate national parameter sets, model projections are compared to one national calibration target that represents the total number of TB- and HIV-related deaths in South Africa. For each accepted regional parameter set in each region, model projections for the number of TB- and HIV-related deaths are calculated using Equation (3.55) in Section 3.7.2. Each candidate national parameter set uses regional projections for the number of TB- and HIV-related deaths for associated accepted regional parameter sets to estimate the total number of TB- and

HIV-related deaths in South Africa. To calculate the total number of deaths in South Africa for each candidate national parameter set, the associated regional model projections of TB- and HIV-related deaths are summed across all regions. Model projections are compared to the national calibration target for South Africa in 2005 and 2017, which represents the 95% confidence interval of the total number of TB- and HIV-related deaths in South Africa from GBD 2019 [44]. The accepted national parameter set is notated as $\mathcal{K} = \{1, \ldots, k, \ldots, K\}$. All 2,513,680 candidate national parameter sets were evaluated against the national calibration target in 2005 and 2017, and 2,429,445 national parameter sets were accepted, such that K =2,429,445. While the total number of accepted national parameter sets was reduced to 2,429,445, the number of accepted regional parameter sets in each region i remained the same, because all regional parameter sets were an element of at least one national parameter set.

Uncertainties in the total number of TB- and HIV-related deaths in South Africa are represented by the accepted national parameter sets, $k \in \mathcal{K}$ as illustrated in Figure 5.1. Figure 5.1 illustrates the mean, minimum, and maximum of the 2,429,445 model predictions for the yearly number of TB- and HIV-related deaths in South Africa aggregated over all regions (as calculated in Equation (3.55) in Section 3.7.2), compared to the national calibration target ranges from GBD 2019 for each year between 1990 and 2017.

Uncertainties in the yearly TB incidence rates, HIV prevalence rates, and TB- and HIV-related mortality rates by region are represented by the accepted regional parameter sets $\bar{k} \in \bar{\mathcal{K}}_i$ as illustrated in Figure 5.2. Figure 5.2 illustrates the mean, minimum, and maximum ranges of model predictions for TB incidence rates (as calculated in Equation (3.52) in Section 3.7.2) in the first column, HIV prevalence rates (as calculated in Equation (3.53) in Section 3.7.2) in the second column, and TB- and HIV-related mortality rates (as calculated in Equation (3.54) in Section 3.7.2) in the third column by region i over the accepted regional parameter sets $\bar{k} \in \bar{\mathcal{K}}_i$, compared to the corresponding regional calibration target ranges from GBD 2019 for each year from 1990 to 2017.

5.3 Formulation of the Multi-Objective Optimization Approach

This section introduces a multi-objective optimization approach that determines the best combinations of care delivery programs to implement by region, given a budget constraint and two

Accepted General Parameter Set ID	**Number of Accepted Regional Parameter Sets in Region i Associated with the Accepted Set of General Parameters**									**Number of Combinations of Regional Parameter Sets**
	$i = 1$	$i = 2$	$i = 3$	$i = 4$	$i = 5$	$i = 6$	$i = 7$	$i = 8$	$i = 9$	
1	2	2	3	4	5	6	3	4	5	86,400
2	4	3	1	4	5	4	4	6	5	115,200
3	4	2	2	4	5	5	3	5	3	72,000
4	2	1	2	3	5	5	1	5	2	3,000
5	4	2	3	4	4	5	1	6	4	46,080
6	3	2	2	4	6	5	2	4	5	57,600
7	5	3	2	3	6	5	3	5	5	202,500
8	4	2	3	3	5	4	2	5	4	57,600
9	4	3	4	4	5	5	1	6	4	115,200
10	6	3	2	3	6	4	5	5	5	324,000
11	5	1	5	4	6	5	2	6	4	144,000
12	4	3	2	4	5	5	3	6	5	216,000
13	5	1	4	3	6	5	2	6	4	86,400
14	3	3	2	3	6	5	3	5	4	97,200
15	5	1	5	3	6	4	2	6	4	86,400
16	3	2	1	3	5	5	1	5	2	4,500
17	3	1	5	5	4	5	1	4	3	18,000
18	3	1	4	4	5	5	2	5	2	24,000
19	4	2	4	3	6	5	1	5	3	43,200
20	5	1	2	4	5	5	2	5	4	40,000
21	5	3	2	3	5	5	3	4	4	108,000
22	4	1	4	4	5	4	3	5	4	76,800
23	5	4	3	4	6	5	3	5	4	432,000
24	5	1	4	4	3	5	2	6	4	57,600
$\bar{K}_i$	97	48	71	87	125	116	55	124	93	
										2,513,680

Table 5.1: Number of accepted regional parameter sets accepted in region i across the 24 accepted general parameter sets. The regions are Eastern Cape ($i = 1$), Free State ($i = 2$), Gauteng ($i = 3$), KwaZulu-Natal ($i = 4$), Limpopo ($i = 5$), Mpumalanga ($i = 6$), Northern Cape ($i = 7$), North-West ($i = 8$) and Western Cape ($i = 9$). The number of accepted regional parameter sets $\bar{K}_i$ in region i across all 24 accepted general parameter sets are provided in the second to last row. The total number of candidate national parameter sets is 2,513,680.

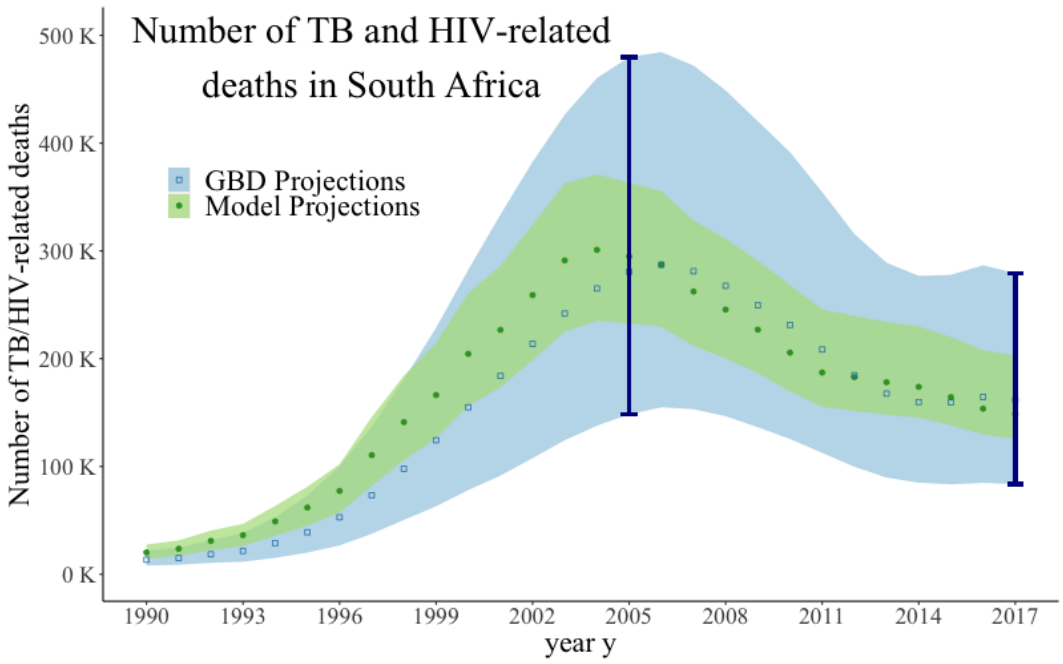

Figure 5.1: Mean, minimum, and maximum of the predicted model results for the yearly number of TB- and HIV-related deaths in South Africa over the 2,429,445 accepted national parameter sets compared to the national calibration target range from GBD 2019 [44] for each year between 1990 and 2017. Model values are shown in green (circles), and estimates from GBD 2019 are shown in blue (squares). In 2005 and 2017, when we compare model values to national target calibration ranges, the ranges are emphasized with lines.

objectives. The decision variables considered in the optimization problem are:

$$u_{i,p} = \begin{cases} 1, \text{if region } i \text{ implements program } p, \\ 0, \text{otherwise} \end{cases}$$

where $i \in \mathcal{I}$, $p \in \mathcal{P}$ and a solution represents a combination of delivery programs, notated as $\{u_{i,p}\}$. A solution must implement exactly one program in each region as in Equation (5.1). The decision variables take on the values of zero or one as in Equation (5.2). I identify a set of the solutions that satisfy both Equation (5.1) and Equation (5.2),

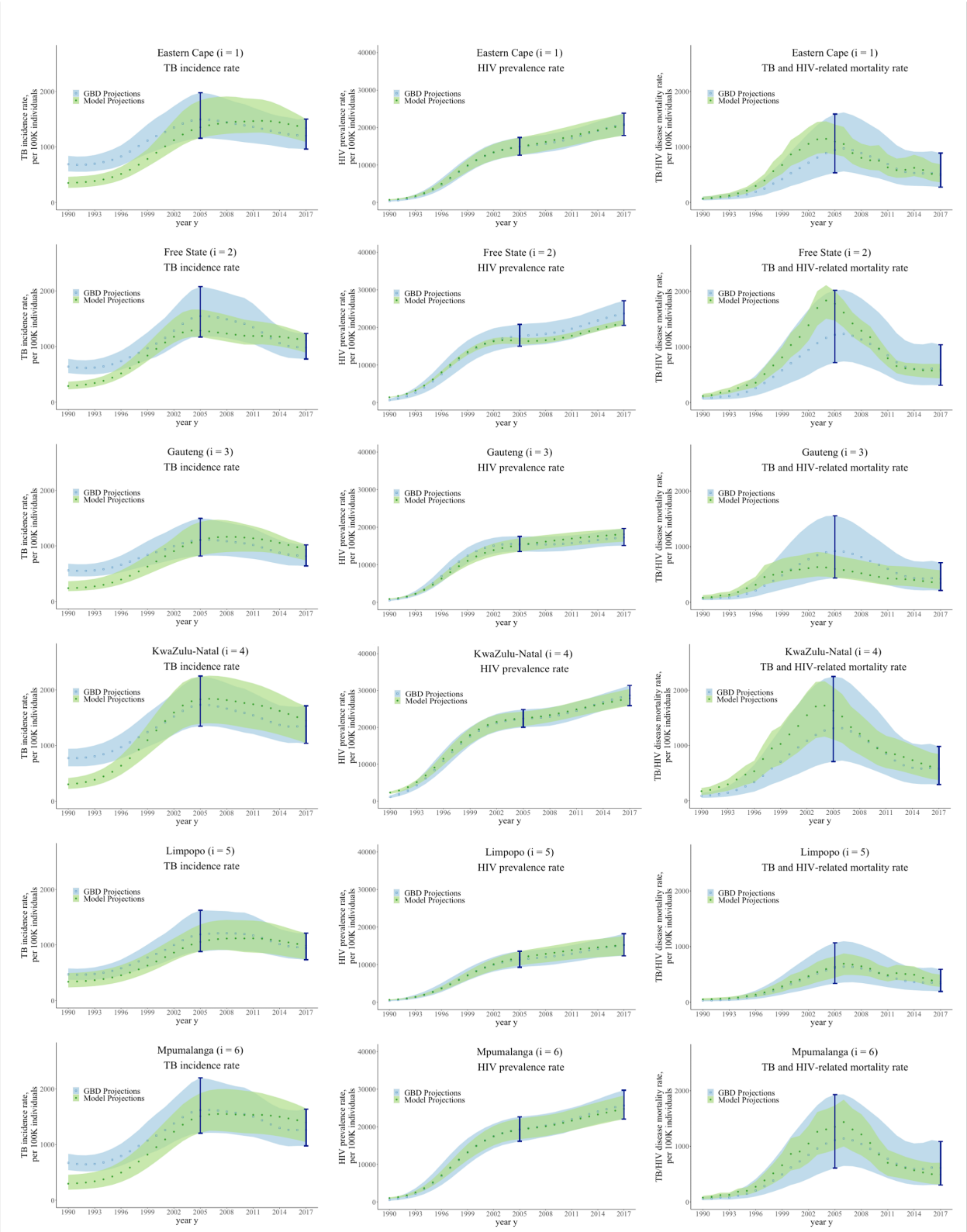

Figure continued on the next page

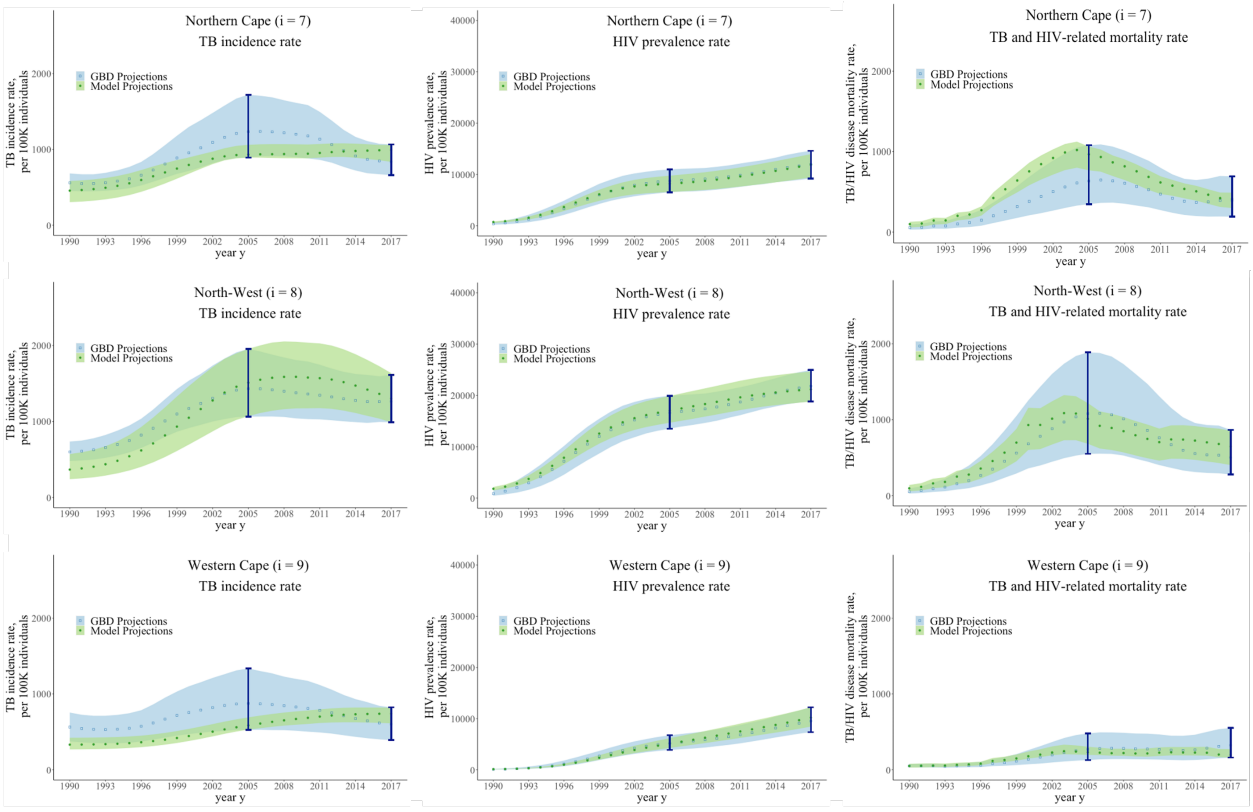

Figure 5.2: Mean, minimum, and maximum model predictions in yearly TB incidence (first column), HIV prevalence (second column), and TB- and HIV-related mortality (third column) rates per 100,000 individuals by region over the accepted regional parameter sets compared to the corresponding regional calibration target ranges from GBD 2019 [44] for each year between 1990 and 2017. Model values are shown in green (circles) and estimates from GBD 2019 are shown in blue (squares). In 2005 and 2017, when we compare model values to regional target calibration ranges, the ranges are emphasized with lines.

$$\sum_{p \in \mathcal{P}} u_{i,p} = 1 \qquad \forall i \in \mathcal{I} \tag{5.1}$$

$$u_{i,p} \in \{0, 1\} \qquad \forall i \in \mathcal{I}, p \in \mathcal{P} \tag{5.2}$$

as $\mathcal{S}$. We evaluate each solution $\{u_{i,p}\} \in \mathcal{S}$ against a budget constraint and two objectives. We use health outcomes and cost projections summarised in Section 5.3.1 and Table 5.2 to estimate a cost function and two objective functions for each solution $\{u_{i,p}\} \in \mathcal{S}$. The budget constraint and two objectives consider uncertainties in program health outcomes and costs across all accepted national parameter sets, notated as $k \in \mathcal{K} = \{1, \ldots, k, \ldots, K\}$.

Section 5.3.1 provides the notation for the projected health outcomes and program costs that are used to quantify the two objective functions and program cost function used in the multi-objective optimization approach. Section 5.3.2 describes how we estimate the total cost function for each solution $\{u_{i,p}\} \in \mathcal{S}$ and evaluate if there is sufficient evidence to say that a solution meets the budget constraint. Section 5.3.3 and Section 5.3.4 describe how we estimate the two objective functions for each solution $\{u_{i,p}\} \in \mathcal{S}$. Section 5.3.5 describes how we determine if there is sufficient evidence to say that a solution is dominated. We also discuss a Pareto optimal solution with sufficient statistical evidence that it is non-dominated and satisfies the budget constraint.

5.3.1 Projections of Health Outcomes and Costs by Region and Program

The notation for program health outcome and cost metrics used in the multi-objective optimization approach is summarised in Table 5.2. To generate these metrics, we run the model with each accepted regional parameter set $\bar{k}$ in each region i under each program p, for all $\bar{k} \in \bar{\mathcal{K}}_i$, $i \in \mathcal{I}, p \in \mathcal{P}$. We calculate the TB- and HIV-related mortality rate for each accepted regional parameter set $\bar{k}$ in each region i under each program p with Equation (3.54) in Section 3.7.2 in Chapter 3. We calculate the number of TB- and HIV-related deaths in each region for each accepted regional parameter set $\bar{k}$ in each region i under each program p with Equation (3.55) in Section 3.7.2 in Chapter 3. We calculate the program costs in each region for each accepted regional parameter set $\bar{k}$ in each region i under each program p with Equation (3.57) in Section 3.7.2 in Chapter 3.

As described in Section 5.2, each accepted national parameter set $k \in \mathcal{K}$ is comprised of a general parameter set and nine regional parameter sets. The projected health outcomes and cost metrics in region i under program p and national parameter set k in year y, make use of the associated nine regional health outcomes and costs in Equation (3.54), Equation (3.55) and Equation (3.57).

Notation	Description
	TB- and HIV-related Mortality
$TBHIVmort\_per_{i,p,k}(y)$	TB- and HIV-related mortality rate per 100,000 individuals in region i under program p and national parameter set k in year y, $i \in \mathcal{I}$, $p \in \mathcal{P}, k \in \mathcal{K}$
$TBHIVmort\_pop_{i,p,k}(y)$	Population-level TB- and HIV-related deaths in region i under program p and national parameter set k in year y, $i \in \mathcal{I}, p \in \mathcal{P}, k \in \mathcal{K}$
	Program Costs
$Cost\_pop_{i,p,k}(y)$	Population-level cost of administering ART and TPT in region i under program p and national parameter set k in year y, $i \in \mathcal{I}, p \in \mathcal{P}, k \in \mathcal{K}$

Table 5.2: Notation for program health outcomes and cost metrics integrated into the multi-objective optimization approach.

5.3.2 Budget Constraint

We compare the program cost function against a budget constraint to determine if there is sufficient evidence to say that a solution meets the budget constraint. The program cost function represents the total cost of implementing exactly one program in each region during the intervention period. We approximate the sample mean of the program cost function for the solution $\{u_{i,p}\}$ with the K realizations of $Cost\_pop_{i,p,k}(y)$ for each region i and program p under national parameter set k and values of the decision variables in solution $\{u_{i,p}\}$ as,

$$\hat{m}^{cost}\Big[\{u_{i,p}\}, \{Cost\_pop_{i,p,k}(y)\}\Big] = \frac{1}{K}\sum_{k\in\mathcal{K}}\left(\sum_{i\in\mathcal{I}}\sum_{p\in\mathcal{P}}\sum_{y\in\mathcal{Y}}\Big(u_{i,p}\Big)Cost\_pop_{i,p,k}(y)\right). \tag{5.3}$$

Similarly, we approximate the sample variance of the program cost function for the solution $\{u_{i,p}\}$ as,

$$\hat{v}^{cost}\Big[\{u_{i,p}\},\{Cost\_pop_{i,p,k}(y)\}\Big] = \frac{1}{K}\sum_{k\in\mathcal{K}}\Bigg(\sum_{i\in\mathcal{I}}\sum_{p\in\mathcal{P}}\sum_{y\in\mathcal{Y}}\Big(u_{i,p}\Big)Cost\_pop_{i,p,k}(y) - \hat{m}^{cost}\Big[\{u_{i,p}\},\{Cost\_pop_{i,p,k}(y)\}\Big]\Bigg)^2. \quad (5.4)$$

A solution is said to meet the budget constraint if the probability that the program cost for the solution $\{u_{i,p}\}$ is less than a budget of B is greater than the probability of α^{budget}. We assume the cost function takes on a normal distribution. This is a reasonable assumption for a large number of accepted parameter sets. We evaluate each solution $\{u_{i,p}\} \in \mathcal{S}$ to determine if it probabilistically meets the budget constraint using a z-distribution for the mean. Letting $z[\alpha^{budget}]$ be the z-score of a one-tailed z-distribution with a tail probability of α^{budget}, we can calculate the upper bound of the confidence interval for the cost function for the solution $\{u_{i,p}\}$, represented by the left-hand side of Equation (5.5). Then we can say that the solution $\{u_{i,p}\}$ meets the budget constraint if

$$\hat{m}^{cost}\Big[\{u_{i,p}\},\{Cost\_pop_{i,p,k}(y)\}\Big] + z[\alpha^{budget}]\left(\sqrt{\frac{\hat{v}^{cost}\Big[\{u_{i,p}\},\{Cost\_pop_{i,p,k}(y)\}\Big]}{K}}\right) \leq B. \quad (5.5)$$

5.3.3 Objective Function 1: TB- and HIV-related Mortality Rate Inequity

The first objective function represents the maximum difference between the TB- and HIV-related mortality rate in each region and the average TB- and HIV-related mortality rate overall I regions in the last year Y of the intervention period. We approximate the sample mean of the first objective function for the solution $\{u_{i,p}\}$ with the K realizations of $TBHIVmort\_per_{i,p,k}(Y)$ as,

$$\hat{m}_1^{obj}\Big[\{u_{i,p}\},\{TBHIVmort\_per_{i,p,k}(Y)\}\Big] = \frac{1}{K}\sum_{k\in\mathcal{K}}\Bigg(\max_{i\in\mathcal{I}}\Bigg\{\sum_{p\in\mathcal{P}}\Big(u_{i,p}\Big)TBHIVmort\_per_{i,p,k}(Y) - \frac{1}{I}\sum_{\bar{i}\in\mathcal{I}}\sum_{p\in\mathcal{P}}\Big(u_{\bar{i},p}\Big)TBHIVmort\_per_{\bar{i},p,k}(Y)\Bigg\}\Bigg). \quad (5.6)$$

Similarly, we approximate the sample variance of the first objective function for the solution

$\{u_{i,p}\}$ as,

$$\hat{v}_1^{obj}\Big[\{u_{i,p}\},\{TBHIVmort\_per_{i,p,k}(Y)\}\Big] = \frac{1}{K}\sum_{k\in\mathcal{K}}\Bigg(\max_{i\in\mathcal{I}}\Bigg\{\sum_{p\in\mathcal{P}}\Big(u_{i,p}\Big)TBHIVmort\_per_{i,p,k}(Y)\Big) - \frac{1}{I}\sum_{\tilde{i}\in\mathcal{I}}\sum_{p\in\mathcal{P}}\Big(u_{i,p}\Big)TBHIVmort\_per_{i,p,k}(Y)\Bigg\} - \hat{m}_1^{obj}\Big[\{u_{i,p}\},\{TBHIVmort\_per_{i,p,k}(Y)\}\Big]\Bigg)^2. \quad (5.7)$$

5.3.4 Objective Function 2: Total TB- and HIV-related Deaths

The second objective function represents the total (population-level) TB- and HIV-related mortality rate summed over all regions and years during the intervention period. We approximate the sample mean of the second objective function for the solution $\{u_{i,p}\}$ with the K realizations of $TBHIVmort\_pop_{i,p,k}(y)$ as,

$$\hat{m}_2^{obj}\Big[\{u_{i,p}\},\{TBHIVmort\_pop_{i,p,k}(y)\}\Big] = \frac{1}{K}\sum_{k\in\mathcal{K}}\Bigg(\sum_{i\in\mathcal{I}}\sum_{p\in\mathcal{P}}\sum_{y\in\mathcal{Y}}\Big(u_{i,p}\Big)TBHIVmort\_pop_{i,p,k}(y)\Bigg). \quad (5.8)$$

Similarly, we approximate the sample variance of the second objective function for the solution $\{u_{i,p}\}$ as,

$$\hat{v}_2^{obj}\Big[\{u_{i,p}\},\{TBHIVmort\_pop_{i,p,k}(y)\}\Big] = \frac{1}{K}\sum_{k\in\mathcal{K}}\Bigg(\sum_{i\in\mathcal{I}}\sum_{p\in\mathcal{P}}\sum_{y\in\mathcal{Y}}\Big(u_{i,p}\Big)TBHIVmort\_pop_{i,p,k}(y) - \hat{m}_2^{obj}\Big[\{u_{i,p}\},\{TBHIVmort\_pop_{i,p,k}(y)\}\Big]\Bigg)^2. \quad (5.9)$$

5.3.5 Probabilistic Dominance and Pareto Optimality

This section defines the concept of probabilistic dominance and Pareto optimality. We assume the two objective functions take on a normal distribution with the means and variances defined in Section 5.3.3 and Section 5.3.4. This is a reasonable assumption for a large number of accepted parameter sets. In this section, we let $F_j(\{u_{i,p}\})$ denote the two objective functions with subscript

$j \in \{1, 2\}$. We let $\hat{m}_j^{obj}(\{u_{i,p}\})$ and $\hat{v}_j^{obj}(\{u_{i,p}\})$ represent the mean and variance for the jth objective function for solution $\{u_{i,p}\}$. For example $\hat{m}_1^{obj}(\{u_{i,p}\}) = \hat{m}_1^{obj}[\{u_{i,p}\}, \{TBHIVmort\_per_{i,p,k}(Y)\}]$. For each objective function $j \in \{1, 2\}$, we consider solution $\{\tilde{u}_{i,p}\}$ to be "better" than solution $\{u'_{i,p}\}$ if the probability that the objective function value of $\{\tilde{u}_{i,p}\}$ is less than or equal to that of $\{u'_{i,p}\}$ is at least α_j^{obj}, that is,

$$P[F_j(\{\tilde{u}_{i,p}\}) \leq F_j(\{u'_{i,p}\})] \geq \alpha_j^{obj}. \tag{5.10}$$

Treating the mean of the objective function j with a z-distribution and letting $z[\alpha_j^{obj}]$ be the z-score of a two-tailed z-distribution with a tail probability of α_j^{obj}, then we say that the solution $\{\tilde{u}_{i,p}\}$ is "better" than solution $\{u'_{i,p}\}$ on the jth objective function if

$$\hat{m}_j^{obj}(\{\tilde{u}_{i,p}\}) - \hat{m}_j^{obj}(\{u'_{i,p}\}) + z[\alpha_j^{obj}] \left(\sqrt{\frac{\hat{v}_j^{obj}(\{\tilde{u}_{i,p}\}) + \hat{v}_j^{obj}(u'_{i,p}\})}{K}} \right) \leq 0. \tag{5.11}$$

We say that a solution is probabilistically dominated if there exists another solution that is "better" on both objective functions. We say a solution is probabilistically non-dominated if there does not exist another solution that probabilistically dominates it.

A solution is Pareto optimal if it satisfies the budget constraint in Equation (5.5) and is probabilistically non-dominated. For each Pareto optimal solution, $\{u_{i,p}\}$, and each objective j the approach returns a confidence interval of α_j^{obj}, where the upper and lower bounds are calculated as,

$$\hat{m}_j^{obj}(\{u_{i,p}\}) \pm z[\alpha_j^{obj}] \sqrt{\frac{\hat{v}_j^{obj}(\{u_{i,p}\})}{K}}. \tag{5.12}$$

The decision maker can use confidence intervals to determine the uncertainty in objective function values for each Pareto optimal solution. In addition, if the confidence intervals of an objective function for two Pareto optimal solutions overlap, it suggests that there is a statistically insignificant difference in the objective function estimates between the two Pareto optimal solutions.

5.4 Results of the Multi-Objective Optimization Approach

This section presents the results of the multi-objective optimization approach. Section 5.4.1 provides the projected health and cost impacts of implementing community-based care by region. Section 5.4.2 provides the statistically valid Pareto optimal solutions.

5.4.1 Regional Impacts of Care Delivery Programs

This section describes projected health outcomes and program costs by region i and program p over the intervention period from the start of 2018 to the end of 2027. Table 5.3 presents the mean, minimum, and maximum model predicted values over the accepted regional parameter sets for TB- and HIV-related mortality rate per 100,000 individuals in the last year of the intervention period Y, $TBHIVmort\_per_{i,p,k}(Y)$ (used to calculate the first objective), the population-level TB- and HIV-related deaths summed over the 10-year intervention period, $\sum_{y\in\mathcal{Y}} TBHIVmort\_pop_{i,p,k}(y)$ (used to calculate the second objective) and population-level program costs summed the 10-year intervention period, $\sum_{y\in\mathcal{Y}} Cost\_pop_{i,p,k}(y)$ (used to calculate the cost function), by region i and program p.

We calculate the incremental health gains by taking the difference between health projections under standard facility-based ART and TPT care delivery ($p = 1$) minus health projections under community-based ART with TPT care delivery ($p = 2$) for each region $i \in \mathcal{I}$ for each regional parameter set, $\bar{k} \in \bar{\mathcal{K}}_i$. Incremental additional costs are calculated by taking the difference between costs under community-based ART with TPT care delivery ($p = 2$) minus costs of standard facility-based ART and TPT care delivery ($p = 1$) for each region $i \in \mathcal{I}$ for each regional parameter set, $\bar{k} \in \bar{\mathcal{K}}_i$.

As shown in Table 5.3, the model projects that implementing the community-based ART with TPT care delivery program ($p = 2$) shows the greatest incremental health gains, compared to standard facility-based ART and TPT care delivery ($p = 1$) in terms of TB- and HIV-related mortality rates in Free State ($i = 2$), KwaZulu-Natal ($i = 4$) and North-West ($i = 8$). The greatest incremental health gains in terms of population-level TB- and HIV-related deaths are seen in KwaZulu-Natal ($i = 4$) and Gauteng ($i = 3$). Table 5.3 also shows that the greatest incremental additional costs from implementing community-based ART with TPT care delivery program ($p = 2$)

instead of standard facility-based ART and TPT care delivery ($p = 1$) are seen in KwaZulu-Natal ($i = 4$) and Gauteng ($i = 3$). This is due, in part, to Guanteng and KwaZulu-Natal having the highest populations [44]. However, the model predicts the incremental health gains and additional costs are, on average, higher in KwaZulu-Natal ($i = 4$) compared to Gauteng ($i = 3$) due to higher projected TB incidence and HIV prevalence rates [44].

5.4.2 Pareto Optimal Solutions

We evaluated 512 solutions, representing all possible combinations of the two programs across the nine regions ($2^9 = 512$). A solution is Pareto optimal if it satisfies the budget constraint in Equation (5.5) and is probabilistically non-dominated.

We set the budget to 15 billion USD, $B = \$15$ billion over 10 years [89]. We set $\alpha^{budget} = 0.95$. Thus, a solution meets the budget constraint in Equation (5.5) if the probability that a solution costs less than 15 billion USD is greater than 95%. Out of the 512 solutions, 195 met the budget constraint.

A solution is probabilistically dominated as defined in Equation (5.11) if there is a solution that is better on the two objective functions with a probability of 95% ($\alpha_1^{obj} = \alpha_2^{obj} = 0.95$). A solution is probabilistically non-dominated if there does not exist another solution that probabilistically dominates it. Out of the 195 solutions that met the budget constraint, ten are probabilistically non-dominated.

Figure 5.3 and Table 5.4 present the ten Pareto optimal solutions and illustrate how the Pareto optimal solutions balance the first objective, inequity in TB- and HIV-related mortality rates between regions, with the second objective, the total TB- and HIV-related deaths summed over all regions. If the approach only considered the first objective, TB- and HIV-related mortality rate inequity, according to the sample mean, then Solution 1 would be the optimal solution. If the approach only considered the second objective, total TB- and HIV-related deaths, according to the sample mean, then Solution 5 would be the optimal solution.

In Figure 5.3 and Table 5.4, Solutions 1-5 are highlighted in blue to indicate that these solutions are non-dominated if we only consider the sample means of the objective functions. Solutions 6-10 are also included because they are non-dominated when considering uncertainty. Figure 5.3 and

Table 5.4 provide the 95% confidence intervals for the two objective functions as calculated in Equation (5.12). Overlapping confidence intervals of objective functions for the Pareto optimal solutions indicate that the differences in objective function values are insignificant. For example, when considering uncertainties, there is insufficient statistical evidence that Solution 5 is better than solutions 4, 8, 9, and 10, as indicated by their overlapping 95% confidence intervals for the second objective, total TB- and HIV-related deaths.

Table 5.4 provides the decision variable results, indicating that region i implements program p. For example, under Solution 1, community-based ART with TPT care delivery ($p = 2$) is implemented in Free State ($i = 2$), KwaZulu-Natal ($i = 4$), and North-West ($i = 8$). Under Solution 5, community-based ART with TPT care delivery ($p = 2$) is implemented in Eastern Cape ($i = 1$), Free State ($i = 2$), KwaZulu-Natal ($i = 4$), and Northern Cape ($i = 7$).

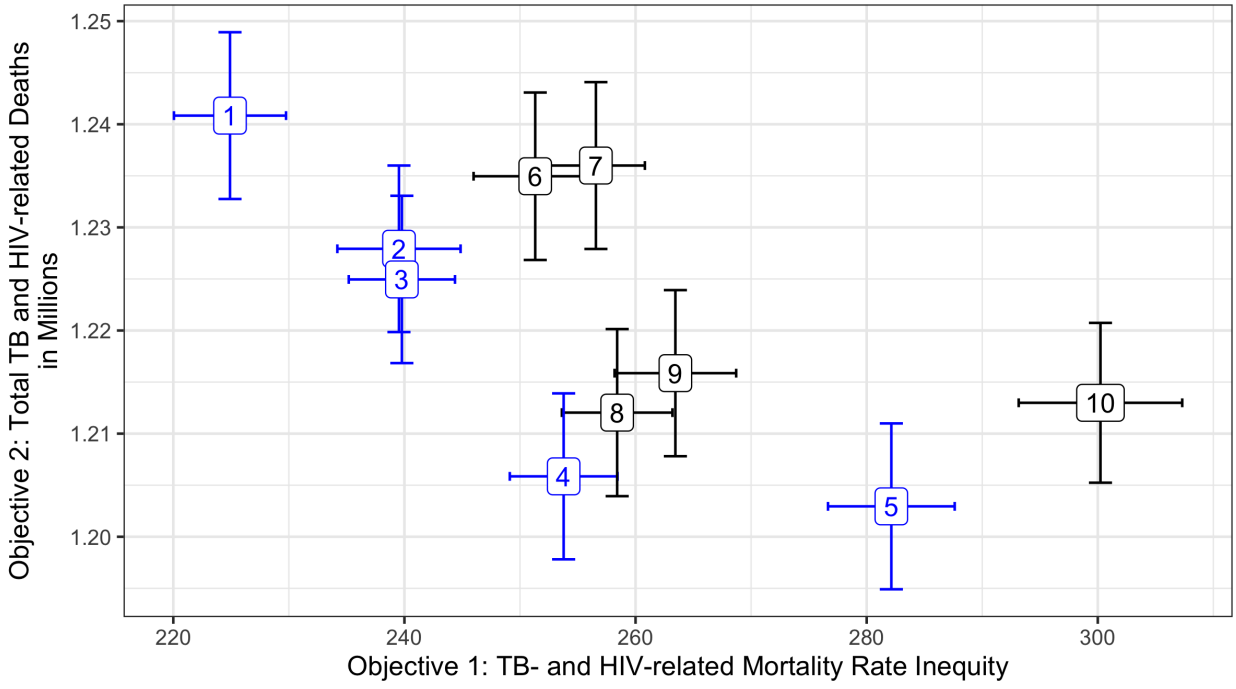

Figure 5.3: Illustration of the trade-offs of the Pareto optimal solutions, including the sample means and 95% confidence intervals over the 2,429,445 accepted national parameter sets for the two objectives with a budget of $15 billion. Solutions 1-5 are highlighted in blue to indicate that these solutions are non-dominated if we only consider the sample means of the objective functions. Solutions 6-10 are also included because they are non-dominated when considering 95% confidence intervals of the objective functions.

5.5 Discussion

The results illustrate the trade-offs of TB- and HIV-related mortality rate inequities between regions and the total TB- and HIV-related deaths between ten Pareto optimal solutions. The approach suggests if the decision makers' only objective is to minimize TB- and HIV-related mortality rate inequities between regions (objective 1), they should consider implementing community-based care delivery ($p = 2$) in Free State ($i = 2$), KwaZulu-Natal ($i = 4$), and North-West ($i = 8$), as suggested by Solution 1 (see Table 5.4). These regions correspond to the provinces with the highest projected TB- and HIV-related mortality rates in the last year of the intervention period under standard facility-based ART and TPT care delivery ($p = 1$), as indicated in Table 5.3.

The approach suggests if the decision maker's only objective is to minimize total TB- and HIV-related deaths, they should consider implementing community-based care delivery ($p = 2$) in Eastern Cape ($i = 1$), Free State ($i = 2$), KwaZulu-Natal ($i = 4$) and Northern Cape ($i = 7$), as suggested by Solution 5 (see Table 5.4). When comparing Solution 1 to Solution 5, the suggested program varies in three of the nine regions, including Eastern Cape ($i = 1$), Northern Cape ($i = 7$), and North-West ($i = 8$). This suggests that while implementing community-based care delivery in regions with high TB- and HIV-related mortality rates can reduce TB- and HIV-related mortality rate inequities between regions, it may not result in the minimum number of total TB- and HIV-related deaths.

Solution 4 balances the two objectives. When comparing Solution 1 to Solution 4, the suggested program varies in two of the nine regions, including Eastern Cape ($i = 1$) and Free State ($i = 2$). When comparing Solution 5 to Solution 4, the suggested program varies in three of the nine regions, including Free State ($i = 2$), Northern Cape ($i = 7$), and North-West ($i = 8$). When comparing Solutions 1, 4, and 5, the suggested program to implement is the same in five of the nine provinces, including Gauteng ($i = 3$), KwaZulu-Natal ($i = 4$), Limpopo ($i = 5$), Mpumalanga ($i = 6$), and Western Cape ($i = 9$).

None of the Pareto optimal solutions suggest the implementation of community-based care delivery ($p = 2$) in Guanteng ($i = 3$) or Western Cape ($i = 9$), whereas, nine out of the ten Pareto optimal solutions suggest implementation of community-based care delivery ($p = 2$) in KwaZulu-Natal ($i = 4$). If the approach only considered the sample means of the objective functions,

none of the Pareto optimal solutions would suggest the implementation of community-based care delivery ($p = 2$) in Limpopo ($i = 5$), as indicated by Solutions 1-5. However, when considering uncertainty in objective function values with 95% confidence intervals, Solutions 7 and 10 suggest the implementation of community-based care delivery ($p = 2$) in Limpopo ($i = 5$).

5.6 Conclusion and Future Work

The proposed approach addresses gaps in modeling methods for allocating a national budget for community-based ART with TPT care delivery to regions. Specifically, we contribute to the development of approaches to budget allocation for regional TB and HIV care delivery programs that: consider regional differences and allow for regional implementation of community-based ART with TPT care delivery, balance equity and effectiveness objectives, and consider uncertainties in health outcomes and costs.

Allowing for the implementation of programs by regions could enhance health outcomes while remaining within a fixed national budget. In order to represent regional differences, we calibrate parameters to three regional calibration targets in each region. Figure 5.2 illustrates how projections reflect regional differences in TB incidence, HIV prevalence, and TB- and HIV-related mortality rates across the nine South African provinces. Capturing the impacts of the two candidate care delivery programs in each region (see Table 5.3) enables us to explore which regions should be prioritized for community-based ART with TPT care delivery.

The two objective functions balance equity and effectiveness of TB- and HIV-related health outcomes. The trade-offs captured by the multi-objective approach are illustrated in Figure 5.3 and highlight the extremes as well as the balanced solution. The ten Pareto optimal solutions give different implementations by region, and can be considered in conjunction with other factors relevant to decision makers that are not captured by the modeling approach (e.g., practicalities and political pressures) [85].

The uncertainties in model projections are captured by estimating the sample means and sample variances of the two objective functions and using statistical tests to determine if a solution is probabilistically non-dominated. Instead of solely relying on sample means and considering Solutions 1-5, this approach provides information to decision makers to consider the additional Solutions 6-10,

which are probabilistically non-dominated as indicated by the overlapping confidence intervals in Figure 5.3.

Stakeholder participation is crucial in the model design and budget allocation process. Clear and reasonable assumptions must be made for the models to be relevant to stakeholders and their needs. We made several simplifying assumptions. We assume no immigration and emigration between regions. We assumed that community-based ART with TPT care would immediately impact ART coverage and TPT initiation rates and could be sustained over ten years. We did not consider programs that allowed partial implementation of community-based care delivery in a province. For simplicity, we do not account for the reduced risk of infection and re-infection while on TPT. This might be particularly important to account for when the TPT course is longer than six months.

Several important future research directions might be worth investigating to address the limitations of the proposed approach. When dealing with a fast-spreading disease (e.g., Ebola), it may not be reasonable to assume that there is no movement of people between regions. It would be interesting to extend the model to relax this assumption and still keep the model computationally tractable for application to fast-spreading diseases. To improve the applicability of the model, it would be interesting to explore modifications to the model that allow for partial implementation of community-based care delivery in a province and consider ramp-up overtime of increased coverage.

Region	Standard facility-based ART and TPT care delivery ($p = 1$)	Community-based ART with TPT care delivery ($p = 2$)	Community-based vs. facility-based care delivery
TB- and HIV-related mortality rate, per 100,000 individuals in region i under program p in the last year of the intervention period			
			Incremental Health Gains
Eastern Cape ($i = 1$)	510 [375, 740]	269 [155, 498]	241 [162, 302]
Free State ($i = 2$)	600 [455, 743]	319 [190, 503]	281 [216, 339]
Gauteng ($i = 3$)	331 [225, 557]	164 [80, 393]	167 [111, 247]
KwaZulu-Natal ($i = 4$)	607 [377, 883]	307 [133, 613]	301 [177, 405]
Limpopo ($i = 5$)	370 [275, 499]	199 [116, 318]	171 [98, 223]
Mpumalanga ($i = 6$)	522 [321, 775]	280 [110, 543]	242 [147, 342]
Northern Cape ($i = 7$)	479 [330, 583]	291 [151, 427]	188 [128, 227]
North-West ($i = 8$)	605 [378, 802]	323 [144, 575]	282 [188, 358]
Western Cape ($i = 9$)	245 [197, 351]	124 [85, 214]	121 [88, 358]
Population-level TB- and HIV-related deaths in thousands in region i under program p summed over all years in the intervention period			
			Incremental Health Gains
Eastern Cape ($i = 1$)	188 [138, 273]	113 [70, 197]	75 [49, 95]
Free State ($i = 2$)	101 [76, 125]	61 [39, 90]	40 [30, 49]
Gauteng ($i = 3$)	317 [215, 538]	182 [99, 405]	136 [88, 201]
KwaZulu-Natal ($i = 4$)	383 [237, 558]	222 [109, 414]	161 [93, 220]
Limpopo ($i = 5$)	114 [89, 154]	69 [43, 107]	45 [25, 62]
Mpumalanga ($i = 6$)	144 [89, 214]	88 [40, 161]	56 [33, 81]
Northern Cape ($i = 7$)	40 [27, 48]	27 [15, 38]	13 [9, 16]
North-West ($i = 8$)	125 [77, 167]	76 [72, 80]	49 [48, 50]
Western Cape ($i = 9$)	93 [76, 133]	55 [39, 90]	38 [27, 55]
Population-level program costs in millions of USD in region i under program p summed over all years in the intervention period			
			Incremental Additional Costs
Eastern Cape ($i = 1$)	1,390 [984, 1,783]	2,172 [1,528, 2,813]	782 [544, 1,031]
Free State ($i = 2$)	634 [459, 745]	995 [713, 1,171]	361 [255, 425]
Gauteng ($i = 3$)	2,975 [2,012, 3,552]	4,748 [3,200, 5,666]	1,773 [1,164, 2,114]
KwaZulu-Natal ($i = 4$)	3,128 [2,050, 3,803]	4,946 [3,221, 6,032]	1,818 [1,145, 2,135]
Limpopo ($i = 5$)	817 [530, 1,050]	1,288 [833, 1,654]	471 [303, 605]
Mpumalanga ($i = 6$)	1,187 [801, 1,579]	1,885 [1,254, 2,523]	698 [454, 944]
Northern Cape ($i = 7$)	175 [112, 239]	274 [172, 376]	99 [60, 137]
North-West ($i = 8$)	730 [465, 949]	1,167 [726, 1,523]	437 [261, 577]
Western Cape ($i = 9$)	838 [607, 1,058]	1,295 [930, 1,638]	457 [324, 579]

Table 5.3: Projected regional health TB- and HIV-related mortality rates per 100,000 individuals, population-level TB- and HIV-related deaths and program costs by program. Values are the mean, minimum, and maximum values over the accepted regional parameter sets. We compare community-based to standard facility-based ART and TPT care delivery for each accepted regional parameter set and present health gains and additional costs.

Solution ID	Objective 1: TB- and HIV-related Mortality Rate Inequity	Objective 2: Total TB- and HIV-related Deaths in Millions	Total Program Costs in Billions	Decision variables results indicating that region i implements program p								
				$i=1$	$i=2$	$i=3$	$i=4$	$i=5$	$i=6$	$i=7$	$i=8$	$i=9$
1	225 [221, 230]	1.241 [1.234, 1.249]	14.570	1	2	1	2	1	1	1	2	1
2	240 [235, 245]	1.228 [1.221, 1.236]	14.664	1	2	1	2	1	1	2	2	1
3	240 [236, 244]	1.225 [1.218, 1.233]	14.889	1	1	1	2	1	2	1	2	1
4	254 [250, 258]	1.206 [1.199, 1.214]	14.968	2	1	1	2	1	1	1	2	1
5	282 [278, 288]	1.203 [1.196, 1.211]	14.991	2	2	1	2	1	1	2	1	1
6	251 [246, 257]	1.235 [1.227, 1.243]	14.828	1	2	1	2	1	2	1	1	1
7	257 [252, 261]	1.236 [1.228, 1.244]	14.674	1	1	1	2	2	1	1	2	1
8	258 [254, 263]	1.212 [1.204, 1.220]	14.985	1	1	1	2	1	2	2	2	1
9	263 [258, 269]	1.216 [1.208, 1.224]	14.895	2	2	1	2	1	1	1	1	1
10	300 [293, 307]	1.213 [1.205, 1.221]	14.778	2	2	1	1	2	2	2	2	1

Table 5.4: Pareto optimal solutions, including the sample means and 95% confidence intervals over the 2,429,445 accepted national parameter sets for the two objectives with a budget of $15 billion. The total program cost represents the upper bound of a one-tailed 95% confidence interval over the accepted national parameter sets. Solutions 1-5 are highlighted in blue to indicate that these solutions are non-dominated if we only consider their sample means. Solutions 6-10 are also included because they are non-dominated when considering their 95% confidence intervals. The set of regions is Eastern Cape ($i=1$), Free State ($i=2$), Gauteng ($i=3$), KwaZulu-Natal ($i=4$), Limpopo ($i=5$), Mpumalanga ($i=6$), Northern Cape ($i=7$), North-West ($i=8$) and Western Cape ($i=9$). Each solution in each region i implements either standard facility-based ART and TPT care ($p=1$) or community-based ART with TPT delivery ($p=2$) as indicated when $u_{i,p}=1$.

Chapter 6

CONCLUSION AND FUTURE RESEARCH

This dissertation focuses on practical approaches that address challenges for decision making in health care related to managing infectious diseases. The approaches address challenges including: (1) dynamics and uncertainties in demand, supply, and health outcomes, (2) multiple objectives, and (3) unique vulnerabilities of populations. To address these challenges, I presented approaches that integrate mathematical optimization, dynamic transmission compartmental modeling, and statistical methodologies to manage infectious diseases. The approaches are applied to three realistic applications, including inventory and order management for multiple healthcare commodities and populations during an infectious disease outbreak; policy analysis of tuberculosis (TB) and HIV health care program interventions in KwaZulu-Natal, South Africa; and budget allocation to regional TB and HIV health care programs across the nine provinces of South Africa.

In Chapter 2, an inventory and order management optimization model for multiple healthcare commodities and populations is introduced. This chapter describes the unique challenges, decisions, and objectives of a healthcare inventory and order management role during a pandemic identified through collaborations with several organizations managing inventory for healthcare commodities during the COVID-19 pandemic. For instance, the model addresses challenges in managing uncertainties in demand and supply over time. The model accounts for the uncertainty of demand and supply over time through chance constraints. Uncertainty in lead times is considered through a discretized probability distribution to project incoming orders. When new information unexpectedly arises, the model is designed to support agile and collaborative decision making in that it can support quick adaptations of decisions that account for the rippling effects of these decisions. The model considers multiple objectives that balance the impacts of delays and substitutions of healthcare commodities against supply, budgeting, and warehouse constraints. The disproportionate impact of delays and substitutions of healthcare commodities on vulnerable populations is accounted for with the use of a new Healthcare Commodity Metric that quantifies the relative

consequences of delays and substitutions on various populations and commodities using suitability- and criticality-based inputs.

In future research, it would be interesting to extend the model to account for dynamic pricing as demand and supply constantly change. Additionally, it would be interesting for the model to consider the implications of reusing commodities and shipping costs, which are excluded to keep the model linear. To further reduce decision-making silos, a model extension that integrates other supply chain management functions (e.g., final-mile distribution) would be beneficial.

In Chapter 3, I introduce two versions of a dynamic transmission compartmental model of TB and HIV disease progression. The two versions of the dynamic transmission compartmental model were built in collaboration with epidemiologists and account for the implications of TB and HIV co-infection by gender and the implications of TB drug resistance. The two versions of the dynamic transmission compartmental model are designed to test the impacts of varying levels of antiretroviral therapy (ART) and TB preventative therapy (TPT) uptake. These models can be used to project health outcomes such as TB incidence, HIV prevalence, TB- and HIV-related mortality, disability-adjusted life years (DALYs), and program costs.

However, these models have their limitations. The first version of the model considers the reduced risk of infection while on TPT, but the parameters that represent the impacts of TPT on reduced risk of developing active TB are difficult to estimate at the regional level. As a result, it would be challenging to apply the first version of the model across regions. To overcome this challenge, the second version of the model was modified to allow for better generalizability across regions; however, for simplicity, it does not consider the reduced risk of infection while on TPT. We recommend developing a future model that considers both factors.

Chapter 4 evaluates the impact of community-based care delivery of ART and TPT in KwaZulu-Natal, South Africa, among 100,000 adults, ages 15-59, in KwaZulu-Natal, South Africa. The dynamic transmission model of TB and HIV transmission and disease progression presented in Chapter 3 (version one) is used to project health outcomes with inputs that are based on findings from the DO ART trial [16] and scientific literature. The model is calibrated over 34 parameters and is used to identify a range of accepted parameter sets that meet 20 calibration targets that represent ten TB- and HIV-related health outcomes across two years from GBD 2019 [44]. To represent

uncertainties, projections of TB- and HIV-related health outcomes and costs are provided across the accepted parameter sets. The policy analysis provides cost-effectiveness rations to provide the trade-offs of health gains and additional costs under community-based and standard facility-based ART with TPT care delivery programs. It also provides insights into how community-based care delivery programs can reduce gender disparities in health outcomes and the indirect benefits of these programs on the HIV negative population, compared to standard facility-based care delivery programs.

In future research, it would be beneficial to test multiple scenarios that account for a ramp-up period where the programs do not take full effect immediately. Additionally, it would be helpful to test realistic scenarios where ART coverage and TPT initiation fluctuate over time instead of assuming sustained programs over ten years. This type of scenario testing may be critical if a decision-maker wants to evaluate the program's impacts over an intervention period of more than ten years.

Chapter 5, introduces an optimal budget allocation approach to regional TB and HIV care delivery programs. The TB and HIV dynamic transmission compartmental model presented in Chapter 3 (version two) is used to capture the dynamics and uncertainties of TB- and HIV-related deaths in each of the nine regions of South Africa under two care delivery programs. The model accounts for uncertainties in TB- and HIV-related health outcomes by identifying a range of parameter sets that meet regional and national calibration targets over two years. Uncertainties in model projections are quantified by estimating the mean and variance of objective functions and cost function across the set of accepted parameter sets identified through calibration. The approach considers two objectives that balance equity and effectiveness of TB- and HIV-related health outcomes against a budget constraint. The first objective function represents inequity in TB- and HIV-related mortality rates between regions. The second objective function is the total TB- and HIV-related deaths summed over all regions. The approach uses statistical tests with the estimated means and variances of the two objective function to evaluate if a solution is probabilistically dominated. The budget constraint captures the risk of exceeding a national budget.

In future research, the approach could be applied to various infectious diseases and locations. It is crucial that any new applications involve stakeholders in the development of the budget allocation

design. The models should be based on clear and reasonable assumptions to meet stakeholders' needs. To improve the approach's applicability to fast-spreading diseases (e.g., Ebola), it would be interesting to extend the model to allow for the movement of infections between regions. To further prioritize vulnerable populations, it would be interesting to explore extensions that allow for partial implementation of community-based care delivery in a province that targets high risk populations.

The research outlined in this dissertation offers practical decision support to address the unique challenges faced by decision makers and stakeholders in the management of infectious diseases. This research paves the way for more effective, practical, and equitable approaches to improve outcomes.

BIBLIOGRAPHY

[1] K. Abedrabboh, M. Pilz, Z. Al-Fagih, O.S. Al-Fagih, J. Nebel, and L. Al-Fagih. Game theory to enhance stock management of personal protective equipment (PPE) during the COVID-19 outbreak. *PLoS One*, 16(2):e0246110, 2021.

[2] A.N. Ackah, H. Digbeu, K. Daillo, A E. Greenberg, D. Coulibaly, I. Coulibaly, K.M. Vetter, and K.M. De Cock. Response to treatment, mortality, and CD4 lymphocyte counts in HIV-infected persons with tuberculosis in Abidjan, Cote d'Ivoire. *The Lancet*, 345(8950):607–610, 1995. https://doi.org/10.1016/S0140-6736(95)90519-7.

[3] O. Ajumobi, P. Uhomoibhi, P. Onyiah, O. Babalola, S. Sharafadeen, M. Ughasoro, A. Adamu, O. Odeyinka, T. Orimogunje, and I. Maikore. Setting a Nigeria national malaria operational research agenda: the process. *BMC health services research*, 18(1):1–7, 2018.

[4] C. Akolo, I. Adetifa, S. Shepperd, and J. Volmink. Treatment of latent tuberculosis infection in HIV infected persons. *Cochrane Database of Systematic Reviews*, (1), 2010. https://doi.org/10.1002/14651858.CD000171.pub3.

[5] I. Ali and D. Kannan. Mapping research on healthcare operations and supply chain management: a topic modelling-based literature review. *Annals of Operations Research*, 315(1):29–55, 2022.

[6] N. Altay and W.G. Green. OR/MS research in Disaster Operations Management. *European Journal of Operational Research*, 175(1):475–493, 2006. https://doi.org/10.1016/j.ejor.2005.05.016.

[7] S.J. Anderson, P. Cherutich, N. Kilonzo, I. Cremin, D. Fecht, D. Kimanga, M. Harper, R L. Masha, P B. Ngongo, W. Maina, and et al. Maximising the effect of combination HIV prevention through prioritisation of the people and places in greatest need: a modelling study. *The Lancet*, 384(9939):249–256, 2014. https://doi.org/10.1016/S0140-6736(14)61053-9.

[8] X. Anglaret, A. Minga, D. Gabillard, T. Ouassa, E. Messou, B. Morris, M. Traore, A. Coulibaly, Kenneth A. Freedberg, C. Lewden, and et al. AIDS and non-AIDS morbidity and mortality across the spectrum of CD4 cell counts in HIV-infected adults before starting antiretroviral therapy in Cote d'Ivoire. *Clin Infect Dis*, 54(5):714–723, 2012. https://doi.org/10.1093/cid/cir898.

[9] L.V.A. Anton and D.W. Hutton. Optimization models for HIV/AIDS resource allocation: A systematic review. *Value in Health*, 23(11):1509–1521, 2020. https://doi.org/10.1016/j.jval.2020.08.001.

[10] G. Arji, H. Ahmadi, P. Avazpoor, and M. Hemmat. Identifying resilience strategies for disruption management in the healthcare supply chain during COVID-19 by digital innovations: A systematic literature review. *Informatics in Medicine Unlocked*, page 101199, 2023.

[11] C. Ash, C. Diallo, U. Venkatadri, and P. VanBerkel. Distributionally robust optimization of a canadian healthcare supply chain to enhance resilience during the COVID-19 pandemic. *Computers & Industrial Engineering*, 168:108051, 2022.

[12] M. Badri, S D. Lawn, and R. Wood. Short-term risk of AIDS or death in people infected with HIV-1 before antiretroviral therapy in South Africa: a longitudinal study. *The Lancet*, 368(9543):1254–1259, 2006. https://doi.org/10.1016/S0140- 6736(06)69117-4.

[13] B. Balcik and B. Beamon. Facility location in humanitarian relief. *International Journal of Logistics*, 11(2):101–121, 2008. https://doi.org/10.1080/13675560701561789.

[14] B. Balcik, C.D.C. Bozkir, and O.E. Kundakcioglu. A literature review on inventory management in humanitarian supply chains. *Surveys in Operations Research and Management Science*, 21(2), 2016. 101–116.

[15] B. Balcik, C.D.C. Bozkir, and O.E. Kundakcioglu. A literature review on inventory management in humanitarian supply chains. *Surveys in Operations Research and Management Science*, 21(2):101–116, 2016. https://doi.org/10.1016/j.sorms.2016.10.002.

[16] R.V. Barnabas, A. Szpiro, H. Van Rooyen, S. Asiimwe, D. Pillay, N C. Ware, T T. Schaafsma, M L. Krows, A. Van Heerden, and P. Joseph. Community-based antiretroviral therapy versus standard clinic-based services for HIV in South Africa and Uganda (DO ART): a randomised trial. *The Lancet Global Health*, 8(10):e1305–e1315, 2020. https://doi.org/10.1016/S2214-109X(20)30313-2.

[17] B.M. Beamon and S.A. Kotleba. Inventory modelling for complex emergencies in humanitarian relief operations. *International Journal of Logistics: Research and Applications*, 9(1):1–18, 2007. https://doi.org/10.1080/13675560500453667.

[18] M. Beaulieu, J. Roy, C. Rebolledo, and S. Landry. The management of personal protective equipment during the COVID-19 pandemic: The case of the province of Quebec. *Healthcare management forum*, 35(1):48–52, 2022.

[19] A. Behl and P. Dutta. Humanitarian supply chain management: A thematic literature review and future directions of research. *Annals of Operations Research*, 283(1):1001–1044, 2019. https://doi.org/10.1007/s10479-018-2806-2.

[20] L. Benkherouf, K. Skouri, and I. Konstantaras. Inventory decisions for a finite horizon problem with product substitution options and time varying demand. *Applied Mathematical Modelling*, 51:669–685, 2017. https://doi.org/10.1016/j.apm.2017.05.043.

[21] A. Bershteyn, L. Jamieson, H. Kim, I. Platais, M.P. Milali, E. Mudimu, D. Ten Brink, R. Martin-Hughes, S.L. Kelly, and A.N. Phillips. Transmission reduction, health benefits, and upper-bound costs of interventions to improve retention on antiretroviral therapy: a combined analysis of three mathematical models. *The Lancet Global Health*, 10(9):e1298–e1306, 2022.

[22] F.M. Bozzani, D. Mudzengi, T. Sumner, G.B. Gomez, P. Hippner, V. Cardenas, S. Charalambous, R. White, and A. Vassall. Empirical estimation of resource constraints for use in model-based economic evaluation: an example of TB services in South Africa. *Cost Effectiveness and Resource Allocation*, 16:1–10, 2018.

[23] J.R. Campbell, N. Winters, and D. Menzies. Absolute risk of tuberculosis among untreated populations with a positive tuberculin skin test or interferon-gamma release assay result: systematic review and meta-analysis. *BMJ*, 368, 2020. https://doi.org/10.1136/bmj.m549.

[24] G. Cao, Y. Wang, Y. Wu, W. Jing, J. Liu, and M. Liu. Prevalence of anemia among people living with HIV: A systematic review and meta-analysis. *EClinicalMedicine*, 44, 2022.

[25] The Center of Disease Control. Personal Protective Equipment (PPE) Burn Rate Calculator, 2020. accessed December, 24 2020, available at https://www.cdc.gov/coronavirus/2019-ncov/hcp/ppe-strategy/burn-calculator.html.

[26] A. Chauhan, H. Kaur, S.K. Mangla, and Y. Kayikci. Data driven flexible supplier network of selfcare essentials during disruptions in supply chain. *Annals of Operations Research*, pages 1–31, 2023.

[27] H. Chen and A. Lim. A network price elasticity of demand model with product substitution. *Journal of Revenue and Pricing Management*, pages 1–13, 2022.

[28] X. Chen, Y. Feng, M.F. Keblis, and J. Xu. Optimal inventory policy for two substitutable products with customer service objectives. *European Journal of Operational Research*, 246(1):76–85, 2015. https://doi.org/10.1016/j.ejor.2015.04.033.

[29] C. Connolly, A. Reid, G. Davies, W. Sturm, K. McAdam, and D. Wilkinson. Relapse and mortality among HIV-infected and uninfected patients with tuberculosis successfully treated with twice weekly directly observed therapy in rural South Africa. *AIDS*, 13(12):1543–1547, 1999.

[30] T.M. Cook. Personal protective equipment during the coronavirus disease (COVID) 2019 pandemic–a narrative review. *Anaesthesia*, 75(7):920–927, 2020. https://doi.org/10.1111/anae.15071.

[31] K.D. Dale, M. Karmakar, K.J. Snow, D. Menzies, J.M. Trauer, and J.T. Denholm. Quantifying the rates of late reactivation tuberculosis: a systematic review. *The Lancet Infect Dis*, 21(10):e303–e317, 2021. https://doi.org/10.1016/S1473-3099(20)30728-3.

[32] L.B. Davis, F. Samanlioglu, X. Qu, and S. Root. Inventory planning and coordination in disaster relief efforts. *International Journal of Production Economics*, 141(2):561–573, 2013. https://doi.org/10.1016/j.ijpe.2012.09.012.

[33] R. Dubey, D.J. Bryde, C. Foropon, G. Graham, M. Giannakis, and D.B. Mishra. Agility in humanitarian supply chain: An organizational information processing perspective and relational view. *Annals of Operations Research*, 2020. https://doi.org/10.1007/s10479-020-03824-0.

[34] L.E. Duijzer, W. Van Jaarsveld, and R. Dekker. Literature review: The vaccine supply chain. *European Journal of Operational Research*, 268(1):174–192, 2018. https://doi.org/10.1016/j.ejor.2018.01.015.

[35] S.R. Earnshaw, K. Hicks, A. Richter, and A. Honeycutt. A linear programming model for allocating HIV prevention funds with state agencies: a pilot study. *Health Care Manage Sci*, 10(3):239–252, 2007. https://doi.org/10.1007/s10729-007-9017-8.

[36] M. Eftekhar, S. Jeannette, S. Jing, and S. Webster. Prepositioning and local purchasing for emergency operations under budget, demand, and supply uncertainty. *Manufacturing & Service Operations Management*, 24(1):315–332, 2022.

[37] T. Egsmose, J. Ang'Awa, and S.J. Poti. The use of isoniazid among household contacts of open cases of pulmonary tuberculosis. *Bulletin of the World Health Organization*, 33(3):419, 1965.

[38] S.H. Ferebee and F.W. Mount. Tuberculosis morbidity in a controlled trial of the prophylactic use of isoniazid among household contacts. *American Review of Respiratory Disease*, 85(4):490–510, 1962.

[39] N. Foster, A. Vassall, S. Cleary, L. Cunnama, G. Churchyard, and E. Sinanovic. The economic burden of TB diagnosis and treatment in South Africa. *Social science & medicine*, 130:42–50, 2015.

[40] G. Galindo and R. Batta. Review of recent developments in OR/MS research in Disaster Operations Management. *European Journal of Operational Research*, 230(2):201–211, 2013. https://doi.org/10.1016/j.ejor.2013.01.039.

[41] R. Geoff. Meeting global health challenges through operational research and management science. *Bulletin of the World Health Organization*, 89:683–688, 2011.

[42] J.A. Gilbert, S.V. Shenoi, A. Moll, G.H. Friedland, D. Paltiel, and A.P. Galvani. Cost-effectiveness of community-based TB/HIV screening and linkage to care in rural South Africa. *PLoS One*, 11(12):e0165614, 2016.

[43] Global Burden of Disease Study 2019. Disability weights, global burden of disease collaborative network, 2020. accessed September, 27 2023, available at https://doi.org/10.6069/1W19-VX76.

[44] Global Burden of Disease Study 2019. Global burden of disease collaborative network, 2020. accessed September, 27 2023, available at http://ghdx.healthdata.org/gbd-results-tool.

[45] J.R. Glynn, P. Khan, T. Mzembe, L. Sichali, P E. Fine, A C. Crampin, and R M. Houben. Contribution of remote M. tuberculosis infection to tuberculosis disease: A 30-year population study. *Plos one*, 18(1):e0278136, 2023. https://doi.org/10.1371/journal.pone.0278136.

[46] R. Granich, J.G. Kahn, R. Bennett, C.B. Holmes, N. Garg, C. Serenata, M.L. Sabin, C. Makhlouf-Obermeyer, C. De Filippo Mack, and P. Williams. Expanding ART for treatment and prevention of HIV in South Africa: estimated cost and cost-effectiveness 2011-2050. *PloS one*, 7(2):e30216, 2012.

[47] A. Grimsrud, H. Bygrave, M. Doherty, P. Ehrenkranz, T. Ellman, R. Ferris, N. Ford, B. Killingo, L. Mabote, T. Mansell, and et al. Reimagining HIV service delivery: the role of differentiated care from prevention to suppression. *J Int AIDS Soc*, 19(1), 2016. https://10.7448/IAS.19.1.21484.

[48] R. Hamilton. Scarcity and coronavirus. *Journal of Public Policy & Marketing*, 40(1):99–100, 2021. https://doi.org/10.1177/0743915620928110.

[49] R. Harpring, A. Maghsoudi, C. Fikar, W.D. Piotrowicz, and G. Heaslip. An analysis of compounding factors of epidemics in complex emergencies: a system dynamics approach. *Journal of Humanitarian Logistics and Supply Chain Management*, 2021.

[50] S.M. Hermans, B. Castelnuovo, C. Katabira, P. Mbidde, J.M.A. Lange, A.I.M. Hoepelman, A. Coutinho, and Y.C. Manabe. Integration of HIV and TB services results in improved TB treatment outcomes and earlier, prioritized ART initiation in a large urban HIV clinic in Uganda. *J Acquir Immune Defic Syndr*, 60(2):e29, 2012. https://doi.org/10.1097/QAI.0b013e318251aeb4.

[51] P. Hooshangi-Tabrizi, H. Doulabi, I. Contreras, and N. Bhuiyan. Two-stage robust optimization for perishable inventory management with order modification. *Expert Systems With Applications*, 193:116346, 2022.

[52] K.C. Horton, A.L Hoey, G. Béraud, E.L. Corbett, and R.G White. Systematic review and meta-analysis of sex differences in social contact patterns and implications for tuberculosis transmission and control. *Emerg Infect Dis*, 26(5):910, 2020. https://doi.org/10.3201/eid2605.190574.

[53] K.C. Horton, T. Sumner, R M. Houben, E L. Corbett, and R G. White. A Bayesian Approach to Understanding Sex Differences in Tuberculosis Disease Burden. *American J of Epidemiology*, 187(11):2431–2438, 2018. https://doi.org/10.1093/aje/kwy131.

[54] K.C. Horton, R.G. White, N.B. Hoa, H. Nguyen, R. Bakker, T. Sumner, E.L. Corbett, and R. Houben. Population benefits of addressing programmatic and social determinants of gender disparities in tuberculosis in Vietnam: A modelling study. *PLOS Global Public Health*, 2(7):e0000784, 2022.

[55] C. Huang, M.C. Becerra, R. Calderon, C. Contreras, J. Galea, L. Grandjean, L. Lecca, R. Yataco, Z. Zhang, and M. Murray. Isoniazid preventive therapy in contacts of multidrug-resistant tuberculosis. *American Journal of Respiratory and Critical Care Medicine*, 202(8):1159–1168, 2020.

[56] C. Huang, E T. Tchetgen, M C. Becerra, T. Cohen, K C. Hughes, Z. Zhang, R. Calderon, R. Yataco, C. Contreras, J. Galea, and et al. The Effect of HIV-Related Immunosuppression on the Risk of Tuberculosis Transmission to Household Contacts. *Clin Infect Dis*, 58(6):765–774, 2014. https://doi.org/10.1093/cid/cit948.

[57] Hyak supercomputer system. Hyak, 2022. https://hyak.uw.edu/.

[58] Gonzatto J., Oilson A., D.C. Nascimento, C.M. Russo, M.J. Henriques, C.P. Tomazella, M.O. Santos, D. Neves, D. Assad, R. Guerra, and E.K. Bertazo. Safety-stock: Predicting the demand for supplies in Brazilian hospitals during the COVID-19 pandemic. *Knowledge-Based Systems*, 247(1):108753, 2022.

[59] John Snow, Inc. *The Supply Chain Manager's Handbook*. 2019. Retrieved February 3, 2022, from https://www.jsi.com/resource/the-supply-chain-managers-handbook/.

[60] John Snow, Inc. *Building Resilient Sexual And Reproductive Health Supply Chains During COVID-19 And Beyond: Community Roadmap for Action and Technical Findings*. 2021. Retrieved February 3, 2022, from https://www.jsi.com/resource/building-resilient-sexual-and-reproductive-health-supply-chains-during-covid-19-and-beyond-community-roadmap-for-action-and-technical-findings/.

[61] John Snow, Inc. *Responding to COVID-19*, 2021. Retrieved February 3, 2022, from https://www.jsi.com/responding-to-covid-19/.

[62] John Snow, Inc. *About Us*. 2022. Retrieved February 3, 2022, from https://www.jsi.com/about-jsi/.

[63] K. Karuppiah, B. Sankaranarayanan, S.M. Ali, and S.K. Paul. Key challenges to sustainable humanitarian supply chains: Lessons from the COVID-19 pandemic. *Sustainability*, 13(11):5850, 2021.

[64] I. Kazancoglu, M. Ozbiltekin-Pala, S.K. Mangla, A. Kumar, and Y. Kazancoglu. Using emerging technologies to improve the sustainability and resilience of supply chains in a fuzzy

environment in the context of COVID-19. *Annals of Operations Research*, 322(1):217–240, 2023.

[65] C C. Kerr, R.M. Stuart, R T. Gray, A J. Shattock, N. Fraser-Hurt, C. Benedikt, M. Haacker, M. Berdnikov, A.M. Mahmood, S.A. Jaber, and et al. Optima: A Model for HIV Epidemic Analysis, Program Prioritization, and Resource Optimization. *J Acquir Immune Defic Syndr*, 69(3):365–376, 2015. https://doi.org/10.1097/QAI.0000000000000605.

[66] S. Khalilabadi, S. Zegordi, and E. Nikbakhsh. A multi-stage stochastic programming approach for supply chain risk mitigation via product substitution. *Computers & Industrial Engineering*, 149:106786, 2020. https://doi.org/10.1016/j.cie.2020.106786.

[67] HY Kim, CF Hanrahan, N Martinson, JE Golub, and DW Dowdy. Cost-effectiveness of universal isoniazid preventive therapy among HIV-infected pregnant women in South Africa. *The International Journal of Tuberculosis and Lung Disease*, 22(12):1435–1442, 2018.

[68] King County. *COVID-19 Emergency Resource Requests*. 2022. Retrieved February 3, 2022, from https://kingcounty.gov/depts/emergency-management/covid-requests.aspx.

[69] C. Ku, P. MacPherson, M. Khundi, R H. Nzawa-Soko, H R. Feasey, M. Nliwasa, K C. Horton, E L. Corbett, and P J. Dodd. Durations of asymptomatic, symptomatic, and care-seeking phases of tuberculosis disease with a Bayesian analysis of prevalence survey and notification data. *BMC medicine*, 19:1–13, 2021. https://doi.org/10.1371/journal.pone.0196003.

[70] P. Kumar, R.K. Singh, and A. Shahgholian. Learnings from COVID-19 for managing humanitarian supply chains: Systematic literature review and future research directions. *Annals of Operations Research*, pages 1–37, 2022.

[71] N. Kunz and G. Reiner. A meta-analysis of humanitarian logistics research. *Journal of Humanitarian Logistics and Supply Chain Management*, 2012.

[72] KwaZulu-Natal Health Department. KwaZulu-Natal Department of Health Strategic Plan 2015-2019, 2020. accessed September, 27 2023, available at http://www.kznhealth.gov.za/Strategic-Plan-2015-2019.pdf.

[73] J.R. Ledesma, J. Ma, A. Vongpradith, E.R. Maddison, A. Novotney, M.H. Biehl, K.E. LeGrand, J.M. Ross, D. Jahagirdar, and D. et al. Bryazka. Global, regional, and national sex differences in the global burden of tuberculosis by HIV status, 1990–2019: results from the Global Burden of Disease Study 2019. *The Lancet Infect Dis*, 22(2):222–241, 2022. https://doi.org/10.1016/S1473-3099(21)00449-7.

[74] J. Little and B. Coughlan. Optimal inventory policy within hospital space constraints. *Health Care Management Science*, 11(2):177–183, 2008. https://doi.org/10.1007/s10729-008-9066-7.

[75] M. Loveday, K. Wallengren, T. Reddy, D. Besada, J C M. Brust, A. Voce, H. Desai, J. Ngozo, Z. Radebe, I. Master, and et al. MDR-TB patients in KwaZulu-Natal, South Africa: Cost-effectiveness of 5 models of care. *PloS one*, 13(4):e0196003, 2018. https://doi.org/10.1371/journal.pone.0196003.

[76] M. Loveday, K. Wallengren, T. Reddy, D. Besada, J.C.M. Brust, A. Voce, H. Desai, J. Ngozo, Z. Radebe, I. Master, and et al. MDR-TB patients in KwaZulu-Natal, South Africa: Cost-effectiveness of 5 models of care. *PloS one*, 13(4):e0196003, 2018. https://doi.org/10.1371/journal.pone.0196003.

[77] J. Ma, W. Lou, and Z. Wang. Pricing strategy and product substitution of bullwhip effect in dual parallel supply chain: aggravation or mitigation? *RAIRO-Operations Research*, 56(4):2093–2114, 2022.

[78] W. Maokola, B. Ngowi, L. Lawson, M. Robert, M. Mahande, J. Todd, and S. Msuya. Coverage of isoniazid preventive therapy among people living with HIV; A retrospective cohort study in Tanzania (2012-2016). *International J of Infect Dis*, 103:562–567, 2021. https://doi.org/10.1016/j.ijid.2020.11.192.

[79] L. Martinez, J N. Sekandi, M E. Castellanos, S. Zalwango, and C C. Whalen. Infectiousness of HIV-seropositive patients with tuberculosis in a high-burden African setting. *American J of Respiratory and Critical Care Medicine*, 194(9):1152–1163, 2016. https://doi.org/10.1164/rccm.201511-2146OC.

[80] L. Martinez, H. Woldu, C. Chen, B D. Hallowell, .E. Castellanos, P. Lu, Q. Liu, C C. Whalen, and L. Zhu. Transmission Dynamics in Tuberculosis Patients With Human Immunodeficiency Virus: A Systematic Review and Meta-analysis of 32 Observational Studies. *Clin Infect Dis*, 73(9):e3446–e3455, 2021. https://doi.org/10.1093/cid/ciaa1146.

[81] S.D. Masuku, R. Berhanu, C. Van Rensburg, N. Ndjeka, S. Rosen, L. Long, D. Evans, and B.E. Nichols. Managing multidrug-resistant tuberculosis in South Africa: a budget impact analysis. *The International Journal of Tuberculosis and Lung Disease*, 24(4):376–382, 2020.

[82] J. McCoy and H. Lee. Using fairness models to improve equity in health delivery fleet management. *Production and Operations Management*, 23(6):965–977, 2014.

[83] J.B. McGillen, S.J. Anderson, M.R. Dybul, and T.B. Hallett. Optimum resource allocation to reduce HIV incidence across Sub-Saharan Africa: a mathematical modelling study. *The Lancet HIV*, 3(9):e441–e448, 2016. https://doi.org/10.1016/S2352-3018(16)30051-0.

[84] McKinsey & Company. COVID-19: Implications for business, 2021. accessed December, 24 2020, available at https://www.mckinsey.com/business-functions/risk/our-insights/covid-19-implications-for-business.

[85] N.A. Menzies, C F. McQuaid, G B. Gomez, A/ Siroka, P. Glaziou, K. Floyd, R G. White, and R.M.G.J. Houben. Improving the quality of modeling evidence used for tuberculosis policy evaluation. *Int J Tuberc Lung Dis*, 23(4):387–395, 2019. https://doi.org/10.5588/ijtld.18.0660.

[86] N.A. Menzies, E. Wolf, D. Connors, M. Bellerose, A.N. Sbarra, T. Cohen, A.N. Hill, R. Yaesoubi, K. Galer, and P.J. White. Progression from latent infection to active disease in dynamic tuberculosis transmission models: a systematic review of the validity of modelling assumptions. *The Lancet Infectious Diseases*, 18(8):e228–e238, 2018.

[87] H.O. Mete and Z.B. Zabinsky. Stochastic optimization of medical supply location and distribution in disaster management. *International Journal of Production Economics*, 126(1):76–84, 2010. https://doi.10.1016/j.ijpe.2009.10.004.

[88] G. Meyer-Rath, A.T. Brennan, M.P. Fox, T. Modisenyane, N. Tshabangu, L. Mohapi, S. Rosen, and N. Martinson. Rates and cost of hospitalisation before and after initiation of antiretroviral therapy in urban and rural settings in South Africa. *Journal of acquired immune deficiency syndromes (1999)*, 62(3):322, 2013.

[89] G. Meyer-Rath, L Jamieson, and L. Johnson. Hiv investment case - full report, 2021. https://www.heroza.org/wp-content/uploads/2021/12/HIV-Investment-Case-2021-Full-report-final.pdf.

[90] G. Meyer-Rath, C. van Rensburg, C. Chiu, R. Leuner, L. Jamieson, and S. Cohen. The per-patient costs of hiv services in South Africa: systematic review and application in the South African hiv investment case. *PloS one*, 14(2):e0210497, 2019.

[91] G. Meyer-Rath, C. Van Rensburg, B. Larson, L. Jamieson, and S. Rosen. Revealed willingness-to-pay versus standard cost-effectiveness thresholds: Evidence from the South African hiv investment case. *PLoS One*, 12(10):e0186496, 2017.

[92] T. Mona, S. Mohsen, A. Ata, and M. Ehsan. A fuzzy programming model for optimizing the inventory management problem considering financial issues: A case study of the dairy industry. *Expert Systems with Applications*, 221:119766, 2023.

[93] S. Moyo, F. Ismail, M. Van der Walt, N. Ismail, N. Mkhondo, S. Dlamini, T. Mthiyane, J. Chikovore, O. Oladimeji, and D. Mametja. Prevalence of bacteriologically confirmed pulmonary tuberculosis in South Africa, 2017–19: a multistage, cluster-based, cross-sectional survey. *The Lancet Infectious Diseases*, 22(8):1172–1180, 2022.

[94] J. Müller, K. Hoberg, and J.C. Fransoo. Realizing supply chain agility under time pressure: Ad hoc supply chains during the COVID-19 pandemic. *Journal of Operations Management*, 2022.

[95] J. Musaazi, C. Sekaggya-Wiltshire, S. Okoboi, S.and Zawedde-Muyanja, M. Senkoro, N. Kalema, P. Kavuma, P.M. Namuwenge, Y.C. Manabe, B. Castelnuovo, et al. Increased uptake of tuberculosis preventive therapy (TPT) among people living with HIV following

the 100-days accelerated campaign: A retrospective review of routinely collected data at six urban public health facilities in Uganda. *PloS one*, 18(2):e0268935, 2023.

[96] M.D. Nglazi, L. Bekker, R. Wood, and R. Kaplan. The impact of HIV status and antiretroviral treatment on TB treatment outcomes of new tuberculosis patients attending co-located TB and ART services in South Africa: a retrospective cohort study. *BMC Infect Dis*, 15(1):1–8, 2015. https://doi.org/10.1186/s12879-015-1275-3.

[97] Y. Niu, Z. Li, L. Meng, S. Wang, Z. Zhao, T. Song, J. Lu, T. Chen, Q. Li, and X. Zou. The collaboration between infectious disease modeling and public health decision-making based on the covid-19. *Journal of Safety Science and Resilience*, 2(2):69–76, 2021.

[98] N. Noyan, M. Meraklı, and S. Küçükyavuz. Two-stage stochastic programming under multivariate risk constraints with an application to humanitarian relief network design. *Mathematical Programming*, pages 1–39, 2022.

[99] P. Nunn, A. Harries, P. Godfrey-Faussett, R. Gupta, D. Maher, and M. Raviglione. The research agenda for improving health policy, systems performance, and service delivery for tuberculosis control: a who perspective. *Bulletin of the World Health Organization*, 80:471–476, 2002.

[100] Occupational Safety and Health Administration (OSHA). *Guidance on Preparing Workplaces for COVID-19*. 2020. Retrieved February 3, 2022, from https://www.osha.gov/sites/default/files/publications/OSHA3990.pdf.

[101] M. Osman, J.A. Seddon, R. Dunbar, H R. Draper, C. Lombard, and N. Beyers. The complex relationship between human immunodeficiency virus infection and death in adults being treated for tuberculosis in Cape Town, South Africa. *BMC Public Health*, 15(1):1–8, 2015.

[102] C. Özlem and I.E. Büyüktahtakın. Stochastic dynamic resource allocation for HIV prevention and treatment: An approximate dynamic programming approach. *Computers & Industrial Engineering*, 118:423–439, 2018. https://doi.org/10.1016/j.cie.2018.01.018.

[103] D.J. Pepper, M. Schomaker, R J. Wilkinson, V. de Azevedo, and G. Maartens. Independent predictors of tuberculosis mortality in a high HIV prevalence setting: a retrospective cohort study. *AIDS Res Ther*, 12(1):1–9, 2015.

[104] A.N. Phillips, V. Cambiano, L. Johnson, F. Nakagawa, R. Homan, G. Meyer-Rath, T. Rehle, F. Tanser, S. Moyo, and M. Shahmanesh. Potential impact and cost-effectiveness of condomless-sex–concentrated prep in kwaZulu-Natal accounting for drug resistance. *The Journal of infectious diseases*, 223(8):1345–1355, 2021.

[105] A. Polater. Dynamic capabilities in humanitarian supply chain management: A systematic literature review. *Journal of humanitarian logistics and supply chain management*, 11(1):46–80, 2021.

[106] N. Privett and D. Gonsalvez. The top ten global health supply chain issues: Perspectives from the field. *Operations Research for Health Care*, 3(4):226–230, 2014. https://doi.org/10.1016/j.orhc.2014.09.002.

[107] M.M. Queiroz, D. Ivanov, A. Dolgui, and S. Fosso Wamba. Impacts of epidemic outbreaks on supply chains: mapping a research agenda amid the COVID-19 pandemic through a structured literature review. *Annals of Operations Research*, pages 1–38, 2022.

[108] N.A.A. Rahman, A. Ahmi, L. Jraisat, and A. Upadhyay. Examining the trend of humanitarian supply chain studies: pre, during and post covid-19 pandemic. *Journal of Humanitarian Logistics and Supply Chain Management*, (ahead-of-print), 2022.

[109] M. Rangaka, R. Wilkinson, A. Boulle, J. Glynn, K. Fielding, G. Van Cutsem, K.A Wilkinson, R. Goliath, S. Mathee, and E. Goemaere. Isoniazid plus antiretroviral therapy to prevent tuberculosis: a randomised double-blind, placebo-controlled trial. *The Lancet*, 384(9944):682–690, 2014.

[110] M.L. Ranney, V. Griffeth, and A.K. Jha. Critical Supply Shortages—the Need for Ventilators and Personal Protective Equipment during the Covid-19 Pandemic. *New England Journal of Medicine*, 382(18):e41, 2020. https://doi.org/10.1056/NEJMp2006141.

[111] D.W. Rao, C.J. Bayer, G. Liu, A. Chikandiwa, M. Sharma, C L. Hathaway, N. Tan, N. Mugo, and R.V. Barnabas. Modelling cervical cancer elimination using single-visit screening and treatment strategies in the context of high HIV prevalence: estimates for KwaZulu-Natal, South Africa. *J Int AIDS Soc*, 25(10):e26021, 2022. https://doi.org/10.1002/jia2.26021.

[112] C. Rawls and M. Turnquist. Pre-positioning of emergency supplies for disaster response. *Transportation research part B: Methodological*, 44(4):521–534, 2010. https://doi.org/10.1016/j.trb.2009.08.003.

[113] A. Rehman, S. Mian, M. Usmani, Yusuf Sand Abidi, and M.K. Mohammed. Modelling and analysis of hospital inventory policies during covid-19 pandemic. *Processes*, 11(4):1062, 2023.

[114] Restart Partners. *About Restart Partners*. 2020. Retrieved February 3, 2022, from https://www.restart.us/about.

[115] M.S. Roni, M. Jin, and S.D. Eksioglu. A hybrid inventory management system responding to regular demand and surge demand. *Omega*, 52:190–200, 2015. https://doi.org/10.1016/j.omega.2014.05.002.

[116] J.M. Ross, A. Badje, M.X. Rangaka, A. Walker, A.E. Shapiro, K.K. Thomas, X. Anglaret, S. Eholie, D. Gabillard, A. Boulle, M. Gary, R.J. Wilkinson, N. Ford, J E. Golub, B.G. Williams, and R.V. Barnabas. Isoniazid preventive therapy plus antiretroviral therapy for the prevention of tuberculosis: a systematic review and meta-analysis of individual participant data. *The Lancet HIV*, 8(1):e8–e15, 2021. https://doi.org/10.1016/S2352-3018(20)30299-X.

[117] J.M. Ross, C. Greene, C. Bayer, D W. Dowdy, A. Van Heerden, J. Heitner, D W. Rao, D.A. Roberts, A E. Shapiro, Z.B. Zabinsky, and R.V. Barnabas. Preventing tuberculosis with community-based care in an HIV-endemic setting: a modeling analysis. *medRxiv*, pages 2023–08, 2023.

[118] J.M. Ross, R. Ying, C L. Celum, J.M. Baeten, K K. Thomas, P M. Murnane, H. Van Rooyen, J.P. Hughes, and R.V. Barnabas. Modeling HIV disease progression and transmission at population-level: The potential impact of modifying disease progression in HIV treatment programs. *Epidemics*, 23:34–41, 2018. https://doi.org/10.1016/j.epidem.2017.12.001.

[119] B. Rottkemper, K. Fischer, A. Blecken, and C. Danne. Inventory relocation for overlapping disaster settings in humanitarian operations. *OR Spectrum*, 33(3):721–749, 2011.

[120] M. Rozhkov, D. Ivanov, J. Blackhurst, and A. Nair. Adapting supply chain operations in anticipation of and during the COVID-19 pandemic. *Omega*, 110:102635, 2022.

[121] M. Sahu, C.J. Bayer, D.A. Roberts, H. van Rooyen, A. van Heerden, M. Shahmanesh, S. Asiimwe, K. Sausi, N. Sithole, R. Ying, et al. Population health impact, cost-effectiveness, and affordability of community-based HIV treatment and monitoring in South Africa: A health economics modelling study. *PLOS Global Public Health*, 3(9):e0000610, 2023.

[122] Salt Lake Chamber. *PPE Resources For Small Businesses*. 2020. Retrieved February 3, 2022, from https://slchamber.com/wp-content/uploads/2020/05/PPE-Resources-for-Small-Businesses.pdf?fbclid=IwAR2z02SmE3Xm-8cKJiy0riyVjTzB4oPBjRPFRmb-QsVkq65DRMdTWq1EbPk.

[123] T. Sawik. Stochastic optimization of supply chain resilience under ripple effect: A COVID-19 pandemic related study. *Omega*, 109:102596, 2022.

[124] S. Sensalire, K.K.N. Esther, J. Nabwire, A. Lawino, D. Kiragga, M. Muhire, H. Kadama, C. Katureebe, P. Namuwenge, J. Musinguzi, J. Calnan, and D. Seyoum. A prospective cohort study of outcomes for isoniazid prevention therapy: a nested study from a national QI collaborative in Uganda. *AIDS Res Ther*, 17(1):1–8, 2020. https://doi.org/10.1186/s12981-020-00285-0.

[125] E. Settanni, T.S. Harrington, and J.S. Srai. Pharmaceutical supply chain models: A Synthesis from a Systems View of Operations Research. *Operations Research Perspectives*, 4:74–95, 2017.

[126] H. Shin, S. Park, E. Lee, and W.C. Benton. A classification of the literature on the planning of substitutable products. *European Journal of Operational Research*, 246(3):686–699, 2015. https://doi.org/10.1016/j.ejor.2015.04.013.

[127] M. Shokouhifar and M. Ranjbarimesan. Multivariate time-series blood donation/demand forecasting for resilient supply chain management during COVID-19 pandemic. *Cleaner Logistics and Supply Chain*, 5:100078, 2022.

[128] J. Silva, A. Claudia, and M. Leonardo. Siloed perceptions in pharmaceutical supply chain risk management: A Brazilian perspective. *Latin American Business Review*, 2020. 1–32.

[129] L. Simbayi, K. Zuma, N. Zungu, S. Moyo, E. Marinda, S. Jooste, M. Mabaso, S. Ramlagan, A. North, J. Van Zyl, and N. Mohlabane. South African national HIV prevalence, incidence, behaviour and communication survey, 2017: towards achieving the UNAIDS 90-90-90 targets. *Human Sciences Research Council*, 2019. Available from https://www.hsrc.ac.za/uploads/pageContent/9234/SABSSMV _Impact_Assessment_Summary_ZA_ADS_cleared_PDFA4.pdf.

[130] K. Soetaert, T. Petzoldt, and R.W. Setzer. Solving differential equations in r: package desolve. *J of statistical software*, 33:1–25, 2010.

[131] South Africa National Department of Health. South Africa master health product list, 2021. available at http://www.health.gov.za/tenders/.

[132] M. Stein. Large sample properties of simulations using latin hypercube sampling. *Technometrics*, 29(2):143–151, 1987.

[133] R.M. Stuart, L. Grobicki, H. Haghparast-Bidgoli, J. Panovska-Griffiths, J. Skordis, O. Keiser, J. Estill, Z. Baranczuk, S L. Kelly, I. Reporter, and et al. How should HIV resources be allocated? lessons learnt from applying optima HIV in 23 countries. *J Int AIDS Soc*, 21(4):e25097, 2018. https://doi.org/10.1002/jia2.25097.

[134] A.B. Suthar, S.D. Lawn, J. Del Amo, H. Getahun, C. Dye, D. Sculier, T.R. Sterling, R.E. Chaisson, B G. Williams, and A.D. Harries. Antiretroviral Therapy for Prevention of Tuberculosis in Adults with HIV: A Systematic Review and Meta-Analysis. *PLOS*, 2012. https://doi.org/10.1371/journal.pmed.1001270.

[135] A.B. Suthar, S.D. Lawn, J. Del Amo, H. Getahun, C. Dye, D. Sculier, T.R. Sterling, R.E. Chaisson, B.G. Williams, and A D. Harries. Antiretroviral Therapy for Prevention of Tuberculosis in Adults with HIV: A Systematic Review and Meta-Analysis. *PloS one*, page e1001270, 2012. https://doi.org/10.1371/journal.pmed.1001270.

[136] M. Takamiya, K. Takarinda, S. Balachandra, M. Godfrey, E. Radin, A. Hakim, M. Pearson, R. Choto, C. Sandy, and T. Maphosa. Isoniazid preventive therapy use among adult people living with HIV in zimbabwe. *International journal of STD & AIDS*, 32(11):1020–1027, 2021.

[137] Temprano ANRS 12136 Study Group. A trial of early antiretrovirals and isoniazid preventive therapy in Africa. *N Engl J Med*, 373(9):808–822, 2015. https://doi.org/10.1056/NEJMoa1507198.

[138] R.H. Teunter and S. Kuipers. Inventory control with demand substitution: new insights from a two-product economic order quantity analysis. *Omega*, 113:102712, 2022.

[139] The Centers for Disease Control and Prevention (CDC). *Maintaining Essential Health Services During COVID-19 in Low Resource, Non U.S. Settings*. 2020. Retrieved February 3, 2022, from https://www.cdc.gov/coronavirus/2019-ncov/global-covid-19/essential-health-services.html.

[140] The Federal Emergency Management Agency (FEMA). *National Incidence Management System*. 2017. Retrieved February 3, 2022, from https://www.fema.gov/sites/default/files/2020-07/fema_nims_doctrine-2017.pdf.

[141] The Federal Emergency Management Agency (FEMA). *Pandemic Response to Coronavirus Disease 2019 (COVID-19): Initial Assessment Report*. 2021. Retrieved February 3, 2022, from https://www.fema.gov/sites/default/files/documents/fema_covid-19-initial-assessment-report_2021.pdf.

[142] The Joint United Nations Programme on HIV/AIDS (UNAIDS). UNAIDS Data. *The Joint United Nations Programme on HIV/AIDS (UNAIDS)*, 2021. Available from https://www.unaids.org/en/resources/documents/2021/2021_unaids_data.

[143] The World Health Organization (WHO). *Coronavirus disease (COVID-19) technical guidance: Essential resource planning.* 2020. Retrieved February 3, 2022, from https://www.who.int/emergencies/diseases/novel-coronavirus-2019/technical-guidance/covid-19-critical-items.

[144] The World Health Organization (WHO). *Rational use of personal protective equipment for coronavirus disease (COVID-19) and considerations during severe shortages.* 2020. Retrieved February 3, 2022, from https://www.who.int/publications/i/item/rational-use-of-personal-protective-equipment-for-coronavirus-disease-(covid-19)-and-considerations-during-severe-shortages.

[145] D. Thompson and R. Anderson. The COVID-19 response: considerations for future humanitarian supply chain and logistics management research. *Journal of Humanitarian Logistics and Supply Chain Management*, 2021. https://doi.org/10.1108/JHLSCM-01-2021-0006.

[146] T. Tirivangani, B. Alpo, D. Kibuule, J. Gaeseb, and B.A. Adenuga. Impact of COVID-19 pandemic on pharmaceutical systems and supply chain–a phenomenological study. *Exploratory Research in Clinical and Social Pharmacy*, 2:100037, 2021. https://doi.org/10.1016/j.rcsop.2021.100037.

[147] S. Tofighi, S. Torabi, and S. Ali-Mansouri. Humanitarian logistics network design under mixed uncertainty. *European Journal of Operational Research*, 250(1):239–250, 2016. https://doi.org/10.1016/j.ejor.2015.08.059.

[148] K.H. Tram, F. Mwangwa, G. Chamie, M. Atukunda, A. Owaraganise, J. Ayieko, V. Jain, T.D. Clark, D. Kwarisiima, M.L. Petersen, et al. Predictors of isoniazid preventive therapy completion among HIV-infected patients receiving differentiated and non-differentiated HIV care in rural Uganda. *AIDS care*, 32(1):119–127, 2020.

[149] UNICEF and World Health Organization. Framework for operations and implementation research in health and disease control programs. *World Health Organization*, 2008.

[150] United Way for Southeastern Michigan. *United Way launches effort to provide personal protective equipment to child care workers and families of essential workers.* 2020. Retrieved

February 3, 2022, from https://unitedwaysem.org/press/united-way-launches-effort-to-provide-personal-protective-equipment-to-child-care-workers-and-families-of-essential-workers/.

[151] R. Uthayakumar and S. Priyan. Pharmaceutical supply chain and inventory management strategies: Optimization for a pharmaceutical company and a hospital. *Operations Research for Health Care*, 2(3):52–64, 2013. https://doi.org/10.1016/j.orhc.2013.08.001.

[152] F. Van Leth, M J. Van der Werf, and M W. Borgdorff. Prevalence of tuberculous infection and incidence of tuberculosis; a re-assessment of the Styblo rule. *Bulletin of the World Health Organization*, 86(1):20–26, 2008.

[153] S. Verver, R.M. Warren, N. Beyers, M. Richardson, G.D. Van Der Spuy, M.W. Borgdorff, D.A. Enarson, M.A. Behr, and P.D. Van Helden. Rate of reinfection tuberculosis after successful treatment is higher than rate of new tuberculosis. *American J of Respiratory and Critical Care Medicine*, 171(12):1430–1435, 2005. https://doi.org/10.1164/rccm.200409-1200OC.

[154] A.R. Vila-Parrish, J.S Ivy, E. King, and S.R. Abel. Patient-based pharmaceutical inventory management: a two-stage inventory and production model for perishable products with markovian demand. *Health Systems*, 1(1):69–83, 2012.

[155] E. Vynnycky and P E. Fine. The natural history of tuberculosis: the implications of age-dependent risks of disease and the role of reinfection. *Epidemiology & Infection*, 119:183–201, 1997.

[156] D. Wang, K. Yang, L. Yang, and J. Dong. Two-stage distributionally robust optimization for disaster relief logistics under option contract and demand ambiguity. *Transportation Research Part E: Logistics and Transportation Review*, 170:103025, 2023.

[157] Washington Global Health Alliance. *Final Mile Event: Kicking off a US chapter of the International Association of Professional Health Logisticians (IAPHL) and the COVID-19 work of Restart Partners.* 2020. Retrieved February 3, 2022,

from https://www.wghalliance.org/event/final-mile-event-kicking-off-a-us-chapter-of-the-international-association-of-professional-health-logisticians-iaphl-and-the-covid-19-work-of-restart-partners/.

[158] B.G. Williams, R. Granich, K.M. De Cock, P. Glaziou, A. Sharma, and C. Dye. Antiretroviral therapy for tuberculosis control in nine african countries. *National Acad Sciences*, 107(45):19485–19489, 2010. https://doi.org/10.1073/pnas.100566010.

[159] World Health Organization. Global tuberculosis report, 2020. full report: `https://www.who.int/teams/global-tuberculosis-programme/tb-reports`.

[160] V.S. Yadavalli, D.K. Sundar, and S. Udayabaskaran. Two substitutable perishable product disaster inventory systems. *Annals of Operations Research*, 233(1):517–534, 2015. https://doi.org/10.1007/s10479-014-1783-3.

[161] X. Yin and I E. Büyüktahtakın. A multi-stage stochastic programming approach to epidemic resource allocation with equity considerations. *Health Care Manage Sci*, 24(3):597–622, 2021. https://doi.org/10.1007/s10729-021-09559-z.

[162] B. Zahiri, P. Jula, and R. Tavakkoli-Moghaddam. Design of a pharmaceutical supply chain network under uncertainty considering perishability and substitutability of products. *Information Sciences*, 423:257–283, 2018. https://doi.org/10.1016/j.ins.2017.09.046.